Laurent Bruckler.

UNIVERSITE CATHOLIQUE DE LOUVAIN
Faculté des sciences agronomiques
Unité de génie rural

HYDRODYNAMIC PROPERTIES OF UNSATURATED POROUS MEDIA AS AFFECTED BY CLAY DISPERSION AND MIGRATION INDUCED BY WATER QUALITY

Marylène MOUTIER
Aspirant du F.N.R.S

Dissertation doctorale présentée en vue de l'obtention du grade de Docteur en sciences agronomiques et ingénierie biologique

Promoteur : Professeur L.W De Backer

Louvain-la-Neuve - Septembre 1996

Thèse soutenue le 20 septembre 1996 à l'Université Catholique de Louvain devant le jury composé de :

T. Avella, Président de jury
L.W De Backer, Promoteur
A. Chabot, Géobel Conseil
B. Delvaux, Faculté des sciences agronomiques, U.C.L
M. Giot, Faculté des sciences appliquées, U.C.L
A. Mermoud, Ecole Polytechnique Fédérale de Lausanne, Lausanne
D. Tessier, Institut National de la Recherche Agronomique, Versailles.

"L'observation est l'investigation d'un phénomène naturel, et l'expérience est l'investigation d'un phénomène modifié par l'investigateur."

Claude Bernard

Remerciements

L'accomplissement de tout travail personnel est le plus souvent le résultat d'une collaboration efficace entre plusieurs personnes, qui d'une manière ponctuelle ou continue y ont participé, et sans lesquelles rien n'aurait été possible.

Ma reconnaissance va en premier lieu à Monsieur le Professeur Louis De Backer, qui m'a acceptée en tant que jeune assistante inexpérimentée au sein de son laboratoire. Ses conseils éclairés, sa confiance, ainsi que sa patience et ses encouragements ont été les ingrédients premiers qui m'ont permis de mener à terme cette recherche, financée par le Fonds National de la Recherche Scientifique.

Les membres de l'unité de génie rural et des sciences du sol, en créant une ambiance détendue et stimulante, ont rendu ces années particulièrement agréables à vivre. L'assistance technique de Messieurs Guido Rentmeesters, Gérard Peeters et Jean Naud a été essentielle à de nombreuses étapes de ce parcours. Les nombreuses discussions que j'ai pu avoir avec Messieurs Badji Moussa, Marnik Vanclooster, Samuel Assouline ont largement contribué à l'établissement et à l'amélioration des aspects théoriques et méthodologiques de ce travail de recherche.

Je tiens également à remercier l'unité de thermodynamique et turbomachines qui a gracieusement mis à ma disposition l'équipement indispensable à la réalisation de certaines mesures expérimentales.

Messieurs André Chabot, Bruno Delvaux, Michel Giot, André Mermoud et Daniel Tessier m'ont fait l'honneur d'accepter d'être membres du jury de cette thèse. Je les remercie du temps qu'ils ont bien voulu consacrer à cette tâche.

Que soit remercié ici mon époux qui a été un collaborateur précieux, que ce soit en m'aidant à réflechir aux aspects statistiques de ce travail ou en réalisant complètement la mise en forme de ce manuscript.

Enfin, je voudrais également remercier mes parents, qui ont certainement été mes plus ardents supporters. En m'offrant l'opportunité de poursuivre mes études, ils ont par la même occasion autorisé la réalisation de ce travail de recherche.

Résumé

Effet de la qualité de l'eau d'infiltration, induisant la dispersion et la migration d'argile, sur les propriétés hydrodynamiques d'un milieu poreux non saturé.

Marylène MOUTIER

Université Catholique de Louvain, Département des sciences du milieu et de l'aménagement du territoire, Unité de génie rural, Place Croix du Sud 2/2, B-1348 Louvain-la-Neuve

Les propriétés hydrodynamiques, comprenant la courbe de rétention en eau et la courbe de conductivité hydraulique, dépendent non seulement de la teneur en eau mais également de la qualité de l'eau, en particulier la concentration totale en électrolytes et la salinité (Sodium Adsorption Ratio). Ainsi, l'utilisation de solutions de faible concentration mais contenant du sodium engendre la dispersion de l'argile, susceptible, ultérieurement, de migrer au sein d'un milieu poreux et d'en affecter les propriétés hydrodynamiques. Si le transport particulaire ou l'effet de la qualité de l'eau sur la conductivité hydraulique sont largement étudiés en milieu saturé en eau, rares sont les travaux effectués en milieu non saturé en eau.

Dans le cadre de cette étude, la modification des propriétés hydrodynamiques d'un milieu poreux sableux non saturé en eau et initialement exempt d'argile (smectite) a été appréhendée en percolant avec des solutions mixtes NaCl-$CaCl_2$. Les percolations ont été conduites sur des milieux stratifiés (bicouches) dont la couche supérieure est constituée d'un matériau à caractère argileux.

Après un rappel de quelques définitions préliminaires, les caractéristiques des matériaux utilisés et les différentes techniques mises en oeuvre sont passées en revue. Les propriétés hydrodynamiques du milieu sableux non saturé en eau sont déterminées en appliquant une approche inverse sous condition d'écoulement permanent. Néanmoins, une approche plus conceptuelle est également présentée.

Il ressort de cette étude que les propriétés hydrodynamiques du milieu considéré sont affectées par la qualité de l'eau induisant la dispersion, la migration et la réorganisation de l'argile. Ces modifications se produisent initialement dans la première couche puis ultérieurement au sein du milieu sableux non saturé en eau. Néanmoins, il subsiste un caractère aléatoire quant à la quantité de smectite qui migrera effectivement et sa distribution spatiale au sein des colonnes expérimentales. La variabilité temporelle des propriétés hydrodynamiques, induite chimiquement, mérite au moins autant d'attention que l'étude de l'hétérogénéité spatiale.

Contents

Introduction

In situ water content observations from an equipped survey well installed in a ponded storm basin on the university site of Louvain-la-Neuve is at the origin of the present study. Abnormally large water content fluctuations were observed in a 6 meter stratified geological profile measured by the means of a coupled neutron-gamma probe *(Hessane, 1995)*. The profile is constituted of sand (150-250 μm), originated from the Bruxellian aquifer, and clay lenses. Three assumptions were proposed i.e. redox processes, calcium carbonate dissolution/precipitation and clay movement, to explain porosity variations which could induce water content fluctuations. Because X-ray analysis of a soil sample highlighted the presence of montmorillonite, clay migration from an upper less permeable layer towards the more sandy layer was proposed to be the major cause of the soil moisture fluctuations. Clay dispersion and migration were further proposed to be linked to the input of deicing salts such as NaCl and $CaCl_2$ in the storm basin during winter.

Conceptual models of water and contaminant transport in soil are based on the soil physical properties such as the soil moisture retention curve (MRC) and the hydraulic conductivity curve (HCC). Yet the use of conceptual models to support water and environmental management issues at different scales is complicated by the heterogeneous nature of the soil hydraulic properties. In the past, considerable attention has been devoted to the characterization of the spatial heterogeneity of the hydraulic properties. Both theoretical and experimental studies *(Russo and Dagan, 1993; Mallants, 1996)* were conducted to show the extent of spatial heterogeneity on the soil water fluxes. The general outcome of these studies is that at the larger scale, due to the huge spatial heterogeneity, the direct estimation of the soil hydraulic properties is nearly impossible. Therefore, indirect methods are currently developed to quantify the spatial distribution of the hydraulic properties*(van Genuchten et al., 1992)*. These methods include the indirect estimation of the MRC and HCC from basic soil properties such as particle size distribution or organic matter contents *(Gupta and Larson, 1979; Arya and Paris, 1981; Rawls et al., 1982; Saxton et al., 1986; Vereecken et al., 1990)* or the indirect estimation of the HCC from the MRC *(Childs and Collis-George, 1950; Burdine, 1953; Mualem, 1976)*. In contrast to the many studies dealing with the spatial variability, only few studies quantified the temporal variability. In the past, it was tacitly assumed that this latter heterogeneity component could be neglected to model water flow in normal rigid field soils. Yet, more and more experimental evidence shows that temporal variability can no longer be ignored.

The soil structure is known to govern the hydraulic properties to an extremely large extent. The soil structure varies considerably in time, especially if affected by different soil management practices. The structural dynamics in clay soils is of particular concern. Heavy clay soils can undergo physical degradation due to swelling. In addition, dispersion of colloidal minerals induce structural changes *(Sumner, 1993)*. On the one hand, clay swelling is a continuous process. It becomes particularly appreciable at high values of salinity or Sodium Adsorption Ratio (SAR) *(Sumner, 1993)*. Clay swelling will further increase with decreasing Total Electrolyte Concentration (TEC) *(Keren and Singer, 1988)*. On the other hand, clay dispersion, is operative throughout the entire range of SAR but is limited if the TEC does not exceed a Critical Flocculation Concentration (CFC) *(Oster et al., 1980)*. The latter is determined under specified conditions of exchangeable cation composition, pH and suspension concentration and is defined as the minimum electrolyte concentration necessary to flocculate a given colloidal suspension in a given time *(Van Olphen, 1977)*. Clay dispersion further depends on the pH *(Suarez et al., 1984; Gupta et al., 1984)*, the presence of oxides or hydroxides *(Alperovitch et al., 1985; Goldberg and Glaubig, 1987)*, the presence of organic matter *(Gupta et al., 1984; Churchman et al., 1993)*, the mineralogy *(Frenkel et al., 1978; Alperovitch et al., 1985)*, the nature of the exchange cations and the presence of organic or inorganic anions *(Frenkel et al., 1992a, 1992b)*.

Two different approaches can be found in the literature to study the effect of salinity and electrolyte concentration on clay dispersion. One consists in the determination of the conditions under which clay suspensions flocculates or disperses, defining some Critical Flocculation Concentration (CFC) *(Goldberg and Glaubig, 1987; Frenkel et al., 1992a, 1992b)*. As it has been mentioned, these CFC are determined under specified conditions (pH, TEC, SAR, mineralogy, etc.) and generally for reference clays characterized by the purity of their clay-size fraction (< 2 μm). Consequently, results cannot be directly extrapolated to clays extracted from soils, referred to as soil clays, due to the fact that they are constituted of various clay minerals.

The other approach consists of following the hydraulic properties of different porous media as affected by the salty experimental conditions *(McNeal, 1968; Bresler et al., 1982; Keren and Singer, 1988; Levy et al., 1988; Frenkel et al., 1992a, 1992b; Russo and Dagan, 1993)*. Most of these studies were carried out under saturated conditions using either dispersed suspensions *(Cayeux, 1990; Somaratne, 1994)* or establishing saturated flow in sand-clay mixtures or soils (*Frenkel et al., 1978; Pupisky and Shainberg, 1979; Alperovitch et al., 1985; Abu-Sharar et al., 1987; Keren and Singer, 1988; Frenkel et al., 1992a, 1992b*). Only recently *Wan and Wilson (1994)* studied colloid transport in unsaturated porous media. According to them, colloid particles preferentially sorb onto the gas-water interface relative to the solid matrix surface under typical groundwater conditions. A stationary gas phase behaves

as a sorbent phase retaining the particles, thereby reducing colloid transport. On the contrary, a mobile gas phase, as it can be obtained during drainage and wetting processes, promotes particle movement. Particle movement in unsaturated zone is of uttermost importance because it constitutes a mobile solid phase and sorbent phase regarding pollutants. Finally, it becomes evident that the presence of clay particles in the unsaturated zone will influence the hydrodynamic properties of the porous media, and hence water flow, solute flow and further particle flow.

This background information allows us to define now the aim and objectives of the study as follows. The aim is to investigate the dispersion and mobility of smectite e.g. smectite of Béthonvilliers in two-layered unsaturated columns induced by means of salty solutions and to study its effect on the hydrodynamic properties of an initial clay-free and unsaturated sand. The objectives can be summarised by simple questions :

- Does smectite of Béthonvilliers migrate when NaCl-$CaCl_2$ solutions prepared with intermediate SAR values and low total electrolyte concentrations are used ?
- How does it influence the matric head, the total hydraulic conductivity, the water content and bulk density profiles during percolation ?
- Where is the dispersed smectite located within an unsaturated sandy layer ?
- How much smectite migrates ?

Given the above and after some theoretical considerations, the following points illustrate how the objectives were achieved and will be discussed later on in the indicated sections :

- Selection and physico-chemical characterization of a soil material whose clay fraction contained mainly smectite (§ 2.3).
- Development and construction of a specific experimental device combined to complementary laboratory equipment, allowing repeated and non destructive volumetric water content and bulk density measurements. The principles of gamma radiation, the calibration requirements, the determinations of the mass attenuation coefficients and, finally, the corrections which have to be considered to calculate the water content and density are discussed in § 2.4.3. The assessment of the error on the measurements is also presented.
- Development of an indirect methodology to quantify small clay amounts (§ 2.5).
- Development and description of the leaching procedures having in mind the numerous factors contributing to the swelling and dispersive behaviour of clay (§ 2.6).
- Development of a conceptual approach to determine soil moisture retention curves (MRCs) for sand-smectite mixtures as a function of the salinity of the leaching solutions and the clay quantities. Because of the lack of data in the literature relating the swelling pressure of

sand-clay mixtures as a function of the retained water content, the conceptual MRC model could not be validated (§ 3.2).

- Determination of the hydrodynamic properties of unsaturated sandy layers affected by the presence of dispersed clay, by applying an inverse approach (§ 3.3).

REFERENCES

Abu Sharar, T.M., F.T. Bingham, and J.D. Rhoades. (1987). Reduction in hydraulic conductivity in relation to clay dispersion and disaggregation. *Soil Science Society of America Journal*, **51**, 342-346.

Alperovitch, N., I. Shainberg, R. Keren, and M.J. Singer. (1985). Effect of clay mineralogy and aluminium and iron oxides on the hydraulic conductivity of clay-sand mixtures. *Clays and Clay Minerals*, **33**, 443-450.

Arya, L.M., and J.F. Paris. (1981). A physico-empirical model to predict the soil moisture characteristic from particle-size distribution and bulk density data. *Soil Science Society of America Journal*, **45**, 1023-1030.

Bresler, E., B.L. Mc Neal, and D.L. Carter. (1982). *Saline and Sodic Soils- Principles-Dynamics - Modelling.* Springer-Verlag, Berlin, 236 p.

Burdine, N.T. (1953). Relative permeability calculations from pore-size distribution data. *Petroleum Trans. Am. Inst. Mining Eng.*, **198**, 71-77.

Cayeux, M.D. (1990). *Contribution à l'Etude de la Migration et de la Rétention de Particules Minérales dans un Milieu Poreux.* LCPC, Rapports des Laboratoires, Série Physique et Chimie PC-8, n° 3585, 107 p.

Childs, E.C., and N. Collis-George. (1950). The permeability of porous materials. *Proc. Roy. Soc.* , **A201**, 392-405.

Churchman, G.J., J.O. Skjemstad, and J.M. Oades. (1993). Influence of clay minerals and organic matter on effects of sodicity on soils. *Australian Journal of Soil Research*, **31**, 779-800.

Frenkel, H., J.O. Goertzen, and J.D. Rhoades. (1978). Effects of clay type and content, exchangeable sodium percentage and electrolyte concentration on clay dispersion and soil hydraulic conductivity. *Soil Science Society of America Journal*, **42**, 32-39.

Frenkel, H., G.J. Levy, and M.V. Fey. (1992a). Clay dispersion and hydraulic conductivity of clay-sand mixtures as affected by the addition of various anions. *Clays and Clay Minerals*, **40**, 515-521.

Frenkel, H., M.V. Fey, and G.J. Levy. (1992b). Organic and inorganic anion effects on reference and soil clay critical flocculation concentration. *Soil Science Society of America Journal*, **56**, 1762-1766.

Goldberg, S., and R.A. Glaubig. (1987). Effect of saturating cation, pH, and aluminium and iron oxide on the flocculation of kaolinite and montmorillonite. *Clays and Clay Minerals*, **35**, 220-227.

Gupta, S.C., and W.E. Larson. (1979). Estimating soil-water retention from particle size distribution, organic matter content and bulk density. *Water Resources Research*, **17**, 1005-1013.

Gupta, R.K., D.K. Bhumbla, and I.P. Abrol. (1984). Effect of sodicity, pH, organic matter and calcium carbonate on the dispersion behavior of soils. *Soil Science,* **137**, 245-251.

Hessane, M.A. (1995). Etude de l'influence des eaux de recharge dans la partie non saturée de l'aquifère du Bruxellien au droit du lac de Louvain-la-Neuve. Thèse de doctorat en Sciences naturelles Appliquées, Université Catholique de Louvain, Louvain-la-Neuve, 101 p.

Keren, R., and M.J. Singer. (1988). Effect of low electrolyte concentration on hydraulic conductivity of sodium/calcium-montmorillonite-sand system. *Soil Science Society of America Journal*, **52**, 368-373.

Levy, G.J., H.V.V. Van Der Watt, and H.M. Du Plesis. (1988). Effect of sodium-magnesium and sodium-calcium systems on soil hydraulic conductivity and infiltration. *Soil Science*, **146**, 303-310.

Mallants, D. (1996). Solute and water transport in heterogeneous soil profiles. Doctoraatschrift n°309 aan de Faculteit Landbouwkundige en Toegepaste Biologische Wetenschappen, Leuven.

McNeal, B.L. (1968). Prediction of the effect of mixed salt solution on soil hydraulic conductivity. *Soil Science Society of America Proceedings*, **32**, 190-193.

Oster, J.D., I. Shainberg, and J.D. Wood. (1980). Flocculation value and gel structure of sodium/calcium montmorillonite and illite suspensions. *Soil Science Society of America Journal*, **44**, 955-959.

Pupisky, H., and I. Shainberg. (1979). Salt effects on the hydraulic conductivity of a sandy soil. *Soil Science Society of America Journal*, **43**, 429-433.

Rawls, W.J., D.L. Brakensiek, and K.E. Saxton. (1982). Estimation of soil-water properties. *Trans. ASAE*, **25**, 1316-1320.

Russo, D., and G. Dagan. (1993). *Water Flow and Solute Transport in Soils-Developments and Applications.* Springer-Verlag, Berlin, 306 p.

Saxton, K.E., W.J. Rawls, J.S. Romberger, and P.I. Papendick. (1986). Estimating generalized soil-water characteristics from texture. *Soil Science Society of America Journal*, **50**, 1031-1036.

Somaratne, N.M. (1994). Characterization and modelling of surface sealing and near surface pore clogging processes. Thesis, Flinders University of South Australia.

Suarez, D.L., J.D. Rhoades, R. Lavado, and C.M. Grieve. (1984). Effect of pH on saturated hydraulic conductivity and soil dispersion. *Soil Science Society of America Journal*, **44**, 3-7.

Sumner, M.E. (1993). Sodic soils : new perspectives. *Australian Journal of Soil Research*, **31**, 683-750.

van Genuchten, M.Th., F.J. Leij, and L.J. Lund. (Eds) (1992). *Indirect methods for estimating the hydraulic properties of soils.* University of California, 730 p.

Van Olphen, H. (1977). *An introduction to clay colloid chemistry.* 2nd ed. John Wiley & Sons, New York, 318 p.

Vereecken, H., J. Maes, and J. Feyen. (1990). Estimating unsaturated hydraulic conductivity from easily measured soil properties. *Soil Science*, **149**, 1-12.

Wan, J., and J.L. Wilson. (1994). Colloid transport in unsaturated porous media. *Water Resources Research*, **30**, 857-864.

1. General theory and definitions

It might be useful for the reader to summarize here below some preliminary definitions before describing the clay fraction (< 2 µm), seat of phenomena such as swelling, dispersion and cation exchange. The common clay minerals will be briefly described in order to understand the specific behaviour of smectite in soils. Finally, the main factors affecting clay swelling and dispersion will be presented.

1.1. Preliminary definitions

The definitions of the following specific terms used in the study such as the particle and bulk density, the water content, the potential energy as well as some parameters related to salinity are given now as references. It will allow a better understanding of the future measurements and experimental procedures which are explained in § 2.

1.1.1. Particle density and bulk density

Consider a three-phase system composed of a solid phase, an aqueous phase and an air phase (figure 1.1). Taking V_s, V_w, V_a and V_t to represent the volume of solid, the volume of liquid, the volume of air and the total volume, respectively, and considering m_s, m_w, m_a and m_t to represent the corresponding masses, the following relations can be defined :

the particle density, $$\rho_s = \frac{m_s}{V_s} \quad [\text{kg/m}^3] , \tag{1.1}$$

the dry bulk density, $$\rho_b = \frac{m_s}{V_t} \quad [\text{kg/m}^3] . \tag{1.2}$$

The often assumed values for the particle density range from 2650 up to 2700 kg/m^3. Nevertheless, strong deviations in the particle density values of volcanic soils were observed by *Bielders et al. (1990)*. They mentioned values ranging from 2380 up to 2720 kg/m^3 and related them to the organic matter content. Furthermore, *Tessier (1984)* presented particle density values varying from 2670 up to 3210 kg/m^3. These high values were related to the iron content. The higher the iron content is, the greater the particle density will be.

The bulk density will mainly depend on the texture and the compaction of the soil sample. The latter can be controlled (§ 2.6.3) but the former can undergo changes, e.g. if the

original soil material becomes enriched in clay due to clay migration. Consequently, it cannot be considered as a constant and it was preferred to measure it during the experiments. Methods for measuring particle density and bulk density of our soil material will be discussed later, respectively in § 2.3.1. and § 2.4.3.

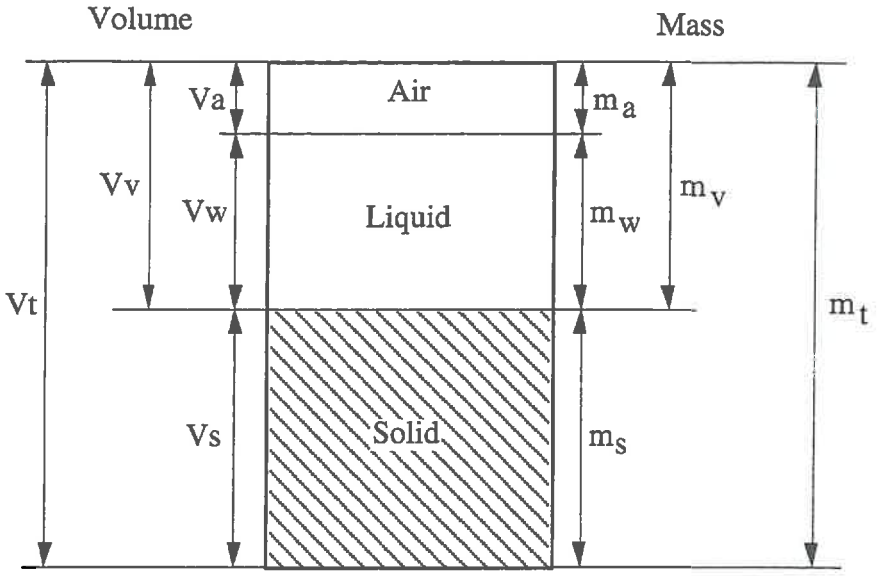

Figure 1.1. The soil as a three-phase system.

1.1.2. Soil water content and soil moisture retention curve

Soil pores will be either occupied by air or water. When the soil pores are filled with a liquid phase, the soil is termed *saturated.* If a gas phase is present, the soil will be referred to as *unsaturated.* The amount of water in soil is defined by the following relationships :

the volumetric water content, $$\theta_v = \frac{V_w}{V_t} \quad [m^3/m^3] , \tag{1.3}$$

the water content on a mass basis, $$\theta_m = \frac{m_w}{m_s} \quad [kg/kg] , \tag{1.4}$$

and $$\theta_v = \frac{\theta_m \rho_b}{\rho_w} . \tag{1.5}$$

In swelling soils, a liquid ratio ϑ is generally used instead of a volumetric water content and is defined as follows :

$$\vartheta = \frac{V_w}{V_s}. \tag{1.6}$$

Nevertheless, in the present study, the use of eqn. (1.3) was preferred to eqn. (1.6) because volumetric water content measurements were directly obtained by gamma-radiation (§ 2.4.3). Furthermore, its calculation is independent of the bulk density of the soil in contrast with the use of eqn. (1.6). Indeed, the liquid ratio can be calculated from the volumetric water content and the porosity ε following :

$$\vartheta = \frac{\theta_v}{1-\varepsilon}, \tag{1.7}$$

and

$$\varepsilon = 1-\frac{\rho_b}{\rho_s}. \tag{1.8}$$

In unsaturated porous media, an empirical relationship exists between the volumetric water content and the matric potential (§ 1.1.3). This relationship referred to as the *soil moisture retention curve (MRC)* can be described with the non-hysteretic parametric functions of van Genuchten (VG)*(van Genuchten, 1980)* :

$$\theta(h) = \theta_r + \frac{(\theta_s - \theta_r)}{\left(1 + (\alpha h)^n\right)^m}, \tag{1.9}$$

where h is the suction as defined in § 1.1.3.1 ;
θ_s is the saturated volumetric water content [m^3/m^3] ;
θ_r is the residual volumetric water content [m^3/m^3] ;
α and n are curve shape parameters, where α is expressed in terms of [m^{-1}] and
$m = 1-1/n$ *(Mualem, 1976).*

Eqn. (1.9) will be used to describe the MRCs of the initial clay-free sandy layer during the flow experiments (§ 3.3). A physical interpretation of the VG parameters is illustrated in figure 1.2.

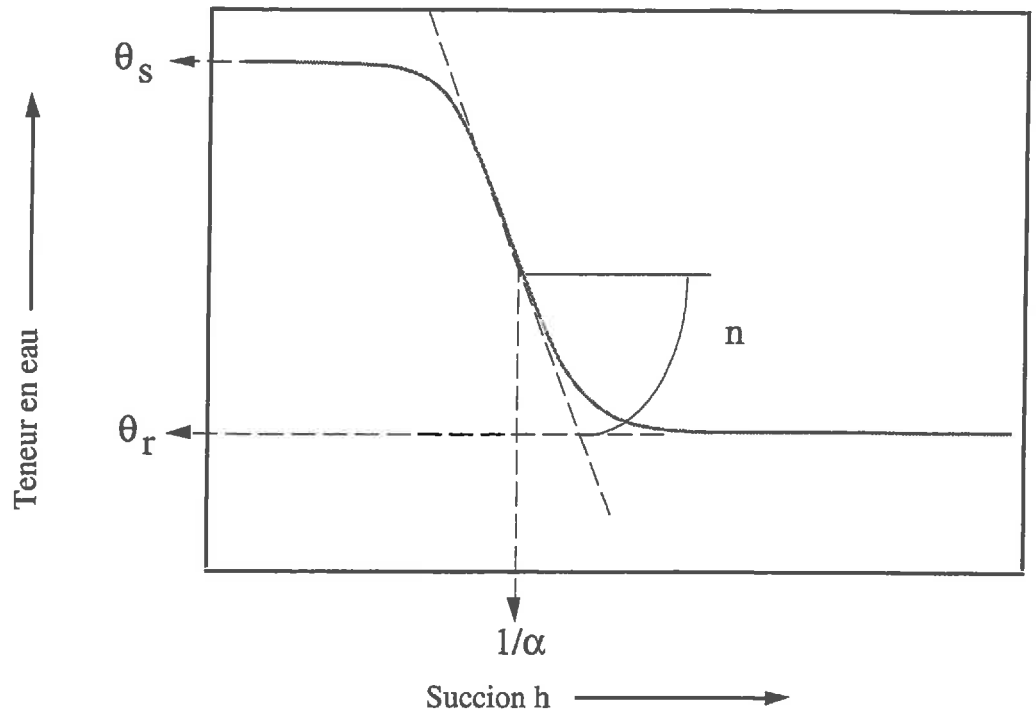

Figure 1.2. A physical interpretation of the *van Genuchten (1980)* parameters used to describe the soil moisture retention curve.

1.1.3. Potential energy of soil water

The *total potential* of soil water Φ_t is the amount of work that must be done per unit quantity of pure water to transfer reversibly and isothermally an infinitesimal quantity of water from a pool of pure water at a reference elevation height, at a standard atmospheric pressure to the soil water at the point under consideration *(Marshall and Holmes, 1979)*.

The total potential of soil water is the summation of the *pressure potential* P (or *matric potential* ψ), the *osmotic potential* Π and the *gravitational potential* Z :

$$\Phi_t = P + \Pi + Z \qquad [J/m^3] , \tag{1.10}$$

where all the potentials are here expressed per unit volume of water. Though, the unit quantity of water on which the potentials are based can also be a mass or a weight.

1.1.3.1. Pressure potential P - matric potential ψ

The pressure potential combines forces between solid soil surfaces and water, cohesion forces between water molecules and forces arising from pressure in the soil gas phase *(Bresler et al., 1982)*. The decrease in the potential energy of water caused by the interaction between soil particles and water is termed the matric potential ψ and has a negative value.

The potentials can either be expressed on a volume basis, a mass basis or a weight basis as follows :

per unit volume	$P_v = \rho_w\ g\ h$	[J/m^3] ,	$\psi_v = -\ \rho_w\ g\ h,$	(1.11)
per unit mass	$P_m = g\ h$	[J/kg] ,	$\psi_m = -\ g\ h,$	(1.12)
per unit weight	$P_w = h$	[m] ,	$\psi_w = -\ h,$	(1.13)

where ρ_w is the density of water [kg/m^3] ;

g is the acceleration due to gravity [m/s^2] ;

h is referred to as the *pressure head* or *matric head* [m].

The term *suction* is widely used to designate the absolute value of the matric head.

1.1.3.2. Osmotic potential Π - Osmotic pressure π

The osmotic potential Π arises from the presence of solutes in soil water. It is equal but of opposite sign to the osmotic pressure π. The osmotic pressure is the pressure to which the solution is subjected in order to be at equilibrium with pure water through a semi permeable membrane albeit the volume of the solution is kept constant *(Marshall and Holmes, 1979; Miyazaki et al., 1993)*. It can be regarded as a solute suction which when added to the matric suction gives the total suction. Denoting the solution pressure p_1 and that of pure water p_2, the osmotic pressure is given by the difference $(p_1 - p_2)$.

The osmotic pressure affects the chemical potential of water in a solution(1). The higher the osmotic pressure is, the smaller the chemical potential will be. The decrease in the chemical potential caused by osmotic pressure in water is referred to as the osmotic potential $\prod$ [J/m^3] and has negative values.

(1) The chemical potential of pure water is taken as reference and is equal to zero.

When the concentration of ions in a given solution differs from that at another point, there is a tendency for the more dilute concentration liquid to diffuse towards the point of higher concentration. This results in a more uniform ion distribution. This means that osmotic gradients may be important only during the early stages of water redistribution *(Bresler et al., 1982)*. Consequently, their contribution to water flow in our experimental columns will be neglected (§ 1.1.3.5).

1.1.3.3. Gravitational potential Z

The gravitational potential Z of water in soil at a given level is determined by the elevation of that point from an arbitrary reference plane. If the point is above (below) the reference plane, the gravitational potential is positive (negative). The soil surface or the water table are generally used as reference. The gravitational potential can also be expressed on a volume basis, a mass basis or a weight basis :

$$Z_v = \rho_w \, g \, z \qquad [\mathrm{J/m^3}] , \qquad (1.14)$$

$$Z_m = g \, z \qquad [\mathrm{J/kg}] , \qquad (1.15)$$

$$Z_w = z \qquad [\mathrm{m}] . \qquad (1.16)$$

The height z is also called the *elevation head.*

1.1.3.4. Hydraulic potential ϕ

The *hydraulic potential* ϕ per unit volume of water only takes into account the pressure potential P and the gravitational potential Z :

$$\phi = P + Z \qquad [\mathrm{J/m^3}] . \qquad (1.17)$$

When the hydraulic potential is expressed on a weight basis, it is termed the *hydraulic head H* :

$$H = h + z \qquad [\mathrm{m}] . \qquad (1.18)$$

1.1.3.5. Darcy's law

The flux of water in soils is described by Darcy's equation :

$$q = - K \nabla H, \tag{1.19}$$

where ∇H is the hydraulic gradient [m/m] ;
K the hydraulic conductivity [m/s] ;
q is the flux density [m/s].

Darcy's equation assumes that the only driving force causing water flow is the hydraulic gradient. Water flow in response to osmotic gradients are generally negligible during infiltration *(Bresler et al., 1982)*. Consequently, Darcy's equation will be used in its form given by eqn. (1.19).

The hydraulic conductivity K is depending on the suction h or the water content θ under unsaturated flow conditions as studied in this work. The hydraulic conductivity curve (HCC) will be described using the functional non-hysteretic van Genuchten relationships *(1980)* :

$$K(h) = K_s \frac{\left[1 - (\alpha h)^{n-1} \left(1 + (\alpha h)^n\right)^{-m}\right]^2}{\left(1 + (\alpha h)^n\right)^{m/2}}, \tag{1.20}$$

where K_s is the saturated hydraulic conductivity [m/s]. The parameters of eqn. (1.20) are those used in eqn. (1.9).

1.1.4. Parameters related to salinity

The quality of a given soil solution depends on the concentration and composition of the salts dissolved in it. The most common parameters related to salinity are the total electrolyte concentration (TEC), the electrical conductivity (EC), the sodium adsorption ratio (SAR) and the exchangeable sodium percentage (ESP), defined as follows :

- the TEC reflects the salinity hazard and is a measure of the total mass of salts per unit volume of solution. It is generally expressed in meq/l.

- the EC is a simplified index of the total electrolyte concentration and is expressed in µS/cm. In this study the EC was measured at 298 K.
- the SAR reflects the alkali hazard and is defined by the following relation *(USSL Staff, 1954)* :

$$SAR = \frac{\left[Na^{+}\right]}{\sqrt{\frac{\left(\left[Ca^{++}\right] + \left[Mg^{++}\right]\right)}{2}}}, \qquad (1.21)$$

where all the concentrations are given in meq/l and the SAR is expressed in $(mmole/l)^{0.5}$.

- the ESP refers to the fraction of the cation exchange capacity (CEC) occupied by exchangeable sodium :

$$ESP = \frac{Na_{exch}}{\sum\left(Ca_{exch} + Mg_{exch} + K_{exch} + Na_{exch}\right)}, \qquad (1.22)$$

and is generally expressed in meq/100 g.

For convenience, units for the SAR and ESP will no longer be added in the text.

1.1.5. Clay structure and mineralogy

The minerals in the clay fraction (< 2 µm) largely consist of aluminosilicates as well as a range of oxides, hydroxides and oxyhydroxides. The type of clay mineral is determined by the arrangement and the chemical composition of their basic structural units or sheets. Two different *sheets*(2) are distinguished : the tetrahedral sheet and the octahedral sheet. The tetrahedron and the octahedron are the basic units of these sheets (figure 1.3). The silicon atom of the silica tetrahedrons can be replaced by Al or Fe^{3+}, whereas the aluminium atom of the octahedron can be replaced by divalent (Fe^{2+}, Mg) or trivalent (Fe^{3+}) cations. These replacements are referred to as isomorphous substitutions. Isomorphous substitution generates a negative charge which can be compensated by various interlayer materials, including cations, hydrated cations and hydroxide octahedral groups and sheets. A *layer* is formed by the combination of tetrahedral and octahedral sheets. The main properties of the most common minerals i.e. kaolinite, illite and smectite, are given in table 1.1 *(Bresler et al., 1982)*.

(2) Following the AIPEA Nomenclature Committee Recommendation *(1980)*.

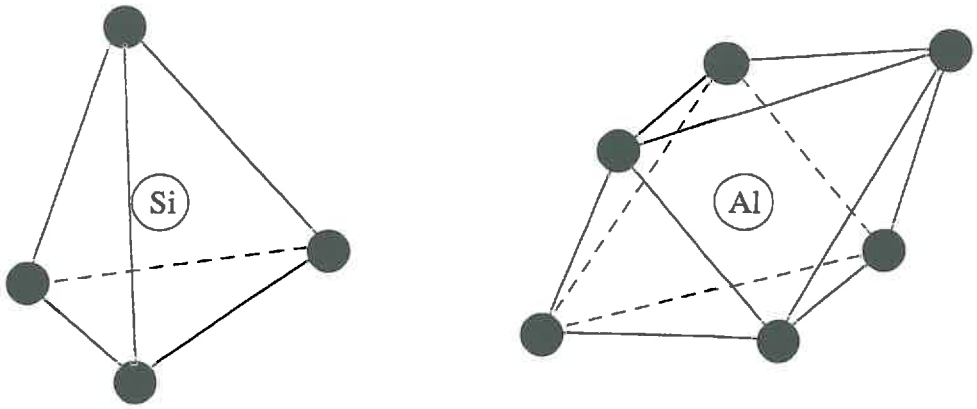

a) b)

Figure 1.3. The two basic units of the sheets : a) the silica tetrahedron and b) the alumina octahedron.

Table 1.1. Major properties of kaolinite, illite and smectite primary particles as defined by *Mering and Oberling (1971).*

Type	Sheet structure	Morphology	CEC(1) meq/100 g	charge per formula unit (2)	Specific surface m^2/g
Kaolinite	1 to 1	flat, thick, platy, regular	3-6	x ~0	30-50
Illite	2 to 1	platy	20-40	x ~1	100-200
Montmorillonite	2 to 1	thin flexible flakes	80-120	x ~0.2-0.6	600-800

(1) Cation Exchange Capacity
(2) Following AIPEA Nomenclature Committee Recommendations (1980)

Kaolinite (figure 1.4) is a typical two-layer mineral having a single tetrahedral sheet joined to a single octahedral sheet to form a 1 to 1 lattice structure. The unit layers are held together by hydrogen bonding. The repetition of the layers is shown by the X-Ray diffraction to occur at intervals of 7 Å. The distance between the corresponding planes is called the basal distance d001.

Illite is a three-layer mineral having two tetrahedral sheets combined with one octahedral sheet between them to give a 2 to 1 lattice structure. Some of the silicon atoms are replaced by aluminium. In addition, non exchangeable potassium ions are present between the tetrahedral sheet and adjacent crystals. The basal distance is about 10 Å.

Smectite (montmorillonite, beidellite, etc.,) is also a three-layer mineral but the bond between the layers is through exchangeable cations. Water molecules attracted to the cations cause the basal spacing to increase progressively. The basal distance varies from 9.6 up to 20 Å *(Norrish, 1954)* corresponding to the progressive adsorption of successive water layers in the interplatelet spaces. Saturating with lithium or sodium can proceed to a further increase of the basal distance, giving irregularly spaced layers. *Tessier (1984)* mentioned for a Greek montmorillonite saturated with NaCl, 10^{-3} N, at a pressure of 0.032 bar a mean basal distance of 57 Å with distances varying in the range 20-150 Å.

Minerals of the smectite group differ from each other primarily with respect to the location, type and degree of mineral-lattice substitution. Montmorillonite *sensu stricto* is a dioctahedral smectite with octahedral substitutions, where some aluminium atoms are replaced by magnesium atoms.

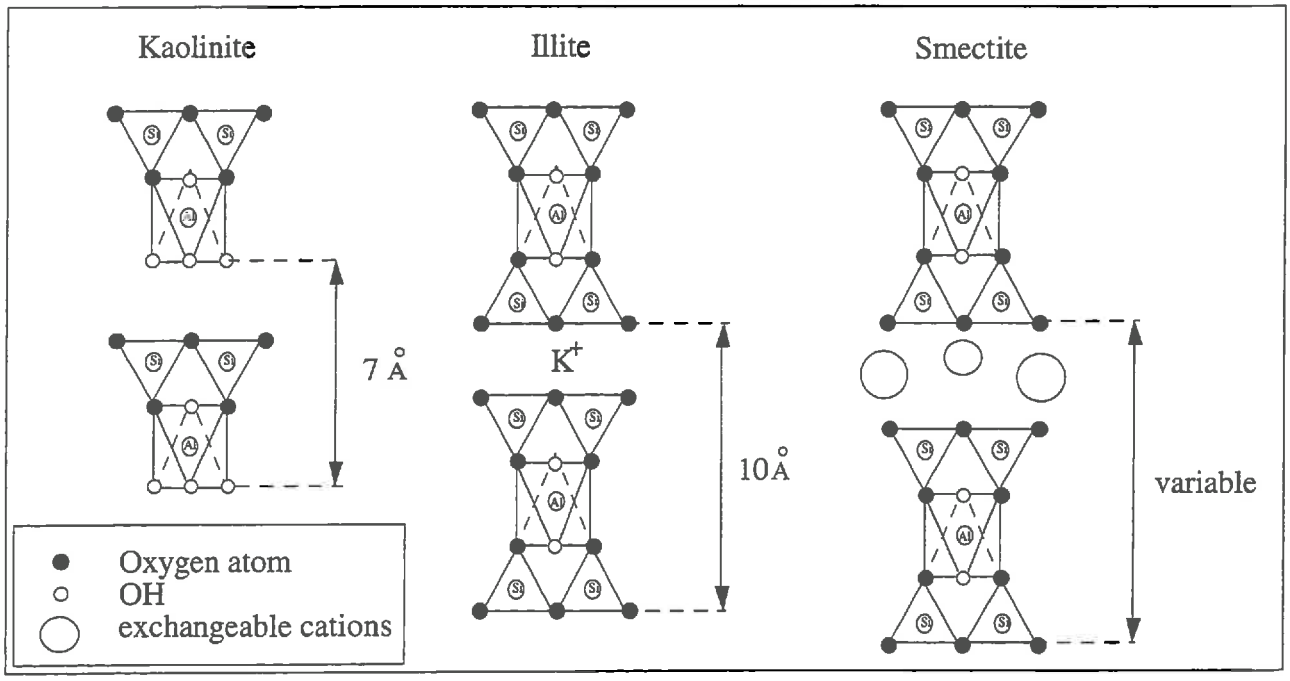

Figure 1.4. A simplified representation of the structure of the most common minerals : kaolinite, illite and smectite.

The smallest clay particle resulting from the superimposed clay layers is referred to as a *primary particle (Mering and Oberling, 1971)*. Such isolated particles are encountered for kaolinite. Nevertheless, in suspensions, clay particles rarely occur as primary particles. They generally form so-called *domains*, *tactoids (Blackmore and Miller, 1961)*. or *quasi-crystals (Quirk and Aylmore, 1971)*.

A domain refers to as an aggregation of primary particles or crystallites, each of them consisting of a small number of layers (3-6) *(Tessier and Pedro, 1987)*. The formation of domains is generally encountered for non swelling clays such as illite.

The term tactoid was initially associated to the microstructure of Na-smectite and K-smectite when the layers are separated from each other by a diffuse double layer (d001 > 35 Å). Though, through the literature few distinction is made between the terms tactoid and quasi-crystal.

Quasi-crystals are packets of clay layers arranged in a more or less parallel alignment. The extent of the packets or the number of layers per packet depends on various factors e.g. the nature of the ion adsorbed, the TEC, the layer charge and the clay concentration *(Tessier and Pedro, 1987)*, the ESP *(Shainberg and Otoh, 1968)*, the maximum pressure applied to the system *(Blackmore and Miller, 1961)*. The number of layers per packet can further be affected by air drying which causes an increase in the average size of quasi-crystals *(Blackmore and Miller, 1961; Shainberg and Otoh, 1968)*.

Tessier and Pedro (1987), who have worked on pastes, mentioned different types of clay particles relating them to the layer charge and saturating cation. They concluded that the quasi-crystal arrangement was characteristic of smectites, including mixed-layer smectites, saturated with divalent cations irrespective to their layer charge. The quasi-crystals are constituted of a great number of layers (up to 50) separated from each other by a restricted number of water sheets (3-4). When Na replaces Ca and in the presence of a dilute solution and low suction (e.g. P = 0.032 bar), Na-smectite consists of packets containing few layers ($\cong$ 10) separated from each other by diffuse double layers. This arrangement is valid for layer charges lower than 0.45 (e.g. true smectites). For layer charges between 0.45 and 0.60, these individual packets are aggregated. Each packet contains approximately 10 layers with interlayer spacings ranging from 10 to 15 Å.

When working with clay suspensions, the number of layers per quasi-crystal is smaller. *Verburg and Baveye, (1994)* summarized the ranges reported in the literature for montmorillonite. The number of layers per quasi-crystal varies between 1 and 1.7 and between 2.7 and 20 for Na-saturated and Ca-saturated montmorillonite, respectively. Such information will be used to establish a conceptual model in order to build up theoretical soil moisture retention curves (§ 3.2).

1.2. Interactions between the liquid phase and clay particles

The basal planes of clay minerals carry negative charges neutralised by a swarm of ions, predominantly of opposite charge. The interaction between these charged particles in colloidal[3] suspensions is usually treated in terms of the DLVO theory, which was developed independently in the 1940s by *Derjaguin and Landau (1941)* and *Verwey and Overbeek (1948) (Yong et al., 1992; Appelo and Postma, 1994).*

The distance from the colloid surface within which these ions occur, $1/\kappa$, gives an estimation of the diffuse double layer thickness and is inversely related to the ionic strength I_s as illustrated in the following equation :

$$\frac{1}{\kappa} = \sqrt{\frac{\varepsilon_r \varepsilon_o RT}{2\,(N_a q_e)^2\ 1000\ I}}\ , \tag{1.23}$$

and

$$I_s = 0.5 \sum C_i Z_i^2\ , \tag{1.24}$$

where $1/\kappa$ is referred to as the Debye screening length [m] ;

ε_r is the dielectric constant of the medium (= 80 for water) ;

ε_o vacuum permittivity (= 8.85e12 F/m) ;

R is the gas constant (= 8.314 J mole^{-1} K^{-1}) ;

T is the absolute temperature (= 298 K) ;

N_a is Avogadro's number (= 6e23 mole^{-1}) ;

q_e is the charge of the elecron (= 1.6e-19 C)

C_i the molal concentration in the bulk solution [mole/kg H_2O] ;

Z_i the ion valency.

It is clearly shown with eqns. (1.23) and (1.24) that the diffuse double layer thickness increases when monovalent ions replace divalents ions. In a similar way, decreasing the TEC will cause the diffuse double layer to increase. The thicker the double layer becomes, the greater is the repulsive force between the colloidal particles.

As planar clay particles approach each other, their mutual interaction energy follows roughly the course indicated in figure 1.5. The mutual interaction energy is composed of contributions due to the London-van der Waals' attractive forces and long distance repulsive forces. At very close particle separation distances, Born repulsive forces and hydration forces, resulting from the hydration of particle surfaces and exchangeable cations *(Chen et al., 1987;*

---

[3] The term colloid refers to particles whose widely accepted upper limit size is 1 µm *(Mills et al., 1991).*

Churchman et al., 1993) have to be taken into account. The combination of all these forces will act on the height of the energy barrier. When particles have sufficient kinetic energy to surmount it, they fall into the primary energy minimum where particles are in a flocculated state.

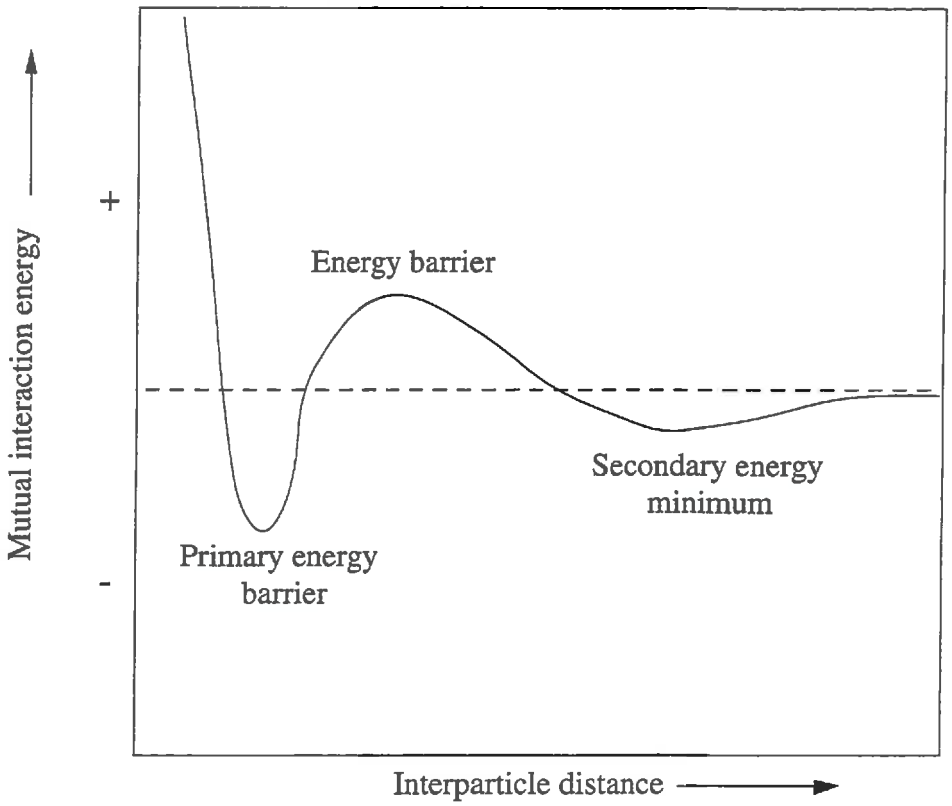

Figure 1.5. Interaction energy vs. interparticle distance *(Chen et al., 1987).*

1.2.1. Swelling and dispersion

Swelling is the moving apart or disjoining of these clay particles until they reach their equilibrium separation or until they fall into the secondary energy minimum. During this process, water is adsorbed and the clay matrix expands in steps corresponding to the degree of hydration of the exchangeable cations *(Norrish, 1954; Chen et al., 1987).* This step-wise swelling, occurring in discrete 2.5-3 Å, is generally referred to as *crystalline* or *limited swelling* and corresponds to the adsorption of the successive water layers in the interplatelet regions. Swelling is a continuous process which increases when the TEC is decreased *(Norrish, 1954; Norrish and Quirk, 1954).* It can be reversed by saturation with K^+.

Saturating with Li^+ or Na^+ results in further swelling. The clay changes from a crystalline solid to a plastic paste in which the swelling is generally termed *osmotic*, *macroscopic* or *extensive*. Extensive swelling becomes particularly appreciable at high SAR values (> 25) *(Shainberg and Caiserman, 1969)* and low TEC. Extensive swelling can be reversed by replacing Na^+ by divalents or by using high electrolyte concentrations *(Churchman et al., 1993)*.

Deflocculation is the moving apart or disjoining particles until they become completely dispersed in the surrounding solution *(Chen et al., 1987)*. Clay dispersion is operative in the entire range of SAR provided that the TEC is below a *Critical Flocculation Concentration* (CFC). The CFC, determined under specified conditions of pH, exchangeable cation composition and suspension concentration, is defined as the minimum electrolyte concentration necessary to flocculate a given colloidal suspension in a given time defined by the authors *(van Olphen, 1977; Goldberg and Glaubig, 1987). Frenkel et al. (1992)* defined the CFC as the total electrolyte concentration required to sediment 80 % of the clay suspension after standing for 24 hours. If the TEC is above the CFC, the repulsive forces are weaker than the attractive forces and clay particles flocculate. These CFC, available in the literature (table 1.2) for reference clays and soil clays containing smectite, were only used as guidelines in order to select relevant TEC and SAR for percolating solutions in our flow experiments (§ 2.6.1).

Table 1.2. Comparison of critical flocculation concentrations (CFC) for reference smectites and soil clays.

Mineral / soil	Saturating cation	pH	SAR/ESP	CFC mmole/l	Source
Smectite	Na	7 8.3 9.5	∞	7-20 28-48 15-68	Arora and Coleman (1979)
Smectite	Ca	7	0	0.25-0.35	Arora and Coleman (1979)
Smectite	Na-Ca	7	15 30	9.6-16.9 18.6-25.3	Arora and Coleman (1979)
Montmorillonite	Na	?	∞	12-16	Oster et al. (1980) van Olphen (1977)
Montmorillonite	Ca	?	0	0.17-0.25	Oster et al. (1980) van Olphen (1977)
Montmorillonite	Na-Ca	7	5 10 20	3 5 6	Oster et al. (1980)
Montmorillonite	Na	6.4 9.4	∞	14 28	Goldberg and Glaubig (1987)
Montmorillonite	Ca	6.1 9.2	0	0.55 0.67	Goldberg and Glaubig (1987)
Montmorillonite	Na-Ca	7	5 ∞	6 26	Goldberg and Forster (1990)
Soil Clays					
Panoche	Na	7 8.3 9.5	∞	7 12 25	Arora and Coleman (1979)
Panoche	Ca	7	0	0.4	Arora and Coleman (1979)
Panoche	Na-Ca	7	15 30 60	5 9 12	Arora and Coleman (1979)
Altamount soil clay (Montmorillonite+illite)	Na-Ca	7	5 ∞	10 210	Goldberg and Forster (1990)

1.2.2. Factors affecting swelling and dispersion

In order to set up the future experimental procedures (§ 2.6), a review of the literature is required, particularly regarding the factors affecting the clay behaviour.

1.2.2.1. Clay mineralogy

Through the literature, authors don't agree on the dispersive behaviour of smectites. On the one hand, smectites are considered to be less dispersive than illites *(Oster et al., 1980; Alperovitch et al., 1985)*. The contrasting behaviour was explained to be due to differences in the shape, size and surface morphology of the crystals of each type. The attractive forces between the thin, flexible smectite particles would be more intimate than between the thick illite particles.

On the other hand, *Velasco-Molina et al. (1971)* showed that smectitic soils released a higher proportion of their clay in the dispersed phase than soils containing illite/kaolinite. The former released 10 % to 20 % of the total clay in weak electrolyte solutions with SAR values ranging from 3 to 12. Smectites are often more concentrated than other minerals in the finest dispersed material *(Churchman et al., 1993)*.

The clay mineralogy was fixed in this study by selecting a material referred to as Béthonvilliers whose clay fraction contained mainly smectite (98 %) (§ 2.3).

1.2.2.2. Layer charge

Swelling of smectites is particularly dependent upon both the magnitude and the location of the layer charge. The lower the charge, the higher the swelling *(Tessier, 1984; Slade and Quirk, 1990)*. Consequently, the amount of water retained by clay particles will increase with a decrease of the layer charge *(Tessier and Pedro, 1987)*.

In this study, the selected smectite is characterized by high layer charge (§ 2.3.3.1). Its swelling will be more restricted if it is compared to the swelling behaviour of e.g. Wyoming bentonite *(Tessier, 1984)*.

1.2.2.3. Nature of the exchangeable cations

The expansion of montmorillonite saturated with polyvalent ions such as Mg^{++}, Ca^{++}, La^{3+} is limited *(Slade and Quirk, 1990)* (eqns. 1.23 and 1.24). This behaviour contrasts drastically with montmorillonite saturated with Na^{+} which exhibits extensive swelling *(e.g. Norrish, 1954)*. Furthermore, if the cations are classified with respect to their promoting dispersive effect, the ranking will be $Na^{+} > K^{+} > Mg^{++} > Ca^{++} > Al^{3+}$ *(Emerson and Bakker, 1973; Levy et al., 1988)*. Consequently, monovalent cations are particularly effective in promoting dispersion whereas divalent and trivalent cations are less prone to induce dispersion. This results in the maintenance of the hydraulic conductivity of the soil. In this study only the effect of Na^{+} and Ca^{++} will be taken into account.

1.2.2.4. Nature of anions

Frenkel et al. (1992) studied the effect of inorganic and organic anions on the dispersive behaviour of clay. The addition of humic acids or other anions influence significantly the dispersive behaviour of clay due to surface charge enhancement *(Shanmuganathan and Oades, 1983)*.

Inasmuch as organic anions seem to be more effective in promoting dispersion that chloride anions, no organic substances were added to the leaching NaCl and $CaCl_2$ solutions because the aim was not to study the effect of wastewater, particularly rich in organic compounds, on the hydrodynamic properties.

1.2.2.5. pH

The pH is a parameter of great importance, especially for the variable charge surfaces which are pH dependent. Increasing the pH will decrease the interactions between oppositely charged surfaces and dispersion will be promoted *(Goldberg and Forster, 1990)*. The effect of the pH is more pronounced for kaolinitic soils *(Gupta et al., 1984; Goldberg and Glaubig, 1987)* than for montmorillonitic soils at all SAR values, due to a greater proportion of pH dependent charge for kaolinite. For example, the CFC of Na-montmorillonite varies from 14 meq/l at pH 6.4 up to 28 meq/l at pH of 9.4 (table 1.2) whereas the CFC of Na-kaolinite ranges from 1 meq/l (pH = 6.2) to 54.6 meq/l (pH = 9.1) *(Goldberg and Glaubig, 1987)*.

1.2.2.6. Organic matter

Organic matter has a stabilizing effect on the aggregates. Swelling is suppressed probably by lowering the specific surface of the clay particles *(Churchman et al., 1993)*. Nevertheless, when present in small quantities, organic matter enhances dispersion *(Goldberg and Glaubig, 1987)*. The addition of organic matter increases the dispersion of soils at high ESP values *(Gupta et al., 1984)*. Adding humic and fulvic acids to sodic montmorillonitic suspensions confirmed it *(Frenkel et al., 1992)*. The dispersive effect of organic matter has been explained by analogy with some anionic dispersants *(Oades, 1984)*. The particular effect of sodium in promoting the dispersive action of organic matter has been explained by its ineffectiveness in acting as a bridging cation *(Varadachari et al., 1991)*. A standard analytical method has been used to detect the presence of organic carbon in the selected material (§ 2.3.2.2).

1.2.2.7. Presence of oxides

The Fe and Al oxides, hydroxides and oxyhydroxides improve the structural stability of the soil and diminishes the dispersion *(Alperovitch et al., 1985; Goldberg and Glaubig, 1987)* by cementing the porous matrix *(Churchman et al., 1993)* or by modifying the charge *(Goldberg and Glaubig, 1987)*. This parameter can be neglected in our study because no oxides were detected.

1.2.2.8. Presence of other weatherable minerals

Weatherable minerals, e.g. $CaCO_3$ and feldspars, supply ions to the soil solution, influencing both swelling and dispersion. Their presence will reduce the sensitivity of soils to sodicity and hence they will be less prone to clay dispersion *(Gupta et al., 1984; Alperovitch et al., 1985; Goldberg and Glaubig, 1987)*. No $CaCO_3$ was detected in the selected soil material. Consequently, this parameter can be neglected in our study.

1.2.2.9. Other parameters

Mechanical disturbance of the soils, including crushing, sieving or centrifugation, affects clay dispersion by increasing the sensitivity to sodicity. The dispersed material might be different in composition from that produced when there is no mechanical disturbance *(Churchman et al., 1993)*. One should also include disturbance of the clay organization by submitting the samples

to various drying and rewetting cycles as it generally occurs during their preparation or saturation *(Tessier, 1984; Tessier et al., 1990).*

Further on, the effect of sodicity on swelling and dispersion is studied on clay suspensions where the ratio soil : solution is low. Results cannot directly be applied to soil systems where these ratios are much more important. The effect of sodicity upon soils is also amplified by the fineness of the texture.

Finally, *Frenkel et al. (1992)* and *Goldberg and Forster (1990)* highlighted the differences between soil clays and reference clays (table 1.2). They concluded that the soil clays are generally more dispersive than their specimen clay counterparts. Their results emphasize the weak quantitative relevance to soils of the physico-chemical investigation of pure clays.

1.3. Conclusions

Considerable attention has been devoted to the effect of salinity and sodicity on clay dispersion and hence on the hydraulic properties of different porous media. Unfortunately, only few studies were carried out under unsaturated conditions. Furthermore, once the hydraulic properties are determined, temporal variability induced by water quality modification is generally not taken into account. It seems evident that in soils affected by salinity, where dispersion and colloidal migration can occur, modifications of the hydrodynamic properties can no longer be ignored.

The introductory part led to the definition of the aim and objectives of this study whose originality consists in the investigation of smectite dispersion and migration in stratified unsaturated flow systems and its effects on the hydrodynamic properties of the original clay-free unsaturated porous media.

This first part summarizes preliminary definitions, such as the water content and density, and those related to the potential energy of soil water. Definitions regarding some parameters related to salinity were added because they will also help the reader in the understanding of the future experimental procedures.

The liquid phase interacts with the components of the soil. Amongst them, the clay fraction, mainly constituted of aluminosilicates, is the most important component because it is the seat of cation exchange, swelling and dispersion. An overview of the literature highlighted the complexity of the interrelationships among the factors contributing to clay dispersion. As proposed by *Sumner (1993)*, an annoted version of the original "threshold concentration" curve *(Quirk and Schofield, 1955)* is presented in figure 1.6. The "threshold concentration" curve corresponds to the combination of TEC and SAR required to produce a 25 % reduction in the HC. Mechanical disturbance of the soil material, the increase of negative charge (increase

of pH, anion adsorption), the presence of smectite or illite, the presence of potassium or/and magnesium, a reduction of the organic content, the absence of oxy-hydroxides result in an increase of the area where dispersion occurs. All these factors will not be taken into account in this study. The selection of one soil material and its chemical characterization will inform us about its dispersive behaviour. This will be discussed in § 2. Furthermore, amongst the ions only Na^+, Ca^{++} and Cl^- will be considered. Finally, the CFC values given in the literature will be used as guidelines to select the combinations of SAR and TEC for the leaching solutions.

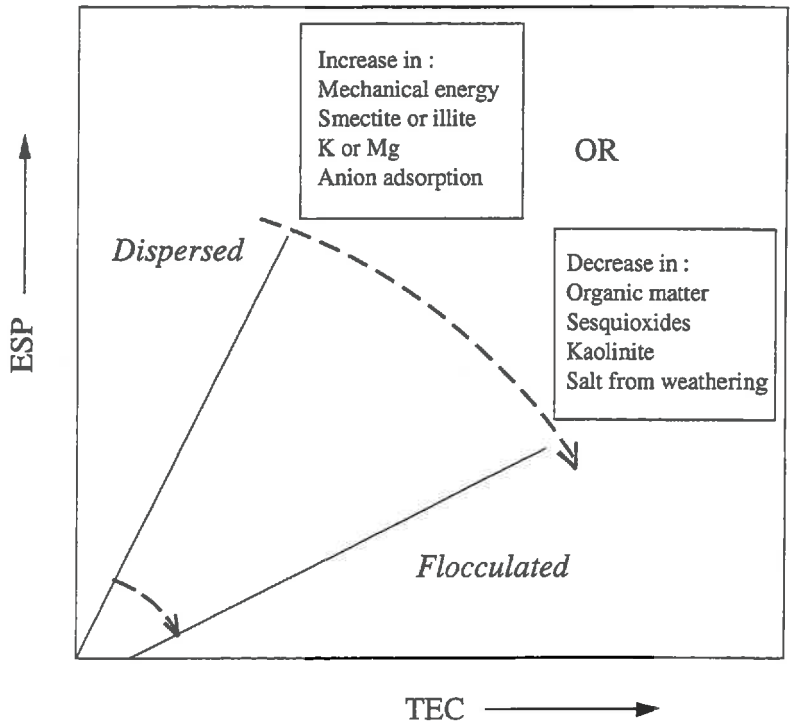

Figure 1.6. Factors affecting the original "threshold concentration" curve proposed by *Quirk and Schofield (1955)* corresponding to the combination of TEC and ESP required to produce a 25 % reduction in the hydraulic conductivity. Changes in these factors will cause the threshold concentration line to shift as indicated by the arrows, increasing the area of dispersed conditions *(from Sumner, 1993)*.

REFERENCES

AIPEA Nomenclature Committee. (1980). Summary of recommendations of AIPEA Nomenclature Committee. *Clays and Clay minerals*, **28**, 73-78.

Alperovitch, N., I. Shainberg, R. Keren, and M.J. Singer. (1985). Effect of clay mineralogy and aluminium and iron oxides on the hydraulic conductivity of clay-sand mixtures. *Clays and Clay Minerals*, **33**, 443-450.

Apello, C.A.J., and D. Postma. (1994). *Geochemistry, Groundwater and Pollution.* A.A. Balkema, Rotterdam, the Netherlands, 536 p.

Arora, H.S., and N.T. Coleman. (1979). The influence of electrolyte concentration on flocculation of clay suspensions. *Soil Science*, **127**, 134-139.

Blackmore, A.V., and R.D. Miller. (1961). Tactoid size and osmotic swelling in calcium montmorillonite. *Soil Science Society of America Journal*, **25**, 169-173.

Bielders, C.L., L.W. De Backer, and B. Delvaux. (1990). Particle density of volcanic soils as measured with a gas pycnometer. *Soil Science Society of America Journal*, **54**, 822-826.

Bresler, E., B.L. Mc Neal, and D.L. Carter. (1982). *Saline and Sodic Soils- Principles-Dynamics - Modelling.* Springer-Verlag, Berlin, 236 p.

Chen, S., P.F. Low, J.H. Cushman, and C.B. Roth. (1987). Organic compound effects on swelling and flocculation of Upton montmorillonite. *Soil Science Society of America Journal*, **51**, 1444-1450.

Churchman, G.J., J.O. Skjemstad, and J.M. Oades. (1993). Influence of clay minerals and organic matter on effects of sodicity on soils. *Australian Journal of Soil Research*, **31**, 779-800.

Derjaguin, B., and L.D. Landau. (1941). *Acta Physicochim*, U.R.S.S, **14**, 635.

Emerson, W.W., and A.C. Bakker. (1973). The comparative effects of exchangeable calcium, magnesium and sodium on some physical properties of aggregates from subsoils of red-brown earths. II. The spontaneous dispersion of aggregates in water. *Australian Journal of Soil Research*, **11**, 151-157.

Frenkel, H., M.V. Fey, and G.J. Levy. (1992). Organic and inorganic anion effects on reference and soil clay critical flocculation concentration. *Soil Science Society of America Journal*, **56**, 1762-1766.

Goldberg, S., and R.A. Glaubig. (1987). Effect of saturating cation, pH, and aluminium and iron oxide on the flocculation of kaolinite and montmorillonite. *Clays and Clay Minerals*, **35**, 220-227.

Goldberg, S., and H.S. Forster. (1990). Flocculation of reference clays and arid-zone soil clays. *Soil Science Society of America Journal*, **54**, 714-718.

Gupta, R.K., D.K. Bhumbla, and I.P. Abrol. (1984). Effect of sodicity, pH, organic matter and calcium carbonate on the dispersion behaviour of soils. *Soil Science,* **137**, 245-251.

Levy, G.J., H.V.V. Van Der Watt, and H.M. Du Plesis. (1988). Effect of sodium-magnesium and sodium-calcium systems on soil hydraulic conductivity and infiltration. *Soil Science*, **146**, 303-310.

Marshall, T.J., and J.W. Holmes. (1979). *Soil Physics*. Cambridge University Press, 345 p.

Mering, J., and A. Oberling. (1971). The smectites. In *The Electron - Optical Investigation of Clays*, Mineralogical Society, London, 135-145.

Mills, W.B., S. Liu, and F.K. Fong. (1991). Literature review and model (COMET) for colloidal/metals transport in porous media. *Groundwater,* **29**, 199-208.

Miyazaki, T., S. Hasegawa, and T. Kasabuchi. (1993). *Water Flow in Soils*. Marcel Dekker Inc., New York, 296 p.

Mualem, Y., (1976). A new model for predicting the hydraulic conductivity of unsaturated porous media. *Water Resources Research*, **12**, 513-522.

Norrish, K. (1954). The swelling of montmorillonite. *Discuss. Faraday Soc.*, **18**, 120-134.

Norrish, K., and J.P. Quirk. (1954). Crystalline swelling of montmorillonite. *Nature*, **173**, 225-256.

Oades, J.M. (1984). Soil organic matter and structural stability : mechanisms and implications for management. *Plant Soil,* **76**, 319-367.

Oster, J.D., I. Shainberg, and J.D. Wood. (1980). Flocculation value and gel structure of sodium/calcium montmorillonite and illite suspensions. *Soil Science Society of America Journal*, **44**, 955-959.

Quirk, J.P., and R.K. Schofield. (1955). The effect of electrolyte concentration on soil permeability. *Journal of Soil Science*, **6**, 163-178.

Quirk, J.P., and L.A.G. Aylmore. (1971). Domains and quasi-crystalline regions in clay systems. *Soil Science Society of America Proceedings*, **35**, 652-654.

Shainberg, I., and O. Otoh. (1968). Size and shape of montmorillonite particles saturated with Na/Ca ions. *Israel Journal of Chemistry*, **6**, 251-259.

Shainberg, I., and A. Caiserman. (1969). Kinetics of the formation and breakdown of Ca-montmorillonite tactoids. *Soil Science Society of America Proceedings*, **33**, 547-551.

Shanmuganathan, R.T., and J.M Oades. (1983). Influence of the anions on dispersion and physical properties of the A horizon of a red brown earth. *Geoderma*, **29**, 257-277.

Slade, P.G., and J.P. Quirk. (1990). The limited crystalline swelling of smectites in $CaCl_2$, $MgCl_2$ and $LaCl_3$ solutions. *Journal of Colloid and Interface Science*, **144**, 18-26.

Sumner, M.E. (1993). Sodic soils : new perspectives. *Australian Journal of Soil Research*, **31**, 683-750.

Tessier, D. (1984). Etude expérimentale de l'organisation des matériaux argileux. Hydratation, gonflement et structuration au cours de la dessication et de la réhumectation. Thèse Université Paris VII, UER des Sciences Physiques de la Terre, 361 p.

Tessier, D., and G. Pedro. (1987). Mineralogical characterization of 2:1 clays in soils : importance of the clay texture : in *Proceedings of the International Clay Conference, Denver, 1985*. Schultz L.G., H. van Olphen, and F.A. Mumpton, eds., The Clay Minerals Society, Bloomington, Indiana, 74-84.

Tessier D., A. Beaumont, and G. Pedro. (1990). Influence of clay mineralogy and rewetting rate on clay microstructure : in *Soil Micromorphology*. Douglas L.A., ed., Elsevier Science Publishers B.V., Amsterdam, the Netherlands, 115-121.

USSL Staff. (1954). *Diagnosis and Improvement of Saline and Alkali Soils*. US Dept. Agric. Handbook 60, 160 p.

van Genuchten, M.Th. (1980). A closed-form equation for predicting the hydraulic conductivity of unsaturated soils. *Soil Science Society of America Journal*, **44**, 892-898.

van Olphen, H. (1977). *An introduction to clay colloid chemistry*. 2nd ed. John Wiley & Sons, New York, 318 p.

Varadachari, C., A.H. Mondal, and K. Ghosh. (1991). Some aspects of clay-humus complexation : effect of exchangeable cations and layer charge. *Soil Science*, **151**, 220-227.

Velasco-Molina, H.A., A.R. Swoboda, and Curtis L. Godfrey. (1971). Dispersion of soils of different mineralogy in relation to sodium adsorption ratio and electrolytic concentration. *Soil Science*, **111**, 282-287.

Verburg K., and P. Baveye. (1994). Hysteresis in the binary exchange of cations on 2:1 clay minerals : A critical review. *Clays and Clay Minerals*, **42**, 207-220.

Verwey, E.J.W., and J.Th.G. Overbeek. (1948). Theory of the stability of lyophobic colloids. Elsevier Science Publishers B.V., Amsterdam, the Netherlands.

Yong, R.N., A.M.O. Mohamed, and B.P. Warkentin. (1992). *Principles of Contaminant Transport in soils*. Elsevier Science Publishers B.V., Amsterdam, the Netherlands, 327 p.

2. Materials and methods

2.1. Introduction

As it has already been mentioned, the main objective of this study is the investigation of smectite dispersion and migration through a two-layered stratified unsaturated porous media, and its consequences on the hydrodynamic properties of the initially clay-free lower sandy layer. The choice concerning the soil material was quite difficult because a smectite rich soil material was required. Amongst the several soil materials initially selected, only one contained a rather pure clay fraction.

The specific experimental device used for the flow experiments is described in details. The methodologies to determine the hydraulic conductivity of the two-layered columns, the non destructive water content and bulk density profiles as well as the amounts of smectite at the end of the percolation period are presented. The determination of the hydrodynamic properties of the lower sandy layer affected by the presence of smectite will be presented separately in § 3.

Leaching solutions required to induce dispersive conditions were chosen based on the literature (table 1.2). Finally, the experimental procedures which were applied to different flow treatments are explained.

2.2. Experimental conditions and assumptions

The main experimental conditions can be summarized as follows :

- experiments are carried out at a laboratory scale, on disturbed stratified columns ;
- smectite dispersion and mobility is investigated in two-layered columns, from an upper clayey layer through an unsaturated sandy porous media ;
- the top layer consists in the raw clayey soil without separation of the sand, the silt or the clay fraction. Clay suspensions or sand-smectite mixtures are voluntarily avoided. The former is generally used to study particle movement in saturated porous media *(Cayeux, 1990)* but is inappropriate for our study, because clay is already dispersed. The use of sand-smectite mixtures could lead to particle segregation during leaching *(Bielders, 1994)* ;
- the stratified porous matrixes are submitted to a constant head by the means of a Mariotte bottle ;
- smectite dispersion and migration is induced by means of salty treatments ;

- the presence of the top clayey layer, which allows to maintain the unsaturated flow condition in the sandy layer, combined to the chemical composition of the leaching solutions, constitutes the upper boundary condition ;
- the top layer is allowed to swell ;
- solute transport through the stratified media is not studied ;
- flow transport through the top layer is not studied ;
- Darcy's law is applicable.

The following assumptions underline the study :

- the effect of the temperature is neglected ;
- the microbiological effects are neglected with the use of gamma-radiation ;
- the flow in the stratified column is assumed to be vertical and unidirectional ;
- the liquid flow is incompressible ;
- the gas phase is continuous and at atmospheric pressure.

2.3. Description of the soil samples

Disturbed soil samples of a vertic soil referred to as Béthonvilliers constituted the upper layer of our experimental columns. They were provided by the National Institute of Agronomy Research (INRA) of Versailles *(Tessier, 1984; Robert et al., 1991)*. The parent bedrock is a weathered glauconic chalk. The main soil properties are summarized in table 2.1. and its physico-chemical characterization is described hereafter. The lower layer of the two-layered stratified experimental columns consisted of a fine textured sand (150-210 µm) which is referred to as the Fontainebleau sand.

Table 2.1. Main soil properties of the Béthonvilliers soil material.

% clay	% silt to loam	% sand	pH_{H2O}(1)	pH_{KCl}(1)	CEC(2) meq/kg	S_0 clay(3) m^2/kg	Mineralogy(4)
65.2	27.8	6.9	7.42	5.61	463	616e3	98 % Sm 1 % K 1 % I

(1) determined for soil : solution ratios of 1 : 5
(2) Cation Exchange Capacity determined at pH = 7 for the soil material
(3) Specific surface determined with EGME
(4) Sm = smectite ; K = kaolinite ; I = illite

2.3.1. Physical characterization of the Béthonvilliers soil material

Physical characterization of Béthonvilliers soil material includes the determination of the particle density, bulk density and particle size analysis. The methodology and results are presented here below.

2.3.1.1. Particle density

Particle density is calculated knowing the mass of the soil material and its volume. The latter was determined on oven-dried samples (48 h - 105°) by the means of an air pycnometer (model 930, Beckman Instruments, Fullerton, CA). The volumetric accuracy claimed by the manufacturer is about 0.05 cm^3. Air-pycnometry measurements revealed highly underestimated volumes and hence overestimated particle densities. *Bielders et al. (1990)* mentioned similar problems on the determination of particle density on volcanic soils when air was used as gas phase. This was assigned to be due to gas adsorption phenomenon and was linearly related to the specific surface. Volume measurements were then performed using helium, a rare gas known to be less adsorbed than air. The vacuum is realized in the pycnometer using a small vacuum pump before introducing helium with an effective pressure of 60 kPa.

The particle density of Béthonvilliers, based on the mean value of four replicates, is equal to 2599 kg/m^3. This value is lower than the particle density mentioned by *Tessier (1984)* (4). One explanation could be found in the experimental procedure which does not allow a complete dehydration of the material, resulting in an underestimation of the particle density.

The absolute error E_a in the estimation of the particle density is given by *(Bielders et al., 1990)* :

$$E_a = \rho_s - \frac{\rho_s}{\left(1 \pm \frac{\rho_s \, A_v}{m_s}\right)}, \qquad (2.1)$$

where ρ_s is the particle density [kg/m^3] ; m_s is the mass of the sample [kg] ; A_v is the volumetric accuracy [m^3]. For ρ_s = 2599 kg/m^3, m_s = 2.5e-2 kg and A_v = 5e-8 m^3, the absolute error equals 13.6 kg/m^3.

(4) *Tessier* (1984) reported a particle density of 2710 kg/m^3. It should be noted that it was obtained from calculation based on the dimensions of the lattice and the structural formula of Bethonvilliers.

2.3.1.2. Bulk density

The bulk density was determined for saturated disturbed soil samples, at an effective pressure of 2 kPa. At saturation, the total volume is then equal to the sum of the water volume and the solid phase volume. The latter is calculated from the weight of the solid phase and the particle density. The bulk density of Béthonvilliers, determined at saturation, is particularly low and equals 580 kg/m^3.

2.3.1.3. Particle size analysis

The texture was determined on disturbed, sieved (< 2 mm) and air dried soil material. Dispersion was achieved by mixing 10 g of soil with sodic resins(5) *(Rouiller et al., 1972; Bartoli et al., 1991)* and ultrasonic waves. Hydrogen peroxide or acid pretreatment to remove respectively the organic matter and carbonates were avoided. These treatments were advantageously replaced by sonication. Particles larger than 50 µm were obtained by sieving. The rate of settling in water (pipette method) was used for the smaller particles. The dispersed soil was washed into a cylinder and made up with water to a known volume. It was stirred into an homogeneous suspension and then allowed to settle. From the amount of soil particles remaining in the suspension at a given depth and after a given settling time, the fraction of soil, with a settling velocity less than the ratio of the depth to the time, was determined *(Marshall and Holmes, 1979)*. Four subdivisions were made for the fraction < 2 µm : 1-2 µm, 0.5-1 µm, 0.2-0.5 µm and < 0.2 µm. (annexe 2.1). The latter fraction is of uttermost importance, because it comprises particles which are the more likely to be mobile. Béthonvilliers contains 65.2 % of clay, with 50.3 % in the fraction < 0.2 µm, 27.8 % of silt to loam, and 6.9 % of sand (table 2.1).

Once the particle size distribution was determined, the remaining clay fraction in the cylinders was collected by successive sedimentations. The dispersed clay suspensions were allowed to settle during 24 hours. The supernatant, which contains the particles of diameter < 2 µm, was siphoned. The height of water in the cylinder was adjusted. The suspension was stirred before it was allowed to settle again. This was repeated till the supernatant was limpid. The clay fraction was flocculated with $CaCl_2$, 1 N. This fraction was used to determine the mineralogy (§ 2.3.3.1), the specific surface area (§ 2.3.3.2) and further, to establish the calibration curves for smectite quantification (§ 2.5.2).

(5) AMBERLITE IR 120 H sodic resin.

2.3.2. Chemical characterization of the Béthonvilliers soil material

Béthonvilliers soil material was chemically characterized using standard methods : the cation exchange capacity, organic carbon and total carbonate content. In addition, the relationship between the sodium adsorption ratio (SAR) and the exchangeable sodium percentage (ESP) has been established for Béthonvilliers soil material.

2.3.2.1. Cation exchange capacity

The cation exchange capacity (CEC) is a measure of the quantity of readily exchangeable cations (K^+, Na^+, Ca^{++}, Mg^{++}) neutralising the negative charges in the soil. It was determined by treatment of disturbed, sieved (< 2 mm) samples with ammonium acetate buffered at pH = 7, followed by washing with denatured ethanol in order to be free of excess saturating salt. The exchangeable cations are measured by the means of the atomic absorption spectrometer(6). Adsorbed ammonium is displaced by KCl 1 N at pH = 3 and quantified by distillation and titration.

Béthonvilliers is characterized by a CEC of 46.3 meq/100 g and is mainly saturated with Ca^{++}. The ratio of exchangeable Ca^{++} to the sum of cations equals 94.5 %. Exchangeable Mg^{++} and K^+ represent respectively 3 % and 1.8 %. Exchangeable sodium only represents 0.7 %. From this analysis, it is concluded that some problems could occur to induce clay dispersion due to the presence of mostly divalent cations.

2.3.2.2. Organic carbon

Organic carbon has been determined using the Walkley and Black wet oxidation by the means of $K_2Cr_2O_7$, 1 N under acid conditions *(Walkley and Black, 1934)*. Oxygen is released from this reaction allowing the oxidation of the organic carbon. The remaining $K_2Cr_2O_7$ is titrated. Using this method, no organic carbon was detected in Béthonvilliers soil material.

(6) SpectrAA - 300 Varian.

2.3.2.3. SAR-ESP relationship for the Béthonvilliers soil material

The ESP of a soil can be estimated from the SAR of the leaching solution if the soil is assumed to be at equilibrium with the latter. If the leaching solution SAR is higher (lower) than that of the original soil solution, the ESP will increase (decrease) *(Chen and Banin, 1975)*. Because the procedure required to obtain ESPs at equilibrium with the solution SAR is quite time-consuming, it was preferred to mix sodic and calcic soil together following an experimental relationship ESP-SAR established for Béthonvilliers soil.

Solutions of SAR = 5, 10 and 20 were used with TEC of 10 meq/l and 1 meq/l. The relationship was established for a soil : solution ratio of 1 : 10. Small quantities (3 g) of air-dried, sieved (< 2 mm) Béthonvilliers soil were shaken with 30 ml solution of a given SAR and TEC in centrifuge tubes. Each SAR-ESP combination was duplicated. After centrifugation, the SAR of the supernatant was measured. Equilibrium was reached for solution of TEC = 10 meq/l (SAR = 5 ; SAR = 10). Problems occurred with the more diluted solutions, as equilibrium has never been reached in spite of the important number of shakings and centrifugations. Nevertheless, these results were used even if the SAR values of the supernatants were far below those of the initial solutions.

Once the SAR was determined, the ESP was measured. The masses of wet soil and dry soil (48 h - 105°C) were weighted respectively at "equilibrium" and after the exchangeable cations were displaced with NH_4Cl 1 N (6 x 25 ml). The difference allowed the volume of entrapped solution to be calculated. The total amount of cations (Ca^{++} and Na^{+}) was measured by the means of the atomic absorption spectrometer. Combined to the knowledge of the volume of entrapped solution and its chemical composition at "equilibrium", the ESP was calculated.

Based on the SAR value of the leaching solution, the ESP is determined as follows :

$$ESP = 2.8375\ SAR - 2.6243. \quad (r = 0.994) \qquad (2.2)$$

Results are given in figure 2.1. Eqn. (2.2) differs from the relationships proposed by the *USSL Staff (1954)* or *Rengasamy et al.(1984)*. These differences could be partly due to the soil : solution ratios. The USSL equation holds for saturated pastes whereas the latter holds for more dilute extracts. Further, the use of low electrolyte concentrations and mechanical disturbance during the procedure could enhance these differences.

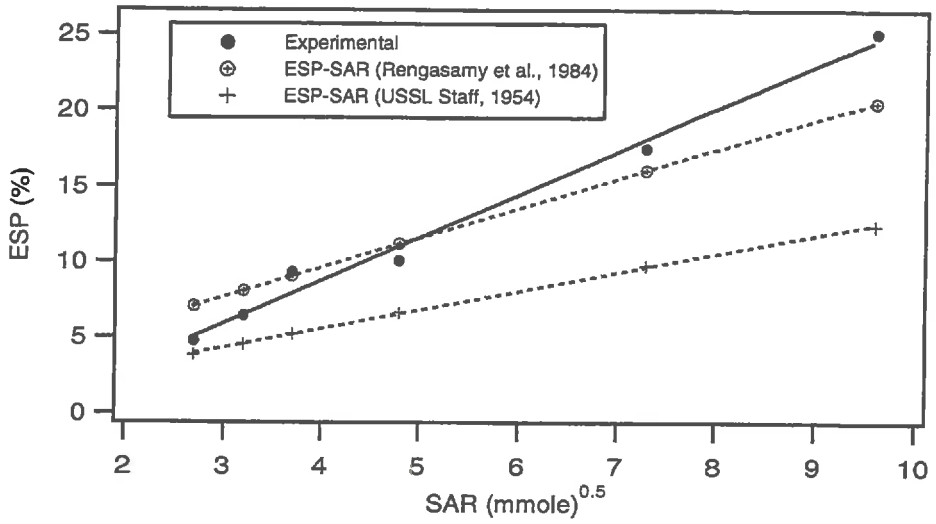

Figure 2.1. Experimental relationship between the exchangeable sodium percentage (ESP) and sodium adsorption ratio (SAR) established with total electrolyte concentrations (TEC) of 1 and 10 meq/l for Béthonvilliers soil material.

Only part of the centrifuge tubes were used to establish the experimental ESP-SAR relationship. The remaining tubes were used to determine a dispersability index for the Béthonvilliers soil. The Index of Dispersion (ID) is defined by the ratio of particles in the range < 0.2 µm to the total clay fraction (< 2 µm). It will give a general idea of the maximum amount of clay that will be dispersed under specified conditions of SAR, TEC and mechanical disturbance. Hence, one knows the amount of clay which can be expected to migrate. Clay in the smallest fraction was quantified by repeated centrifugations (4000 rpm - 10 minutes) until the supernatant was limpid. Results are given in figure 2.2. As it has already been discussed, equilibrium was obtained only for solutions of SAR = 5 and 10 and TEC of 10 meq/l. For higher SAR values or lower TEC, the SAR of the supernatants were lower than that of the original solution and ranged from 2.6 to 4.8. Consequently, the indexes of dispersion are underestimated. It can be seen (figure 2.2) that no dispersion occurs with an "equilibrium" SAR of 3.9 and TEC = 10 meq/l. The ID increases with an increasing SAR value, i.e. 16.7 % and 36.4 % for "equilibrium" SARs of 7.2 and 9.8, respectively. For low SAR values and low TEC (1 meq/l), the ID ranged from 19.4 % up to 29.3 %. Therefore, clay is expected to disperse and eventually to migrate within the limits of our SAR and TEC treatments (§ 2.6.1).

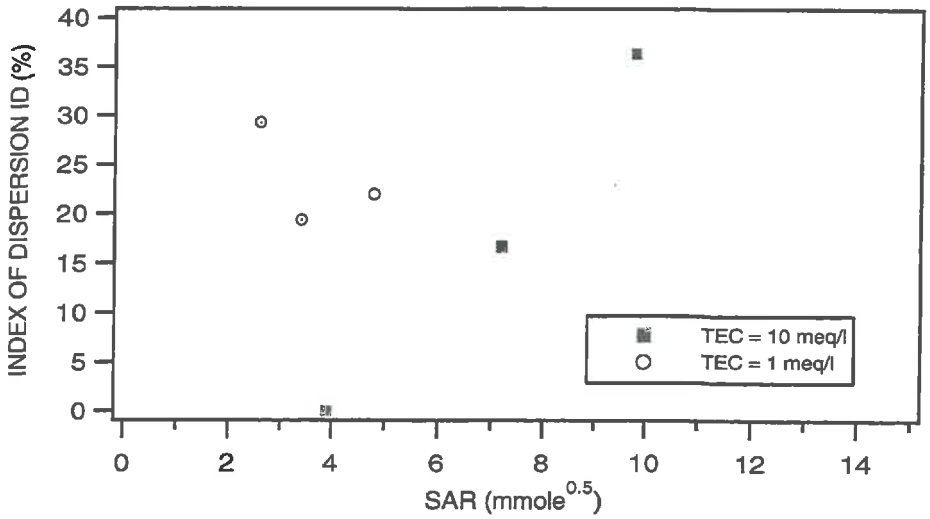

Figure 2.2. Index of dispersion (ID), given by the ratio of particles < 0.2 µm to the total clay fraction of Béthonvilliers soil material, as a function of the "equilibrium" SARs and TECs.

2.3.3. Characterization of the Béthonvilliers clay fraction

Mineralogical composition of the Béthonvilliers clay fraction has been determined qualitatively and quantitatively. The specific surface has been measured using ethylene glycol monoethyl ether adsorption.

2.3.3.1. Clay mineralogical composition

Clay mineralogy was determined qualitatively by X-ray diffraction analysis(7), using a Cu-Kα ray (Ni filter). Oriented clay samples were prepared by saturating the clay fraction either with KCl or $MgCl_2$ 1 N. A small amount of the suspension is then placed on a glass plate and is allowed to dry. The Mg-saturated and K-saturated samples were submitted to standard treatments i.e. air-dry and ethylene glycol monoethyl ether treatment (16 h) for the former ; air-dry, 300°C (4 h) and 550°C (4 h) for the latter.

(7) PHILPS PW 1349/30 diffractometer - X-Ray generator PHILIPS PW 1130/00/60.

From the analysis, it was concluded that Béthonvilliers contained kaolinite, illite and smectite. A quantitative X-ray diffraction was required[8] in order to quantify the fraction of smectite compared to the illite and kaolinite fraction. Béthonvilliers contained mainly smectite (98 %). This will avoid X-ray diffraction to be used for the dispersed clay in the experimental columns after leaching.

Furthermore, *Tessier, (1984)* mentioned a layer charge per formula unit equal to 0.6 with a tetrahedral layer charge of 0.18 and an octahedral charge of 0.40. As it has been mentioned before (§ 1.2.2.2), swelling is directly related to the layer charge. The lower the layer charge is, the higher the swelling will be.

2.3.3.2. Specific surface area

The specific surface area was measured by a gravimetric method using ethylene glycol monoethyl ether (EGME) *(Dyal and Hendricks, 1950)* and a sodic Camp Berteau as reference clay (S_o = 750e3 m^2/kg). The measured surface implies the formation of a monomolecular film and corresponds to the measurement of the total basal surface *(Tessier, 1984)*. The specific surface area of Béthonvilliers clay fraction equals 616e3 m^2/kg, and its high value is directly related to the smectite content. This value will be used for the calculation of the theoretical soil moisture retention curves for mixtures composed of smectite and Fontainebleau sand (§ 3).

2.3.4. Characterization of the Fontainebleau sand

The Fontainebleau sand has been chosen for its narrow particle range (150-210 µm) and its common use in percolation studies *(Martins, 1993; Novy Quadri, 1993)*. Based on their soil moisture retention curve (figure 2.3) established under draining conditions, an unsaturated water content profile can be obtained in a sandy layer of 60 cm height without any suction at the bottom of the sandy layer. If the length of the lower layer is decreased, suction has to be increased in order to generate an equivalent water content profile. An acceptable compromise was obtained with a sandy layer of 28.5 cm height and a suction of 25 cm (2.5 kPa), resulting in volumetric water contents ranging from saturation (32 %) at the bottom to approximately 10 % in the upper part of the experimental column.

---

(8) The quantitative X-ray diffraction has been performed by the laboratory of geology and mineralogy, at the Catholic University of Louvain, Belgium, using a sequential X-ray spectrometer (SRS 3000 - Siemens).

The Fontainebleau sand is washed with acid and has a specific surface of 19 m^2/kg. The mass spectrometer analysis reveals 340 mg/kg Al and 70 mg/kg Fe in the form of amorphous oxides and hydroxides *(Novy Quadri, 1993)*. The bulk density varies from 1647 kg/m^3 to 1691 kg/m^3, depending on the filling of the experimental columns. The particle density is approximately equal to 2650 kg/m^3.

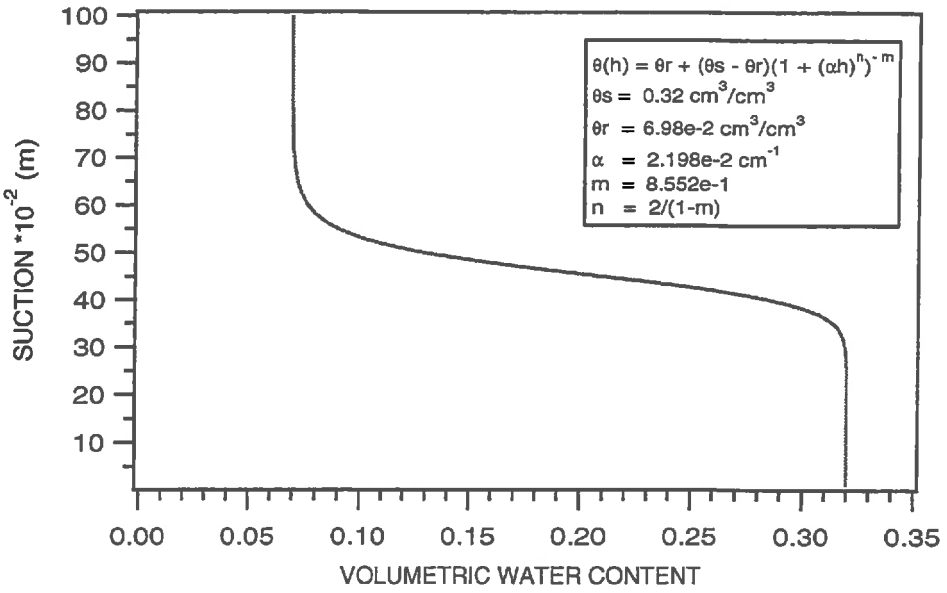

Figure 2.3. Soil moisture retention curve established for Fontainebleau sand under draining conditions *(Martins, 1993)*.

2.4. Description of the experimental device

A specific experimental device was developed for the flow experiments due to some constraints, i.e. an easy recovery of the soil samples at the end of the percolation period (§ 2.4.1). The equipment will be described before discussing the measurements of the total hydraulic conductivity (§ 2.4.2) and the water content - bulk density profiles (§ 2.4.3). An indirect method (§ 2.5) was used to quantify dispersed smectite within the sandy subsamples, because the clay amount was too small to be determined by a standard particle size analysis. Finally, the experimental leaching procedures will be presented in detail in § 2.6.

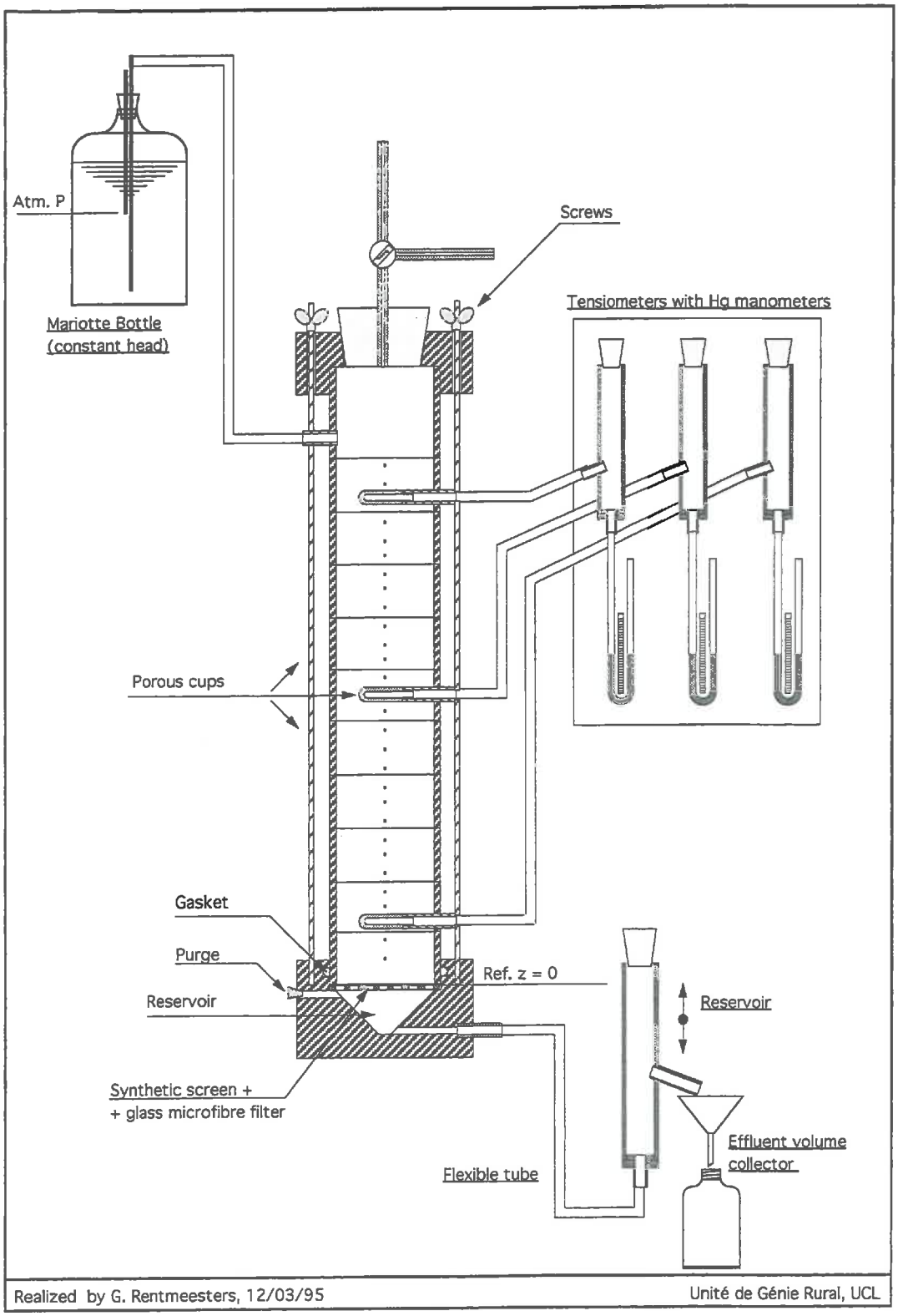

Figure 2.4. Experimental device

2.4.1. General description

The columns were constructed with 10 small transparent PVC cylinders (5.7 cm inside diameter, 3 cm length) tightly joined to each other by the means of two long screws and bolts (figure 2.4 and annexes 2.2 through 2.4). Small holes separated from each other every centimetre are made in the cylinders allowing the gas phase to remain at atmospheric pressure during leaching (§ 2.2). Each column was equipped with three tensiometers connected to mercury manometers allowing for the measurement of the hydrostatic and hence the hydraulic heads. The column was placed on top of a reservoir, covered with a rigid synthetic screen and a glass microfibre filter(9) to support the column. A purge avoided the entrapment of gas bubbles below the rigid screen. The reservoir was connected to an outer mobile reservoir by means of a flexible tube enabling the control of the suction at the lower end of the column and, hence, the desaturation of the porous matrix. At the outlet of the mobile reservoir, small bottles allowed to collect the effluent volumes.

A constant head was applied by the means of a Mariotte bottle. Total hydraulic measurements were performed daily using the falling head method for 8 to 10 weeks (§ 2.4.2). In between the conductivity measurements, the head was kept constant at the top of the column.

The water content and bulk density profiles were measured by gamma-radiation (§ 2.4.3). Two radioactive sources (^{137}Cs- 406 mCi or 15 GBq - ^{241}Am - 200 mCi or 7.4 GBq) were placed in a cross position, following the study of *Stroosnijder and De Swart (1974)*, on a mobile frame which moved in an upward or downward direction along the column.

2.4.2. Measurement of the total hydraulic conductivity : the falling head method

The hydraulic conductivity (HC) of the stratified column was measured using the falling head method, more appropriate for low HC values. In this method (figure 2.5), the upper water level is allowed to fall. The fall of the hydraulic head dH in the small tube above the soil material is related to the flux density of solution q through it within a given time dt according to :

$$- A_1 \, dH = A_2 \, q \, dt, \qquad (2.3)$$

(9) Whatman GF/A glass microfibre filters are characterised by high infiltration rates. Solid particles of diameter > 1.6 µm are retained.

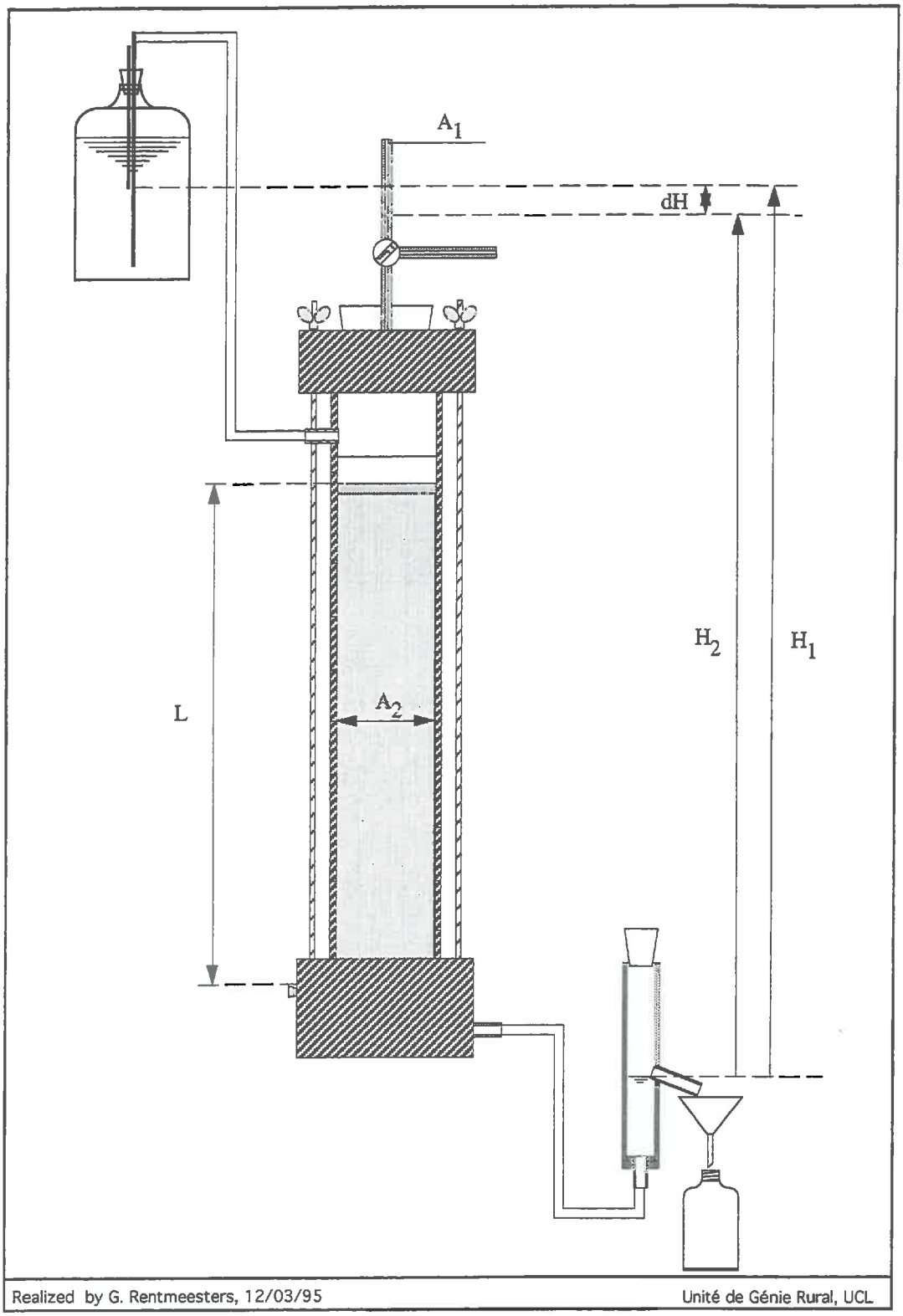

Figure 2.5. Meaning of the terms required to calculate the total hydraulic conductivity of the two-layered experimental columns using the falling head method (eqn. 2.5).

where A_1 and A_2 are respectively the cross-sectional areas of the small tube and the soil column. Substituting the flux density given by eqn. (1.19) into eqn. (2.3) results in :

$$\frac{A_1\ L}{A_2\ K_T} \int_{H_1}^{H_2} \frac{dH}{H} = \int_0^t dt\ . \tag{2.4}$$

Integrating and rearranging the terms gives :

$$K_T = \frac{A_1\ L}{A_2\ t} \ln\left(\frac{H_1}{H_2}\right). \tag{2.5}$$

Eqn. (2.5) was used to determine the total hydraulic conductivity K_T for the stratified experimental columns, where H_1 and H_2 are the initial and the final hydraulic head, respectively, and L is the height of the soil column. The latter is the sum of the unsaturated sandy layer thickness and the upper Béthonvilliers layer whose thickness was expected to vary with the SAR and TEC of the leaching solution. Consequently, it was measured approximately every two days during 8 to 10 weeks.

2.4.3. Measurement of the water content and bulk density profiles

Simultaneous and non-destructive measurements of the bulk density and volumetric water content in the columns were obtained by the means of two radioactive sources. The dual energy gamma beam attenuation method has proven to be a powerful technique for studying water redistribution in swelling soils *(Corey et al., 1971; Nofziger and Swartzendruber, 1974; Stroosnijder and De Swart, 1974)*. The apparatus used is quite identical to that of *Stroosnijder and De Swart (1974)*. Calibration requirements and the determination of the mass attenuation coefficients are indubitably the most important steps. Furthermore, accurate water contents and bulk densities cannot be obtained without corrections for the dead time and the Compton scatter. Finally, the accuracy on the measurements of the water content and density will be assessed.

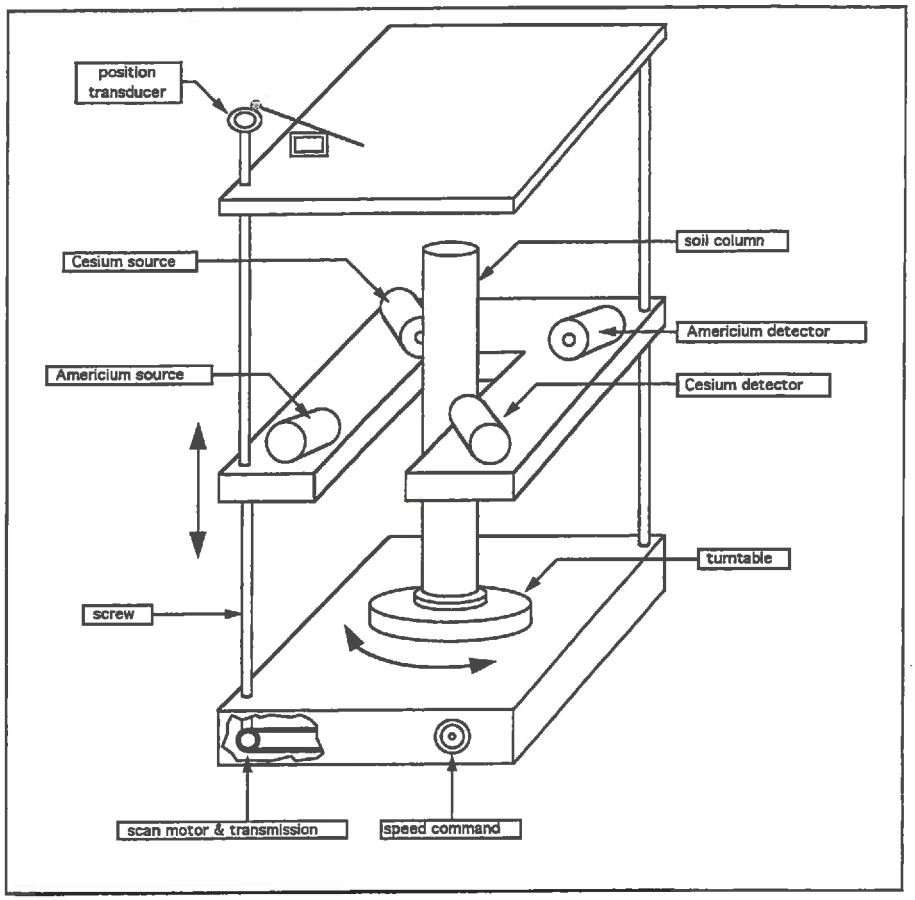

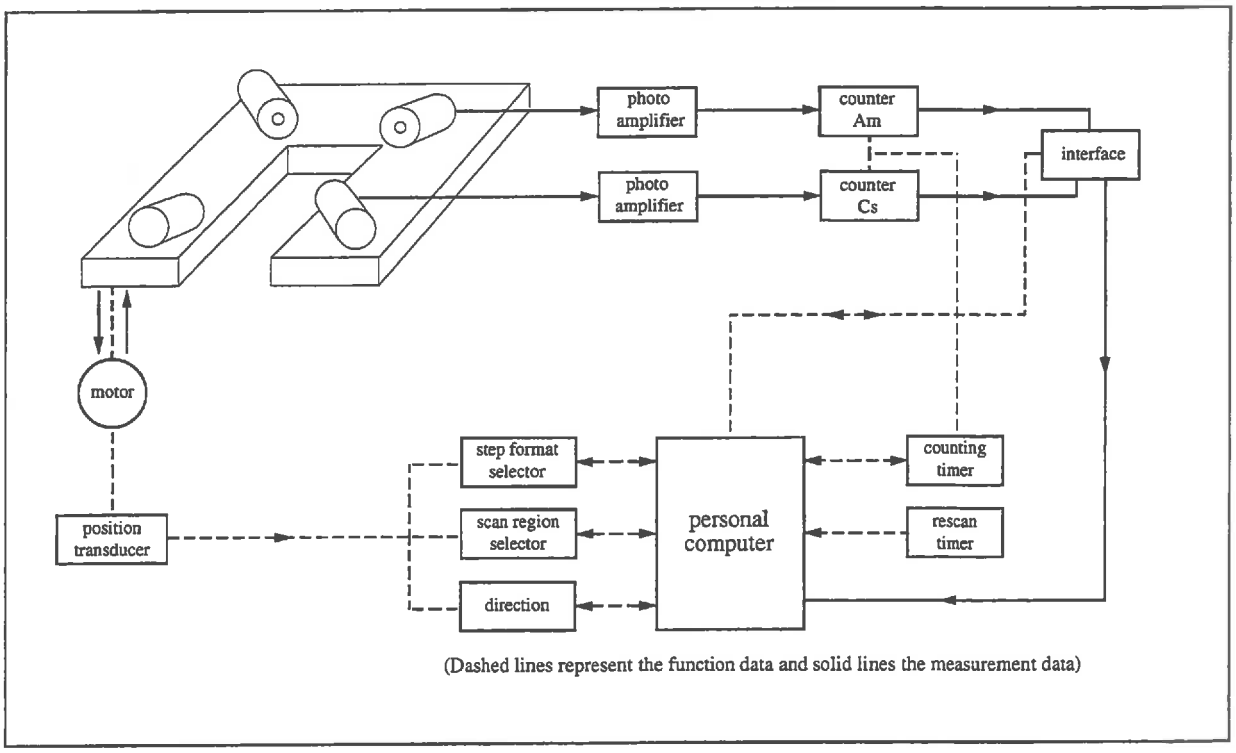

Figure 2.6. General presentation of the gamma-radiation equipment.

2.4.3.1. Apparatus

The two radioactive sources (^{137}Cs- 406 mCi or 15 GBq - ^{241}Am - 200 mCi or 7.4 GBq) and detectors are placed at fixed cross positions on a moveable platform. The ^{137}Cs source is imbedded in a steel cylinder surrounded by a 5 cm thickness lead shield, totalling a quantity of 250 kg lead. The beam is collimated to approximately 5 mm.

The scintillation probe consists of a Thallium-activated sodium iodide crystal connected in series with a photomultiplier, energized with a high-voltage power supply, and a preamplifier. This is in connection with a amplifier-discriminator and an individual counter. The two counters are slaved together in order to start and stop simultaneously. The counting rates are then automatically transferred to a personal Macintosh computer (figure 2.6).

The platform is mobile in the vertical direction by the means of four screw spills driven by a same motor. The speed is operated by a hand-turned gear mechanism. The measurements are realized stepwise either in the downward or upward direction. The step size is controlled by a position-transducer mounted on top of the apparatus. The minimum step size is 0.1 cm, but measurements were realized with step sizes of 1 cm. The direction and the step can be chosen by the user from its personal computer. The column is installed on a turntable and is rotated during measurements, allowing to measure average water contents and bulk densities at a given height.

The repetitiveness of the platform position depends on its speed of mobility. With a movement of 1 cm/minute, the mobile frame is repositioned with an accuracy of about 0.25 mm. The maximum cumulative error on the total displacement is about 1 %.

2.4.3.2. Attenuation equations

The basic attenuation equation is given by Beer's law :

$$\left(\frac{N}{N_o}\right) = \exp\left(-\mu_s \rho_b x_s - \mu_w \rho_w \theta_v x_s\right), \qquad (2.6)$$

where N is the total corrected gamma count through soil ;
N_o is the total corrected gamma count through an empty column ;
x_s is the uniform thickness of the soil material [m] ;
ρ_b is the dry bulk density [kg/m^3] ;
ρ_w is the density of water (= 1000 kg/m^3) ;
μ_s is the mass attenuation coefficient of the soil [m^2/kg] ;
μ_w is the mass attenuation coefficient of water [m^2/kg].

Accurate water contents and bulk densities can be obtained provided that the recorded ^{241}Am and ^{137}Cs count rates are corrected to yield the true count rates. The main corrections are the dead time and the ^{137}Cs interference in the low energy band of ^{241}Am, also referred to as the Compton scatter.

2.4.3.3. ^{137}Cs interference in the low-energy band

When a percentage of the ^{137}Cs gamma rays (662 keV) is scattered, pulses equivalent to lower energy gamma rays are produced *(Goit et al., 1978)* and are able to be recorded by the ^{241}Am detector. As mentioned by *Stroosnijder and De Swart (1974)*, cross-positioned sources minimizes the ^{137}Cs influence on the ^{241}Am detector. In their study, a fixed correction on the ^{241}Am count rate of about 10 counts per second (cps) was used. Nevertheless, it was important to verify it for the present experimental device.

Nofziger and Swartzendruber (1974) further concluded that the Compton scatter was independent of the sample material placed in the γ-ray beam and that it could be expressed with good accuracy using the following equation :

$$c = A + BI_r + CI_r^2 + DI_r^3, \tag{2.7}$$

where c represents the Compton scatter [cps] ;

$I_r = N_r/t$ is the recorded count rate without any correction [cps] ;
with t the counting time [s] ;

A, B, C, D are constants.

The determination of the above mentioned constants is given in annexe 2.5. From this study, it is concluded that for count rates ranging from 2500 cps and 3500 cps which envelop the encountered experimental values through sandy unsaturated columns, corrections due to ^{137}Cs interference on ^{241}Am detector are of about 65 - 70 cps. The corrections are higher than that proposed by *Nofziger and Swartzendruber (1974)* but remains, nevertheless, relatively small (2 - 2.4 %).

2.4.3.4. Dead time correction

The dead time of a counting system can be defined as the minimum amount of time to separate two events in order to be recorded as two separated pulses. Because of the random nature of radioactive decay, there is always some probability that a true event will be lost because it

occurs too quickly after the preceding event. The most familiar equation is the nonparalysable model *(Nofziger and Swartzendruber, 1974; Stroosnijder and De Swart, 1974)* which assumes that a fixed dead time follows each true event. The fraction of all time that the detector is dead is given by the product of the recorded count rate I_r and the dead time τ. The rate at which true events are lost is given by :

$$I - I_r = I\,(I_r\tau). \tag{2.8}$$

Solving it for I yields :

$$I = \frac{I_r}{1 - I_r\tau}\,. \tag{2.9}$$

The use of eqn. (2.9) is valid both in the high-energy range and in the low-energy range, provided that for the latter the ^{137}Cs source is closed.

The dead times are determined independently for each counting system. Firstly, based on Beer's law, the true count rate is related exponentially to the linear attenuation coefficient of an absorbing material of given thickness :

$$\left(\frac{N}{N_o}\right) = \exp\left(-\mu_l x\right)\,, \tag{2.10}$$

where N is the total corrected gamma count through the absorbing material ;
N_o is the total corrected gamma count through air ;
x is the uniform thickness of the absorbing material [m] ;
μ_l is the linear attenuation coefficient of the absorbing material, product of the mass attenuation coefficient and the density [1/m].

A relatively reliable linear attenuation coefficient can be obtained by plotting the logarithm of the recorded countings $\ln(N_r)$, instead of the corrected ones, versus the material thickness. For the high energy-range band, flat plates of lead were used, allowing to vary the thickness from 0.1 cm up to 1.6 cm. In the low-energy band, due to the low recorded count rates, plexiglass was used (from 0.795 cm up to 3.975 cm). Once the linear attenuation coefficient is determined, the dead time can be calculated following eqn. (2.9). Combining eqn. (2.9) and eqn. (2.10) yields :

$$\frac{I_r}{1 - I_r\tau} = I_o \exp\left(-\mu_l x\right)\,, \tag{2.11}$$

and finally :

$$I_r \exp\left(\mu_l x\right) = I_o - I_o I_r \tau\,. \tag{2.12}$$

Plotting the term on the left-hand side versus the recorded count rate I_r will give a straight line whose negative slope is equal to $(I_o\tau)$. By extrapolation for $x = 0$, the corrected count rate through air I_o is obtained.

The dead time for the ^{137}Cs measurement system equals 106 µs/count, whereas that of the ^{241}Am equals 23.3 µs/count. This is particularly important for ^{137}Cs because of the high count rates and the great dead time value. It means that for count rates ranging from 2500 cps to 3500 cps, the corrected count rates vary from 3400 cps to 5560. Depending on the water content and the bulk density in the columns, 900 cps up to 2060 cps are lost.

2.4.3.5. Attenuation coefficients

The use of eqn. (2.6), written for the ^{137}Cs and the ^{241}Am sources, requires the knowledge of the mass attenuation coefficients which were calculated as follows :

$$\mu_s = \frac{-\ln\left(\overline{N}_o/\overline{N}_s\right)}{\rho_b x_s}, \tag{2.13}$$

$$\mu_w = \frac{-\ln\left(\overline{N}_o/\overline{N}_w\right)}{\rho_w x_w}, \tag{2.14}$$

where $\overline{N}_o$, $\overline{N}_w$, $\overline{N}_s$ are the corrected mean values of 248 countings through an empty column, through a column filled with water and through a column filled with sand, respectively. In the high-energy band, ^{137}Cs count rates were corrected for the dead time using eqn. (2.9). The ^{241}Am count rates were corrected using :

$$I_{Am} = \frac{\left(I_{r_{Am}} - c\right)}{1 - \left(I_{r_{Am}} - c\right)\tau_{Am}}, \tag{2.15}$$

because the Compton scatter has to be taken into account *(Nofziger and Swartzendruber, 1974)*. The following mass attenuation coefficients were obtained and employed during series I flow experiments :

$\mu_{s_{Cs}}$ = 6.71e-3 m²/kg ; $\mu_{w_{Cs}}$ = 9.59e-3 m²/kg ;
$\mu_{s_{Am}}$ = 2.35e-2 m²/kg ; $\mu_{w_{Am}}$ = 1.98e-2 m²/kg.

The values of the attenuation coefficients were verified before the series II flow experiments were launched. Changes were feared because between these two series, the apparatus was switched off. The coefficients for water remained identical, but those concerning the Fontainebleau sand changed, and the following values were obtained :

$$\mu_{s_{Cs}} = 6.95\text{e-}3 \text{ m}^2/\text{kg} ;$$
$$\mu_{s_{Am}} = 2.60\text{e-}2 \text{ m}^2/\text{kg}.$$

2.4.3.6. Calculation of the volumetric water content and bulk density

The volumetric water content and bulk density can be calculated directly using eqn. (2.6) applied to ^{137}Cs and ^{241}Am countings. Nevertheless, as it had been mentioned by *Bruckler (1983)*, double scrutation gives a better theoretical solution. However, the calculated error on the estimation of the water content and density is considerably increased, due to the increased number of terms.

The general calculation of the water content and bulk density takes as reference count rates through air or through an empty column. Adding countings obtained for dry experimental columns allows the basic equations to be modified. This further results in a smaller total calculated error (§ 2.4.3.7). Firstly, the water content is calculated as follows :

$$\theta_v = \frac{-\ln\left(N_{ws}/N_{ds}\right)_{Cs}}{\mu_{w_{Cs}} x_s \rho_w}, \tag{2.16}$$

where N_{ws} and N_{ds} are respectively the total corrected ^{137}Cs countings for the wet and the dry soil column. The ^{137}Cs countings were preferred to those of ^{241}Am which has much lower mass attenuation coefficient values. It should be noted that the measured water contents correspond to both capillary water and water retained by dispersed clay particles. It is assumed that this will not affect the value of $\mu_{w_{Cs}}$. This seems quite reasonable if one considers the study of *Goit et al. (1978)* in which a single mass attenuation coefficient was used both for water and ice.

The bulk density is then calculated using the ^{241}Am countings with the following equation :

$$\rho_b = \frac{\ln\left(N_o/N_{ws}\right)_{Am} - \mu_{w_{Am}} \theta_v x_s \rho_w}{\mu_{s_{Am}} x_s}. \tag{2.17}$$

Table 2.2. Overview of the terms required to calculate the volumetric water content error. Values given for the variances of some terms are originated from *Bruckler (1978).*

Variable X_i	Units	$(\partial G/\partial x_i)^2$	σ_i^2
$(N_{ws})_{Cs}$	-	$\left(\mu_{w_{Cs}} x_s (N_{ws})_{Cs} \rho_w\right)^{-2}$	$(N_{ws})_{Cs}$
$(N_{ds})_{Cs}$	-	$\left(\mu_{w_{Cs}} x_s (N_{ds})_{Cs} \rho_w\right)^{-2}$	$(N_{ds})_{Cs}$
$\mu_{w_{Cs}}$	m^2/kg	$\left(\theta_v/\mu_{w_{Cs}}\right)^2$	$\sigma^2_{\mu_{w_{Cs}}}$ = 1e-8
x_s	m	$\left(\theta_v/x_s\right)^2$	$\sigma^2_{x_s}$ = 1e-8

Table 2.3. Overview of the terms required to calculate the bulk density error. Values given for the variances of some terms are originated from *Bruckler (1978).*

Variable X_i.	Units	$(\partial G/\partial x_i)^2$	σ_i^2
$(N_o)_{Am}$	-	$\left(\mu_{s_{Am}} x_s (N_o)_{Am}\right)^{-2}$	$(N_o)_{Am}$
$(N_{ws})_{Am}$	-	$\left(\mu_{s_{Am}} x_s (N_{ws})_{Am}\right)^{-2}$	$(N_{ws})_{Am}$
$\mu_{w_{Am}}$	m^2/kg	$\left(\rho_w \theta_v/\mu_{s_{Am}}\right)^2$	$\sigma^2_{\mu_{w_{Am}}}$ = 1e-8
$\mu_{s_{Am}}$	m^2/kg	$\left(\rho_b/\mu_{s_{Am}}\right)^2$	$\sigma^2_{\mu_{s_{Am}}}$ = 1e-8
θ_v	m^3/m^3	$\left(\mu_{w_{Am}} \rho_w/\mu_{s_{Am}}\right)^2$	$\sigma^2_{\theta_v}$
x_s	m	$(1/x_s)^2\left(\rho_b + \mu_{w_{Am}} \theta_v \rho_w/\mu_{s_{Am}}\right)^2$	$\sigma^2_{x_s}$ = 1e-8

In eqn. (2.17), it is assumed that the presence of small clay amounts has a negligible effect on the mass attenuation coefficient of the soil sample. Measurements are realized with counting times of 60 seconds.

2.4.3.7. Assessment of the error on the water content and bulk density measurements

Let $Y = G(X_1, X_2, ..., X_n)$ be a function of n independent random variables X_i. The total variance σ_Y^2 can then be estimated, assuming that all the derivatives exist, by *(Meyer, 1978)*:

$$\sigma_Z^2 \approx \sum_{i=1}^{n} \left(\frac{\partial G}{\partial x_i} \right)^2 \sigma_i^2 . \qquad (2.18)$$

The number of terms for the determination of the error on θ_v equals 4, i.e. N_{ws}, N_{ds}, $\mu_{w_{Cs}}$, and x_s. For the error on ρ_b, the number of terms equals 6, i.e. N_o, N_{ws}, $\mu_{w_{Am}}$, $\mu_{s_{Am}}$, θ_v, and x_s. The water density is not taken into account because it is not a random variable. The terms relative to the countings constitute a minimal error linked to the random nature of the process. The remaining terms constitute a residual error *(Bruckler, 1983)*. The expression of each second partial derivative and variance corresponding to the variable taken into account are given in tables 2.2 and 2.3.

It can be seen that both errors increase with the water content. The major part of the total error is linked to the random nature of the process (table 2.4) which can be reduced by increasing the counting time. Inasmuch as the counting time equals 60 seconds, the random error represents more than 70 % of the total error. The standard deviation on the calculation of the water content is less than 1 % (< 8e-3 m^3/m^3 for 30 second counting times, and less than 6e-3 m^3/m^3 when countings are recorded for 60 seconds).

The total error on the bulk density is less influenced by the random nature of the process (table 2.5). For countings recorded during 30 s, half of the error is explained by the residual error. When the counting time is doubled, the error due to the random nature is decreased twofold whereas the residual error is less reduced. Consequently, approximately 40 % of the total error is linked to the randomness and 60 % to the residual error. For a bulk density of 1600 kg/m^3, the standard deviation ranges from 10.5 kg/m^3 to 14.1 kg/m^3, depending on the water content and the counting time, thus corresponding to less than 1 % of the value.

Table 2.4. Composition of the error on the calculation of the volumetric water content by gamma-radiation using eqn. (2.18) for two different counting times.

Counting time [s]	θ_v [m^3/m^3]	Random error [m^6/m^6]	%	Residual error [m^6/m^6]	%	σ_{θ_v} [m^3/m^3]
30	0.30	4.86e-5	82.8	1.01e-5	17.2	7.7e-3
	0.20	4.72e-5	91.3	4.47e-6	8.7	7.2e-3
	0.15	4.65e-5	94.9	2.52e-6	5.1	7.0e-3
	0.10	4.59e-5	97.6	1.12e-6	2.4	6.9e-3
	0.05	4.52e-5	99.4	2.80e-7	0.6	6.7e-3
60	0.30	2.43e-5	70.7	1.01e-5	29.3	5.9e-3
	0.20	2.36e-5	84.1	4.47e-6	15.9	5.3e-3
	0.15	2.33e-5	90.2	2.52e-6	9.8	5.1e-3
	0.10	2.29e-5	95.4	1.12e-6	4.6	4.9e-3
	0.05	2.26e-5	98.8	2.80e-7	1.2	4.8e-3

with ρ_b = 1600 kg/m^3 ; x_s = 5.7e-2 m ; $\mu_{w_{Cs}}$ = 9.59e-3 m^2/kg ; $(N_{ds})_{Cs}$ = 1.5e+5 counts (30 s) and 3e+5 counts (60 s).

Table 2.5. Composition of the total error on the calculation of the bulk density determined by gamma-radiation (eqn. 2.18) as a function of the volumetric water content and two different counting times.

Counting time [s]	θ_v [m^3/m^3]	Random error [kg^2/m^6]	%	Residual error [kg^2/m^6]	%	σ_{ρ_b} [kg/m^3]
30	0.30	9.95e+1	49.8	1.00e+2	50.2	1.41e+1
	0.20	8.97e+1	49.0	9.34e+1	51.0	1.35e+1
	0.15	8.52e+1	48.4	9.08e+1	51.6	1.33e+1
	0.10	8.09e+1	47.7	8.86e+1	52.3	1.30e+1
	0.05	7.69e+1	46.9	8.70e+1	53.1	1.28e+1
60	0.30	4.97e+1	37.5	8.29e+1	62.5	1.15e+1
	0.20	4.48e+1	36.9	7.66e+1	63.1	1.10e+1
	0.15	4.26e+1	36.5	7.42e+1	63.5	1.08e+1
	0.10	4.05e+1	35.9	7.23e+1	64.1	1.06e+1
	0.05	3.85e+1	35.1	7.10e+1	64.9	1.05e+1

with ρ_b = 1600 kg/m^3 ; x_s = 5.7e-2 m ; $\mu_{s_{Am}}$ = 2.35e-2 m^2/kg ; $\mu_{w_{Am}}$ = 1.98e-2 m^2/kg ; $(N_o)_{Am}$ = 7.26e+4 counts (30 s) and 1.45e+5 counts (60 s).

2.5. X-ray fluorescence spectrometry for clay quantification

The X-ray fluorescence spectrometry was used to quantify the clay fraction within the sandy subsamples at the end of the percolation period using a calibration curve established on Fontainebleau sand-Béthonvilliers smectite mixtures. Firstly, the X-ray fluorescence technique will be briefly explained. The experimental calibration curves will then be presented.

2.5.1. Methodology

X-ray fluorescence spectrometry is considered as a reliable and non-destructive method for elemental analysis of soils *(Page et al., 1982)*. X-ray emission spectrometry depends on the fact that when a beam of X-rays is directed onto the surface of a sample, secondary (fluorescent) X-radiation is emitted. The latter contains wavelengths that are characteristic of each element present in the sample. The X-rays initially required to excite matter are obtained, in our specific case, using an X-ray tube with a Rd anode. Once the beam has stroken the matter, electrons from the inner levels of the atoms are ejected and electrons from higher energy levels replace the ejected ones. This releases energy that appears as a characteristic X-radiation. Consequently, for a given element and electron transmission, the wavelength of the X-rays produced is unique. Further, the intensity of radiation emitted is linearly related to the concentration of an element *(Eberhart, 1989)*.

Quantitative analysis depends on the determination of precise intensity of emitted radiation at a selected spectral position by counting. X-ray fluorescence spectrometry requires dead time and matrix corrections. These corrections take into account the effect of the presence of other elements than the element being analysed. The error in quantitative analysis arises from the variable quality of the prepared standards and samples, the equipment used, the counting procedures, and finally the procedures used to correct for inter-element absorption. The effect of the sample heterogeneity, in terms of particle radii, can be minimized by grinding.

Based on the structural formula[10] of Béthonvilliers clay fraction, Mg, Al and Fe were used to establish the calibration curves.

---

[10] The structural formula of Bethonvilliers smectite (per half unit cell) is :
$\{Si_{3.82}\,Al_{0.18}\}\{Al_{1.32}\,Fe^{3+}_{0.39}\,Mg_{0.23}\}O_{10}(OH)_2\,Ca_{0.23}K_{0.11}Na_{0.1}$ *(Tessier (1984)*

2.5.2. Calibration curves

Calibration curves were established with the original Fontainebleau sand and Ca-smectite mixtures with known clay contents (0 - 0.1 - 0.2 - 0.3 - 0.4 - 0.5 - 0.7 and 1 % of clay). The clay fraction (< 2 µm) obtained by successive sedimentation (§ 2.3.1.3) was saturated with $CaCl_2$, and washed to be free of excessive salts, first with water then with water and acetone till the AgCl test was negative *(Charlot, 1963)*. Acetone has been used in the washing procedure only to facilitate clay flocculation. The clay fraction was then dried at low temperature (70 °C) and crushed.

Ca-smectite was mixed with acetone wetted Fontainebleau sand. Samples were then allowed to dry again. The spectrometry measurements[11] are performed on small discs which consisted in a mixture of crushed and ground Fontainebleau sand and Ca-smectite mixed up with an acrylic resin (10 % - helvacite) diluted in acetone. The mixture is then finally submitted to a pressure of approximately 94 MPa using an automatic hydraulic press.

To establish the calibration curves, the total corrected countings N_{X-ray} due to Mg, Al or Fe were linearly related to the mass percentage of clay $\%_c$ as follows :

$$\%_c = A\ N_{X-ray} + B, \tag{2.19}$$

with $A = 3.26e{-}3\ \%_c/cps$; $B = 1.32e{-}1\ \%_c$ for Mg ;
$A = 3.34e{-}3\ \%_c/cps$; $B = 1.31e{-}1\ \%_c$ for Fe ;
$A = 1.58e{-}3\ \%_c/cps$; $B = 1.17e{-}1\ \%_c$ for Al.

The accuracy on smectite quantification is of about 0.06 %, 0.09 % and 0.1 % for Mg, Fe and Al measurements, respectively. Smectite was finally quantified using only Fe and Mg calibration curves, because the former has an intense signal and an intermediate standard deviation, whereas Mg has a lower intensity but presented the lowest standard deviation.

2.5.3. Presentation of the results

Results for clay quantification can either be expressed in terms of mass or volume ratios. The latter has been used in the study of *Somaratne (1994)*. It is easily calculated following :

(11) The sample preparation required for spectrometry analysis was realized by the laboratory of geology and mineralogy at the Catholic University of Louvain, Louvain-la-Neuve, Belgium.

$$\frac{V_c}{V_t} = \frac{m_c\ \rho_b}{m_t\ \rho_{sc}}\ , \qquad (2.20)$$

where m_c is the mass of clay [kg] ;
m_t is the total mass of soil [kg] ;
ρ_b is the bulk density of the soil [kg/m^3] ;
ρ_{sc} is the clay particle density of Béthonvilliers [kg/m^3] ;
V_c is the volume of clay [m^3] ;
V_t is the total soil volume [m^3].

Volume ratios instead of mass ratios will be used to compare our experimental results to those of *Somaratne (1994)* (§ 4).

2.6. Description of the experimental leaching procedures

Having in mind the general description of the experimental device the leaching procedures for the two different series of flow experiments are now described.

2.6.1. Leaching solution quality

The leaching solutions consisted of NaCl -$CaCl_2$ solutions prepared with various SAR and TEC values i.e. with SAR = 5, 10, and 20, and TEC = 1, 5 and 10 meq/l. The SAR and TEC values were chosen based on the literature (table 1.2) and on the results of the dispersion test realized on the Béthonvilliers clay fraction (figure 2.2). Both the SAR and the electrolyte concentration were verified by the determination of the Na and Ca concentrations by atomic absorption spectrometry (AAS) and DCP[12]. Electrical conductivity and pH of the leaching solutions were also measured (annexe 2.3).

Finally, one should also mention that the use of leaching solutions of total electrolyte concentrations lower than 10 meq/l will not greatly affect the water content and bulk density measurements*(Mermoud, 1982)*. Therefore, we will not take care of additional corrections in these measurements.

(12) DCP Direct Current Plasma.

2.6.2. The achievements of Béthonvilliers soil materials at given ESP values

The ESP values corresponding to the SAR of the leaching solutions were obtained "artificially" by mixing calcic with sodic Béthonvilliers soil material, based on the knowledge of the ESP-SAR relationship (eqn. 2.2). Soil either saturated with calcium or sodium were obtained by mixing fifty grams of air-dried, sieved (< 2 mm) soil material with NaCl or $CaCl_2$ 2N for 5 hours, and with NaCl or $CaCl_2$ 1N for four days. The soil materials were then first washed with deionized water, water and acetone and finally with acetone till the AgCl test *(Charlot, 1963)* was negative. Soil samples were dried at 50°C and again sieved to 2 mm.

2.6.3. Experimental procedure

In order to investigate smectite dispersion and mobility in a stratified porous media induced by means of salty solutions, and to quantify its effect on the hydrodynamic properties, two series of flow experiments were carried out. Each series was performed on six two-layered columns.

The main objective of series I experiments is to study the effect of one leaching solution of intermediate salinity and low TEC on the behaviour of the Béthonvilliers soil material, and its consequences on the hydrodynamic properties of the initial clay-free Fontainebleau sand under unsaturated flow conditions.

The objective of the flow experiments of the second series was to establish the change of the soil moisture retention curve (MRC) and the unsaturated hydraulic conductivity curve (HCC), initially at equilibrium with a solution of given SAR and TEC, by inducing conditions which are more favourable to clay dispersion. These conditions were obtained by an increase of the SAR, a reduction of the TEC, or both simultaneously.

The experimental procedure explained below has been applied to each column :

- Once the elements of the columns are fitted together, the small holes are filled up with silicone, and molten paraffin is poured at the junction of two consecutive cylinders.
- The dry fine textured Fontainebleau sand is then uniformly packed in the column. This is performed by placing the empty column on a vibration table (6000 oscillations/minute) and by progressively filling it within a given time, ranging from 2'30" to 3'05". The homogeneity of compaction within each column is verified using the gamma-radiation (^{137}Cs- 406 mCi or 15 GBq - ^{241}Am - 200 mCi or 7.4 GBq).

- The 28.5 cm sandy subsoil is then progressively wetted from the bottom by capillary rise with a solution of known SAR and TEC, in order to minimize air entrapment.

Series I experiments :

For series I flow experiments, solutions of SAR equal to 5 or 20 and TECs of 1, 5 and 10 meq/l were used.

Series II experiments :

All the columns are first leached with SAR = 5 and TEC = 5 meq/l based on the experimental results obtained with the flow experiments of series I. This allowed to test the reproducibility of the results.

- The silicone is removed from the holes of the PVC cylinders.
- The lower boundary condition is then fixed to a constant suction of 25 cm (2.5 kPa) and drainage is started. At equilibrium, the first water content and density profiles were measured before the tensiometers were connected to the mercury manometers. The first profile corresponds to the soil moisture retention curve of Fontainebleau sand in the low suction range.
- The top layer of the dry Béthonvilliers soil material is gently placed after the drainage occurred (45 g for series I and 20 g for series 2). Without draining first, smectite movement induced mechanically was feared due to the increase of the suction at the bottom of the column, and not especially due to water quality. The top layer is covered with a glass microfibre filter to reduce surface disturbance during the leaching experiments and progressively wetted in order to minimize particle disaggregation. The wetting of the soil material is performed with the same solution of known SAR and TEC, before a constant head is applied by means of a Mariotte bottle.

Series I experiments :

In series I flow experiments, each column is leached during a period of approximately 8 to 10 weeks.

Series II experiments :

In series II flow experiments, each column is leached during 3 to 4 weeks, corresponding to pore volumes ranging from 15 up to 19, before the leaching solution is changed. Each column is then submitted to a different solution in order to study the effect of an increase of the SAR (SAR = 10 ; TEC = 5 meq/l), a decrease of the TEC (SAR = 5 ; TEC = 1 meq/l), or both (SAR = 10 ; TEC = 1 meq/l). The effect of leaching with deionized water, which simulates rainfall, has also been tested on one column.

- During percolation, independently of the series, the matric head and the total hydraulic conductivity are measured daily, whereas the volumetric water content and bulk density profiles are determined weekly. All the effluent volumes are collected and the EC, pH and the respective concentrations of calcium and sodium determined. The upper layer thickness is regularly measured.
- At the end of the percolation period, the water content profile is verified by the gravimetric method. The small cylinders of the PVC column are then separated from each other. The water content on a mass basis are determined by weighting the wet sample and after drying at 105°C during 48 h.
- The sandy samples are washed to remove the excess of soluble salts and dried again at 50°C.
- The amount of smectite within the sandy subsamples is quantified by the means of X-ray fluorescence spectrometry.

2.7. Conclusions

The soil materials chosen for the leaching experiments, were chemically and physically characterized. The upper layer of the two-layered systems is a smectite rich soil material mainly saturated with divalents and referred to as Béthonvilliers. Due to the fact that the clay fraction contains mainly smectite, the use of X-ray for the determination of the dispersed clay within the sandy samples at the end of the leaching period is circumvented.

To get around the problem of the presence of divalent cations, artificial exchangeable sodium percentages (ESP) were obtained by mixing calcic and sodic soil together, based on an experimental relationship ESP - salinity (SAR). The high clay content characterizing the soil material has both a positive and negative effect. Indeed, high clay contents increase the dispersive behaviour of clay but, once dispersed, clay movement is reduced within the clayey layer.

We described in details the experimental device which has been constructed for the flow experiments, and the different methodologies to measure the water content and bulk density profiles, the hydraulic head, and the total hydraulic conductivity.

The errors on the measurement of the water content and bulk density were assessed using values including the range of experimental values. The standard deviations on the determination of these parameters are smaller than 1 %, provided that the recorded countings are corrected. These corrections concern the dead time and the Compton scatter.

An indirect method, referred to as X-ray fluorescence spectrometry, has been used to quantify dispersed smectite. Quantification is performed by the means of calibration curves relating linearly the countings to the concentration of the measured structural element (Mg, Fe). The accuracy on smectite quantification is of about 0.06 % for Mg and 0.09 % for Fe measurements.

Finally, the leaching procedures applied to each column during the two flow series experiments were described. Justification of the total electrolyte concentrations and SAR are based on values given in the literature (table 1.2).

REFERENCES

Bartoli, F., G. Burtin, and A.J. Herbillon. (1991). Disaggregation and clay dispersion of oxisols : Na resin, a recommended methodology. *Geoderma*, **49**, 307-377.

Bielders, C.L., L.W. De Backer, and B. Delvaux. (1990). Particle density of volcanic soils as measured with a gas pycnometer. *Soil Science Society of America Journal*, **54**, 822-826.

Bielders, C.L. (1994). Spatial distribution and formation mechanisms of rainfall-induced crusts on coarse-textured soils. Thesis, Faculty of Graduate School, Cornell University, USA, 219 p.

Bruckler, L. (1983). Analyse théorique des erreurs de mesure de la teneur en eau et de la masse volumique par atténuation gamma. *Bulletin du G.F.H.N*, **13**, 7-34.

Cayeux, M.D. (1990). *Contribution à l'étude de la migration et de la rétention de particules minérales dans un milieu poreux.* LCPC, Rapports des Laboratoires, Série Physique et Chimie PC-8, n° 3585, 107 p.

Charlot, G. (1963). *L'analyse Qualitative et les Réactions en Solution.*. 5e éd., Masson et Cie. Eds., Paris, France.

Chen, Y., and A. Banin. (1975). Scanning electron microscope (SEM) observations of soil structure changes induced by Na-Ca exchange in relation to hydraulic conductivity. *Soil Science*, **120**, 428-436.

Corey, J.C., S.F. Peterson, and M.A. Wakat. (1971). Measurement of attenuation of ^{137}Cs and ^{241}Am gamma rays for soil density and water content determinations. *Soil Science Society of America Journal*, **35**, 215-219.

Dyal, R.S., and S.B. Hendricks. (1950). Total surface of clays in polar liquids as a characteristic index. *Soil Science*, **69**, 421-432.

Eberhart, J.P. (1989). *Analyse Structurale et Chimique des Matériaux : Diffraction des Rayons X, Electrons et Neutrons ; Spectrométrie des Rayons X, Electrons et Ions ; Microscopie Electronique*. Dunod, 614 p.

Goit, J.B., P.H. Groenevelt, B.D. Kay, and J.G.P. Loch. (1978). The application of dual gamma scanning to freezing soils and the problems of stratification. *Soil Science Society of America Journal*, **42**, 858-863.

Marshall, T.J., and J.W. Holmes. (1979). *Soil Physics*. Cambridge University Press, 345 p.

Martins, J. (1993). Les aspects hydrodynamiques, physico-chimiques et biologiques du devenir des pesticides dans les sols : application au transfert du Pentachlorophenol en colonnes. Thèse de doctorat, Université Joseph Fourier, Grenoble I, France, LTHE-INPG-UJF-CNRS (URA 1512).

Mermoud, A. (1982). Contribution à l'étude de transferts simultanés d'eau et de soluté en milieu poreux. Thèse n°432, Ecole Polytechnique Fédérale de Lausanne, Suisse, 255 p.

Meyer, P.L. (1978). *Introductory Probability and Statistical Applications*. 2nd ed., Addison-Wesley Publishing Company, 367 p.

Nofziger, D.L., and D. Swartzendruber. (1974). Material content of binary physical mixtures as measured with a dual energy beam of gamma rays. *Journal of Applied Physics*, **45**, 5443-5449.

Novy Quadri, M.G. (1993). Transfert de solutés dans les sols saturés et non saturés. Application au Pentachlorophenol. Thèse de doctorat, Université Joseph Fourier, Grenoble I, France, LTHE-INPG-UJF-CNRS (URA 1512).

Page, A.L., R.H. Miller, and D.R. Keeney. (1982). *Methods of Soil Analysis. Part II. Chemical and Microbiological Properties*. Agronomy monograph n°9 (2nd ed.), Madison, WI 53711, USA, 1159 p.

Rengasamy, P., R.S. Greene, G.W. Ford, and A.H. Mehanni. (1984). Identification of dispersive behaviour and the management of red-brown earths. *Australian Journal of Soil Research*, **22**, 413-431.

Robert, M., M. Hardy, and F. Elsass. (1991). Cristallochemistry, properties and organization of soil clays derived from major sediment rocks in France. *Clay Minerals*, **26**, 409-420.

Rouiller, J., G. Burtin, and B. Souchier. (1972). La dispersion des sols dans l'analyse granulométrique. Méthode utilisant les résines échangeuses d'ions. *Bulletin ENSAIA*, Nancy, **XIV**, 193-205.

Somaratne, N.M. (1994). Characterization and modelling of surface sealing and near surface pore clogging processes. Thesis, Flinders University of South Australia.

Stroosnijder, L., and J.G. De Swart. (1974). Column scanning with simultaneous use of ^{241}Am and ^{137}Cs gamma radiation. *Soil Science*, **118**, 61-69.

Tessier, D. (1984). Etude expérimentale de l'organisation des matériaux argileux. Hydratation, gonflement et structuration au cours de la dessication et de la réhumectation. Thèse Université Paris VII, UER des Sciences Physiques de la Terre, 361 p.

USSL Staff. (1954). *Diagnosis and Improvement of Saline and Alkali Soils*. US Dept. Agric. Handbook 60, 160 p.

Walkley, A., and I.A. Black. (1934). An examination of the Degtjareff method for determining soil organic matter and a proposed modification of the chromic acid titration method. *Soil Science*, **37**, 29.

3. Determination of the hydrodynamic properties of unsaturated sandy layers affected by the presence of smectite

3.1. Introduction

The hydrodynamic properties of soils, especially the hydraulic conductivity curve, can be inferred from steady or quasi-steady flow experiments if the flow is driven by Darcy's law. If unsteady water flow experiments are carried out, appropriate initial and boundary conditions have to be imposed to allow the direct inversion of the governing transport equations by analytical or semi-analytical methods. Such procedures allow direct computation of the specific functional form of deterministic coefficients. Unfortunately, these direct inversion methods show some difficulties. Experimental analyses based on direct methods *(Klute, 1972)* are generally quite time-consuming, and steady state or equilibrium hydraulic conditions have to be achieved repeatedly. In addition, the governing transport equations have to be linearized and finally, parameter uncertainty is not readily available from the direct inversion methods.

An alternative approach uses parameter estimation techniques to solve the inverse problem. With this approach, the physical problem is solved for given boundary and initial conditions with an appropriate analytical or numerical method. Parameterized functional relationships are assumed to describe the system to a sufficient degree of approximation. The parameters are determined by minimising an objective function *(Kool et al., 1987)*. Finally, information concerning parameter uncertainty is obtained with little additional effort.

In a similar way, the soil moisture retention curve (MRC) can also be obtained either directly or indirectly e.g. from basic soil properties such as particle size distribution or organic matter contents *(Gupta and Larson, 1979; Arya and Paris, 1981; Rawls et al., 1982; Saxton et al., 1986)*. Within this study two different approaches were followed. Firstly, theoretical MRCs were established using relationships or/and data sets found in the literature (§ 3.2). This conceptual approach allows us to determine MRCs for sand-smectite mixtures, depending on the clay content and exchangeable sodium percentages (ESP). In the second approach, the MRCs were determined based on the knowledge of the water content-bulk density profiles and the mean flux densities using an inverse methodology.

Before presenting in detail the inverse approach, one will go through the conceptual model for the MRC of sand-smectite mixtures.

3.2. A conceptual model for the MRC of sand-smectite mixtures

Theoretical soil moisture retention curves were constructed taking into account the specific arrangements of the layers in sodic and calcic smectite suspensions. Relationships between the number of layers per quasi-crystal (§ 1.1.5) as a function of the exchangeable sodium percentage (ESP) and the maximal pressure applied to the system could be established based on data from the literature. Finally, applying a similar approach to that of *Low (1980)*, one was able to relate the pressure, which was put equal to the swelling pressure of the clay in a confined media, to the ESP and the distance separating the layers, both for Na-saturated or Na-Ca systems.

The establishment of these theoretical soil moisture retention curves can be criticized. Indeed, this conceptual approach utilizes different data sets concerning both pure or reference clays and soil clays *(Low, 1980)*. Furthermore, in their critical review, *Verburg and Baveye (1994)* put forth experimental evidence of cation exchange reactions having limited reversibility i.e. that exhibits hysteresis. On the basis of the experimental evidence they proposed a conceptual model for binary exchange reactions Ca-Li. In this study, a non-hysteretic cation exchange reaction involving Ca and Na is assumed.

3.2.1. Particle arrangement in sodic and calcic smectites

Particle arrangement is different in pure Na-systems compared to mixed Na-Ca systems (figure 3.1). In pure Na systems, tactoids *(Blackmore and Miller, 1961)* consist in more or less single layers *(Verburg and Baveye, 1994)*. High swelling pressures predictable by the diffuse double layer theory are developed (§ 1.1.5). When the layers are saturated with Ca, the quasi-crystals *(Quirk and Aylmore, 1971)* are constituted of four to nine layers. This quasi-crystal formation reduces the surface area of smectite which behaves as a larger particle. Unfortunately, double layer theory is unable to predict this behaviour without empirical adjustments to the number of layers in a tactoid.

The formation and breakdown of these quasi-crystals is influenced by the composition of the exchange complex *(Shainberg and Caiserman, 1969)*. Na and Ca are not randomly distributed but a "demixing" of cations occurs. Indeed, Ca mainly neutralizes the charges of the inner surfaces, whereas the outer surfaces are mainly covered with Na^+ *(Glaeser and Mering, 1954)*. The introduction of more than 20 % Na into the exchange complex results in the breakdown of the quasi-crystals *(Shainberg et al., 1971)*. Finally, increasing the amount of adsorbed sodium, the cations are distributed more homogeneously on the adsorption sites. Swelling of the mixed system behaves then as a pure Na-system.

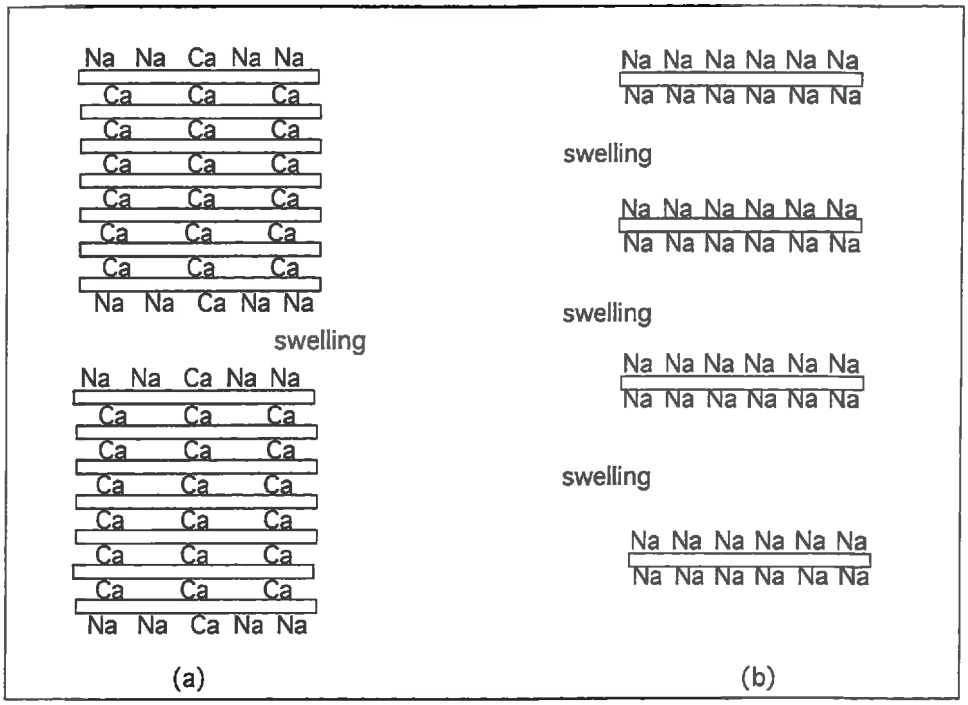

Figure 3.1. Particle arrangement for (a) Na-Ca-smectite and for (b) Na-smectite, illustrating the formation of "tactoids" *(Blackmore and Miller, 1961)* or "quasi-crystals" *(Quirk and Aylmore, 1971)* (according to *Sumner, 1993).*

3.2.2. Expression for the mass ratio of water to smectite

In mixed Ca-Na systems the mass ratio of water to smectite m_w/m_c (subscript c refers to clay) is directly related to the number of layers and the thickness of the water film in between them *(Bresler et al., 1982; Tessier, 1984)* :

$$\frac{m_w}{m_c} = \rho_w S_o \left(\frac{\lambda_i}{2N_p} + \frac{b_o}{2} - \frac{b_o}{2N_p} \right), \tag{3.1}$$

where ρ_w is the density of water [kg/m^3] ;

S_o represents the total specific surface area of the clay, and is also referred to as the total basal surface [m^2/kg] ;

λ_i is the distance between the adjacent quasi-crystals [m] ;

$b_o/2$ is the average half spacing between the layers in the quasi-crystals as determined by X-ray measurements (= 4.5e-10 m) *(Shainberg et al., 1971)* ;

N_p is the number of layers per quasi-crystal ;

S_o/N_p represents the external basal surface [m^2/kg].

Na-saturated smectite has also a tendency to form quasi-crystals but they consist in 1.0 up to 1.7 layers *(Verburg and Baveye, 1994)* e.g. the number of layers per quasi-crystal was found to be about 1.4 for the pure Na-Camp Berteau montmorillonite *(Dufey et al., 1976).* Consequently, in homoionic sodic systems and considering that N_p equals 1, eqn. (3.1) becomes :

$$\frac{m_w}{m_c} = \frac{\rho_w S_o}{2} \lambda_i. \qquad (3.2)$$

Reconsidering eqn. (3.2), one should note that for a given mass ratio of water to smectite and taking into account the total specific area developed by a Na-saturated smectite, a mean distance can be estimated (§ 3.2.4). *Low (1980)* demonstrated a constant value for the ratio $(m_w/S_o m_c)$ for different soil clays. However, this has been criticized by *Tessier and Pedro (1987)* who mentioned that this ratio was no longer constant for a layer charge lower than 0.45 per half unit cell. For such values, the lower the layer charge, the higher the amount of water associated with exchangeable cations.

Eqn. (3.2) represents the fraction of intracrystalline[13] water. *Tessier (1984)* mentioned that the fraction of intercrystalline[14] water for Na-saturated clay pastes only represented 19 % up to 36 % of the total water content and was pressure dependent. However, in Ca-saturated systems, water between the super imposed layers represents a minor fraction. The major part is located between the crystals (92 % for a pF = 1.5 or - 3.2 kPa and 69 % for pF = 3 or - 101.3 kPa) *(Tessier, 1984).*

---

[13] or water in between the platelets or internal water *(Tessier, 1984).*

[14] or extracrystalline water, water that occupies the interstices (pores) between the crystals, external water *(Tessier, 1984).*

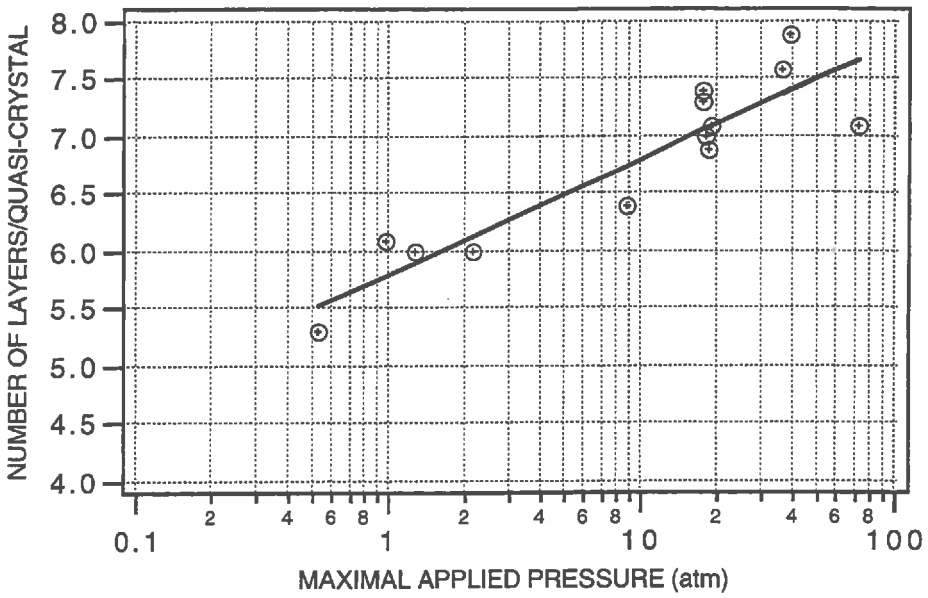

Figure 3.2. Relationship between the number of layers per quasi-crystal for Ca saturated smectite as a function of the maximal applied pressure (according to *Blackmore and Miller, 1961).*

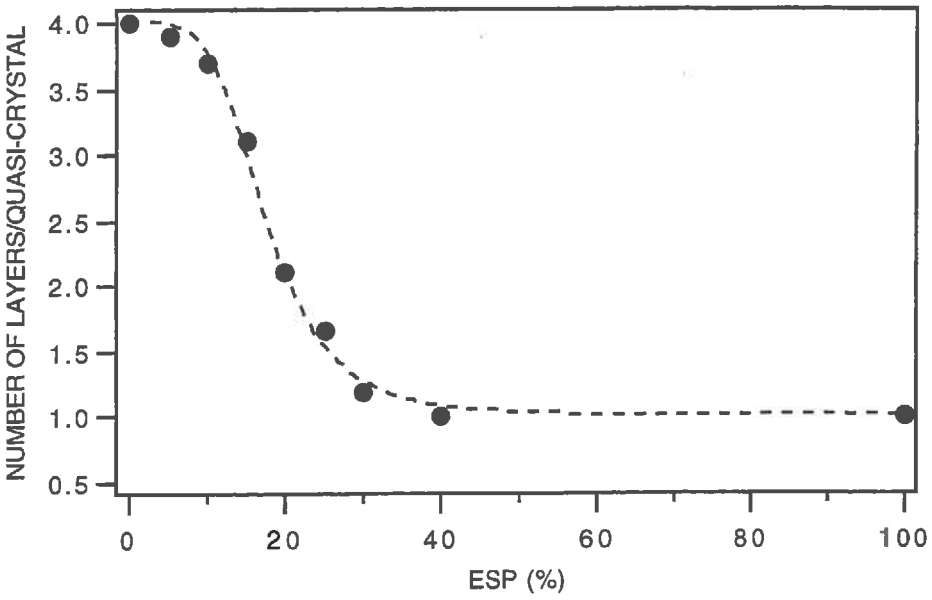

Figure 3.3. Relationship between the number of layers per quasi-crystal as a function of the ESP without any external pressure. The filled circles represent the original data for Wyoming Bentonite from *Shainberg and Otoh (1968),* whereas the dashed line gives the fitting when eqn. (3.4) is used.

3.2.3. Number of layers per quasi-crystal as a function of the pressure and ESP

For smectites saturated with Ca (ESP = 0), *Blackmore and Miller (1961)* highlighted an increase of the number of layers per quasi-crystal $N_{p_{Ca}}$ with the logarithm of the maximal pressure P_{max} applied to the system, following an empirical relationship given by :

$$N_{p_{Ca}} = C_1 + C_2 \log(P_{max}), \tag{3.3}$$

where the values of the estimated coefficients are respectively :

$$\hat{C}_1 = 5.82 \pm 1.53\text{e-}1 \text{ and } \hat{C}_2 = 1 \pm 1.33\text{e-}1$$

for the pressures expressed in [atm] (figure 3.2). If the pressure is expressed in [Pa], it should be divided by a factor equal to 98100. For a small pressure value, i.e. 981 Pa or 0.01 atm, the number of layers/tactoid equals 3.82. *Dufey et al. (1976)* found that the number of single layers/quasi-crystal was about 3.9 for pure Ca-Camp Berteau, without any external pressure.

The number of layers per quasi-crystal N_p can be related to the exchangeable sodium percentage (ESP) using the data of *Shainberg and Otoh (1968)* (figure 3.3). We fitted these data with an empirical expression :

$$N_p = N_{p_{Na}} + \frac{\left(N_{p_{Ca}} - N_{p_{Na}}\right)}{1 + \left(C_3 ESP\right)^{C_4}}, \tag{3.4}$$

where $\hat{C}_3 = 5.59\text{e-}2 \pm 8.90\text{e-}4$ (meq/100g)$^{-1}$;

$\hat{C}_4 = 4.39 \pm 2.78\text{e-}1$.

It should be noted that the inverse of C_3 could be compared to a characteristic ESP value separating the quasi-crystal from the single layers arrangement. The second parameter (C_4) gives the slope of the linear part of the curve joining these two typical arrangements. The higher the value of C_4 is, the steeper the slope will be. This means that the breakdown of the quasi-crystals occurs in a narrower ESP range.

However, *Shainberg et al. (1971)* demonstrated that for low pressures, 7 % of Na on the exchangeable complex were sufficient to break down the quasi-crystals, but at higher pressures, the quasi-crystal arrangement is still existing, even with ESP values of 20. Nevertheless, the constants in eqn. (3.4) will be assumed to be pressure independent. Only N_{pCa} will depend on the maximal pressure applied to the system. These curves are presented in figure 3.4.

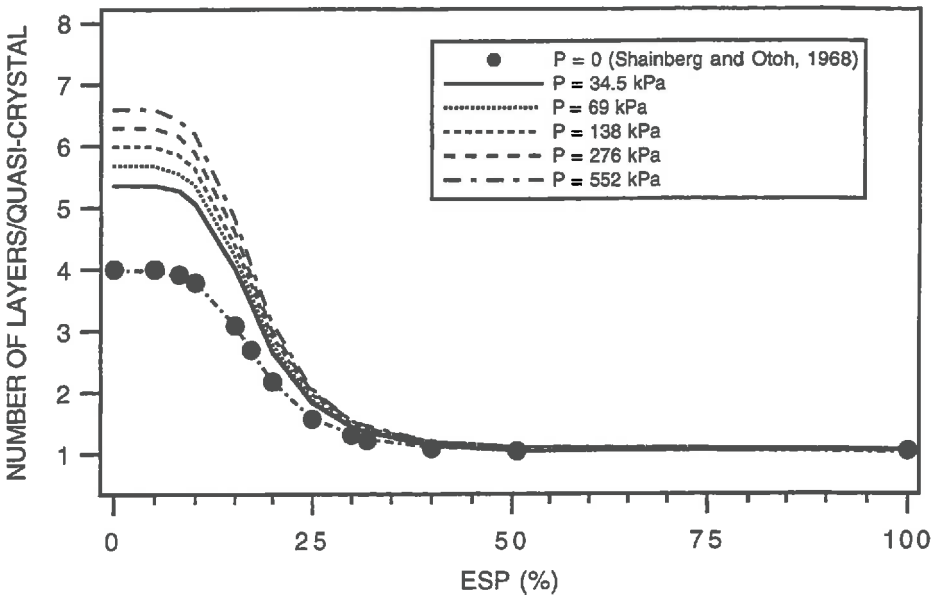

Figure 3.4. Relationships between the number of layers per quasi-crystal as a function of the ESP and the pressure according to eqns. (3.3) and (3.4). The filled circles are the experimental data from *Shainberg and Otoh (1968)*.

3.2.4. Distance between adjacent quasi-crystals

Assuming that the Na-saturated quasi-crystals consist in a uniform distribution of parallel oriented particles a mean distance can be estimated. Rearranging the terms of eqn. (3.2), Na-saturated quasi-crystals are separated from each other by a distance proportional to the mass ratio of water to clay according to :

$$\lambda_{iNa} = \frac{2}{\rho_w S_o}\left(\frac{m_w}{m_c}\right)_{Na} . \tag{3.5}$$

Rearranging the terms of eqn. (3.1) for mixed Na-Ca systems, it can be seen that the distance is no longer equal to the ratio $\left(2m_w/(\rho_w S_o m_c)\right)$, but is given by :

$$\lambda_{i\,Na-Ca} = \frac{2m_w}{\rho_w S_o m_c} N_p - b_o\left(N_p - 1\right). \tag{3.6}$$

This means that for clay systems where the water content, the total specific surface area and the number of layers are known, the distance separating the adjacent quasi-crystals can be estimated.

3.2.5. Swelling pressure as a function of the corrected distance and ESP

If a clay system is prevented from swelling to the full extent of the double layer, it exerts a swelling pressure which depends on the difference in concentration between the outer bathing solution and the solution containing exchangeable cations between the clay surfaces *(Marshall and Holmes, 1979; Bresler et al., 1982)*. In a confined system a hydraulic pressure develops between the clay layers and will be equal in magnitude to the swelling pressure.

On the one hand, *Bresler (1972)* related a scaled swelling pressure of homoionic and mixed systems as a function of the sodium adsorption ratio (SAR), the total electrolyte concentration (TEC), the distance between layers, and the effective charge density of the clay (Γ_s). The latter is given by the ratio of the cation exchange capacity (CEC) to the total specific surface area. The main problem is that the typical quasi-crystal arrangement is not taken into account. Consequently, for given conditions of SAR, ESP, TEC and Γ_s, the distances and hence the water contents are overestimated for mixed Na-Ca systems.

On the other hand, *Low (1980)* investigated the behaviour of 35 Na-saturated montmorillonites in relation with the applied pressure. He developed an empirical equation in which the swelling pressure, which was taken to be equal to the confining pressure, depended exponentially on the water content. The latter was directly related to the distance between the layers, following a relation close to that of eqn. (3.5). Consequently, he established a single curve between the swelling pressure of Na-montmorillonite and the distance between the layers. This relationship, valid in the pressure range 2.45 kPa to 6.87e2 kPa, was assumed to be independent of the nature of the montmorillonite.

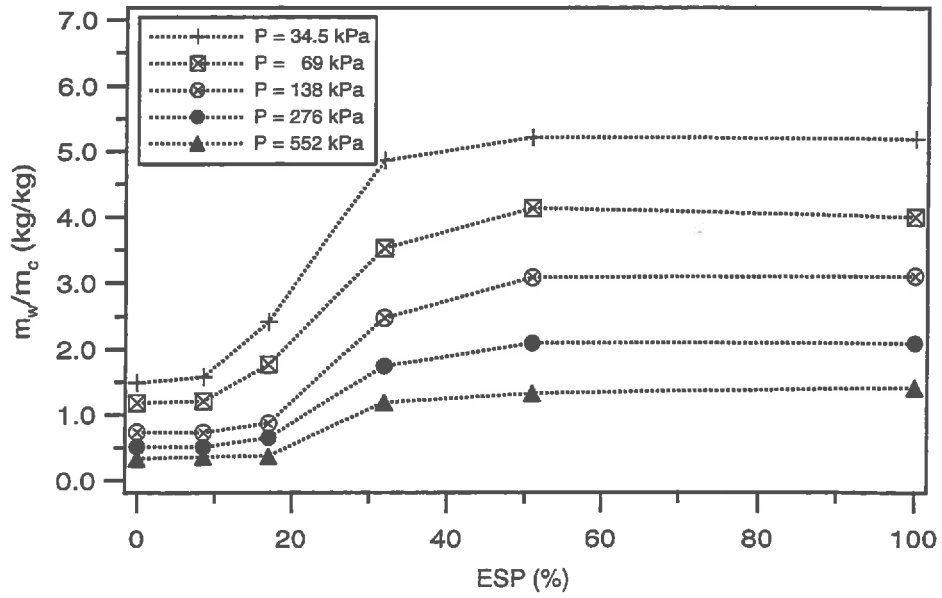

Figure 3.5. Mass ratios of water to Wyoming Bentonite as a function of the pressure applied to a confined system and different ESP values (from *Shainberg et al., 1971).*

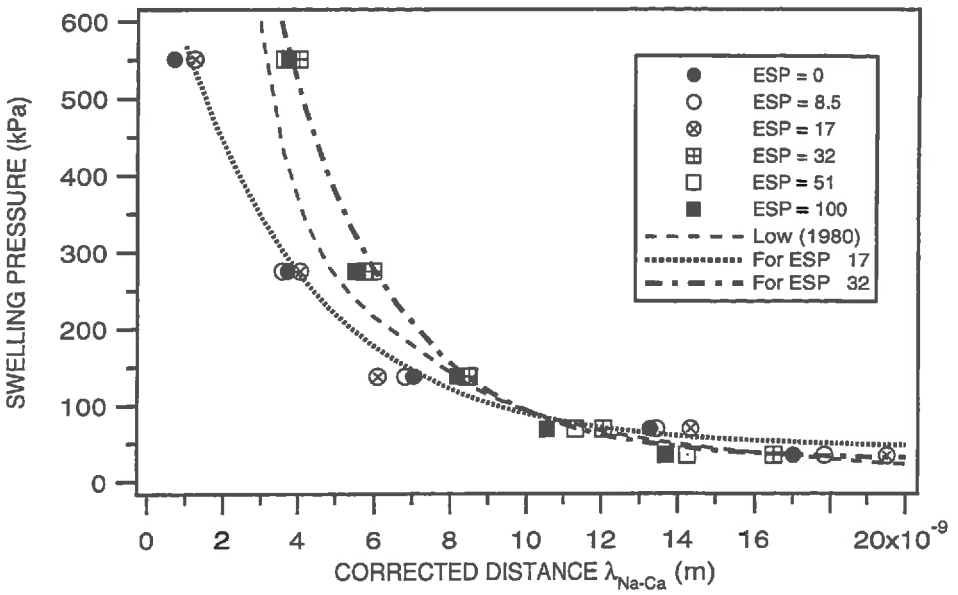

Figure 3.6. Relationships between the pressure occurring between clay layers (Wyoming Bentonite) vs. a corrected distance calculated from eqn. (3.6) as a function of the ESP. Data from *Shainberg et al. (1971)* were used.

Based on these studies, it was thought that similar relationships could be established for mixed Na-Ca montmorillonites, provided corrected distances are used for the quasi-crystal arrangement. Data from *Shainberg et al. (1971)* were used (figure 3.5). The mass ratios of water to Wyoming Bentonite (S_o = 760e3 m²/kg), characterized by different ESPs, are related to the pressure in the range 34.5 kPa up to 5.52e2 kPa. The experiment has been carried out under confined conditions. Consequently, the swelling pressure is considered to be equal to the applied pressure *(Warkentin et al., 1957)*. For a given pressure and ESP, the number of layers per quasi-crystal is calculated following eqns. (3.3) and (3.4). Based on the knowledge of N_p, a corrected distance is determined with eqn. (3.6). The latter is associated to the corresponding pressure applied to the system. The equations for the curves of figure 3.6 were found to be :

$$P = C_5 + C_6 \exp\left(- C_7 \lambda_{iNa-Ca}\right), \tag{3.7}$$

with the following values for the coefficients :

$$\begin{aligned} & \hat{C}_5 = 2.88e1 \pm 4.74\ kPa\ ; \\ \text{ESP} \geq 32 \quad & \hat{C}_6 = 1.89e3 \pm 7.57e1\ kPa\ ; \\ & \hat{C}_7 = 3.38e8 \pm 1.05e7\ m^{-1}; \end{aligned}$$

$$\begin{aligned} & \hat{C}_5 = 4.49e1 \pm 6.19\ kPa\ ; \\ \text{ESP} \leq 17 \quad & \hat{C}_6 = 6.88e2 \pm 1.71e1\ kPa; \\ & \hat{C}_7 = 2.74e8 \pm 1.28e7\ m^{-1}. \end{aligned}$$

These equations are valid in the range 34.5 kPa up to 5.52e2 kPa. For lower pressures, Low's curve is applicable down to 2.45 kPa.

Three curves can be distinguished (figure 3.6). The dashdotted and dotted curves correspond to the data of *Shainberg et al. (1971),* whereas the dashed curve was proposed by *Low (1980)*. For ESP values greater than 32 and for distances lower than 70 Å, the experimental data belong to the confidence limit of Low's curve. Differences could be due to the fact that Low's samples were saturated with Na but the pastes were prepared with deionized water. In contrast with *Shainberg et al. (1971)*, the pastes, leached with solutions of a given SAR, were prepared with the equilibrium solutions. For ESP values lower or equal to 17 where the quasi-crystal arrangement mainly occurs, data are fitted by the dotted curve. It should be noted that for a given swelling pressure, the distance separating Na-Ca layers will be smaller than for sodic saturated single layers.

Low (1980) assumed that the distance between Na-layers was the same for all the montmorillonites at any value of the pressure. A similar assumption will hold for Na-Ca layers, even if the relationships given by eqn. (3.7) were only established with Wyoming Bentonite.

3.2.6. Calculation of theoretical MRC for sand-smectite of Béthonvilliers

Having in mind the above mentioned considerations, one is able to establish theoretical soil moisture retention curves (MRCs) for sand-smectite mixtures based on the use of eqns. (3.3), (3.4) and (3.7). Before presenting them, the errors on the calculations of the water contents will be assessed. These are due to errors in the estimation of the coefficients which were obtained from independent data sets found in the literature.

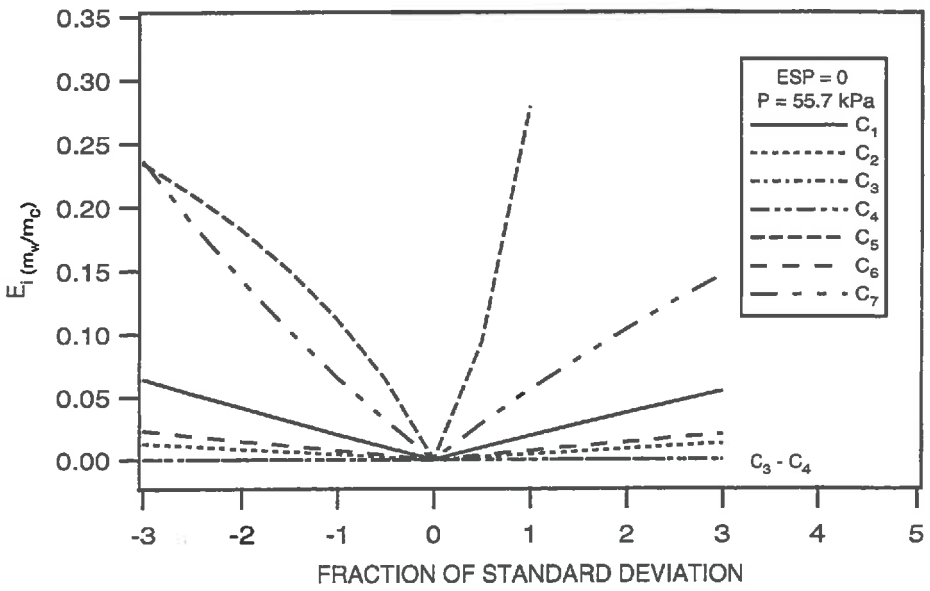

Figure 3.7. The relative error on the calculation of the water ratio to clay in the low pressure range (P = 55.7 kPa) for Ca saturated clay layers (ESP = 0). The model is particularly sensitive to the coefficients C_5 and C_7.

3.2.6.1. Sensitivity analysis

The estimated coefficients $\hat{C}_i$ (i = 1, 2,..., 7) of eqns. (3.1) through (3.7) and their associated standard deviation (SD) were obtained by fitting the experimental data found in the literature. Consequently, one is able to assess the influence of an error on the estimation of each coefficient on the calculation of the mass ratio of water to clay, depending on the ESP and the pressure applied to the system. In order to perform this analysis, the coefficients are independently varied in the range of their standard deviation (SD), and the mass ratios are calculated following eqn. (3.1). A relative error on the calculation of the mass ratio is defined as follows :

$$E_{i_{(m_w/m_c)}} = \left| \frac{(m_w/m_c)_{\hat{C}} - (m_w/m_c)_{C_i}}{(m_w/m_c)_{\hat{C}}} \right|, \tag{3.8}$$

where $(m_w/m_c)_{\hat{C}}$ is the mass ratio of water to clay for the optimal estimated coefficient vector $\hat{C} = (\hat{C}_1, ..., \hat{C}_7)$;

$(m_w/m_c)_{C_i}$ is the mass ratio of water to clay when the coefficient C_i is varied around its optimal value $\hat{C}_i$.

In the low pressure range, for clay layers saturated with Ca, the calculation of the ratio of water to clay is particularly sensitive to the coefficients $\hat{C}_5$ and $\hat{C}_7$ of eqn. (3.7) (figure 3.7). A variation of these two coefficients is illustrated in figures 3.8a and 3.8c. For a given corrected distance, an increase of $\hat{C}_5$ induces a shift of the curve towards higher pressures. A similar effect is obtained when for a given corrected distance the coefficient $\hat{C}_7$ is decreased. In the low pressure range, this results in a considerable variation of the distance between layers (and the amount of water retained by clay) and hence an increase of the relative error. Errors of about 28 % can be obtained when $\hat{C}_5$ in increased by a fraction equal to one standard deviation. Relative errors are smaller when its value is underestimated (11 % for $\hat{C}_5 - 1\ SD$). The model remains sensitive to these coefficients in the entire ESP range (annexe 3.1), but the error is smaller when the ESP is increased (14 % instead of 28 % when the coefficient is overestimated and 9 % instead of 11 % when it is underestimated). The importance of $\hat{C}_7$ increases with an increase of the ESP.

When higher pressures are applied to the system, the model is sensitive to $\hat{C}_6$ and $\hat{C}_7$, but only for ESP values higher than 35 (annexe 3.2). The variation $\hat{C}_6$ is illustrated in figure 3.8b. As it can be seen an increase of $\hat{C}_6$ in the higher pressure range results in an increase of the distance between layers for a given pressure. Its effect will be more accentuated

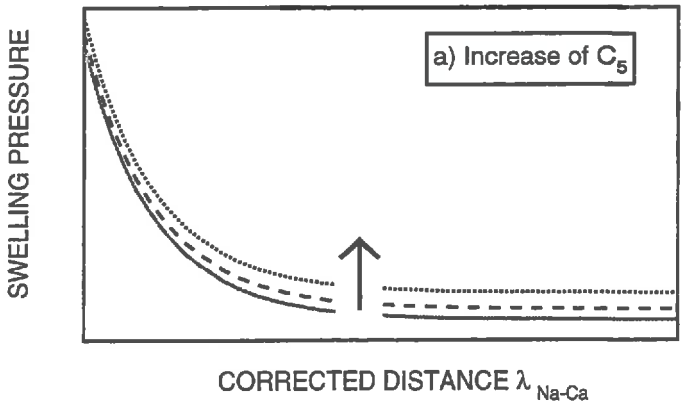

(a)

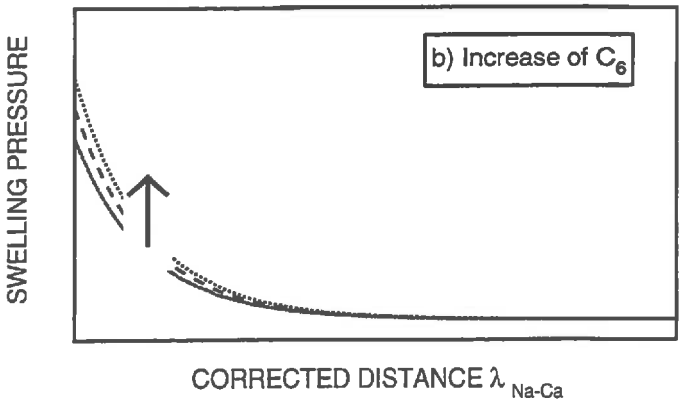

(b)

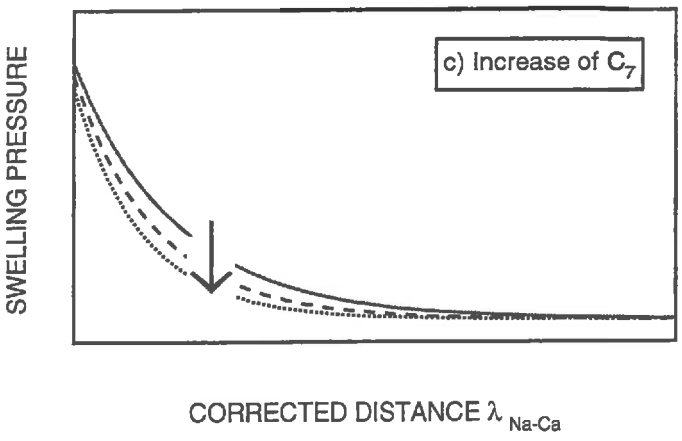

(c)

Figure 3.8. Assessment of an increase of a) C_5, b) C_6 or c) C_7 on the relationship between the swelling pressure and the corrected distance separating adjacent quasi-crystals (eqn. 3.7). The solid lines correspond to the lowest values of a given coefficient and the dotted lines to the highest values.

for ESP values greater than 35. As a consequence, varying the coefficients $\hat{C}_6$ or $\hat{C}_7$ around their respective optimal value by ± 1 SD results in relative errors lower than 8 %.

The model constituted eqns. (3.3), (3.4) and (3.7) seems quite insensitive to the other coefficients even if the optimal value is overestimated or underestimated by a fraction equal to ± 3 SD. From this analysis, it is concluded that the model is particularly sensitive to the coefficients of eqn. (3.7), relating the pressure to the corrected distance as a function of the exchangeable sodium percentage. These coefficients could eventually be better estimated if independent data sets could be added.

3.2.6.2. Calculation of the MRCs

Let us consider a homogeneous and isotropic soil, whose clay fraction contains mostly smectite. The soil is characterized by a uniform porosity which according to *Baver et al. (1972)* can be divided into structural and textural porosity. The structural porosity [15] refers arbitrarily to the pores drained under suction head of less than one meter of water column. The textural porosity can be regarded as an intrinsic property of the soil arising from the size and arrangement of basic particles within the soil mass. In these textural pores, water retention curve is determined quantitatively from the pressure that occurs between clay layers. In a confined system the pressure applied is equal to this swelling pressure. Consequently, the volume of water retained by the clay fraction per unit volume of soil (V_w/V_t) i.e. the volumetric water content θ_v, can be calculated as a function of the pressure and ESP according to :

$$\frac{V_w}{V_t} = \frac{m_c}{m_s}\rho_b S_o\left(\frac{\lambda_i}{2N_p} + \frac{b_o}{2} - \frac{b_o}{2N_p}\right), \tag{3.9}$$

where (m_c/m_s) represents the mass percentage of clay ;

ρ_b is the bulk density of the soil [kg/m^3].

On the other hand, the structural pores are sensitive to external forces arising e.g. from interactions between the clay layers within the textural porosity. In the structural pores, at

[15] The structural porosity or sometimes referred to as the inter-ped porosity is due to soil cracks, biological activity or aggregates arrangement *(Monnier et al., 1973)*.

equilibrium, the suction increases as the pore radius decreases, according to the capillarity equation :

$$h = \frac{2\ \sigma \cos \gamma}{\rho_w\ g\ r}, \tag{3.10}$$

where σ is the surface tension (7.28e-2 J/m^2 at 20° C) ;
γ is the contact angle (assuming here $\gamma = 0$ °) ;
h is the suction [m] ;
ρ_w is the water density [kg/m^3] ;
g is the gravitational acceleration at the earth's surface (9.81 m/s^2).

The water retention curve in the structural porosity will be affected by changes in the volume occupied by the clay mass within the textural porosity. For a given suction, an increase of the SAR and a decrease of the TEC will result in an increase of the distance between the layers. Consequently, the volume of water retained by the clay mass and the volume occupied by the clay will be increased.

In a constant volume system, changes in the volume of the clay matrix and, hence, in the amount of water retained by the clay, are at the expense of the structural porosity and its distribution *(Bresler et al., 1982)*. For a given amount of water, the pore radii is reduced due to swelling of the layers, hence increasing the suction (eqn. 3.10). In other words, for a given suction, the amount of water retained by the soil will also increase. To estimate soil moisture retention curves (MRC) as a function of ESP and percentage of clay, it will be further assumed that for a given pressure applied to the system, the total amount of water retained by the soil will be equal to the sum of both capillary water and water retained by the clay layers.

Results are given in figure 3.9 for a mixture sand of Fontainebleau-Béthonvilliers smectite in the low suction range (2.5 kPa up to 10.1 kPa). Calculations were performed with a specific surface area of 616e3 m^2/kg (§ 2.3.3.2) and a bulk density of 1679 kg/m^3, which corresponds to a mean bulk density value for all the columns of the flow experiments. The MRCs were calculated for arbitrary ESP values equal to 0, 17, 35 and 55 and a clay fraction of 0.5 %. The amount of water retained by the clay fraction has been added to the water contents of Fontainebleau sand. The MRC of the latter was calculated, obtained from the experimental volumetric water contents measured by gamma-radiation on the columns after drainage occurred (§ 4). If these theoretical MRCs are valid, one should note that, for a given suction, the volumetric water contents increase of about 5.5 % when the ESP is increased from 0 up to 55.

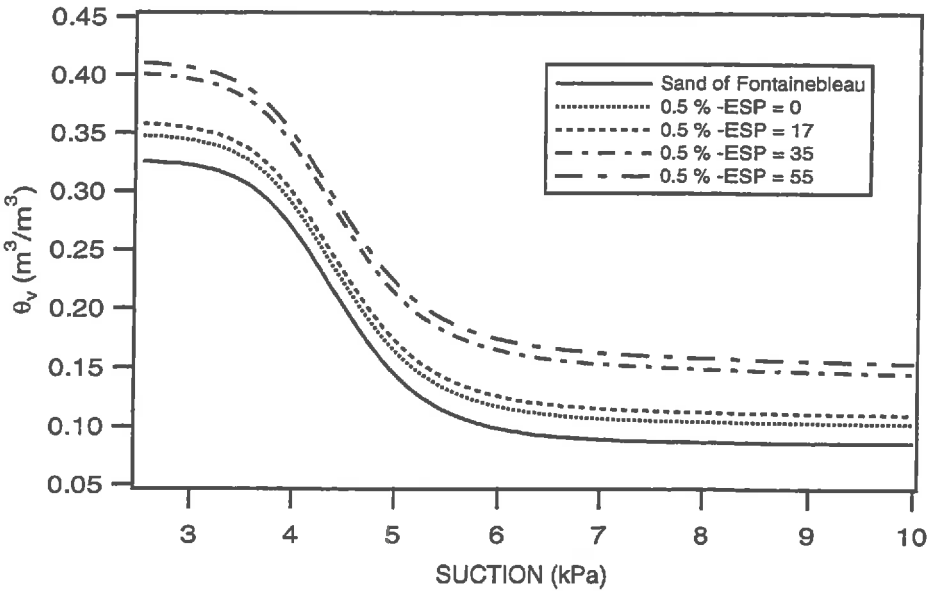

Figure 3.9. Theoretical soil moisture retention curves (MRCs) calculated for sand-clay mixtures, constituted of Fontainebleau sand and 0.5 % Béthonvilliers smectite. The MRC for the initially clay-free sand determined by gamma-radiation (§ 4) has been added.

The calculated mass ratios of water to clay (eqn. 3.1) were also compared to the experimental ratios given in *Tessier (1984)*. Water contents on a mass basis were determined at pressure values of 1, 3.2, 10, 32 and 100 kPa for Na and Ca-Béthonvilliers prepared with a dilute solution (10^{-3} M) of NaCl or $CaCl_2$. The calculations were performed with a calculated specific surface area of 769e3 m^2/kg (ρ_b = 2710 kg/m^3). Results are given in (figure 3.10). The diagonal line represents a perfect correlation between the calculated and experimental ratios (m_w/m_c). A rather good correlation is observed except for one point. This ratio, corresponding to the water content measured at 1 kPa, is highly overestimated. The overestimation could be due to the equation relating the swelling pressure to the corrected distance (eqn. 3.7).

One should remember that the ratio $(m_w/S_o m_c)$ was assumed to be constant and that this assumption would be no longer valid for layer charges lower than 0.40 (Tessier and Pedro, 1987). The lower the layer charge, the higher the swelling. Consequently, the water content on a mass basis for smectites characterized by such layer charges e.g. Wyoming montmorillonite or Greek montmorillonite will be underestimated.

Inasmuch the conceptual approach developed *ut supra* seems to be coherent to obtain theoretical MRCs, it should be confirmed with independent experimental data sets. Two main problems were then encountered. Firstly, only one data set was found in the literature and was used to establish the relationships between the swelling pressure and the corrected distance between the clay layers. Secondly, such data set requires a specific pressure cell. This equipment was unfortunately not available. Consequently, these theoretical curves could not be validated and it seemed hazardous to use them in order to solve the direct problem. Finally, the MRCs were determined applying an inverse approach which will be explained here below and discussed later on (§ 4).

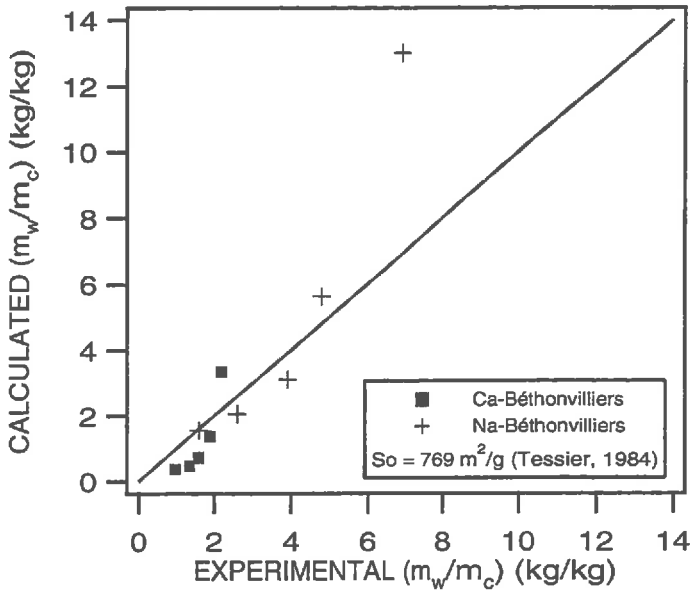

Figure 3.10. Correlation between the experimental and calculated ratio of water to clay in the pressure range 1 kPa up to 100 kPa for Na and Ca-Béthonvilliers (S_0 = 769e3 m^2/kg) prepared with NaCl or $CaCl_2$, 10^{-3} M. Original data from *Tessier (1984)* were used.

3.3. An inverse approach under steady state conditions

3.3.1. The governing equations and functional relationships

To determine the effect of clay migration on the hydraulic properties of the sandy layer, the initial steady-state conditions before the addition of the clay and the final steady-state conditions at the end of the percolation period were recorded. At any moment during the flow experiment, the flux through the sandy column is given by Darcy's law :

$$q = -K(h)\left(\frac{dh}{dz} + 1\right), \tag{3.11}$$

where q is the steady flux density [m/s] ;
$K(h)$ is the hydraulic conductivity of the sandy layer which depends on h [m/s] ;
h is the suction [m] ;
z is the space coordinate taken as positive in the upward direction [m].

The steady downward fluxes can either be measured directly at the outlet of the reservoir, or calculated from the product of the measured total hydraulic conductivity, using the falling head method and the total hydraulic gradient.

For the description of the moisture retention curve (MRC) and the hydraulic conductivity curve (HCC), the non-hysteretic parametric functions of van Genuchten (VG) *(van Genuchten, 1980)* were adopted :

$$S_e = \left(1 + (\alpha h)^n\right)^{-m}, \tag{3.12}$$

and

$$K(h) = K_s \frac{\left[1 - (\alpha h)^{n-1}\left(1 + (\alpha h)^n\right)^{-m}\right]^2}{\left(1 + (\alpha h)^n\right)^{m/2}}, \tag{3.13}$$

where $K_s = K(h = 0)$ is the saturated hydraulic conductivity [m/s] ;
$S_e = (\theta - \theta_r)/(\theta_s - \theta_r)$ is the effective saturation [m^3/m^3] ;
θ_s and θ_r are the saturated and residual volumetric water content, respectively [m^3/m^3] ;
α and n are curve shape parameters, where α is expressed in terms of [m^{-1}] and $m = 1-1/n$.

The following considerations should be made :

- By adopting the VG relationships (eqns. 3.12 and 3.13), we implicitly assume that they accurately represent the system. Even if the sandy profile becomes more and more heterogeneous due to the migration of clay colloids, the MRC will be described using a unimodal model which assumes a unimodal pore size probability density function. Applying a more flexible bimodal model results in an increasing number of parameters, which are difficult to obtain by an inverse approach *(Durner, 1994)*.
- The residual water content is defined by *van Genuchten and Nielsen (1985)* as the water content at a high suction for which the water capacity $d\theta/dh$ becomes zero. If θ_r is inferred from parameter estimation techniques, it should be considered as purely empirical. Its value depends on observed retention data and on the adopted retention model itself *(Kosugi, 1994)*.
- The curve shape parameters are quite empirical and strict definitions have not been proposed yet. The n parameter is an increasing function of the slope determined at a point located halfway between θ_r and θ_s *(van Genuchten, 1980)*. The narrower the pore size distribution is, the higher n is. *Russo (1988)* assumed that n was related to the width of the pore radius distribution.

  The α parameter can be considered as a scaling factor that determines the position of the pore size maximum for the continuous, bell-shaped pore size distribution *(Durner, 1994)*. It tends to be equal to the inverse of the air entry value of the *Brooks and Corey (1964)* relationship for high n values. The capillary pressure at the inflection point h_g can be obtained by differentiating twice eqn. (3.12) with respect to h:

$$h_g = \frac{m^{1-m}}{\alpha}. \tag{3.14}$$

  For high n values, m tends to 1 and α becomes equal to $1/h_g$.
- The restrictive case $m = 1-1/n$ *(Mualem, 1976)* was chosen to minimize the number of unknown parameters. This constraint eliminates some flexibility, but it allows for the simplification of the solution for the hydraulic conductivity models. *van Genuchten (1980)* showed that this assumption can be reasonably adopted in soils with narrow pore-size distributions, i.e. high values of n.

It should be noted that the entire sandy layer is supposed to be accurately characterized with only one MRC or one estimated parameter vector $\hat{b}$ (§ 3.3.3).

Further, as indicated by the results of *van Genuchten and Nielsen (1985)*, a reliable estimated value of K_s is difficult to obtain. We therefore estimated K_s with the empirical expression of *Mbagwu (1995)* :

$$K_s = 1.166e^{-5}(e^{0.08P_e}), \tag{3.15}$$

where P_e is the macroporosity [%] defined as the pore space volume fraction draining at -10 kPa, i.e. the structural porosity. This experimental model was successful in predicting K_s of sandy loam and sandy clay loam soils with high porosity values and relatively high water intake rates *(Mbagwu, 1995)*. In a first approximation, the saturated hydraulic conductivities will be estimated in our study with eqn. (3.15). Experimental data of the hydraulic conductivity related to a mean suction for the unsaturated porous media will be used as matching points in order to determine K_s more accurately.

To further reduce the number of unknown parameters, the residual water content was initially kept constant, based on the fact that inverse estimation of the MRC and HCC parameters is not very sensitive to θ_r *(Kool et al., 1987)*.

The integral form of the Darcy eqn. (3.11) was solved for dz and integrated from h_o to h :

$$z(h) = \int_0^z dz = \int_{h_0}^{h} \frac{dh}{1 + q/K(h)}, \tag{3.16}$$

where h_o is the matric potential at the bottom of the column (in our case equal to - 25 cm water column or - 2.5 kPa). This integral with $K(h)$ given by eqns. (3.13), (3.16) and the calculated flux within the column q cannot be solved directly and requires numerical integration.

3.3.2. Numerical integration

Numerical integration of eqn. (3.16) has been carried out using a five terms Gauss-Legendre quadrature *(Gerald and Wheatley, 1994)*. If the limits of a given integral are a and b, then it can be rewritten as :

$$\int_a^b f(x)\,dx = \frac{(b-a)}{2}\int_{-1}^{1} f\left(\frac{(b-a)t+b+a}{2}\right)dt, \tag{3.17}$$

Changing the interval of integration to (-1, 1) allows the use of the tabulated Gaussian quadrature parameters. If needed, it can be extended beyond two terms :

$$\int_{-1}^{1} f(t)\,dt = \sum_{i=1}^{p} w_i\, f(t_i), \tag{3.18}$$

where p gives the number of terms and w_i are the weighting factors. For a non-linear system and for a given number of terms p, the tt_i's are the roots of the p-th degree Legendre polynomial defined by recursion :

$$(p+1)\,L_{p+1}(x) - (2n+1)\,x\,L_p(x) + n\,L_{p-1}(x) = 0, \tag{3.19}$$
$$L_0(x) = 1\ ;\ L_1(x) = x.$$

This procedure has been applied to the wet range for $0 < |\alpha h| < 1$. In the dry range ($|\alpha h| > 1$), however, the integral (eqn. 3.16) can only successfully be evaluated if the $u = \ln(-h)$ transformation is used *(Warrick, 1991)* :

$$\int_h f(h)\,dh = -\int_u e^u\, f\left(e^u\right)du. \tag{3.20}$$

3.3.3. Optimization algorithm

After numerical integration, the remaining unknown parameters were determined by minimising the ordinary least-squares (OLS) objective function :

$$O(\hat{b}) = \sum_i \left(\theta_{calc}(z_i,\hat{b}) - \theta_{meas}(z_i)\right)^2, \tag{3.21}$$

where $\theta_{meas}(z_i)$ is the measured water content profile obtained by gamma-radiation and $\theta_{calc}(z_i,\hat{b})$ the calculated water content profile. The latter is calculated from the estimated parameter vector $\hat{b} = (\theta_s,\alpha,n)$ or $(\theta_r,\theta_s,\alpha,n)$, the integrated $z(h)$ and the MRC model (eqn.

3.12). To determine $\hat{\boldsymbol{b}}$, the simplex algorithm *(Nelder and Mead, 1965)* was adopted tominimize the objective function $O(\hat{\boldsymbol{b}})$. The simplex algorithm avoids the problem of local optima encountered when using the gradient optimization method, but converges much more slowly. As the time of calculation was not a limiting factor, the simplex method has been preferred.

The OLS method yields unbiased optimal parameter estimates, but their variances are not minimum *(Kool et al., 1987)*. Parameter uncertainty can be assessed by calculating an unbiased estimated variance-covariance matrix C_b, according to :

$$C_b = \frac{SS}{(n_{obs} - p)} H\left(\hat{\boldsymbol{b}}\right)^{-1}, \tag{3.22}$$

where n_{obs} is the number of observations ;

p is the dimension of the parameter vector ;

SS is the sum of the squared residuals calculated at the solution $\hat{\boldsymbol{b}}$ following eqn. (3.21) ;

$H(\hat{\boldsymbol{b}})$ is the Hessian matrix or the matrix of second partial derivatives of the objective function and is given by :

$$H\left(\hat{\boldsymbol{b}}\right) = \begin{pmatrix} \frac{\partial^2 O}{\partial b_1^2} & \frac{\partial^2 O}{\partial b_1 \partial b_2} & \frac{\partial^2 O}{\partial b_1 \partial b_3} \\ \frac{\partial^2 O}{\partial b_2 \partial b_1} & \frac{\partial^2 O}{\partial b_2^2} & \frac{\partial^2 O}{\partial b_2 \partial b_3} \\ \frac{\partial^2 O}{\partial b_3 \partial b_1} & \frac{\partial^2 O}{\partial b_3 \partial b_2} & \frac{\partial^2 O}{\partial b_3^2} \end{pmatrix}. \tag{3.23}$$

The second partial derivatives were approximated numerically by applying a forward difference scheme.

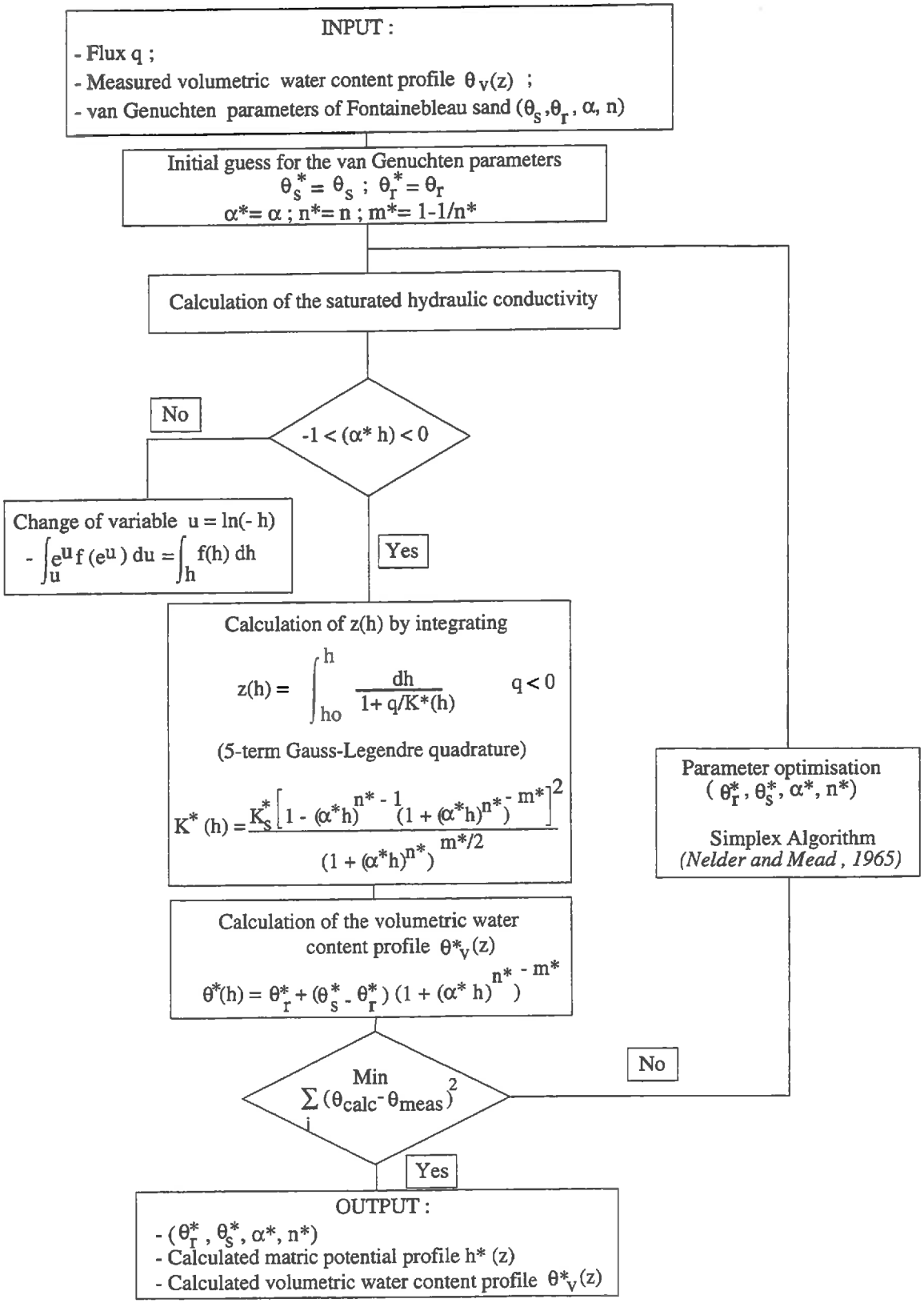

Figure 3.11. Flow chart to estimate the van Genuchten parameters of the MRCs and HCCs affected by clay migration under steady state conditions.

3.3.4. Flow chart

The flow chart is given in figure 3.11. The saturated hydraulic conductivity was calculated. The VG parameter vector (θ_s,α,n) or $(\theta_r,\theta_s,\alpha,n)$, depending on the assumption that the residual water content is unaffected by clay migration or not, was determined using the inverse approach. The input variables to estimate the parameters describing the modified hydraulic properties for each column are the downward flux density and the measured volumetric water content profile. The matric potentials are facultative. The steady downward fluxes were calculated based on the total hydraulic conductivities and the constant hydraulic gradient. The VG parameters of the clay-free sand were taken to initialize the parameter procedure.

3.4. An objective criterion to compare the estimated soil-water retention curves

There is no simple criterion to test statistically the difference between optimized MRCs. A general objective discrimination method is developed below. Let us consider a number of k MRCs. Each curve is characterized by an estimated parameter vector $\hat{\boldsymbol{b}}_j$ $(j = 1...k)$ and an estimated variance-covariance matrix $\hat{V}_j$. An arbitrary new parameter vector $\overline{\hat{\boldsymbol{b}}}$ and variance-covariance matrix $\overline{\hat{V}}$ is built as follows :

$$\overline{\hat{V}} = \frac{1}{k}\sum_{j=1}^{k}\hat{V}_j , \tag{3.24}$$

$$\overline{\hat{\boldsymbol{b}}} = \frac{1}{k}\sum_{j=1}^{k}\boldsymbol{b}_j , \tag{3.25}$$

where $\overline{\hat{\boldsymbol{b}}}$ and $\overline{\hat{V}}$ are respectively the arithmetic mean of the k estimated parameter vectors and variance-covariance matrices. The assumption underlying eqns. (3.24) and (3.25) is that the k MRCs are similar and belong to the same parent population of MRCs. Differences between the estimated curves are only due to parameter error taken into account in $\overline{\hat{V}}$.

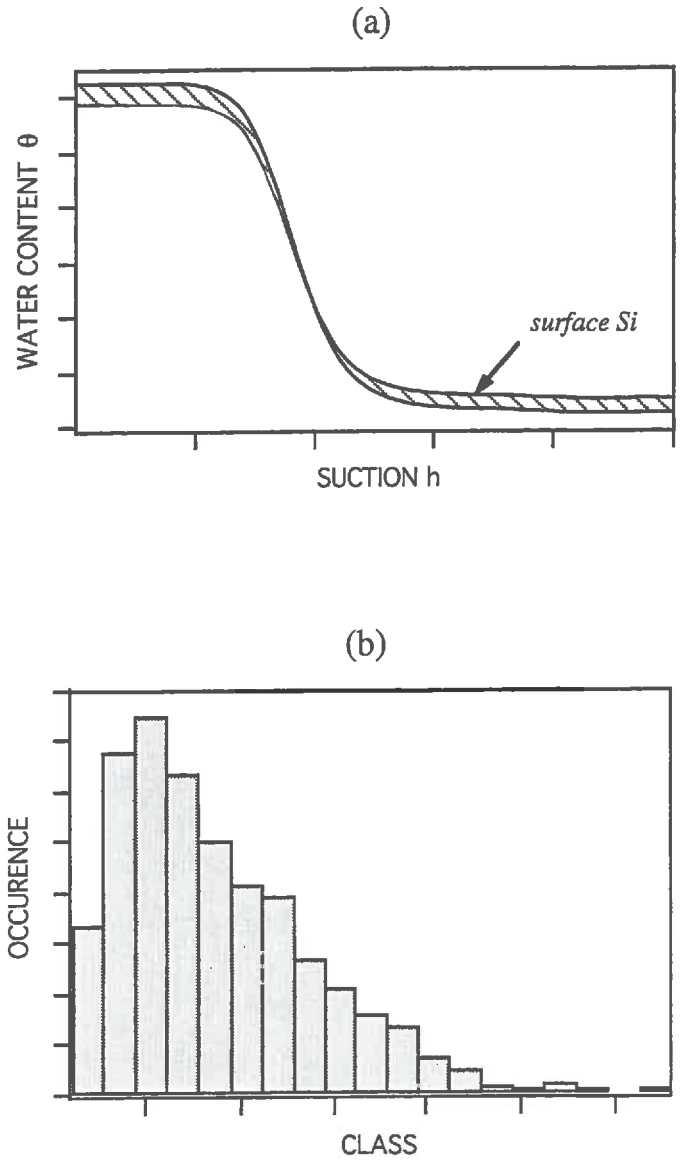

Figure 3.12. Hypothetical probability density function estimate (b) of the surfaces Si between two generated soil-moisture retention curves (a).

Based on the knowledge of the mean variance-covariance matrix $\overline{\hat{V}}$ corresponding to $\overline{\hat{b}}$, new parameter sets $\overline{\hat{b}_g}$ can be generated by applying the Cholesky's decomposition (*Horn and Johnson, 1988*). All of these sets are different in terms of their parameters, but are characterized by the same variance-covariance matrix $\overline{\hat{V}}$. Each set can then be used to draw a MRC_g. Subsequently, the surface between two generated moisture retention curves, i.e. MRC_{g1} and MRC_{g2}, is calculated in a given suction range according to :

$$S_i = \int_h \left| \theta_i(h, \overline{\hat{b}_{g1}}) - \theta_i(h, \overline{\hat{b}_{g2}}) \right| , \text{ i} = 1..1000, \tag{3.26}$$

where $\theta_i(h, \overline{\hat{b}_{g1}})$ and $\theta_i(h, \overline{\hat{b}_{g2}})$ are the water content data of the MRCs calculated respectively with $\overline{\hat{b}_{g1}}$ and $\overline{\hat{b}_{g2}}$. The integral was arbitrarily evaluated for suctions ranging from 1 kPa up to 7.5 kPa, which includes the measured suction range.

The estimate of the probability density function (pdf) can be drawn (figure 3.12) and a 95 % or 99 % confidence limit can be defined. Two MRCs were considered as significantly different at a level of 0.05 or 0.01 if the surface in between them, defined as :

$$S_{jl} = \int_h \left| \theta(h, \hat{b}_j) - \theta(h, \hat{b}_l) \right|, \quad j, l = 1...k, \tag{3.27}$$

did not belong to the 95 % or 99 % confidence limit.

3.5. Sensitivity analysis

The sensitivity analysis allows to evaluate the effect of changes in the input parameters on the final response. The input in the parameter estimation procedure were the constant downward flux and the measured volumetric water content profile. The final response was the estimation of each parameter $\hat{b}_i$ of the four-term vector $\hat{b} = (\theta_r, \theta_s, \alpha, n)$.

These parameters can be considered *a posteriori* as new input parameters. The effect of VG parameter changes were studied individually, performing a monodimensional sensitivity analysis *(Badji, 1984)* again. The latter allows the ranking of the VG parameters, whereas the former only gives relative errors on the estimation of each parameter due to flux or water content changes.

3.5.1. Assessment of an error of the flux on the estimated hydraulic parameters

To check the sensitivity of the downward flux on each parameter $\hat{b}_i$, a relative error E_{iq} is defined as follows :

$$E_{iq} = \frac{\left(\hat{b}_i(q_j) - \hat{b}_i(q_{j-1})\right)}{\hat{b}_i(q_{ref})}, \tag{3.28}$$

where E_{iq} is the relative error on the estimation of parameter $\hat{b}_i$ due to flux modifications;

$\hat{b}_i(q_{ref})$ is the optimal parameter $\hat{b}_i$ determined by the inverse approach with the reference downward flux q_{ref} ;

$\hat{b}_i(q_j)$ is the optimal parameter $\hat{b}_i$ for a modified downward flux q_j ;

j is an index giving the degree of variation of the downward flux ($j \geq 1$).

When the index $j = 1$, corresponding to a variation of the downward flux of ± 1%, then $q_{j-1} = q_{ref}$.

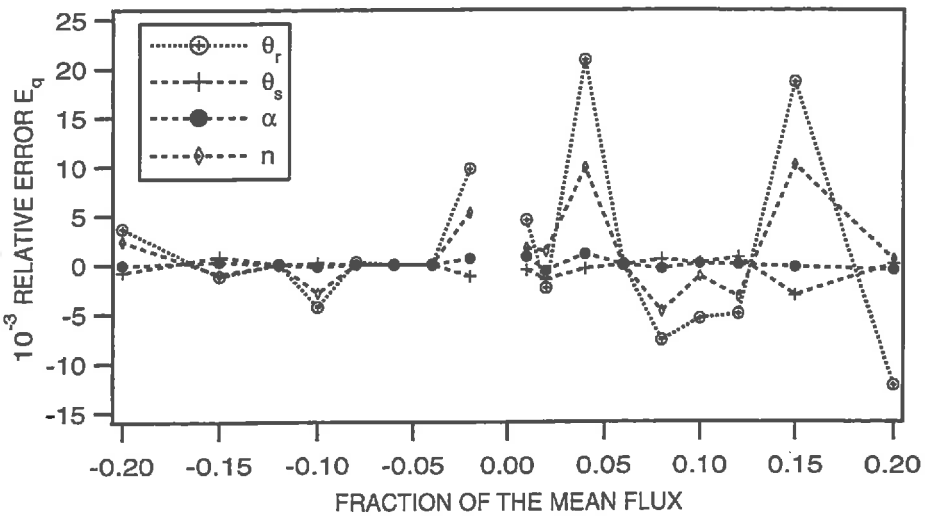

Figure 3.13. Relative errors on the estimation of each VG parameter $\hat{b}_i$ due to flux modifications. Fluxes were varied up to 20 % of the mean downward flux calculated for the last 30 days of the leaching period. Reference data from the column percolated with SAR = 5 and TEC = 5 meq/l were used (series I).

Data from the column leached with a SAR = 5 and a TEC = 5 meq/l (series I) were used. Calculations were performed with the profile obtained at the end of the percolation period. Downward fluxes were modified by adding or subtracting a fraction of the mean downward flux calculated for the last 30 days. The additional fraction ranged from ± 1 % ($j = 1$) up to ± 20 % of the mean value. The VG parameters from the reference data were used as initial guess to reduce the number of iterations. Convergence occurred between the 47th and the 70th iterations. From this analysis, we conclude that the effect of flux changes on the parameter vector estimation is very small. It is less than 2.5 % with a maximum relative error on the estimation of θ_r and a minimum for α (figure 3.13).

3.5.2. Assessment of an error on the measured water content profile on the estimated hydraulic parameters

To assess the effect of experimental errors on the estimated parameters, the following procedure was used. The measured volumetric water contents were obtained by gamma-radiation means. Such measurements are characterized by a Poisson distribution. For high counting rates, the Poisson distribution tends to a Gaussian distribution. To simulate experimental errors and their effect on parameter estimation, a random error is added to each measured value. The noise has a Gaussian distribution with a mean value equal to zero and a standard deviation of 6e-3 m^3/m^3 (table 2.4). A relative error similar to eqn. (3.28) can be defined as follows :

$$E_{i\theta(z)} = \frac{\left(\hat{b}_i(\theta(z)) - \hat{b}_i\left(\theta(z)_{ref}\right)\right)}{\hat{b}_i\left(\theta(z)_{ref}\right)}, \tag{3.29}$$

where

$E_{i\theta(z)}$ is the relative error on the parameter vector $\hat{b}_i$ taking into account experimental error on the water content data ;

$\hat{b}_i(\theta(z))$ is the optimal parameter vector $\hat{b}_i$ obtained with a modified water content profile ;

$\hat{b}_i\left(\theta(z)_{ref}\right)$ is the optimal parameter vector $\hat{b}_i$ obtained with the reference water content profile.

Results are given in figure 3.14. Data from the column percolated with a SAR = 5 and a TEC = 5 meq/l (series I) was used. Calculations were performed with the mean downward flux for the last 30 days. Ten water content profiles were created by adding normally distributed errors to each value of the reference profile obtained at the end of the percolation period. The VG parameters from the reference data were again used as initial guess. Convergence occurred between the 50th and the 98th iterations. From this analysis, it was concluded that the relative errors on the estimation of θ_s, α or n are small (less than 5 %). In contrast with this, the estimation of θ_r may be associated with large uncertainties (up to 17 %). The available data may lead to an objective function that lacks sensitivity for this parameter. *Parker et al. (1985)*, who used a one-step outflow procedure to determine the hydraulic properties, mentioned poor estimates for the residual water content. This problem was alleviated by including additional direct measurements of water contents at high suctions in their objective function. Direct measurements of low water contents could not be performed with our experimental device.

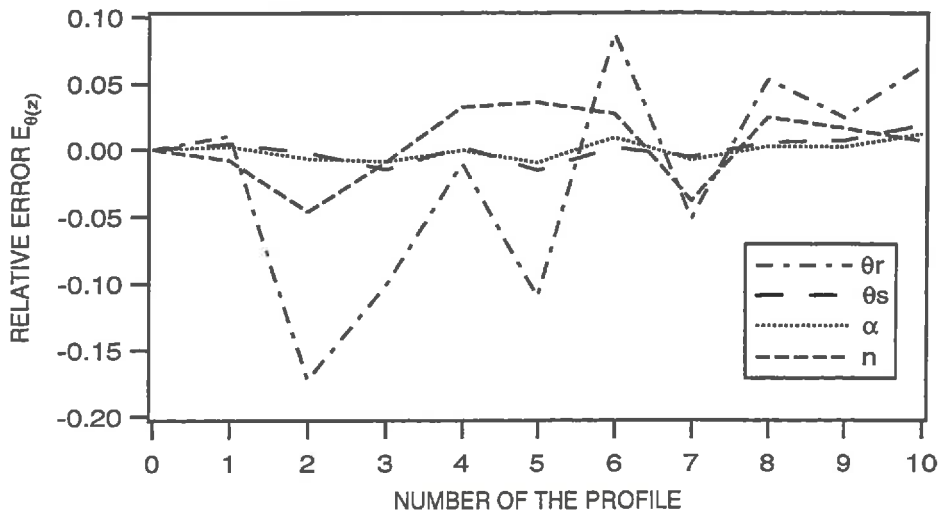

Figure 3.14. The relative error on the estimation of each parameter $\hat{b}_i$ due to experimental error on the measured volumetric water content data. Reference data from the column percolated with SAR = 5 and TEC = 5 meq/l (series I) were used.

3.5.3. Assessment of changes in the VG parameters on the relative sensitivity

The effect of an error in the downward fluxes or in the measured water content profiles on the estimation of the VG parameters has been assessed. The estimated values could be used *a posteriori* as new input parameters. Consequently, their relative importance should be known.

A ranking is obtained by studying the effect of a variation of one parameter on the relative sensitivity, defined as follows *(Badji, 1984)* :

$$RELS_j = \frac{\Delta O_j}{\Delta\left(\hat{b}_i\right)_j}, \tag{3.30}$$

$$\Delta O_j = \frac{\left| O_j\left(\hat{\boldsymbol{b}}_j\right) - O_{j-1}\left(\hat{\boldsymbol{b}}_{j-1}\right) \right|}{O\left(\hat{\boldsymbol{b}}\right)}, \tag{3.31}$$

and

$$\Delta\left(\hat{b}_i\right)_j = \frac{\left| \left(\hat{b}_i\right)_j - \left(\hat{b}_i\right)_{j-1} \right|}{\left(\hat{b}_i\right)}, \tag{3.32}$$

where $RELS_j$ is the relative sensitivity ;

ΔO_j is the relative variation of the objective function following eqn. (3.22) ;

$\Delta\left(\hat{b}_i\right)_j$ is the relative variation of the i-th parameter ;

$O_j\left(\hat{\boldsymbol{b}}_j\right)$ is the value of the objective function when the parameter vector equals $\hat{\boldsymbol{b}}_j$;

$O\left(\hat{\boldsymbol{b}}\right)$ is the value of the objective function for the optimal parameter vector $\hat{\boldsymbol{b}}$;

$\left(\hat{b}_i\right)_j$ is the optimal value of the i-th parameter of the vector $\hat{\boldsymbol{b}}_j$;

$\hat{b}_i$ is the optimal value of the i-th parameter of the vector $\hat{\boldsymbol{b}}$;

j is an index giving the degree of variation of each VG parameter (§ 3.5.1).

The parameters are varied individually around their optimal value, performing a monodimensional sensitivity analysis again. An increasing value of the relative sensitivity with an increasing variation around the optimal value of the parameter means that the importance of the parameter becomes more and more pronounced. However, a decreasing relative sensitivity value means that the importance of the parameter is decreasing when its value is progressively increased.

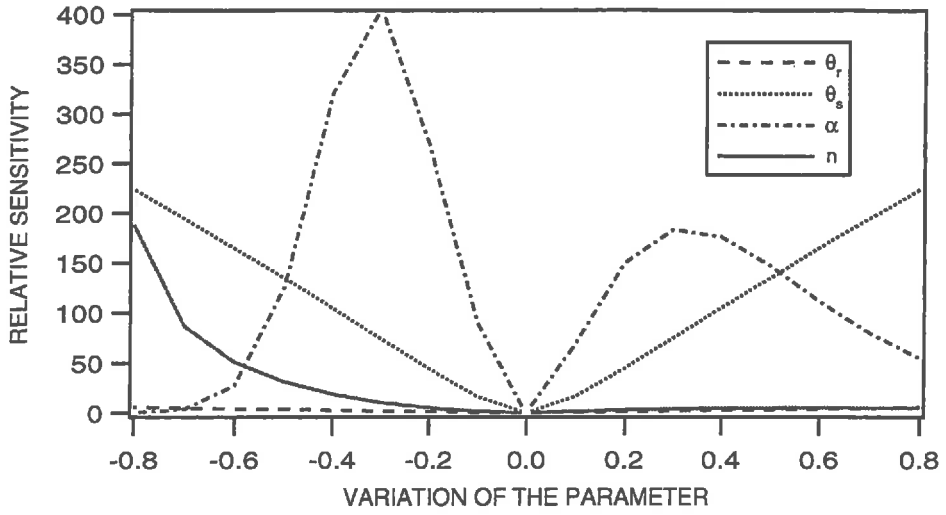

Figure 3.15. Results of the monodimensional sensitivity analysis based on the relative sensitivity. Each parameter was varied from ± 1 % up to ± 80 % around its optimal value. Reference data from the column percolated with SAR = 5 and TEC = 5 meq/l (series I) were used.

Result of the monodimensional sensitivity analysis are given in figure 3.15. Data from the column percolated with a SAR = 5 and a TEC = 5 meq/l was used (§ 4). Calculations were performed with the mean downward flux for the last 30 days and the reference water content profile obtained at the end of the percolation period. Each VG parameter was varied from 1 % up to 80 % around its optimal value. From this analysis, it is concluded that :

- to the right of the optimal value, the α curve shape parameter and the saturated water content θ_s are the most important parameters. The ranking is $\alpha > \theta_s > n \cong \theta_r$ for variations of approximately 30 %. The importance of α decreases with an increasing variation around its optimal value. The model is not sensitive to n and θ_r.

- to the left of the optimal value, the same ranking is obtained for variations of 30 %. When the parameters are further decreased, the ranking becomes $\theta_s > n > \alpha \cong \theta_r$. The parameter n has an increasing importance with a progressive decrease of its value.

It has been shown that errors in the measured water content profile could lead to significant errors in the estimation of the residual water content. Fortunately, the model is not sensitive to the residual water content. The α curve shape parameter and the saturated water content are the most critical parameters who are well estimated and quite independent of errors in the downward flux or the measured water contents.

3.6. Conclusions

Theoretical soil moisture retention curves (MRCs) can be obtained based on few equations and coefficients resulting from the literature. The model is particularly sensitive to those of the expression relating the swelling pressure to a corrected distance between the layers. The effects of errors in the estimation of each coefficient and its consequence on the calculation of the mass ratios of water to clay has been assessed as a function of the exchangeable sodium percentage and the pressure applied to the system. Errors of 28 % can be obtained, especially in the low pressure range, even if the coefficients are varied in the range ± 1 standard deviation around their optimal value.

Inasmuch as the procedure seems to be coherent, the MRCs could not be validated due to the lack of complementary data relating water contents on a mass ratio to the swelling pressure determined in a confined media. Furthermore, these data could not be obtained experimentally, because a specific miniature pressure apparatus was required. Consequently, it was preferred not to use these theoretical MRCs in solving the direct problem.

The soil moisture retention curves (MRCs) and the unsaturated hydraulic conductivity curves (HCCs) for the sandy substratum were determined by applying an inverse approach. The proposed inverse approach, assuming steady state conditions and using the *van Genuchten* (VG) non hysteretic functional relationships in the soil water transport equation, allows the determination of the VG parameters. A general objective criterion has been proposed in order to determine significant differences between estimated MRCs.

The effect of variable input on the estimated four-term parameter vector was assessed. It was concluded that parameter estimation was not very sensitive to errors in the calculated fluxes. Increasing or decreasing the downward flux up to 20 % has small effects. The maximum relative errors (2.5 %) were obtained on the estimated residual water contents. In addition, the estimation of θ_r is excessively sensitive to errors in the measured water content data. This could be explained by the lack of measurements in the high suction range. The relative errors on the estimation of the remaining parameters are lower than 5 %.

Performing a monodimensional sensitivity analysis based on the calculation of the relative sensitivity, it was concluded that the α curve shape parameter and the saturated water content were the most critical parameters. Fortunately, both parameters are well estimated and are quite independent of errors in the downward flux or the measured water contents.

REFERENCES

Arya, L.M., and J.F. Paris. (1981). A physicoempirical model to predict the soil moisture characteristic from particle-size distribution and bulk density data. *Soil Science Society of America Journal*, **45**, 1023-1030.

Badji, M. (1984). Utilisation de l'eau du sol par une culture (Brachiaria Ruziziensis) en conditions climatiques semi-arides. Analyse expérimentale et simulation numérique. Thèse de doctorat, Katholieke Universiteit te Leuven, 157 p.

Baver, L.D., W.H. Gardner, W.R. Gardner. (1972). *Soil Physics*. 4th ed. John Wiley & Sons, New-York.

Blackmore, A.V., and R.D. Miller. (1961). Tactoid size and osmotic swelling in calcium montmorillonite. *Soil Science Society of America Journal*, **25**, 169-173.

Bresler, E. (1972). Interacting diffuse layers in mixed mono-divalent ionic systems. *Soil Science Society of America Proceedings*, **36**, 891-896.

Bresler, E., B.L. McNeal, and D.L. Carter. (1982). *Saline and Sodic Soils - Principles-Dynamics - Modeling*. Springer-Verlag, Berlin, 236 p.

Brooks, R.H., and A.T. Corey. (1964). Hydraulic properties of porous media. *Hydrol. Pap. n°3*, Colorado State University, Fort Collins, Colorado.

Dufey, J., A. Banin, H.G. Laudelout, and Y. Chen. (1976). Particle shape and sodium self-diffusion coefficient in mixed sodium-calcium montmorillonite. *Soil Science Society of America Journal*, **40**, 310-314.

Durner, W. (1994). Hydraulic conductivity estimation for soils with heterogeneous pore structure. *Water Resources Research*, **30**, 211-223.

Gerald, C.F., and P.O. Wheatley. (1994). *Applied Numerical Analysis*. Fifth edition. Addison Wesley Publishing Company, 748 p.

Glaeser, R., and J. Mering. (1954). Isothermes d'hydratation des montmorillonites bi-ioniques (Na, Ca), *Clay Miner. Bull.*, **2**, 188-193.

Gupta, S.C., and W.E. Larson. (1979). Estimating soil-water retention from particle size distribution, organic matter content and bulk density. *Water Resources Research*, **17**, 1005-1013.

Horn, R.A., and C.R. Johnson. (1988). *Matrix Analysis*. Cambridge University Press, New York, 561 pp.

Klute, A. (1972). The determination of the hydraulic conductivity and diffusivity of unsaturated soils. *Soil Science*, **113**, 264-276.

Kool, J.B., J.C. Parker, and M.Th. van Genuchten. (1987). Parameter estimation for unsaturated flow and transport models - a review. *Journal of Hydrology*, **91**, 255-293.

Kosugi, K. (1994). Three-parameter lognormal distribution model for soil water retention. *Water Resources Research*, **30**, 891-901.

Low, P.F. (1980). The swelling of clay II montmorillonite. *Soil Science Society of America Journal*, **44**, 667-676.

Marshall, T.J., and J.W. Holmes. (1979). *Soil Physics*. Cambridge University Press, 345 p.

Mbagwu, J.S.C. (1995). Saturated hydraulic conductivity in relation to physical properties of soils in the Nsukka Plains, southeastern Nigeria. *Geoderma*, **68**, 51-66.

Monnier, G., P. Stengel, and J.C. Fiès. (1973). Une méthode de mesure de la densité apparente de petits agglomérats terreux. Application à l'analyse des sytèmes de porosité du sol. *Ann. Agron.*, **24**, 523-545.

Mualem, Y. (1976). A new model for predicting the hydraulic conductivity of unsaturated porous media. *Water Resources Research*, **12**, 513-522.

Nelder, J., and R. Mead. (1965). A simplex method for functional minimization. *Computer Journal*, **7**, 308-313.

Parker, J.C., J.B. Kool, and M.Th. van Genuchten. (1985). Determining soil hydraulic properties from one-step outflow experiments by parameter estimation : II. Experimental studies. *Soil Science Society of America Journal*, **49**, 1354-1360.

Quirk, J.P., and L.A.G. Aylmore. (1971). Domains and quasi-crystalline regions in clay systems. *Soil Science Society of America Proceedings*, **35**, 652-654.

Rawls, W.J., D.L. Brakensiek, and K.E. Saxton. (1982). Estimation of soil-water properties. *Trans. ASAE*, **25**, 1316-1320.

Russo, D. (1988). Determining soil hydraulic properties by parameter estimation : on the selection of a model for the hydraulic properties. *Water Resources Research*, **24**, 453-459.

Saxton, K.E., W.J. Rawls, J.S. Romberger, and P.I. Papendick. (1986). Estimating generalized soil water characteristics from texture. *Soil Science Society of America Journal*, **50**,1031-1036.

Shainberg, I., and O. Otoh. (1968). Size and shape of montmorillonite particles saturated with Na/Ca ions. *Israël Journal of Chemistry*, **6**, 251-259.

Shainberg, I., and A. Caiserman. (1969). Kinetics of the formation and breakdown of Ca-montmorillonite tactoids. *Soil Science Society of America Proceedings*, **33**, 547-551.

Shainberg, I., E. Bresler, and Y. Klausner. (1971). Studies on sodium/calcium montmorillonite systems. I. The swelling pressure. *Soil Science*, **111**, 214-219.

Tessier, D. (1984). Etude expérimentale de l'organisation des matériaux argileux. Hydratation, gonflement et structuration au cours de la dessication et de la réhumectation. Thèse Université Paris VII, UER des Sciences Physiques de la Terre, 361 p.

Tessier, D., and G. Pedro. (1987). Mineralogical characterization of 2:1 clays in soils : importance of the clay texture : in *Proceedings of the International Clay Conference, Denver, 1985*. Schultz L.G., H. van Olphen, and F.A. Mumpton, eds., The Clay Minerals Society, Bloomington, Indiana, 74-84.

van Genuchten, M.Th. (1980). A closed-form equation for predicting the hydraulic conductivity of unsaturated soils. *Soil Science Society of America Journal*, **44**, 892-898.

van Genuchten, M.Th., and D.R Nielsen. (1985). On describing and predicting the hydraulic properties of unsaturated soils. *Annales Geophysicae*, **3**, 615-628.

Verburg K., and P. Baveye. (1994). Hysteresis in the binary exchange of cations on 2:1 clay minerals : A critical review. *Clays and Clay Minerals*, **42**, 207-220.

Warkentin, B.P., G.H. Bolt, and R.D. Miller. (1957). Swelling pressure of montmorillonite. *Soil Science Society of America Proceedings*, **21**, 495-497.

Warrick, A.W. (1991). Numerical approximations of Darcian flow through unsaturated soil. *Water Resources Research*, **27**, 1215-1222.

4. Results and discussion

4.1. Introduction

After the theoretical introduction, the second part of the study presented the leaching procedures, the specific experimental device and the different techniques required to achieve our objective. In the third part, the methodology applied to determine the hydrodynamic properties of the unsaturated sandy porous media was explained. Having in mind these theoretical and technical considerations, the results concerning the different flow experiments are presented hereafter and discussed. In this fourth part of the study, we will go through the following points :

- the assessment of the homogeneity of the dry bulk densities (§ 4.2) ;
- the effect of water quality on the total hydraulic conductivities (§ 4.3) ;
- the calculation of the downward flux densities required in the inverse approach (§ 4.3.4) ;
- the spatial distribution of smectite within the experimental columns (§ 4.4) ;
- the evolution of the hydrostatic heads and, hence, the hydraulic gradients (§ 4.5) ;
- the evolution of the volumetric water content and bulk density profiles (§ 4.6).

Finally, the hydrodynamic properties of the unsaturated sandy layer are obtained under steady state flow conditions achieved during the last 30 days of the leaching period. They were determined applying the above-mentioned inverse approach (§ 3.3) with a mean downward flux calculated for the last 30 days. The soil moisture retention curves (MRCs) are described with the functional and non hysteretic van Genuchten (VG) relationships with a four-term parameter vector $(\theta_r, \theta_s, \alpha, n)$. In a first approximation and in order to reduce the number of parameters, the residual water content was assumed to be unaffected by clay migration. Consequently, only three parameters were required to characterize the MRCs. This assumption was analyzed and discussed (§ 4.8).

The hydraulic conductivity curves (HCCs) are described using the same van Genuchten parameters but additional data is required to estimate the saturated hydraulic conductivity (§ 4.9). For the two series of flow experiments, a parameter estimation is presented. The MRCs and HCCs obtained for the unsaturated sandy layer at the end of the percolation periods are presented and discussed.

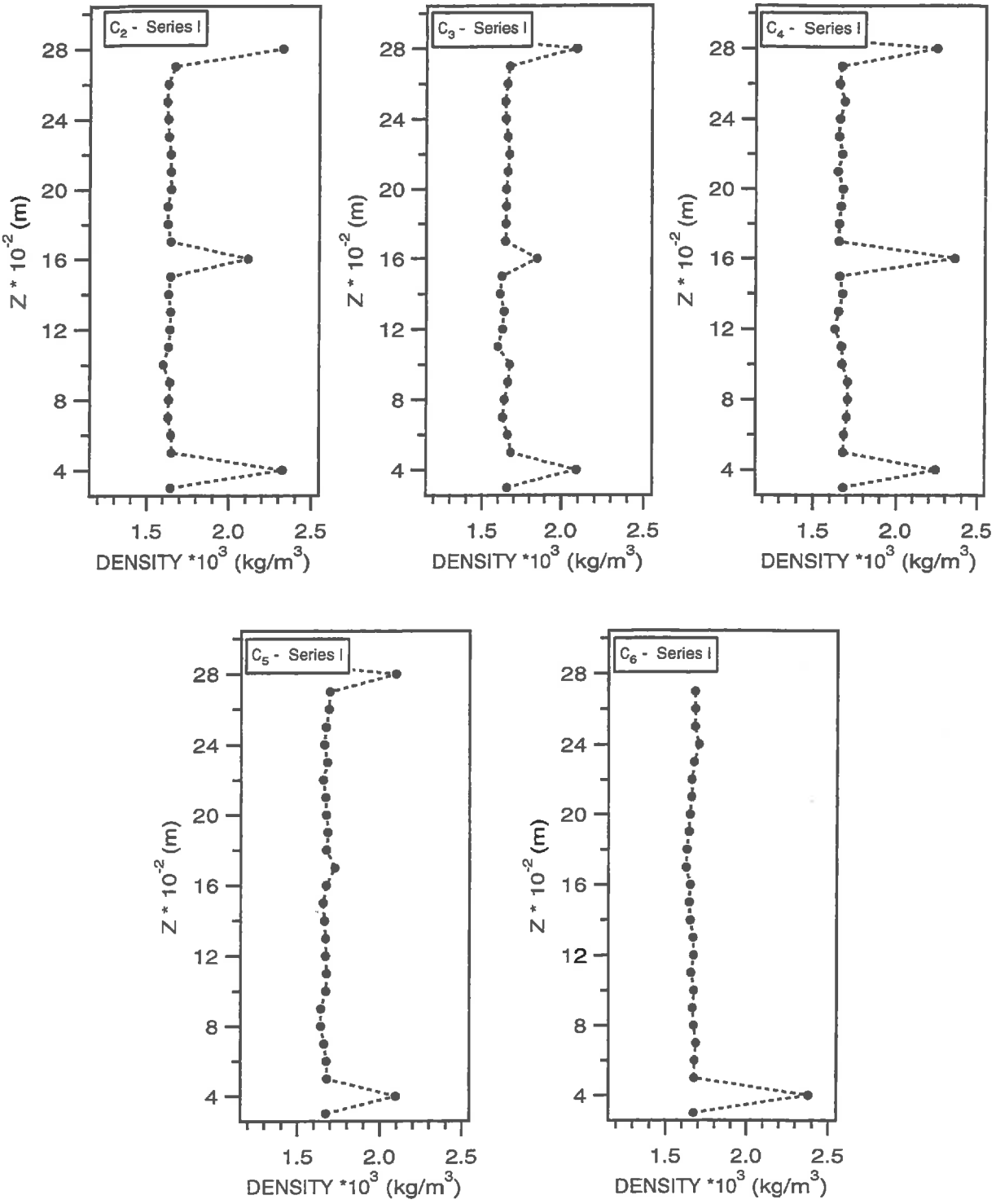

Figure 4.1. Typical dry bulk density profiles, obtained by gamma-radiation, demonstrating the homogeneity of packing within the columns of series I. The increase of the bulk density is due to the presence of the tensiometers.

One should remember the specific aim of each flow experiment series. With the first series the aim was to observe the first migration of clay into clay-free sand under various physico-chemical conditions. The experiments were initially carried out on six columns. Some experimental problems occurred with the first one, leached with a solution of SAR = 5 and TEC = 10 meq/l. The remaining five columns were either percolated with solutions of SAR = 5 (TEC = 5 or 1 meq/l), or SAR = 20 (TEC = 1, 5 or 10 meq/l) during 8 to 10 weeks.

The flow experiments of the second series allowed to assess the change of the MRCs and HCCs, initially at equilibrium with a given SAR and TEC, as a function of the quality of the percolating solution. Flow experiments were carried out on five columns, but again technical problems appeared with one of them. The four remaining columns, hereafter often referred to as C_1, C_2, C_3 and C_5, were first percolated with a solution of SAR = 5 and TEC = 5 meq/l for 3 to 4 weeks. During this first leaching period, total pore volumes ranged from 16 up to 20[16]. Solutions were then changed to simulate the effect of a decreasing total electrolyte concentration (TEC) (C_1), an increasing sodium adsorption ratio (SAR) (C_2), or both (C_3). The last column was leached with deionized water (C_5).

As it will be seen through the discussion hereafter, the flow experiments of series II were conditioned by the results of the first series. It has been observed that leaching with a solution of SAR = 5 and TEC = 5 meq/l induced clay migration and allowed to maintain relatively high hydraulic conductivities. Consequently, this solution was used for the first percolation period of series II. Further, the mass of air-dry Béthonvilliers constituting the upper clayey layer was diminished in order to increase its hydraulic gradient and to generate a higher downward flux density.

The basic results will be first presented, i.e. the bulk densities, the total hydraulic conductivities, and the distribution of water and clay within the columns. These data will be later used in the determination of the VG parameters, describing the MRCs and HCCs.

4.2. Assessment of the homogeneity of the density

The sand of Fontainebleau was packed in the columns by placing the empty ones on a vibrating table and pouring the sand progressively in it during a given filling time (§ 2.6.3). The homogeneity within each column was verified by the means of gamma-radiation. The dry bulk density profiles were obtained from the ^{241}Am countings during 60 seconds (figure 4.1). The presence of the three tensiometers is clearly seen by a considerable increase of the bulk density, except for the columns C_5 and C_6. In these cases the gamma-radiation measurements occurred

(16) It is generally assumed that hydrodynamic equilibrium is obtained after 10 pore volumes.

on both sides of the porous cups located in the middle (C_5 and C_6) and in the upper part of the column (C_6 only).

The profiles for the columns of series II were verified twice by performing an upward and downward scanning because it was observed that the bulk densities of the columns C_1 and C_2 (annexe 4.1) seemed to decrease with depth, in the lower and upper part of the columns, respectively. After verification, it was concluded that it was due to differential packing and not to a shift in the counting rates.

The 99 % confidence limits, associated to the mean bulk densities measured by gamma-radiation, include those obtained on a weight basis (tables 4.1 and 4.2) except for one column of series I. For series I and II, average bulk densities of 1671 kg/m^3 ± 17.5 kg/m^3 and 1685 kg/m^3 ± 7.5 kg/m^3 were respectively obtained.

It was concluded that the dry bulk densities measured by gamma-radiation were reliable, provided the countings were corrected (§ 2.4.3.3 and § 2.4.3.4). The methodology also allowed to conclude that the procedure followed for packing was appropriate and that the columns could be considered to be homogeneously packed.

Table 4.1. Comparison between the bulk densities obtained on a weight basis for the dry columns of series I and the mean values obtained by gamma-radiation (counting time = 60 s) associated to their 99 % confidence limit. The standard deviation on the determination of the dry bulk densities is approximately of 10 kg/m^3.

	Solution	ρ_b (kg/m^3)	$\overline{\rho}_b - 2\ SD$ (kg/m^3)	$\overline{\rho}_b + 2\ SD$ (kg/m^3)
C_2	SAR = 5 ; TEC = 5 meq/l	1647	1619	1659
C_3	SAR = 5 ; TEC = 1 meq/l	1659	1628	1668
C_4	SAR = 20 ; TEC = 10 meq/l	1676	1647	1687
C_5	SAR = 20 ; TEC = 5 meq/l	1686	1651	1691
C_6	SAR = 20 ; TEC = 1 meq/l	1687	1645	1685

Table 4.2. Comparison between the bulk densities obtained on a weight basis for the dry columns of series II and the mean values obtained by gamma-radiation (counting time = 60 s) associated to their 99 % confidence limit. The standard deviation on the determination of the dry bulk densities is approximately of 10 kg/m^3.

	2nd solution :	ρ_b (kg/m^3)	$\overline{\rho}_b - 2\ SD$ (kg/m^3)	$\overline{\rho}_b + 2\ SD$ (kg/m^3)
C_1	SAR = 5 ; TEC = 1 meq/l	1683	1645	1685
C_2	SAR = 10 ; TEC = 5 meq/l	1674	1639	1679
C_3	SAR = 10 ; TEC = 1 meq/l	1691	1671	1711
C_5	deionised water (DW)	1686	1650	1690

4.3. Total hydraulic conductivities

Flow experiments were carried out on the two-layered experimental columns. The upper layer was necessary to maintain the unsaturated flow condition in the lower sandy layer. The presence of the upper layer combined to the chemical composition of the leaching solutions constituted the upper boundary condition. The measurement of the total hydraulic conductivity K_T (eqn. 2.5) is then particularly interesting because it is highly affected by the SAR and the salt solution concentration. The total hydraulic conductivities were measured daily by the falling head method (eqn. 2.5). Before presenting the results, it seemed important to discuss about the change in thickness of the upper layer as a response to the different leaching solutions. Indeed, an increase of the upper layer thickness due to swelling affects the hydraulic gradient through the upper clayey layer (Béthonvilliers soil material). Swelling of this layer was quantified and is discussed hereafter (§ 4.3.1).

The validity of Darcy's law in columns leached with various solutions was verified and will also be discussed. Finally, the total hydraulic conductivities combined to the total hydraulic gradient allowed for the calculation of the downward flux densities required in the inverse approach.

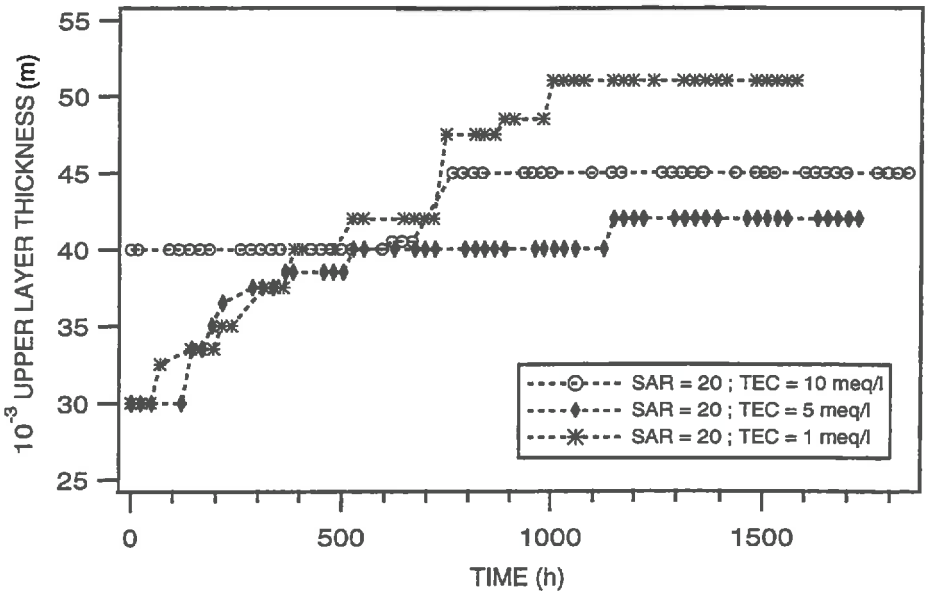

Figure 4.2. Evolution of the upper clayey layer average thickness in response to leaching solutions of SAR = 20 and TECs of 1, 5 and 10 meq/l. The thicknesses remained constant for the columns leached with a solution of SAR = 5 and were not added.

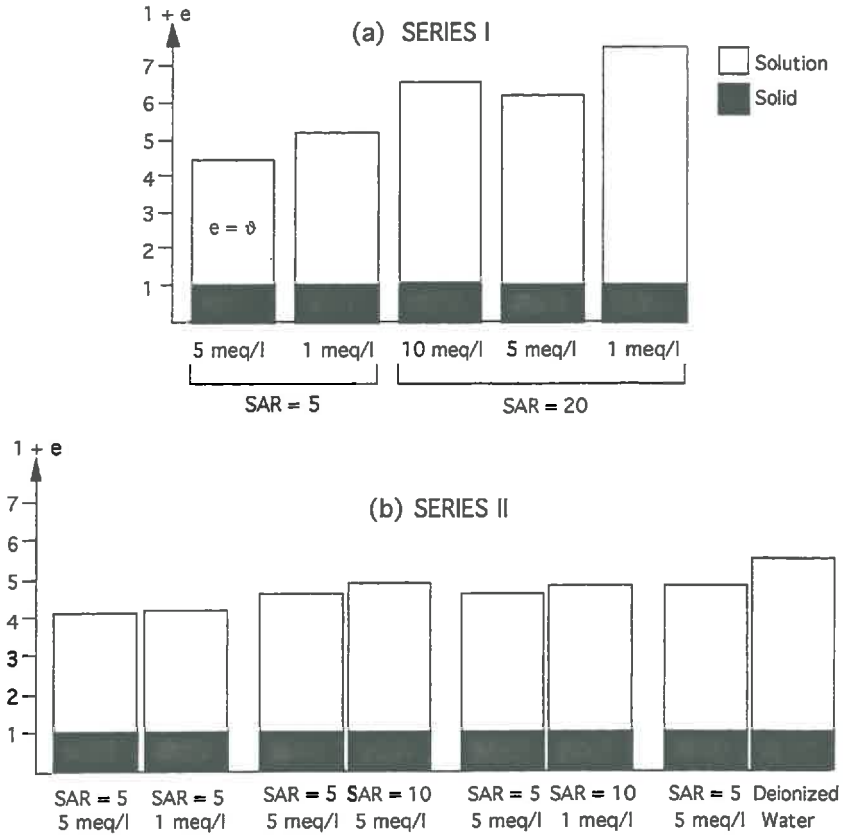

Figure 4.3. Apparent volumes occupied by the upper clayey layer at the end of the percolation periods, respectively for series I (a) and II (b).

4.3.1. Upper layer behaviour in response to the leaching solutions

For an identical mass of air-dried soil material (45 g in series I) characterized by a given ESP it was observed that the average thickness of the upper layer remained constant during the percolation period for the columns leached with a solution of SAR = 5 and TECs of 5 meq/l (3 cm) and 1 meq/l (3.5 cm). For the other columns leached with SAR = 20, differences appear between a TEC = 10 meq/l and TEC values of 1 and 5 meq/l. For the latters, the thicknesses increased progressively until a plateau was obtained (figure 4.2). This evolution suggests more a progressive step-wise macroscopic swelling induced by the use of low TECs (1 and 5 meq/l) and a high SAR value (20). The higher the SAR and the lower the TEC, the more the clayey Béthonvilliers layer swoll. When a higher TEC was used, the observations seem to suggest a more rapid hydration of the Béthonvilliers soil material. Indeed, from the very beginning of the leaching procedure a constant thickness was measured (4.0 cm) for more than 600 hours before slightly increasing and stabilizing then till the end of the experiment. One should also note that the upper layer for the column leached with SAR = 20 and TEC = 10 meq/l is thicker than that of SAR = 20 and TEC = 5 meq/l. This could eventually be explained by differences in packing of the Béthonvilliers soil material though the same procedure has been applied to all the columns. Finally, one can conclude that limited swelling was induced with the solutions of SAR = 5, but extensive swelling occurred during leaching with SAR = 20.

The swelling can be quantified in terms of apparent volumes at the end of the percolation period, given by the ratio of the total volume to the volume of solid *(Tessier, 1984)*. Assuming that the total void volume is occupied by water, i.e. $e = \vartheta$, it can be written that :

$$\frac{V_s + V_v}{V_s} = 1 + \vartheta, \tag{4.1}$$

where e and ϑ are respectively the void ratio and the liquid ratio given by eqn. (1.7). It is clearly seen that the volume of water per unit volume of solid increases with the SAR (figure 4.3). For a TEC of 1 meq/l the apparent volume equals 5.16 and 7.51 for a SAR of 5 and 20, respectively. Those corresponding to a higher electrolyte concentration (5 meq/l) are equal to 4.42 (SAR = 5) and 6.19 (SAR = 20). Comparing the apparent volumes for a given SAR, the apparent volume should increase with a decrease of the TEC. Though a greater apparent volume is obtained with TEC = 10 meq/l rather than 5 meq/l. One explanation could be found in a differential packing of the Béthonvilliers soil material.

For the flow experiments of series II the apparent volumes at the end of the first percolation period varied from 4.14 up to 4.81 when the columns were leached with SAR = 5 and TEC = 5 meq/l. These small discrepancies can be explained by differences in the packing of the Béthonvilliers soil material.

Swelling caused by a change in the electrolyte concentration and SAR of the leaching solutions was quantified by the use of a more appropriate parameter. It takes into account the evolution of the void ratio when the solution is changed Δe and the initial apparent volume determined for the dry clay soil material $(1 + e_o)$. This parameter is given by $(\Delta e/(1 + e_o))$ *(Tessier, 1984).*where Δe is the difference between the void ratios calculated at the end of the first and second percolation period, respectively. Results are presented in table 4.3. Extensive swelling was not expected because solutions of low SARs (5 and 10) and low TECs (1 and 5 meq/l) were used *(Shainberg and Caiserman, 1969)* and due to the high layer cell of the Béthonvilliers smectite (§ 2.3.3.1). The effect of a decrease of the TEC (C_1), an increase of the SAR (C_2) or both (C_3) induced limited swelling, even when deionized water (C_5) replaced the leaching solution. Limited in situ clay swelling due to a gradually decreasing of the TEC has also been mentioned by *Keren and Singer (1988).*

It is obvious that the behaviour of the clayey layer can also been explained by remembering the specific arrangement of smectite (§ 3.2.1) or even the hypothesized distribution of cations as proposed by *Verburg and Baveye (1994).* Small quantities of sodium are assumed to adsorb preferentially on the external surfaces of the quasi-crystals while calcium would remain in the interlayer positions. For low TEC, the repulsive forces act between the quasi-crystals but its integrity is maintained. This is accompanied by little swelling. For higher amounts of sodium (corresponding to higher SAR), sodium would invade the interlayer positions. Consequently, interlayer swelling develops at the expense of the destruction of the quasi-crystal arrangement.

Table 4.3. Assessment of the upper layer swelling due a change of the electrolyte concentration or the salinity of the leaching solutions (series II). The number of the columns refers to the chemical treatment of table 4.2.

	e_1 (1)	e_2 (2)	$\Delta e/(1 + e_o)$
C_1	3.14	3.22	0.03
C_2	3.64	3.89	0.11
C_3	3.64	3.81	0.07
C_5	3.81	4.55	0.32

with $(1 + e_o) = 2.32$

(1) void ratio calculated at the end of the first percolation period ;

(2) void ratio calculated at the end of the second percolation period.

4.3.2. Total hydraulic conductivities

Taking into account the variable length of the stratified columns, the total hydraulic conductivities (HCs) were measured daily according to the falling head method. Calculations were performed with cross-sectional areas for the small tube and the soil sample of respectively 2.83e-5 m^2 and 2.55e-3 m^2 (eqn. 2.5). The initial and final hydraulic heads were specific to each column. The total hydraulic conductivities are given as a function of time in figures 4.4a and 4.4.b for the columns of series I and II, respectively.

The two mechanisms which are suggested for HC reductions are swelling and dispersion *(Quirk and Schofield, 1955)*. Under our experimental conditions and due to the large amount of smectite, the observed decrease of the total hydraulic conductivity is probably mainly due to swelling as proposed by *McNeal et al. (1966)*. According to them, a two-step process would occur in soils containing large amounts of expansible clay. The first step consists in swelling which initiates the second step, i.e. dispersion and clay movement by weakening the interparticle bonds resulting from swelling. Further, dispersion can occur in the whole SAR range provided the TEC is below a critical flocculation concentration (CFC). However, due to the constraints induced by swelling, migration of dispersed clay particles within such samples is highly reduced *(Chen and Banin, 1975)*. Clay quantification by the means of X-ray fluorescence spectrometry (§ 2.5) at the end of the percolation period confirmed that clay dispersion and particle movement from the upper layer towards the unsaturated layer of Fontainebleau sand, occurred in all the columns (§ 4.4).

The measured hydraulic conductivities decreased rapidly before stabilising after approximately 200 hours and 500-600 hours of percolation for solutions of SAR = 5 and SAR = 20, respectively. Limited swelling was induced by leaching with SAR = 5 and TEC = 5 meq/l and, hence, a relatively high HC could be maintained (annexe 4.2). However, with the use of a more diluted solution (TEC = 1 meq/l), the total hydraulic conductivity dropped from 1.39e-7 m/s to 7.94e-9 m/s. Extensive swelling of the upper clayey layer which occurred when the columns were leached with SAR = 20 (10, 5 or 1 meq/l) explains the very low hydraulic conductivity values, ranging from 1.26e-9 m/s to 1.55e-9 m/s.

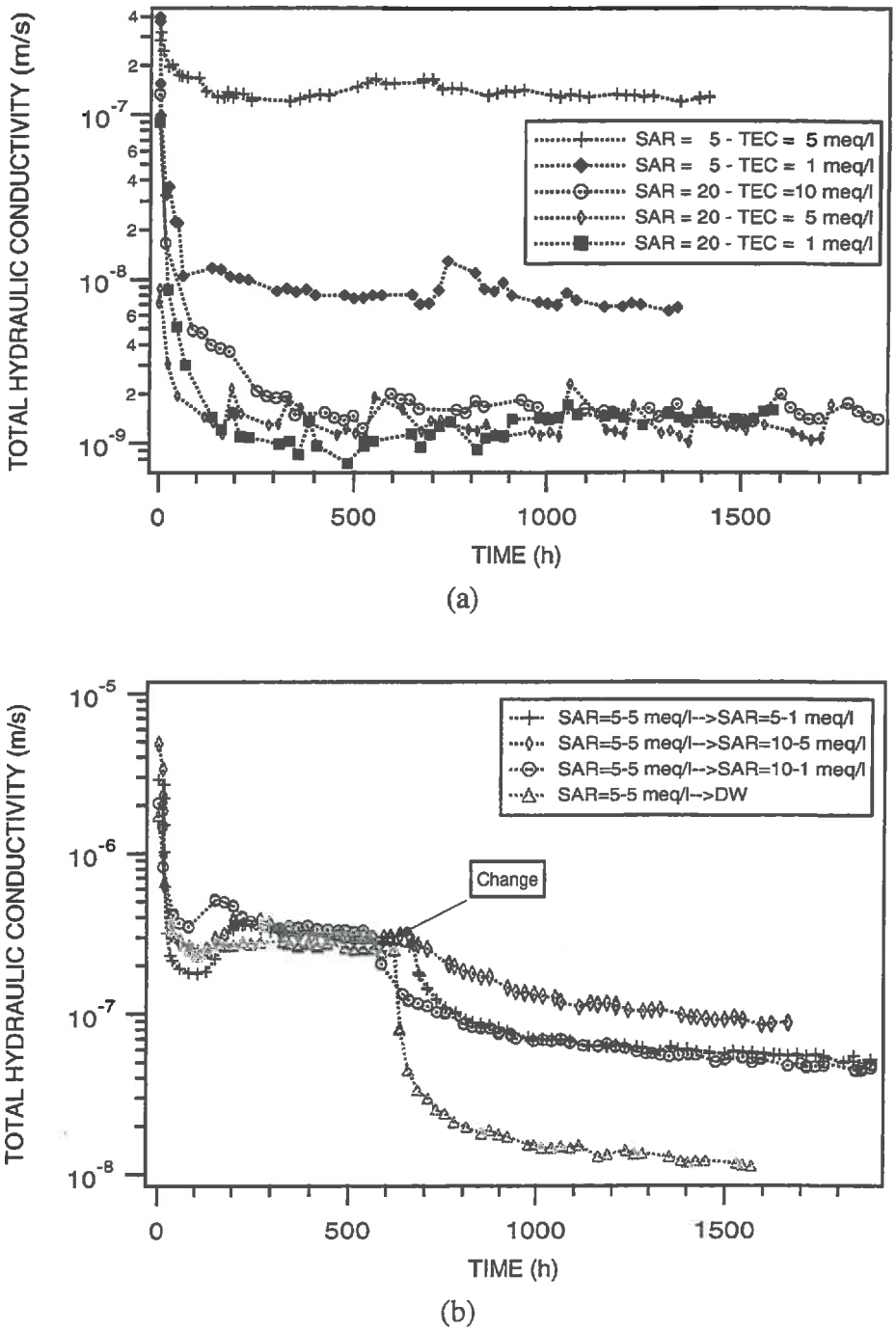

Figure 4.4 Total hydraulic conductivities, measured by means of the falling head method, for the columns of the first (a) and second (b) flow experiments.

Comparing the total hydraulic conductivities measured for columns leached with a same solution (series II), it was observed that they decreased rapidly to a certain extent, before increasing and stabilising after 200 hours (figure 4.4b). The increase in the total hydraulic conductivity could neither be explained by the renewal of the solution nor by a change in the experimental conditions. Consequently, it was concluded that the increase of the measured HC was due to particle translocation from the clayey layer, allowing higher HC to be maintained. In this case, the difference between the minimum measured HC and the relatively constant values of the plateau would be proportional to the amount of clay that migrated. The reason for the occurrence of dispersion and particle translocation with such leaching solutions will be discussed later, and its consequences on the measurement of the hydraulic heads (§ 4.5), on the volumetric water contents (§ 4.6), on the bulk density profiles (§ 4.6) as well as on the hydrodynamic properties (§ 4.8 and § 4.9) will be assessed hereafter.

When the solution of SAR = 5 and TEC = 5 meq/l was replaced by a more diluted one of equal SAR, the HC decreased of about 81 % of the mean HC obtained with the former solution. A similar effect was obtained with SAR = 10 and TEC = 1 meq/l (reduction of about 86 %), but it should be noted that the HC diminished slowly. Maintaining a constant TEC but increasing the SAR of the leaching solution induced a reduction of about 69 %. Finally, when deionized water replaced the solution of SAR = 5 and TEC = 5 meq/l, the total hydraulic conductivity dropped sharply (94 % reduction). The observed rapidity of the HC decrease suggests an abrupt sealing of the pore space due to entrapped dispersed clay whereas a gradual sealing occurs probably due to a re-orientation of dispersed clay particles. This is the case when leaching with SAR = 10 for both TECs. Similar observations were made by *McNeal et al. (1966)* and *Frenkel et al., (1978)* amongst others.

4.3.3. Validity of Darcy's law in stratified experimental columns

Darcy's law application is valid if a linear relationship between the cumulated effluent volume versus the cumulated time exists. The total hydraulic conductivity is then constant and does not decrease with time due to particle rearrangement as proposed by *Aringhieri and Capurro (1994)*. The slope of that linear relationship is proportional to the total hydraulic conductivity, the soil sample cross-sectional area and the total hydraulic gradient. The hydraulic gradient can be considered constant within the columns of a given series - it ranges from 2.40 to 2.51 for series I and from 2.62 to 2.68 for series II. The value of the hydraulic conductivity obtained by assuming a mean total hydraulic gradient represents an average value obtained for a given solution as a function of the SAR and the TEC (figures 4.5 and 4.6). The total HC calculated from the slope of the linear part relating the effluent volume *versus* time (annexes 4.4 and 4.5)

are generally slightly higher than those calculated for the last 30 days of the corresponding leaching period (annexe 4.2 and 4.3).

Dispersion and particle migration are proposed to occur at the early beginning of the experiments (§ 4.3.2). Due to limited clay migration later on through the clayey layer, a constant hydraulic conductivity and a linear effluent volume-time relationship occurred.

It was concluded that Darcy's law was applicable. This is justified by the fact that first, the cumulated effluent volume was linearly related to the time. Second, the total hydraulic conductivity and the total hydraulic gradient remain physically independent variables despite the chemical leaching conditions.

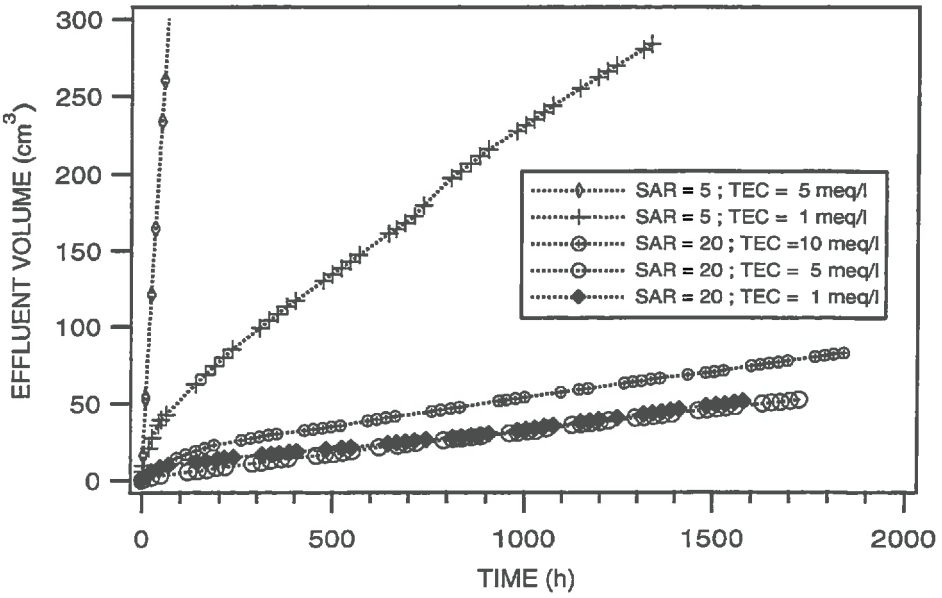

Figure 4.5. Verification of the applicability of Darcy's law for stratified columns leached with intermediate SARs (5 and 20) and low electrolyte concentrations (1, 5, 10 meq/l) by relating the effluent volume versus the cumulated time.

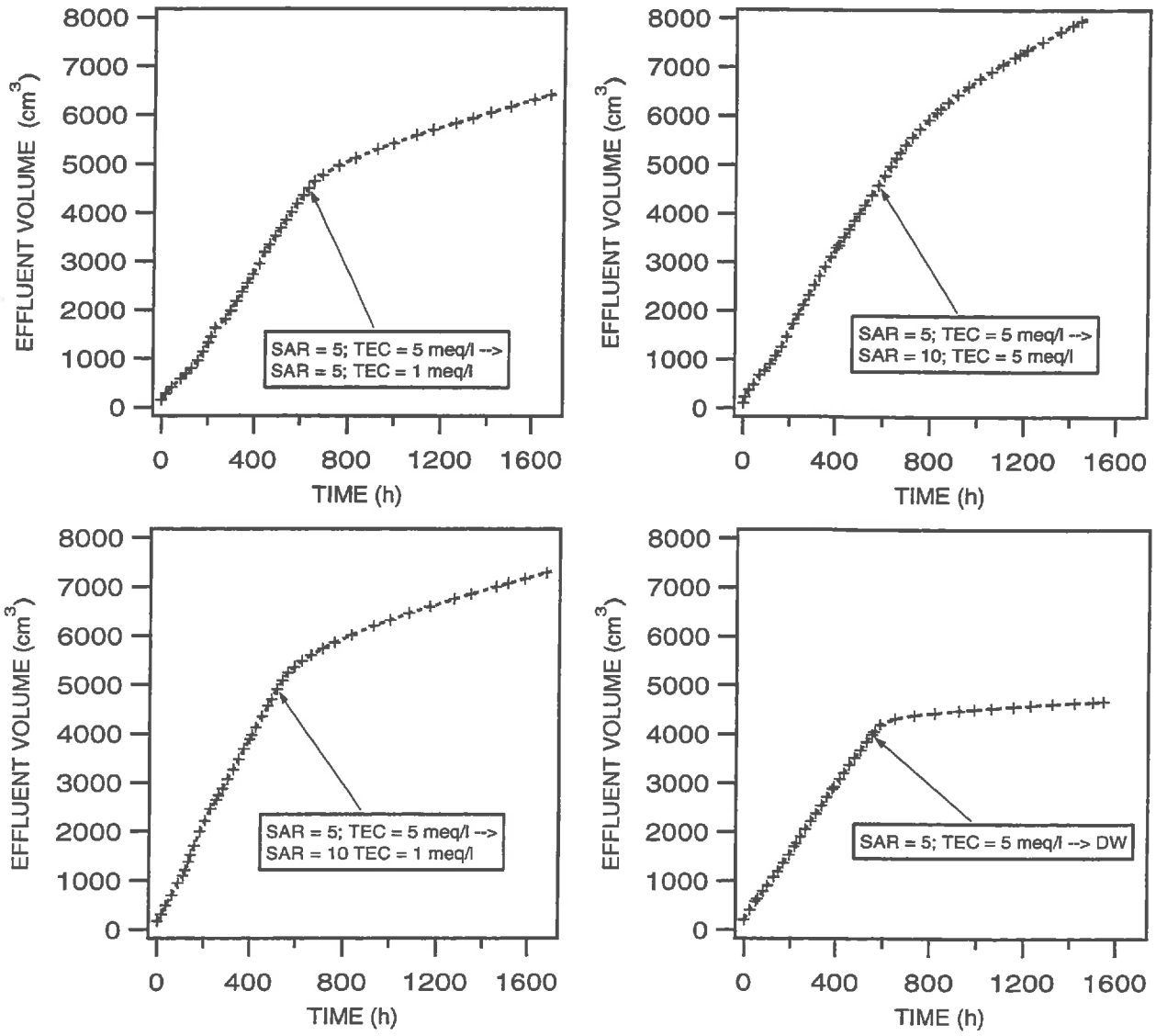

Figure 4.6. Relationships between the effluent volume versus the cumulated time to verify the applicability of Darcy's law for stratified columns first leached with a solution of SAR = 5 and a TEC = 5 meq/l. The solution is replaced by decreasing the TEC, increasing the SAR or both.

Table 4.4. Mean flux densities calculated for the last 30 days of the leaching period and the standard deviations used to estimate the van Genuchten parameters describing the MRCs at the end of the percolation period (series I). Each flux density was obtained from the product of the total hydraulic conductivity and the total hydraulic gradient.

Solution	$\overline{q}$ (m/s)	SD (m/s)
SAR = 5 ; TEC = 5 meq/l	3.49e-7	3.16e-8
SAR = 5 ; TEC = 1 meq/l	1.96e-8	3.23e-9
SAR = 20 ; TEC = 10 meq/l	3.72e-9	4.02e-10
SAR = 20 ; TEC = 5 meq/l	3.04e-9	6.24e-10
SAR = 20 ; TEC = 1 meq/l	3.18e-9	4.60e-10

Table 4.5. Mean flux densities and standard deviations used to estimate the van Genuchten parameters describing the MRCs at the end of the first (SAR = 5 ; TEC = 5 meq/l) and second percolation period (series II).

	$\overline{q}$ (m/s)	SD (m/s)	2nd solution	$\overline{q}$ (m/s)	SD (m/s)
C_1	7.53e-7	6.92e-8	SAR = 5 ; TEC = 1 meq/l	1.47e-7	6.20e-9
C_2	8.22e-7	6.48e-8	SAR = 10 ; TEC = 5 meq/l	2.56e-7	2.18e-8
C_3	9.41e-7	1.28e-7	SAR = 10 ; TEC = 1 meq/l	1.33e-7	9.24e-9
C_5	6.98e-7	2.97e-8	deionised water	4.30e-8	1.44e-8

4.3.4. Downward flux densities

Parameter estimation for the determination of the hydrodynamic properties requires the knowledge of the downward flux densities corresponding to each column. For the flow experiments within series I, fluxes could not accurately be measured without significant errors due to the small effluent volumes. Therefore, they were calculated based on the measured total hydraulic conductivity, applying the falling head method and the measured total hydraulic gradient (table 4.4). The standard deviations associated to the mean values calculated for the last 30 days of the leaching period take into account the fluctuations of both measurements. Even though the effluent volumes were greater for the series II flow experiments, especially during the first percolation period, it was preferred to apply the same procedure (table 4.5).

In series I flow experiments, mean flux densities were extremely low, ranging from 1.26 mm/h for SAR = 5 and TEC = 5 meq/l down to approximately 0.01 mm/h for SAR = 20. To avoid similar problems in the second series, the mass of Béthonvilliers soil material was reduced to 20 g instead of 45 g. This resulted in a thinner upper layer, a greater hydraulic gradient through it and hence in higher downward flux densities values. The mean downward flux densities for the first percolation period of series II (SAR = 5 ; TEC = 5 meq/l) varied in the range 2.5 mm/h and 3.4 mm/h. Depending on the solution used for the second period, the values ranged from 0.9 mm/h (SAR = 10 ; TEC = 5 meq/l) down to 0.15 mm/h (deionized water).

4.3.5. Partial conclusions

The hydraulic conductivity (HC) is particularly sensitive to the SAR and electrolyte concentration of leaching solutions but no clear relationship could be established between the measured total hydraulic conductivity, SAR, TEC and clay amount. The total hydraulic conductivities for the two-layered experimental columns were determined daily by means of the falling head method. The calculations were performed taking into account the changes in thickness of the upper layer which were expected in response to the SAR and TEC of the leaching solutions. Swelling was quantified and it was concluded that only limited swelling was induced by leaching with SAR = 5. However, extensive swelling occurred with SAR = 20.

The HC measurements were also used to justify particle translocation from the upper saturated clayey layer towards the unsaturated sandy layer. This was initially not expected.

Despite the fact that the columns were leached with saline solutions, the hydraulic conductivity and hydraulic gradient remained physically independent variables. Furthermore,

the cumulated effluent volume was still linearly related to the time. These considerations allowed to conclude that Darcy's law was applicable in our study.

Finally, the measurements of the total hydraulic conductivity combined to those of the total hydraulic gradient allowed to calculate the downward flux densities required for the determination of the soil moisture retention curves (MRCs) and hydraulic conductivity curves (HCCs) by the inverse approach. One should also note that due to differences in the hydraulic conductivities, the columns of a given series were not submitted to the same upper boundary conditions.

4.4. Clay contents

Dispersion of smectite occurred with solutions of SAR = 5 and TEC = 5 meq/l. This concentration is higher than some critical flocculation concentrations (CFC) mentioned in the literature. This can be explained by the observations of *Frenkel et al (1992a, 1992b)* and *Goldberg and Forster (1990)* who highlighted the differences between soil and reference clays in terms of CFC. Soil clays are generally more dispersive than reference clays, requiring greater salt concentrations at all SARs and pH values. Furthermore, mechanical disturbance, i.e. crushing of the sample and sieving, affects clay dispersion by increasing their sensitivity to sodicity *(Sumner, 1993)*. Further, the sensitivity to excessive exchangeable sodium and low TECs increases with the clay contents *(Frenkel et al., 1978)*. Consequently, it is not surprising to observe dispersed smectite within the sandy subsamples, even with solutions of SAR = 5 and TEC = 5 meq/l.

At the end of experiment, clay was quantified from an elevation head z = 3 cm up to z = 28 cm using X-ray fluorescence spectrometry (§ 2.5). The last sample collected in the upper part of the sandy column has a smaller length equal to 1 cm. The clay content profiles are presented in figures 4.7 and 4.8 in terms of volumetric ratios, i.e. the volume of smectite per unit volume of soil (eqn. 2.20). Smectite was found at all the depths and not only in the first centimetres of the unsaturated sandy layer, though absent from the effluent volumes. This has been proved by filtering the effluent volumes using a 0.22 µm filter. X-ray measurements were performed on these filters but neither illite or kaolinite, nor smectite were detected. This has been performed also without filtering the effluents and no clay has been detected in the solutions. Nevertheless, it should be noted that the amounts of smectite are particularly low, less than 0.004 m^3/m^3, but these results are in complete agreement with those of *Somaratne (1994)*. In his study achieved under saturated flow conditions deposits ranged from 9e-3 m^3/m^3 down to 6e-6 m^3/m^3 in the upper 5 cm, except in the top first centimeters where most of the particles were deposited.

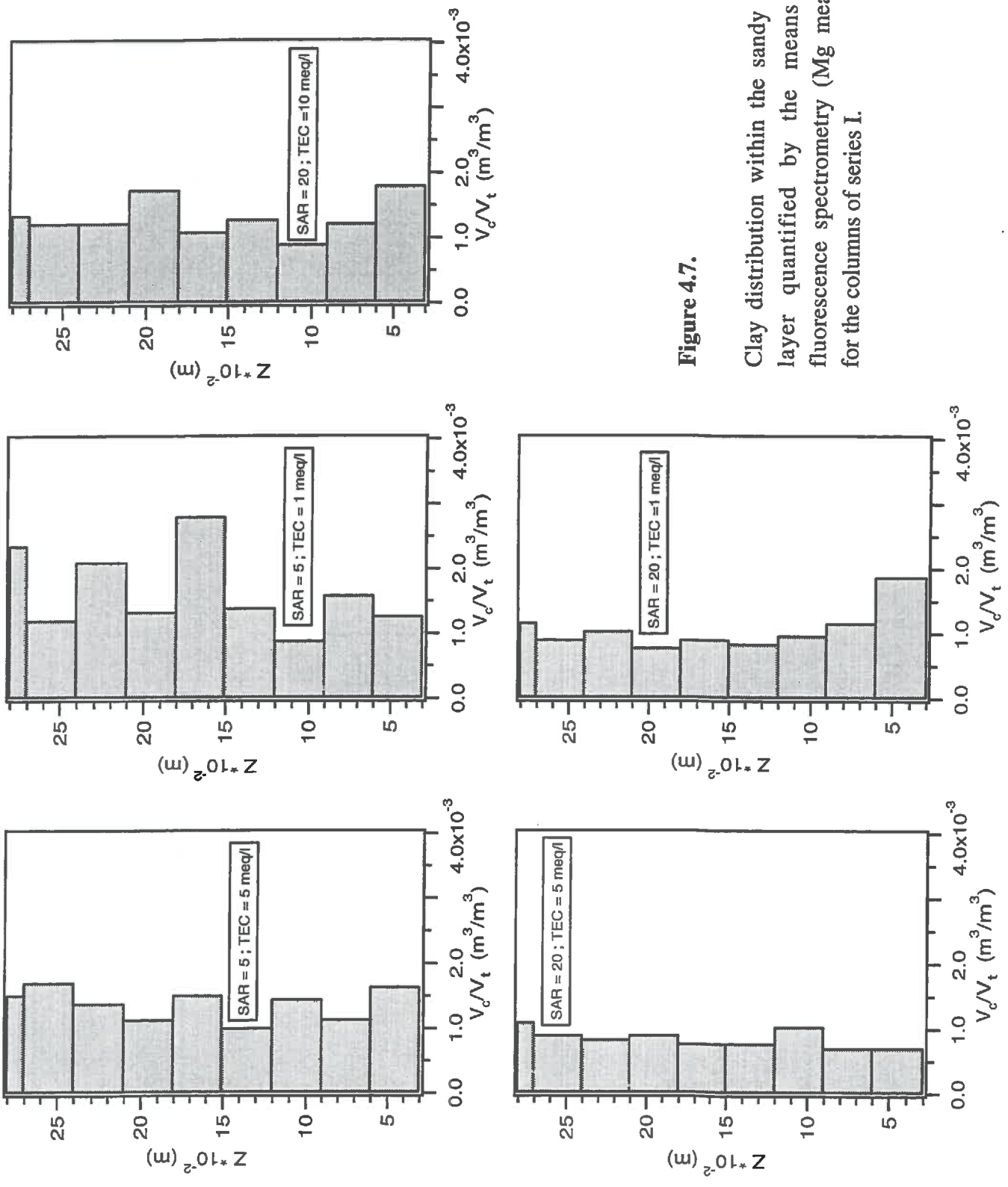

Figure 4.7.

Clay distribution within the sandy unsaturated layer quantified by the means of X-ray fluorescence spectrometry (Mg measurements) for the columns of series I.

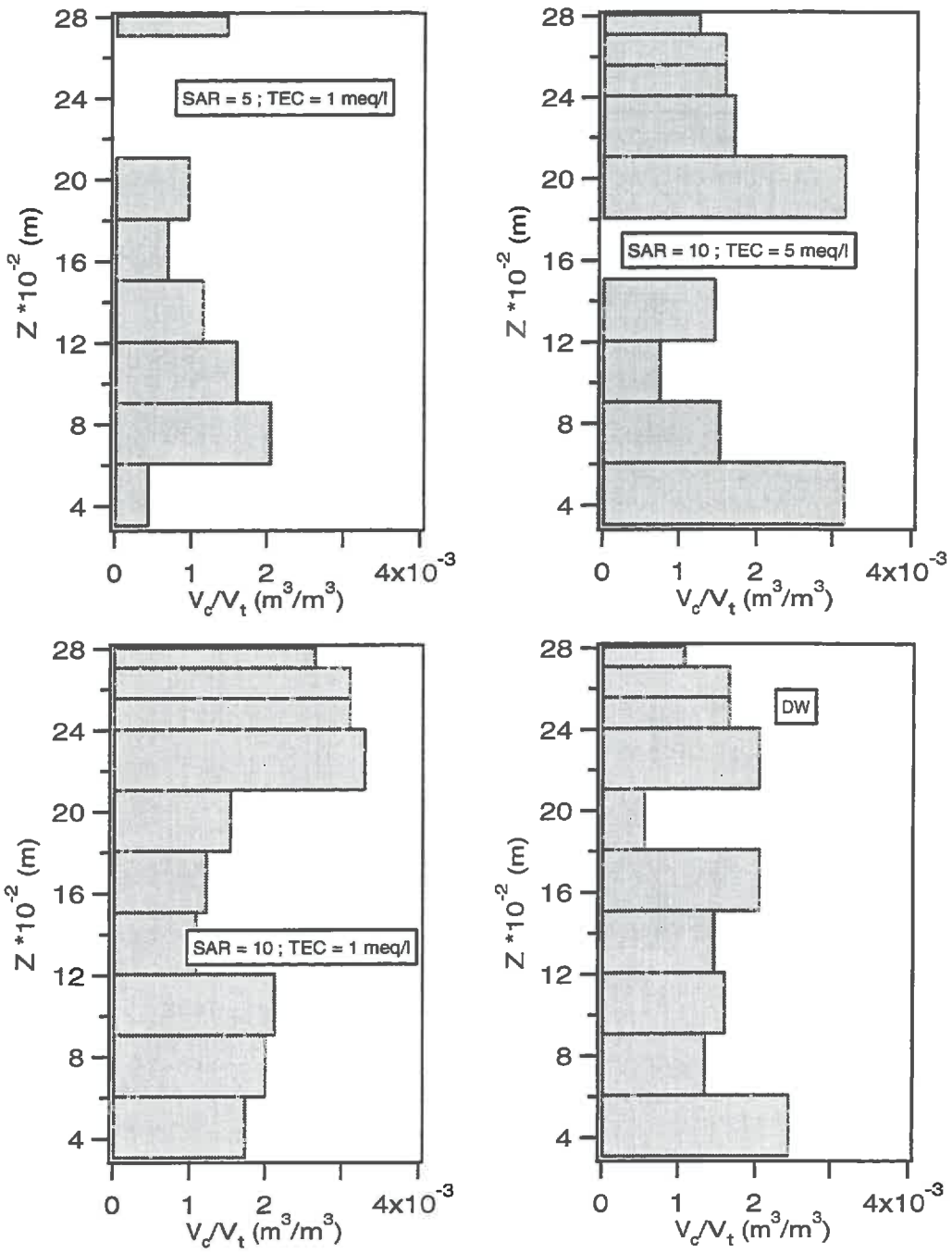

Figure 4.8. Clay distribution within the sandy unsaturated layer quantified by the means of X-ray fluorescence spectrometry for the columns of series II.

Furthermore, the presence of clay particles everywhere in the column seems to be in contradiction with the conclusions of *Wan and Wilson (1994)*. They mentioned that the presence of a gas phase would act as a barrier and would slow down clay movement through a porous media. According to them, colloid particles would preferentially sorb onto the gas-water interface relative to the solid matrix surface under typical groundwater conditions. Under our experimental conditions, the presence of smectite can be justified in two ways. First the smallest particles probably migrated, i.e. those whose size is less than 0.2 µm. Second, gamma-radiation measurements required to disconnect the three tensiometers and the small reservoir which was used to apply the suction at the bottom of the column. The gas phase is then no longer stationary. This induces a redistribution of water within the column, though limited as it was verified by performing consecutively an upward and downward volumetric water content-bulk density profile. In contrast with the role of a stationary sorbent gas phase, moving interfaces could explain the movement of clay particles further down the column. This has also been suggested by *Wan and Wilson (1994)*.

4.5. Evolution of the suctions

It seems obvious that particle migration within an initial clay-free sand will induce changes in the soil-water pressure, negative hydrostatic heads or matric potentials, called suction. An augmentation of the amount of clay at a given depth in the column will result in an increase in the amount of water retained by the dispersed smectite particles. This is accompanied by a reduction of the suction. This is in complete agreement with the general understanding of the soil moisture retention curves (MRCs).

The suctions were measured daily by the means of three tensiometers installed respectively in the upper, middle and lower part of the sandy unsaturated layer of each experimental column. The tensiometers were connected to mercury manometers. For each porous cup, a simple equation was established in order to calculate the suction (annexe 4.6).

Results concerning series I are given in annexe 4.7 and the most significant ones are illustrated in figure 4.9. These results were obtained for the column leached with SAR = 20 and TEC = 1 meq/l. In the upper part of the unsaturated layer, the hydrostatic head increased from - 0.52 m of water column (- 5.2 kPa) to approximately - 0.20 m (- 2 kPa). For this column especially the reduction of the suction was accompanied by a considerable increase of the volumetric water content of about 15 % (figure 4.10). However, the clay profiles (figure 4.7) do not exhibit a high clay amount though the presence of brownish stains one centimetre beneath the clayey layer.

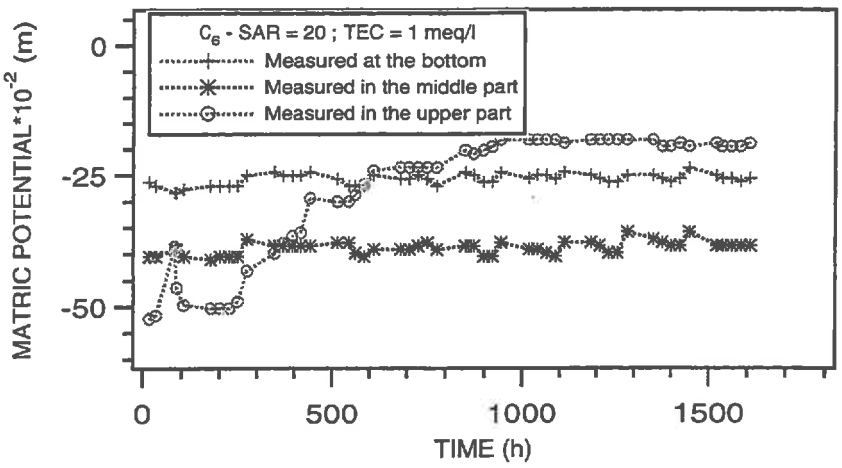

Figure 4.9. Evolution of the suctions measured at three different depths in the column leached with SAR = 20, TEC = 1 meq/l (series I).

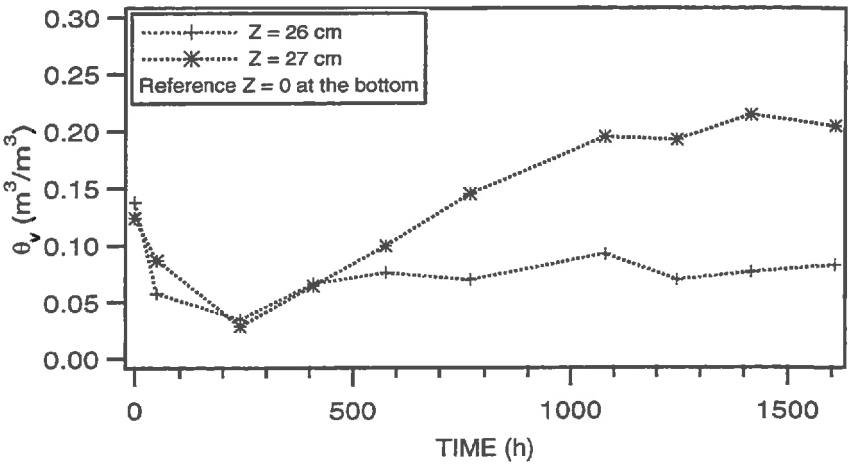

Figure 4.10. Evolution of the measured volumetric water contents in the column leached with SAR = 20 and TEC = 1 meq/l in the top centimeters of the unsaturated layer whose total thickness equals 28.2 cm (series I).

This is due to the fact that clay quantification by X-ray fluorescence spectrometry was performed after mixing the sand of each column ring. A better estimation of the clay amount could have been obtained if clay had been quantified by sampling only the first top millimeters of this ring.

A progressive decrease of the suction was also observed in the first tensiometer of the column leached with SAR = 5 and TEC = 5 meq/l (C_2), and to a lesser extent for the columns leached with a solution of a TEC of 5 meq/l (C_5) and 10 meq/l (SAR = 20) (C_4) (annexe 4.7). Hydrostatic head decreases only in the upper part of the unsaturated layer. The measurements exhibit rather stable values in the middle and lower part of the columns except for C_4.

For the series II flow experiments (figure 4.11), the matric potentials are presented as a function of the pore volume ($\cong$ 260 cm^3). To facilitate their interpretation, the total hydraulic conductivities were added. At the very beginning of the percolation period, the rapid decrease of the total hydraulic conductivity induced a reduction of the water contents (annexe 4.9) and an increase of the suctions. This is particularly clear for C_5. For instance, after approximately 5 pore volumes a constant matric potential of about - 0.42 m is measured in C_5. In the columns C_1 and C_2 it should be noted that the reduction of the suctions is observed together with an increase of the volumetric water contents and the total hydraulic conductivity (§ 4.3.2) which was explained by clay migration. Then the matric potentials remained constant until the solution was changed.

With the change of the leaching solutions, two typical behaviours were observed. For columns leached with a SAR = 10, a gradual sealing due to a re-orientation of dispersed clay particles was proposed to explain the total hydraulic conductivity decrease (§ 4.3.2). Particle translocation from the top layer towards the unsaturated layer is allowed, inducing a reduction of the suction which was measured in the column leached with SAR = 10 and TEC = 1 meq/l (C_3 - figure 11c). This reduction of about 0.05 m of water column occurred only 2 pore volumes after changing the leaching solution. The suction then further progressively decreased for the more diluted solution (1 meq/l), but stabilized matric potentials were measured with 5 meq/l (C_2 - figure 4.11b). It seems reasonable to assert that the amount of clay which induces a reduction of the suction is small because no change in the total hydraulic conductivity was observed after the solution was changed.

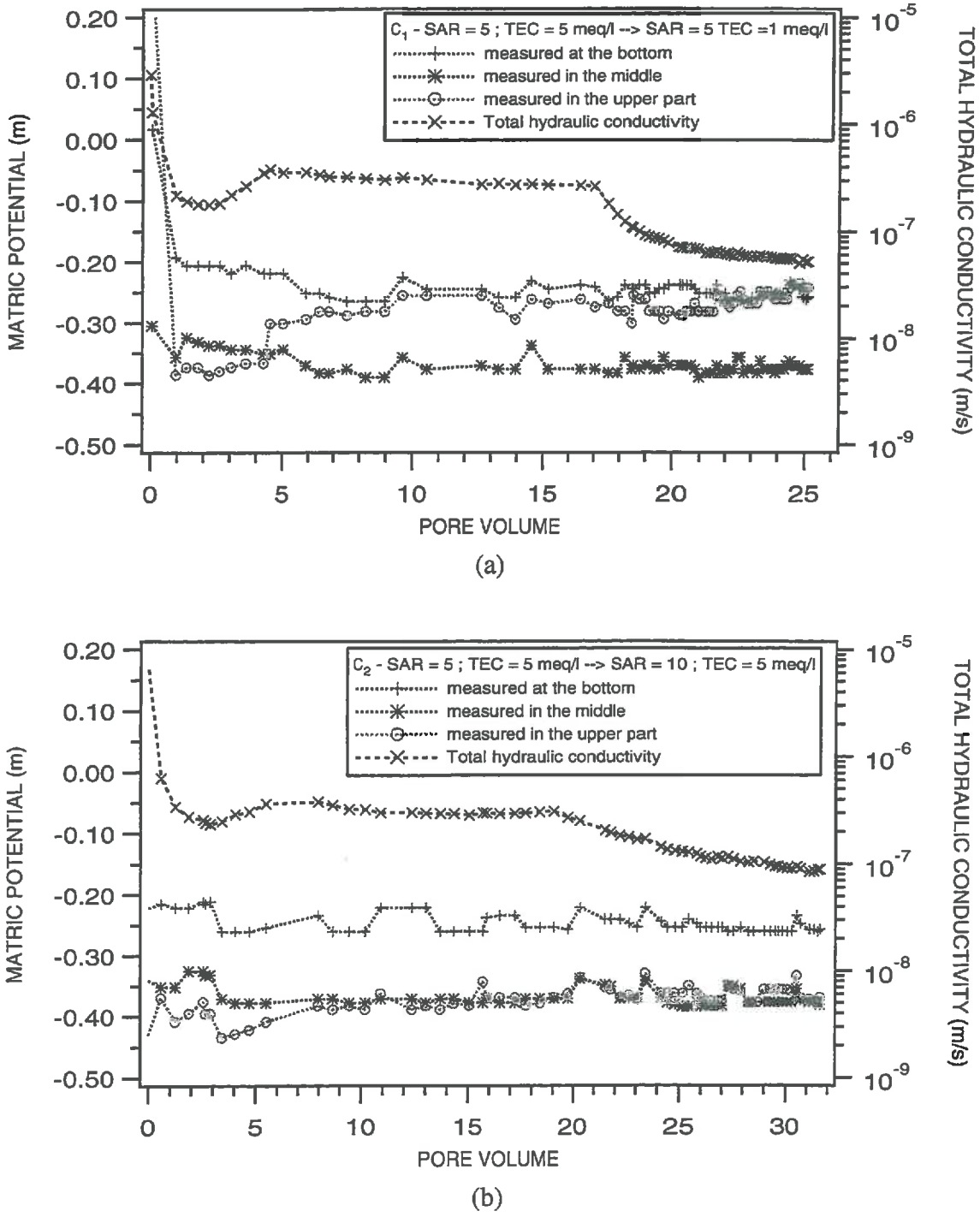

Figure 4.11. Evolution of matric potentials measured at three different depths in the experimental columns as a function of the pore volume (1 pore volume is approximately equal to 260 cm^3). The total hydraulic conductivities were added.

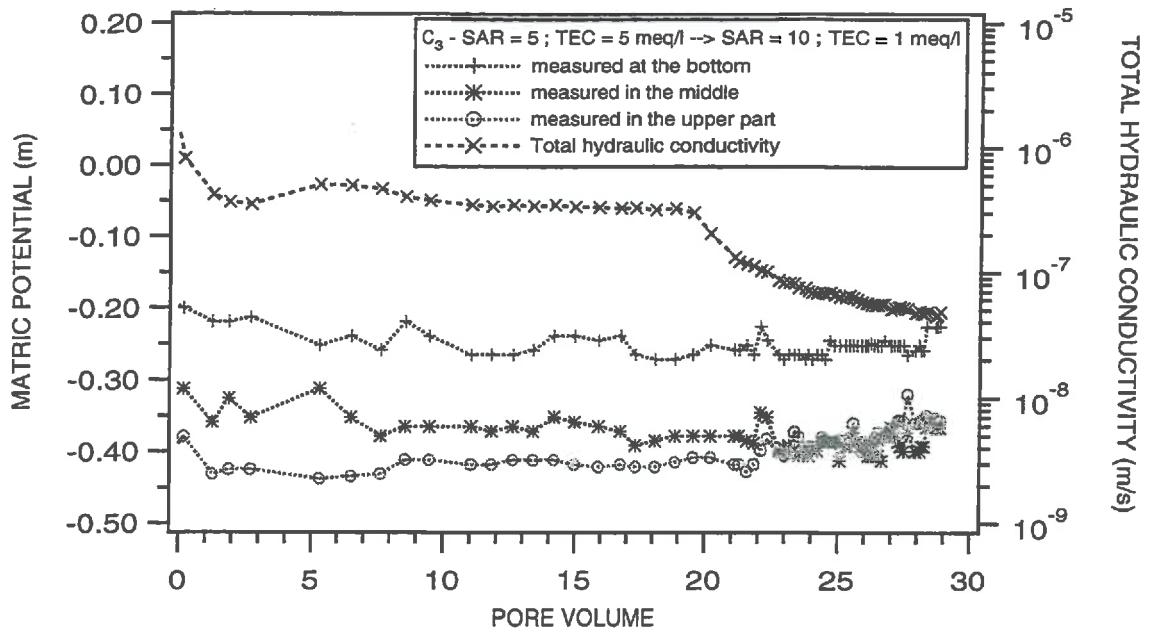
C3 - SAR = 5 ; TEC = 5 meq/l --> SAR = 10 ; TEC = 1 meq/l
measured at the bottom
measured in the middle
measured in the upper part
Total hydraulic conductivity
MATRIC POTENTIAL (m)
TOTAL HYDRAULIC CONDUCTIVITY (m/s)
PORE VOLUME
0.20
0.10
0.00
-0.10
-0.20
-0.30
-0.40
-0.50
0
5
10
15
20
25
30
10-5
10-6
10-7
10-8
10-9

(c)

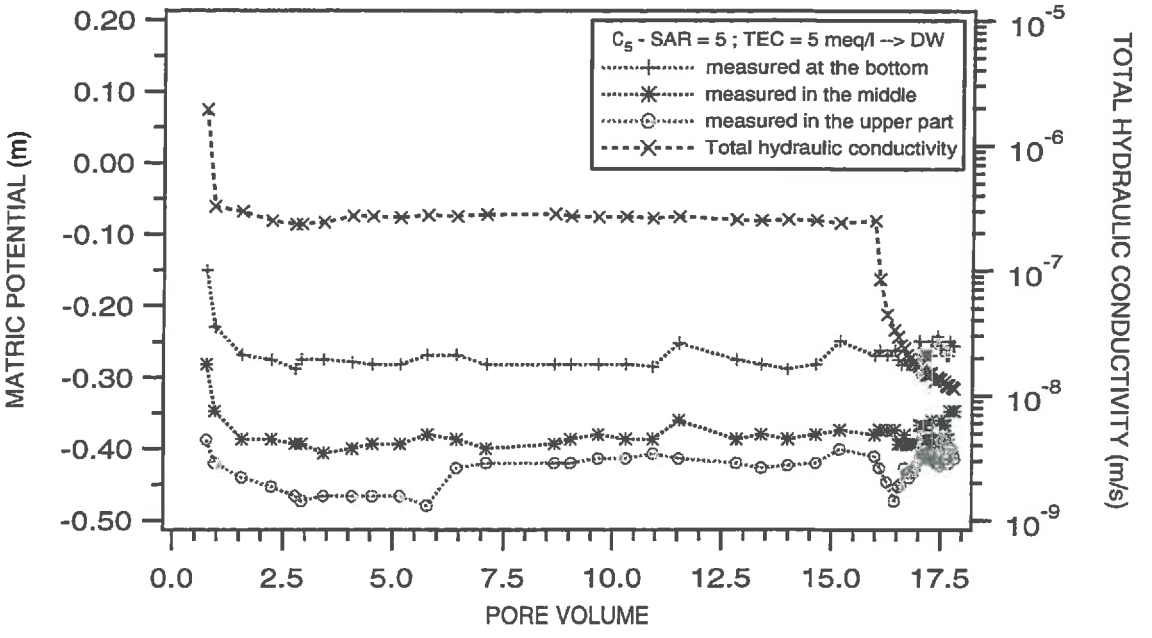
C5 - SAR = 5 ; TEC = 5 meq/l --> DW
measured at the bottom
measured in the middle
measured in the upper part
Total hydraulic conductivity
MATRIC POTENTIAL (m)
TOTAL HYDRAULIC CONDUCTIVITY (m/s)
PORE VOLUME
0.20
0.10
0.00
-0.10
-0.20
-0.30
-0.40
-0.50
0.0
2.5
5.0
7.5
10.0
12.5
15.0
17.5
10-5
10-6
10-7
10-8
10-9

(d)

In contrast with this, an increase of the suction was observed in the columns leached with SAR = 5, TEC = 1 meq/l (C_1 - figure 4.11a) and deionized water (C_5 - figure 4.11d). In these cases, a stronger sealing of the upper clayey layer should have highly limited particle movement within this layer while the clay present in the unsaturated layer below it is able to move. Then if the fraction of clay which quits the upper part of the sandy layer is greater than the amount of clay arriving from the upper clayey layer, an increase of the suction should occur and this was observed (figure 4.11a and 4.11d). This increase of the suction is particularly clear in the column leached with deionized water (C_5 - figure 4.11d) where the suction varied from 0.41 m to 0.47 m of water column, and to a lesser extent in the column leached with SAR = 5, TEC = 1 meq/l (C_1 - figure 4.11a). These differences could be explained by the study of *Emerson and Bakker (1973)* who examined the favourable conditions for clay dispersion and migration when dilute solutions are used. Two conditions were proposed to favour clay dispersion : i) a quick drop of the concentration of the soil solution below the critical flocculation concentration, ii) a steep salt gradient between the dilute solution in the macropores and the more concentrated solution between the clay layers. Both conditions are better fulfilled when deionized water is applied rather than SAR = 5 and TEC = 1 meq/l.

Then, the increase of the suction is followed by a decrease to approximately the previous values. In addition, due to particle movement, a reduction of the bulk density should also occur as discussed in § 4.6. Simultaneously, with the change of the water quality, the clay layers expand, increasing the distance between them. This resulted in an increase of the water contents, though different in the columns leached with deionized water and with a solution of SAR = 5, TEC = 1 meq/l (§ 4.6). This will be explained hereafter (§ 4.6).

Finally, one should note that if the matric potentials had not been measured daily, nothing concerning these behaviours could have been observed.

From this discussion, we should keep in mind that due to the fact that the upper boundary conditions were different for each column, various water content profiles and suctions were induced. These measurements were further affected by an arrival of dispersed clay from the upper clayey layer or/and a change in the chemical conditions. As a consequence, variations in the measured suctions are not necessarily combined to changes in the measured water contents and *vice-versa*, though the MRCs were affected (§ 4.8).

4.6. Water content and bulk density profiles

The volumetric water content and bulk density profiles were measured weekly by gamma-radiation. At the end of the percolation period, the water content profiles were verified by means of the gravimetric method. Good agreement was obtained with the profiles on a weight basis and those obtained by gamma-radiation. One should insist on the adequacy of this methodology for water content measurements (§ 2.4.3). Upward or downward scanning could be performed repeatedly with any step chosen by the supervisor of the experiment. In addition, the section of the column available for the water flow remains unaffected by these measurements. This is not the case with the presence of the tensiometers. Furthermore, water content measurements should be preferred rather than matric potential ones. Indeed, significant variations in the water contents can be measured without significant changes in the suctions or in the hydraulic gradients.

The evolution of the volumetric water contents for the different columns are presented as a function of the depth and time in annexe 4.8 and annexe 4.9 for series I and series II, respectively. The most interesting result was measured for the column leached with a solution of SAR = 20 and a TEC of 1 meq/l (series I - C_6) (figure 4.10). It is also interesting to observe the increase of the water contents after the solution was changed (series II) e.g. in columns leached with deionized water (C_5) or with a solution of SAR = 5 and TEC = 1 meq/l (C_1), despite the reduction of the downward flux density (annexe 4.9a and 4.9d). One should note the progressive rise of the water content in the column leached with SAR = 5, TEC = 1 meq/l (C_1 - annexe 4.9a) and the small abrupt increase (of about 5 %) when deionized water was used (C_5 - annexe 4.9d). In the column C_1, the water contents progressively increased of about 10 % in the top three centimeters after the solution was changed together with a progressive reduction of the suction (figure 4.11a). The increase in the water content observed can be caused by *in situ* limited swelling of already dispersed particles in the unsaturated layer or/and by the arrival of particles from the upper clayey layer. In our laboratory conditions, both could occur and we cannot conclude whether the former is more important than the latter.

When the solution of SAR = 5, TEC = 5 meq/l is replaced by SAR = 10 (C_2 - TEC = 5 or C_3 - 1 meq/l) the water contents first decrease as a response of a reduction of the downward flux before observing an increase of the water contents, probably linked to the arrival of clay particles (§ 4.5).

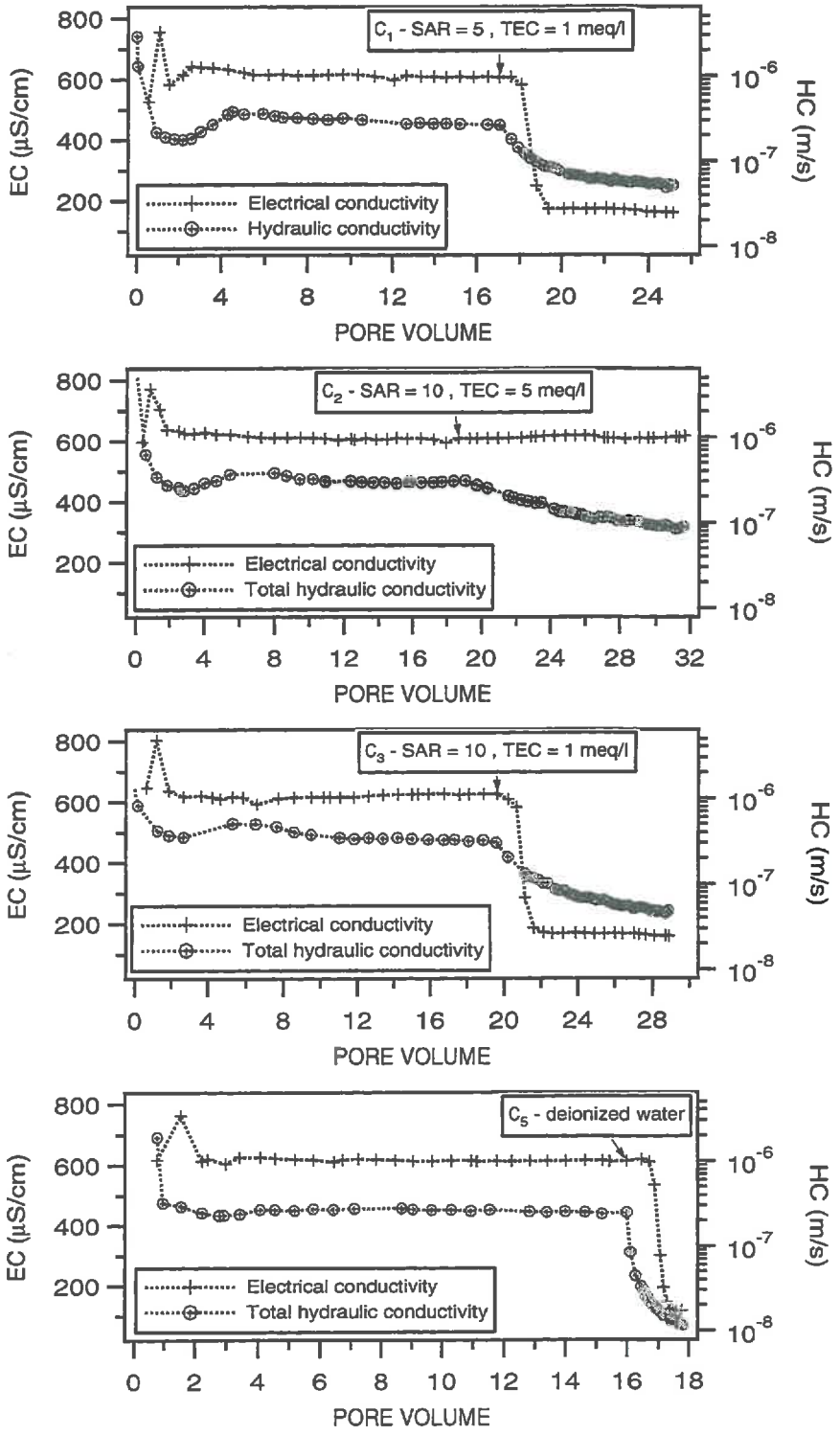

Figure 4.12. Evolution of the electrical conductivities (EC) in the effluents as a function of the pore volume (series II). The total hydraulic conductivities HC measured by the means of the falling head were added. All the columns were first leached with SAR = 5, TEC = 5 meq/l.

The influence of the chemical treatments was also observed in the measurements of the bulk densities (annexe 4.10a). In series I experiments, the mean bulk densities tend to increase with time. The columns were leached with only one kind of solution. All treatments provoked clay dispersion and clay particle migration through the unsaturated porous media (figure 4.7). Then a straight forward reasoning leads to explain the increase in the bulk density. Let us consider a subsample characterized by a total mass of solid, initially constituted of Fontainebleau sand, and a constant total volume. With the arrival of dispersed smectite particles, the mass of solid increases whereas the volume remains constant. This results in an increase of the bulk density, which was observed.

In the second series of experiments (annexe 4.10b), mean bulk density values tend to decrease after the change of solution. The confidence limits associated to the mean bulk densities do no longer overlap. This seemed to take three to four weeks except for the column where deionized water replaced the salty solution. For this latter treatment, the mean bulk densities decreased right away from the first water content - bulk density profile after deionized water was applied. To explain this behaviour, let us consider now that dispersed clay is already present in a given sandy subsample having a constant total volume. Increasing the SAR or decreasing the TEC results in more dispersive conditions. With the departure of clay from this subsample, the total mass of solid diminishes. The bulk density is lowered and, hence, the total porosity increases (eqn. 1.8). In addition, due to the expansion of the clay layers in response to the salty conditions, more water is retained. Considering that the clay layers are saturated with water, when the liquid ratio increases, the void ratio also increases and the bulk density decreases. However, this increase of the porosity is not effective for the water flow.

4.7. Evolution of the EC, pH and concentrations

The effluent volumes were collected and the electrical conductivity (EC), pH and the respective concentrations of sodium and calcium were measured. The electrical conductivity and pH were measured using standard methods. The electrolyte concentrations were measured by the means of the atomic absorption spectrometer and the direct current plasma (§ 2.6.1). Results concerning the EC are illustrated in figure 4.12 and those concerning the electrolyte concentrations are given in annexe 4.11. The total hydraulic conductivities were added to compare their evolution to that of the measured EC.

At the early beginning of the percolation period, the total hydraulic conductivities decrease was accompanied by an increase of the total EC (figure 4.12). The maximum EC

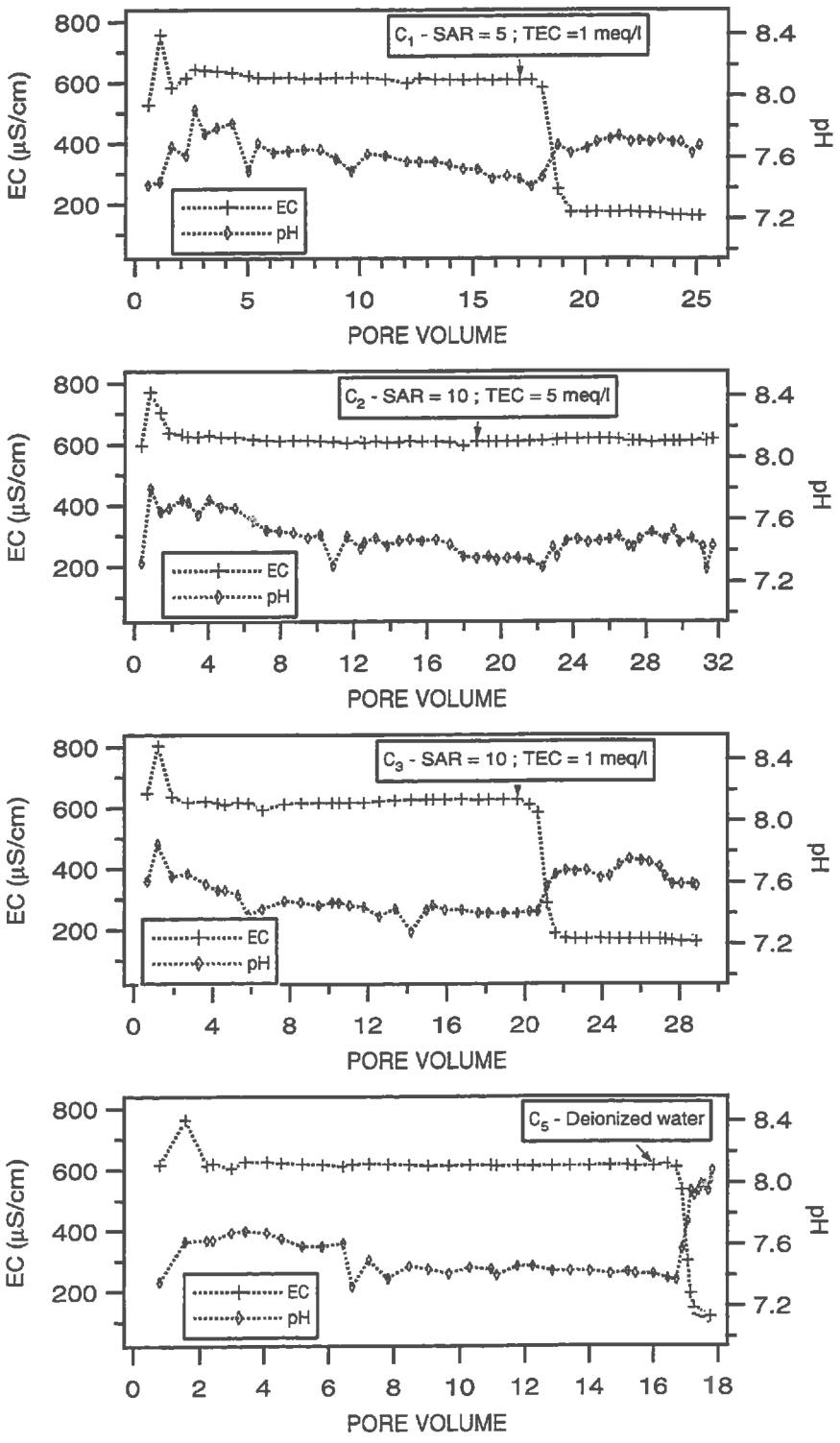

Figure 4.13. Evolution of the pH values and electrical conductivities (EC) of the effluents as a function of the pore volume (series II). All the columns were first leached with SAR = 5, TEC = 5 meq/l.

occurs within 0.85 and 1.55 pore volumes. This increase could be caused by a release of soluble salts due to an insufficient washing during the preparation of the sodic soil (§ 2.6.2). A more reasonable explanation could be found in an exchange reaction. Indeed, the upper clayey layer was obtained by mixing together homoionic Na and Ca saturated soil material in various proportions to obtain a given ESP. The leaching solutions used were not those which saturated the soil material. Consequently, when these solutions are employed, an exchange of cations can occur to be at equilibrium with the leaching solution. This can result in a release of salts. Nevertheless, after approximately 2 pore volumes, constant ECs are measured.

When the TEC is decreased (C_1 - SAR = 5, TEC = 1 meq/l), one should remark that the EC dropped sharply. The leachate concentration reached the steady state after only 1.8 pore volumes. During this short time the HC of the column leached with SAR = 5, TEC = 1 meq/l dropped of about 62 % of the HC measured with the former solution (SAR = 5, TEC = 5 meq/l). This means that 77 % of the total reduction already occurred. The effect of a decreasing TEC on the hydraulic conductivity is immediately observed, even before the EC began to decrease. This is probably due to the fact that with the arrival of the displacing solution, salt is leached out of the soil aggregates, maintaining the EC at a higher value. One should also remember that the most favourable dispersive conditions are obtained at this particular moment (§ 4.5), causing the reduction of the HC.

When both the SAR is increased and the TEC is decreased (C_3 - SAR = 10, TEC = 1 meq/l), similar observations hold. Chemical steady state conditions are obtained after 2.5 pore volumes. During this period, 77 % of the total HC reduction also occurred. For these two examples, this signifies that the system was not at equilibrium when the electrolyte concentration reached the steady state value. On the contrary, when deionized water was used (C_5), constant EC values were measured after 1.4 pore volumes. Within this time almost the entire reduction occurred.

One should also note that the EC remains constant for C_2 (SAR = 10, TEC = 5 meq/l) while the total hydraulic conductivity decreases.

In addition, it seems that the time necessary to observe chemical equilibrium depends on the SAR. Indeed, it takes 2.5 and 1.8 pore volumes for SAR = 10 and SAR = 5, respectively. The most rapid chemical equilibrium conditions are obtained with deionized water.

The pH was also measured in the effluent volumes (figure 4.13). The most interesting observation concerned the augmentation of the pH after the solution was changed. The increase of the pH could be due to the hydrolysis of exchangeable sodium through exchange by H^+ from dissociated water as proposed by *Frenkel et al. (1978)*. They measured an increase of 0.5 unit when the electrolyte concentration was decreased below 10 meq/l. Furthermore, *Pupisky and Shainberg (1979)* concluded that no hydrolysis of exchangeable ions occurred when neutral pH were maintained. This is the case with SAR = 10, TEC = 5 meq/l (C_2).

In addition, this pH augmentation seems to be related to the TEC rather than the SAR. Indeed, relatively constant pH values are maintained with SAR = 10, TEC = 5 meq/l whereas this exchange reaction caused an increase in pH of nearly 0.3 unit for SAR = 10, TEC = 1 meq/l and 0.7 unit for deionized water. The column leached with SAR = 5, TEC = 1 meq/l exhibit a similar pH variation as SAR = 10, TEC = 1 meq/l.

Finally, the increase of the pH promotes the negative charges on the clay layers (§ 1.2.2.5) which in his turn promotes clay dispersion. This should be associated to the increase of the suctions observed especially when deionized water was applied (figure 4.11d).

4.8. Determination of the MRCs

The hydrodynamic properties i.e. the soil moisture retention curve (MRC) and the hydraulic conductivity curve (HCC), determined by an inverse approach under steady state conditions (§ 3.3) are presented and discussed in detail. The MRCs were described with the functional and non hysteretic van Genuchten relationships with a four-term parameter vector $(\theta_r,\ \theta_s,\ \alpha,\ n)$. In order to reduce of the number of parameters, the residual water content was initially assumed to be unaffected by clay migration. Consequently, only three parameters were required to characterize the MRCs. This assumption was analyzed and discussed (§ 4.8.2).

Parameter vector estimation of the initially clay-free Fontainebleau sand was obtained with the first measured volumetric water content - bulk density profiles under drying conditions with a constant suction of 2.5 kPa (25 cm of water column at the bottom) and a zero downward flux. The last experimental water content profiles for each column was used to determine the unknown parameters of the modified MRC and HCC. Taking into account all the measured profiles for each column and assuming temporarily steady state conditions, the temporal variability of these parameters will be discussed only for series I.

Finally, the effect of the different leaching procedures on the estimated MRCs and HCCs are presented and discussed (§ 4.8.2 and § 4.8.3).

4.8.1. Soil moisture retention curves for the Fontainebleau sand

The MRC of the initially clay-free sandy material has been calculated using data from all the columns. Fitting the experimental measured volumetric water content data to the solution of the flow equation allowed for the calculation of the MRCs and HCCs parameters (table 4.6). The parameters $(\theta_s,\ \theta_r)$ and $(\alpha,\ \theta_s)$ are slightly negatively correlated, whereas $(\alpha,\ \theta_r)$, $(n,\ \theta_r)$ and $(n,\ \alpha)$ are highly positively correlated. $(n,\ \theta_s)$ is highly negatively correlated.

Table 4.6. The van Genuchten parameters with their variances σ^2 and correlation matrix for the mean soil moisture retention curve (drying branche) of Fontainebleau sand (series I).

Parameter	Estimated Value	σ^2	Parameter	θ_r	θ_s	α	n
θ_r	0.086	8.089e-4	θ_r	1			
θ_s	0.326	2.469e-5	θ_s	-0.55	1		
$\alpha^{(*)}$	0.023	2.599e-7	α	0.94	-0.31	1	
n	10.537	2.811	n	0.91	-0.72	0.78	1

(*) here expressed in [1/cm]

Based on these optimal parameters, the MRCs of Fontainebleau sand were calculated (figure 4.14). An estimated 95 % confidence limit to the MRCs was constructed by generating 1000 parameter sets applying the Cholesky's decomposition. The new parameter sets were characterized by the same variance-covariance matrix (table 4.6) as the parameter vector $(\theta_r,\ \theta_s,\ \alpha,\ n)$ estimated with the inverse approach. For each generated parameter set, a MRC was calculated. For each depth or matric potential, the thousand volumetric water contents were classified. The 95 % confidence limit at a given depth corresponds to the 50th and 950th water content values. It should be noted that the interval is narrow except in the dry range, at the top of the sandy layer.

The estimated parameter vector, appropriate to the initial flow conditions, describes the main drying curve. Soil moisture retention curves under wetting conditions, described by the parameter vector $\left(\theta_r^w,\ \theta_s^w,\ \alpha^w,\ n^w\right)$, can be estimated assuming that the main hysteresis loop is closed, i.e. $\theta_r^w = \theta_r^d$, $\theta_s^w = \theta_s^d$, where the superscript d refers to drying and w refers to wetting. Another simplification may be obtained by setting $n^w = n^d$ and $\alpha^w = 2\alpha^d$ *(Kool and Parker, 1987)*. The confidence limit associated to the main wetting curve is larger because the variance of the parameter α has been multiplied by a factor 4 and the covariance has been doubled.

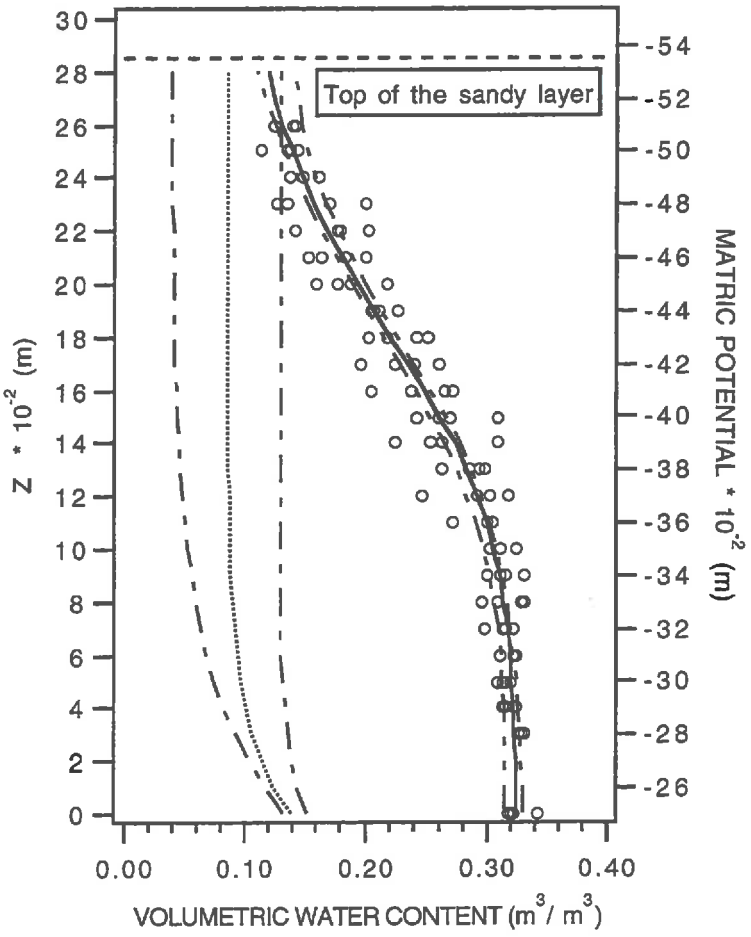

Figure 4.14. Soil moisture retention curves for the clay-free Fontainebleau sand and the estimated 95 % confidence limit to the MRCs. The solid line represents the main drying branche obtained by fitting the experimental volumetric water content data (o). The dotted lines represents the estimated wetting branche (series I).

4.8.2. The modified MRCs due to clay migration : series I

The VG parameter vector describing the MRC of the initially clay-free Fontainebleau sand was taken as reference. The determination of the VG parameter vectors at the end of the leaching procedure of the series I flow experiments was performed by first assuming that the residual water content remained unaffected. Finally, when steady state flow conditions were considered, one was able to examine the variability of the VG parameters. A clear relationship could be observed for the α curve shape parameter.

4.8.2.1. Estimation of the final van Genuchten parameter vector : series I

Parameter estimation requires the knowledge of the last measured water content profiles (annexes 4.12a and 4.12b) and the mean downward flux densities for each column (table 4.4). Initially, θ_r was assumed to equal the residual water content of the clay-free sand. Minimising the residual error between the calculated and the measured water content profile, the three-term parameter vector and its corresponding variance-covariance matrix (annexe 4.13) were estimated. To avoid numerical instabilities during the calculation of the second partial derivatives, the increment used was put equal to 0.01. It must be noted that the three parameters are highly correlated : $(n,\ \theta_s)$ and $(n,\ \alpha)$ are negatively correlated whereas $(\alpha,\ \theta_s)$ are positively correlated. An increase in θ_s value will cause a shift of the parameter n toward a smaller value. A similar effect will be caused by increasing α.

The same procedure has been followed to determine the four-term VG parameter vector without imposing any constraint (figure 4.15). Convergence was slower and the number of iterations was significantly increased (from 80 up to 204 for the column percolated with solution of SAR = 20 and TEC = 1 meq/l) when the optimisation was performed with the same initial VG parameters. Slow convergence could be explained by the correlation between the parameters *(van Genuchten et al., 1988)*. Parameter uncertainty was assessed. Results are given in annexe 4.14.

Comparing the estimated variances of the residuals σ^2_{res}, given by the ratio of the sum of squared residuals and the difference between the number of observations and the number of estimated parameters, it can be observed that the experimental water content profiles are better estimated with a four-term parameter vector. The lower this variance is, the better the model describes the experimental data. It quantifies the goodness of the fit. In addition, the variances relative to each parameter are generally lower for a three-term parameter vector, because parameter estimates are conditioned to the constant θ_r.

Concerning the correlations between parameters, some differences should be noted. The $(\alpha,\ \theta_s)$, which are highly positively correlated for a three-term parameter vector, remains positively correlated for the four-term vector but ranges from 0.36 to 0.80. Correlations between $(n,\ \alpha)$ are highly variable when a four-term parameter vector is estimated. No correlation appears for $(\alpha,\ \theta_r)$ whereas a high positive correlation appeared when the VG parameters were determined for the initial Fontainebleau sand.

The calculated soil moisture retention curves of the sandy layers as affected by the different treatments when three or four parameters are estimated are given in figure (4.16). Estimated 95 % confidence limits were added only for the four-term parameter vector. In the dry range, when $(d\theta/dh)$ tends to zero, it is clearly shown that the residual water content θ_r does not always belong to the defined confidence limit. Furthermore, imposing a constraint on this parameter results in high correlations between the remaining parameters.

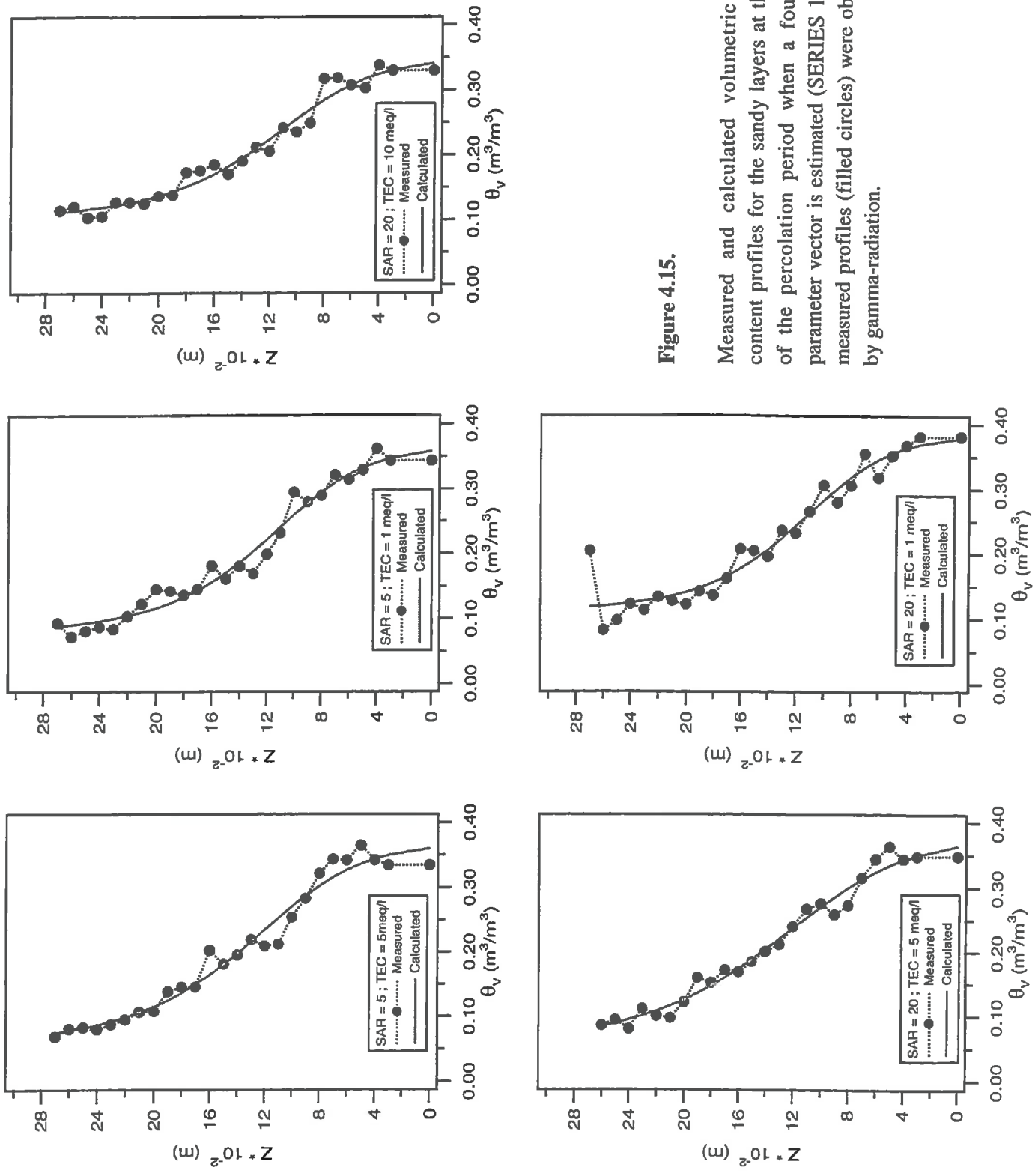

Figure 4.15.

Measured and calculated volumetric water content profiles for the sandy layers at the end of the percolation period when a four-term parameter vector is estimated (SERIES 1). The measured profiles (filled circles) were obtained by gamma-radiation.

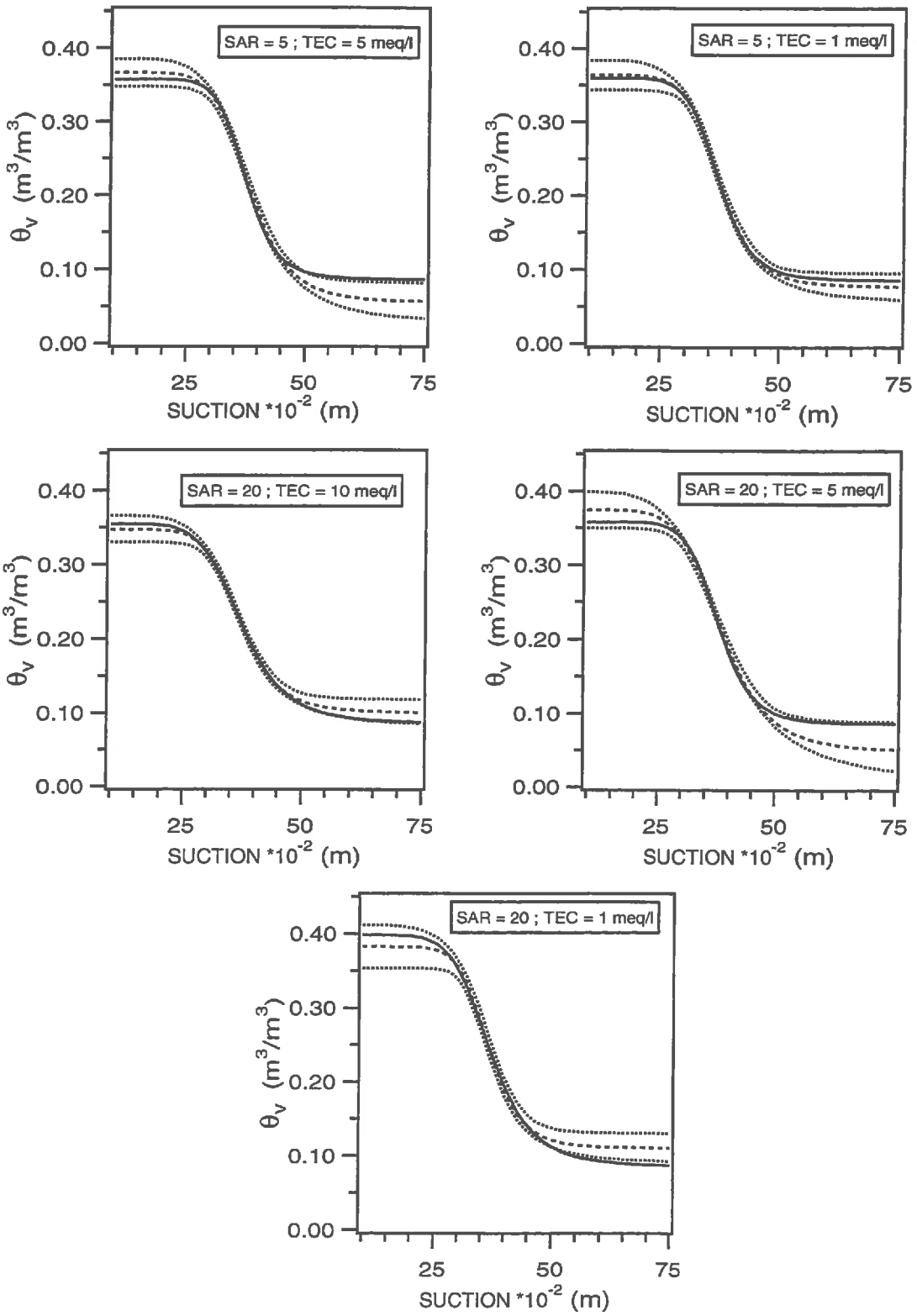

Figure 4.16. Mean MRCs (---) estimated with a four-term parameter vector and its corresponding 95 % estimated confidence limit (...). The solid line represents the MRCs estimated with the three-term parameter vector.

Highly correlated parameters can lead to some parameter estimation problems *(Kool et al., 1987)* because a change in one parameter is balanced by a corresponding change in the correlated parameter. Consequently, none of these parameters are accurately estimated. These reasons justify the estimation of the four-term parameter vector $(\theta_r,\ \theta_s,\ \alpha,\ n)$ instead of the three-term parameter vector $(\theta_s,\ \alpha,\ n)$.

4.8.2.2. Final soil moisture retention curves : series I

Parameter estimation for Fontainebleau sand has been determined under drying conditions. Once the upper clayey layer has been placed and the constant head has been applied, the columns were simultaneously wetted and drained. Consequently, the MRC obtained at the end of the percolation period are not the main drying branches.

The modified MRCs (figure 4.17) are differently affected and must be interpreted having in mind the distribution of clay within the sandy layers and the solution used, in terms of SAR and TEC. Theoretically, for a given solution, the volumetric water content increases with the clay percentage. For a given amount of clay and a given matric potential, the distance between clay layers increases when the SAR increases or the TEC decreases. Consequently, the amount of water retained increases.

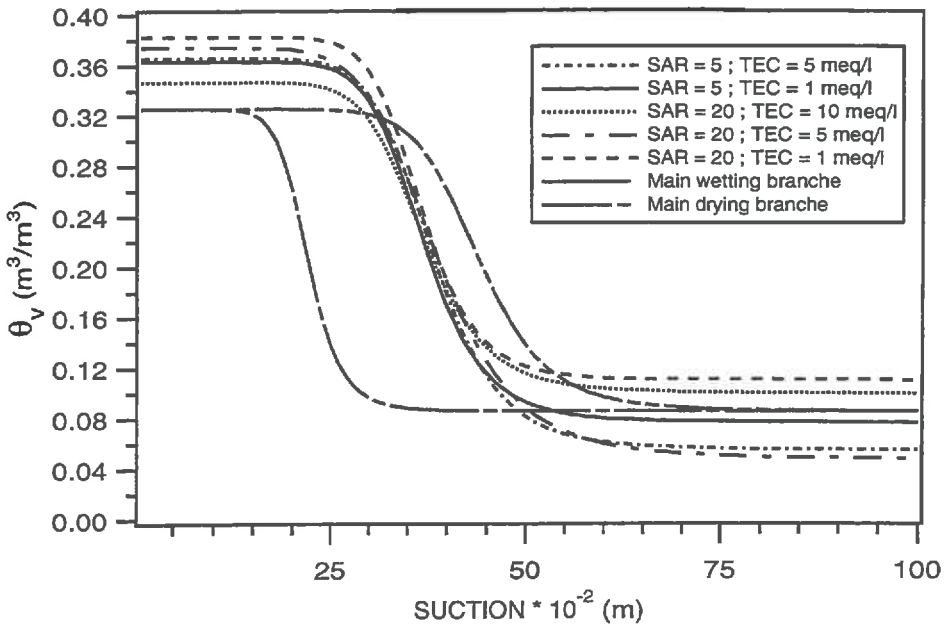

Figure 4.17. Calculated soil moisture retention curves of the sandy layers at the end of the leaching period obtained with a 4-term parameter vector (series I). The main calculated wetting and drying branches of the initially clay-free Fontainebleau sand are added.

All the estimated MRCs were compared to one another applying the objective criterion developed in (§ 3.4). The comparison is summarized in table 4.7 and the corresponding values of the surfaces between two estimated curves are given in annexe 4.15.

Saturated water contents vary from 35.5 % (SAR = 20 ; TEC = 10 meq/l) up to 39.8 % (SAR = 20 ; TEC = 1 meq/l). In the low suction range and for SAR = 20, it can be observed that volumetric water contents for a TEC = 1 meq/l exceed those for a TEC = 5 meq/l (significantly different at the 0.05 level), which in turn exceed those for a TEC = 10 meq/l (significant at the 0.05 level). If we compare columns percolated with the same TEC but with different SAR values, the greater the SAR is, the greater the water content will be. The MRC obtained with a SAR = 20 and a TEC = 1 meq/l is significantly different at the 0.05 level from the curve obtained for SAR = 5. The increase of the amount of water retained diminishes with an increase of the TEC.

When comparing columns percolated with SAR = 20 and for suctions > 0.40 m, it can be seen that more water will be retained with a TEC of 10 meq/l than with a TEC of 5 meq/l. The presence of a greater amount of smectite (0.28 $\%_c$) combined with a TEC = 10 meq/l explains the higher water contents, compared to the case with lower clay amounts (0.11 $\%_c$) clay and a TEC = 5 meq/l. The reasons of occurrence of higher clay contents with TEC = 10 meq/l compared to TEC = 5 meq/l remains unclear.

Table 4.7. Comparison of the soil moisture retention curves obtained at the end of the leaching period (series I).

Solution	SAR = 5 TEC = 5 meq/l	SAR = 5 TEC = 1 meq/l	SAR = 20 TEC = 10 meq/l	SAR = 20 TEC = 5 meq/l	SAR = 20 TEC = 1 meq/l
SAR = 5 TEC = 5 meq/l	=				
SAR = 5 TEC = 1 meq/l	-	=			
SAR = 20 TEC = 10 meq/l	+	-	=		
SAR = 20 TEC = 5 meq/l	-	-	+	=	
SAR = 20 TEC = 1 meq/l	++	+	-	+	=

\- not significantly different at a level of 0.05
\+ significant different at a level of 0.05
++ significant different at a level of 0.01

The MRCs obtained from the inverse approach were compared to those obtained with the conceptual model (§ 3.2). The calculations (eqn. 3.9) required the knowledge of the mass ratio of clay to solid (m_c/m_s), the bulk density and the specific surface area (= 616e3 m^2/kg). A mean mass clay percentage was assumed for each experimental column and a mean bulk density of 1679 kg/m^3. The latter corresponds to a mean bulk density value for all the columns of the two flow experiments. Results are given in annexe 4.16. The main differences does not appear for θ_s, θ_r or n if one bears in mind the 95 % estimated confidence limit corresponding the MRC obtained from the inverse approach. Discrepancies appear with the α VG parameter. On the one hand, the amount of water retained by a given percentage of smectite is added to the amount of water retained by the initially clay-free Fontainebleau sand. In the conceptual model, these MRCs are further considered to be the main drying branches. This results in MRCs characterized by a lower α VG parameters (or a higher air entry value for high n values). On the other hand, the MRCs obtained at the end of the leaching period by the inverse approach are not the main drying branches. Consequently, the α VG parameters obtained with each method are not comparable.

4.8.2.3. Assessment of the variation of the curve shape parameter α

Assuming temporarily steady state flow conditions, the four-term parameter vectors were determined for each column and for each measured water content-bulk density profile. No clear relationship could be observed for the VG parameters except for the α curve shape parameter. When plotted versus the cumulated percolation time, α increased progressively following a logarithmic evolution.

The cumulated time is linearly related to the cumulated effluent volume (§ 4.3.3), which can be expressed adimensionally in terms of pore volume. Consequently, α is logarithmically related to the pore volume (figure 4.18). The latter expression has been preferred because it allows an easy comparison between columns and takes into account the effect of SAR and electrolyte concentration.

The following empirical equation was fitted to the data :

$$\frac{d\alpha}{dV} = C\, e^{(-b\,V)}, \qquad (4.2)$$

where $d\alpha/dV$ represents the amount of variation of the VG α_o curve shape parameter in a given period of time expressed in terms of pore volumes, C is the variation of α_o at the beginning of the process and is equal to α_o and b is the rate constant. The higher the rate

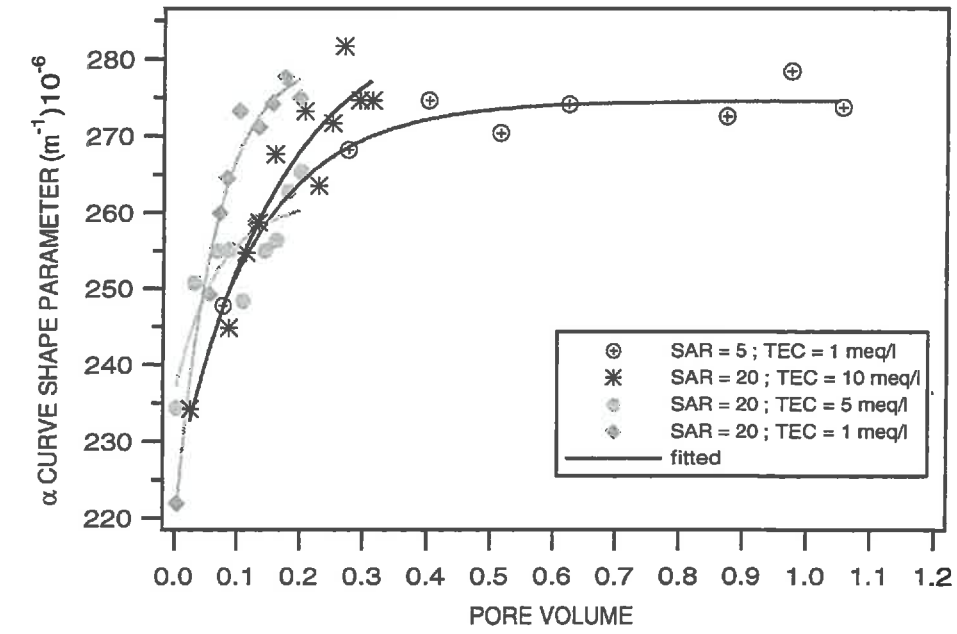

(a)

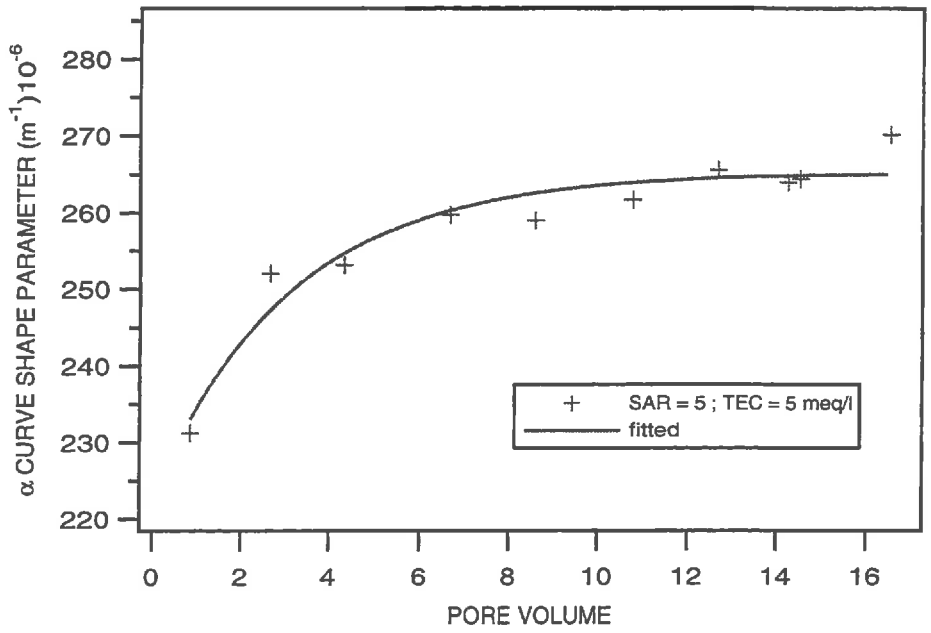

(b)

Figure 4.18. Estimated α curve shape parameter versus the pore volume obtained for the columns of series I.

constant b , the more accentuated is the variation of the α curve shape parameter in comparison with its initial value α_o. This constant could be compared to the speed by which the inflection point of the estimated MRC is shifted towards lower suctions according to the original MRC of the clay-free sand.
By integrating eqn. (4.2), one obtains :

$$\alpha = -\frac{C}{b} e^{(-bV)} + constant. \tag{4.3}$$

After a sufficient long time, it is assumed that α will be equal to a final constant value α_f. In addition, at the beginning of the process, when $V = 0$, it can be written that :

$$\alpha = \alpha_o = -\frac{C}{b} + \alpha_f, \tag{4.4}$$

Replacing the value of $(-C/b)$ with $(\alpha_o - \alpha_f)$ in eqn. (4.3) yields :

$$\alpha = (\alpha_o - \alpha_f) e^{(-bV)} + \alpha_f. \tag{4.5}$$

Rearranging the terms, eqn. (4.5) can be rewritten as follows :

$$\alpha = (\alpha_f - \alpha_o)\left(1 - e^{(-bV)}\right) + \alpha_o. \tag{4.6}$$

A dimensionless curve shape parameter can be expressed as :

$$\alpha_{adim} = \frac{\alpha - \alpha_o}{\alpha_f - \alpha_o} = 1 - e^{(-bV)}. \tag{4.7}$$

Finally, in the logarithmic form, one obtains :

$$\ln(1 - \alpha_{adim}) = -bV. \tag{4.8}$$

Plotting $\ln(1 - \alpha_{adim})$ versus the pore volume will give a straight line whose negative slope is equal to b, the rate of the MRC displacement (figure 4.19). Because the number of different treatments and columns were small, results must be interpreted with criticism. Nevertheless, it can be seen that the higher the SAR and the lower the TEC, the more accentuated is the variation of the α VG curve shape parameter in comparison to its initial value.

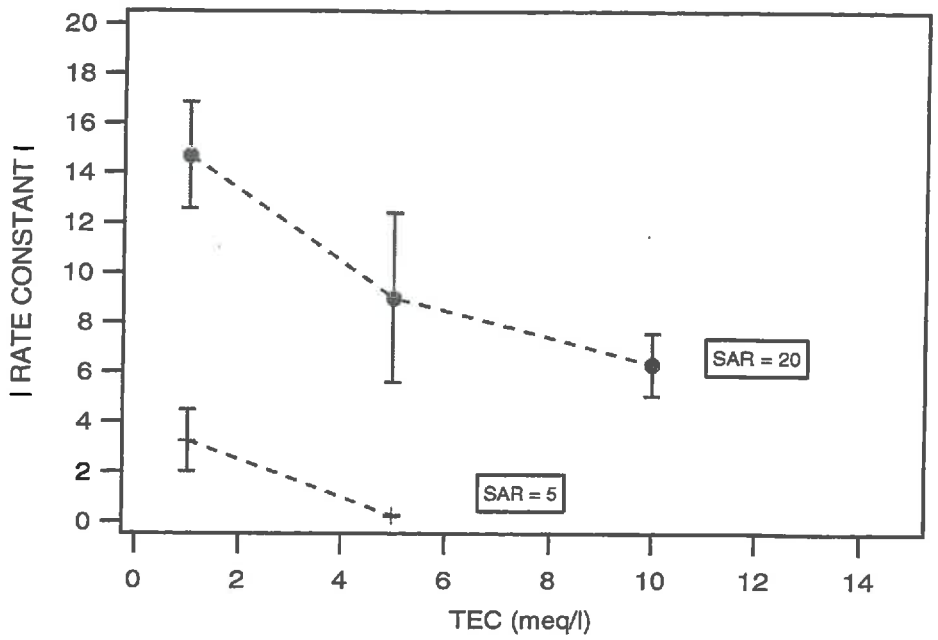

Figure 4.19. Rate of the soil-moisture retention curve displacement (eqn. 4.2) as a function of SAR and TEC (series I). Each filled circle and cross represents the rate constant corresponding to one column and to one chemical treatment. The vertical bars are the standard deviations.

4.8.3. The modified MRCs : series II

For the second flow experiments, each MRC and each HCC were characterized with a four-term parameter vector $(\theta_r, \theta_s, \alpha, n)$. The water content profiles and MRCs obtained with SAR = 5 and TEC = 5 meq/l will be first compared. The effect of an increasing SAR, a decreasing TEC or both are also discussed.

4.8.3.1. The MRCs as affected by clay migration at the end of the first stage : series II

The four stratified columns were first leached with a solution of SAR = 5 and TEC = 5 meq/l. The columns were submitted to the same experimental boundary conditions. The upper layer was constituted of an equal soil material quantity (20 g Béthonvilliers soil material - an approximate thickness of 0.7-cm) and the same proportion of sodic and calcic soil material. A constant suction (25 cm of water column or 2.5 kPa) was applied at the bottom of each column. The total hydraulic gradients range from 2.62 to 2.68. Consequently, these four

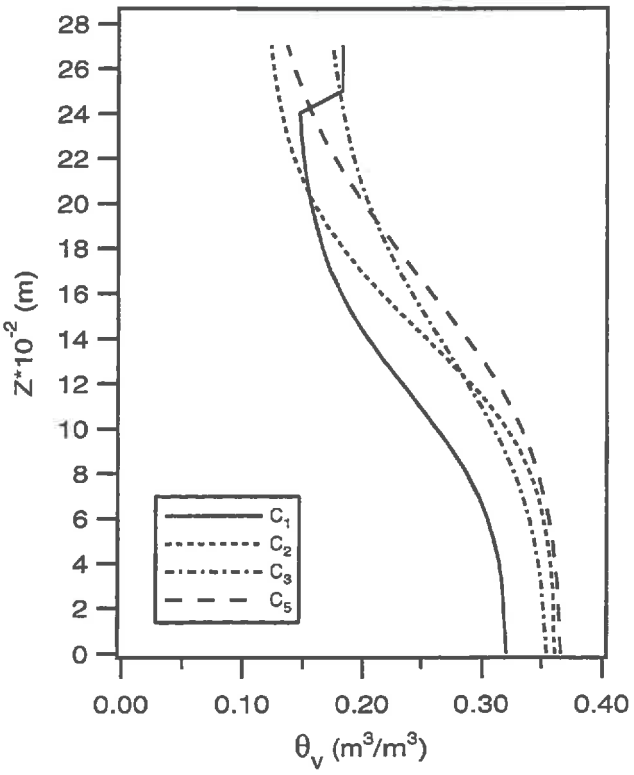

Figure 4.20. Calculated volumetric water content profiles in the sandy layers at the end of the first percolation period differing from each other due to differences in the clay content profiles (series II - SAR = 5 meq/l, TEC = 5 meq/l).

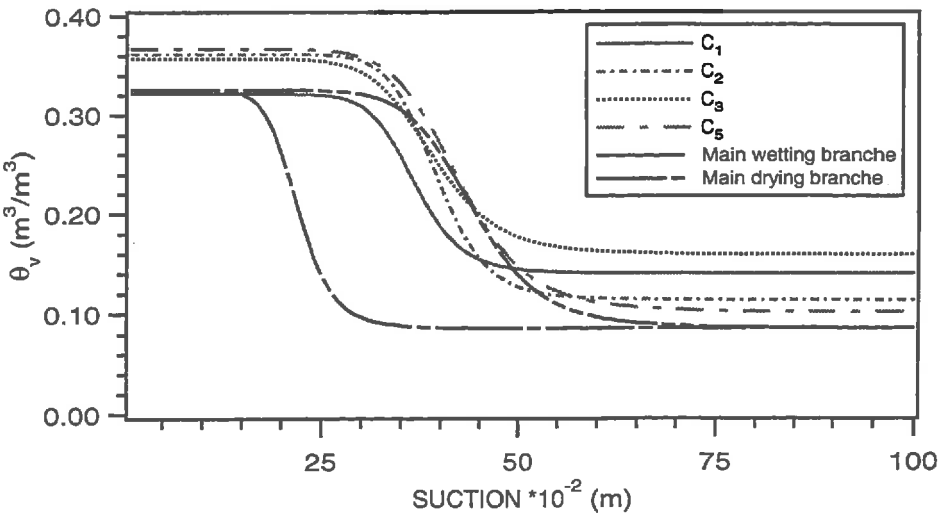

Figure 4.21. Calculated MRCs of the sandy layers at the end of the first leaching period (series II - SAR = 5, TEC = 5 meq/l). The columns can be considered as replicates and differences in the MRCs are probably due to different clay profiles.

columns can be considered as replicates and differences in themeasured water content profiles (figure 4.22), MRCs and HCCs could be explained by the differences in the clay content profiles. For technical reasons, clay quantification could not be realized without a complete destruction of the columns and has been performed only at the end of the second stage.

The calculated water content profiles obtained from the estimated VG parameter vector and corresponding flux density are compared in figure (4.20). Three water content profiles are comparable in the lower part of the column (C_2, C_3 and C_5). The water content profile of C_1, which exhibits a volumetric water content equal to that of the initial sand (32 %), contains probably less clay. In the upper part of the sandy layers, clay has been accumulated, constituting progressively a third layer (C_1). This can be explained by a massive arrival of dispersed clay at the early beginning of the percolation, provoking a decrease of the suction and an increase of the total hydraulic conductivity (figure 4.4b). The presence of clay probably blocked the further movement of colloids. The increase in the hydraulic conductivities, due to clay movement from the upper clayey layer, has been observed for the other columns but was of less importance.

The MRCs are calculated using the four-term VG parameter vector minimising the sum of the squared residuals (figure 4.21). Results are given in annexe 4.17. The matrix of second derivatives (eqn. 3.23) has been calculated with an increment equal to 0.01 of the optimal VG parameter value, except for C_1 who exhibits large numerical instabilities. For the latter an increment of 0.001 has been used.

The estimated MRCs were compared statistically (annexe 4.18). The MRC obtained for C_2 and C_5 are not significantly different at the 0.05 level. All the remaining curves are significantly different at the 0.01 level.

The presence of less clay in the saturated zone of column C_1 could explain the differences in the estimated water contents (32.2 % for C_1 and $\approx$ 36 % for C_2, C_3 and C_5). For a suction of 40 cm (4 kPa), volumetric water content ranges from 18 % (C_1) to 26 % (C_5). When the suction is further increased, more water is retained by C_3 rather than by C_5 whose water contents are close to those of the initially clay-free sand.

An important conclusion can be drawn at this stage. For identical chemical and hydraulic conditions, different water content profiles and hence soil moisture retention curves can be obtained. Indeed, leaching with SAR = 5 and TEC = 5 meq/l induces clay dispersion and migration. Though, the amount of smectite and its spatial distribution within the sandy unsaturated layer are characterized by a highly stochastic behaviour.

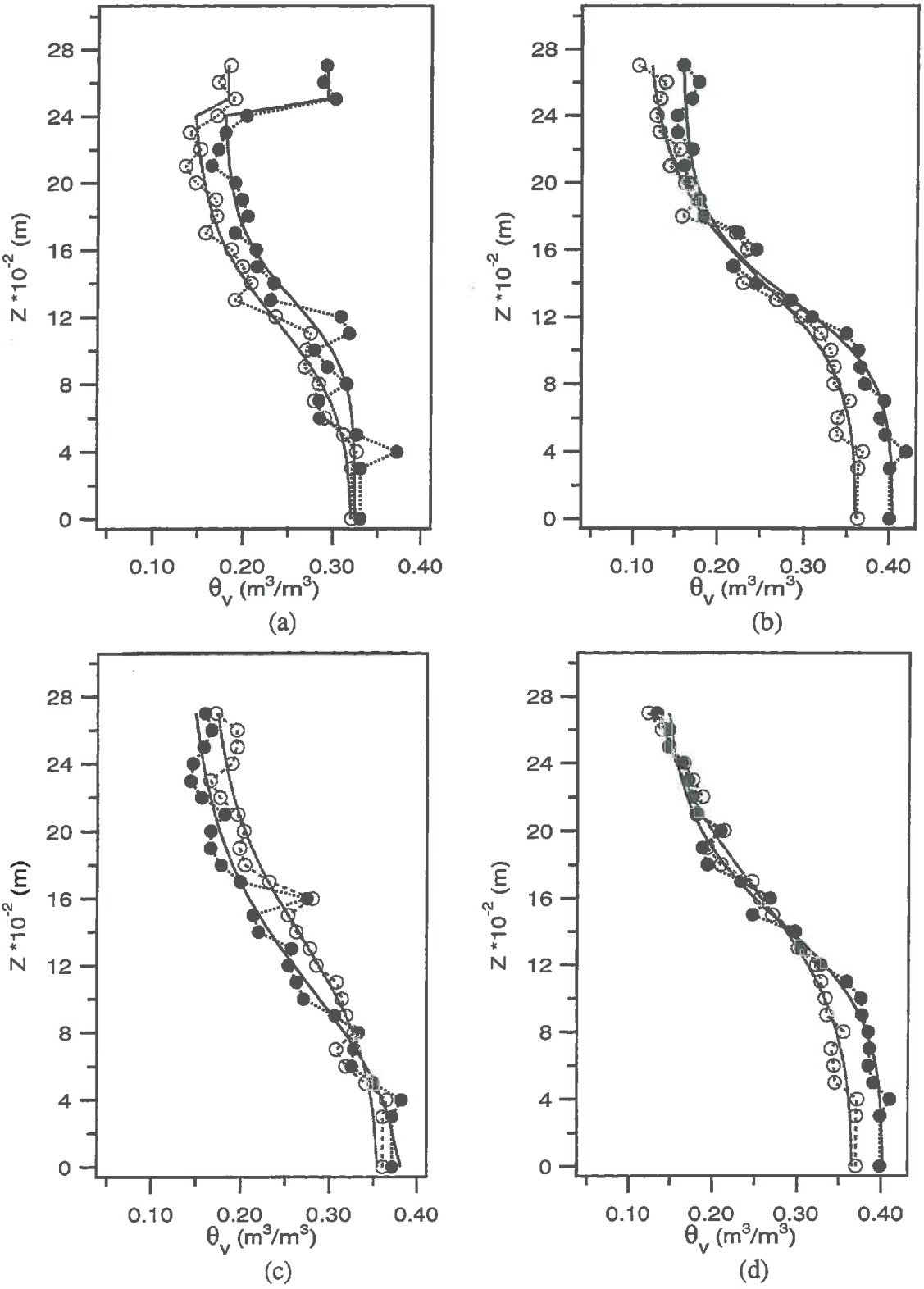

Figure 4.22. Comparison between the measured (circles) and calculated (solid line) water content profiles at the end of the first (o) and second percolation period (•) (series II) when a) SAR = 5, 1 meq/l, b) SAR = 10, TEC = 5 meq/l, c) SAR = 10, TEC = 1 meq/l or d) deionized water replaces SAR = 5, TEC = 5 meq/l.

4.8.3.2. Effect of a change of the SAR and TEC

An increase in the SAR or a decrease in the TEC reduced the total hydraulic conductivities as mentioned before (§ 4.3.2). If the total hydraulic gradient is maintained constant, a decrease in the hydraulic conductivity will cause a decrease of the downward flux. What generally happens is a shift of the water content profile towards lower water content values. If clay has migrated in the sandy layer during the first percolation period, an increase of the SAR or a decrease in the TEC will induce an increase of the water content because the distance between layers will increase. Consequently, the amount of water retained is also increased. Furthermore, when the leaching solutions are changed, a redistribution and a reorganisation of clay colloids occur within the column. When the TEC remains below the CFC, dispersion takes place, both in the clayey layer and in the sandy layer. Because of the large dimensions of the pores, dispersed colloids are more likely to be mobile in the sandy layer *(Sumner, 1993)* than in the upper clayey layer. In the latter, movement becomes limited due to pore constriction.

The effect of a change in the percolating solution on the water content profiles can be clearly seen and has already been discussed. Results of parameter estimation at the end of the second percolation period are summarized in annexe 4.19. They were obtained using the mean downward fluxes (table 4.5) and minimising the squared differences between the measured and the calculated water content profiles at the end of the second stage (figure 4.22).

The initial MRCs obtained with a SAR = 5 and TEC = 5 meq/l were different probably due to the clay amount and their distribution within the column. The effect of an increase in the SAR or a decrease of the TEC will be analysed by comparing the two MRCs for each column (figure 4.23). The parameter vector and variance-covariance matrix are the arithmetic means of those obtained at the end of the first and second percolation period. An estimated pdf is built for each column associated with their 95 % or 99 % confidence limits. The surfaces between the MRCs for a given column are calculated and compared to the respective confidence limits of the pdf (annexe 4.20).

The moisture retention curves determined after the solutions were changed are all significantly different at the 0.01 level, except for the column where the SAR of the leaching solution has been increased and the TEC decreased (C_3). The latter is only significantly different at the 0.0713 level.

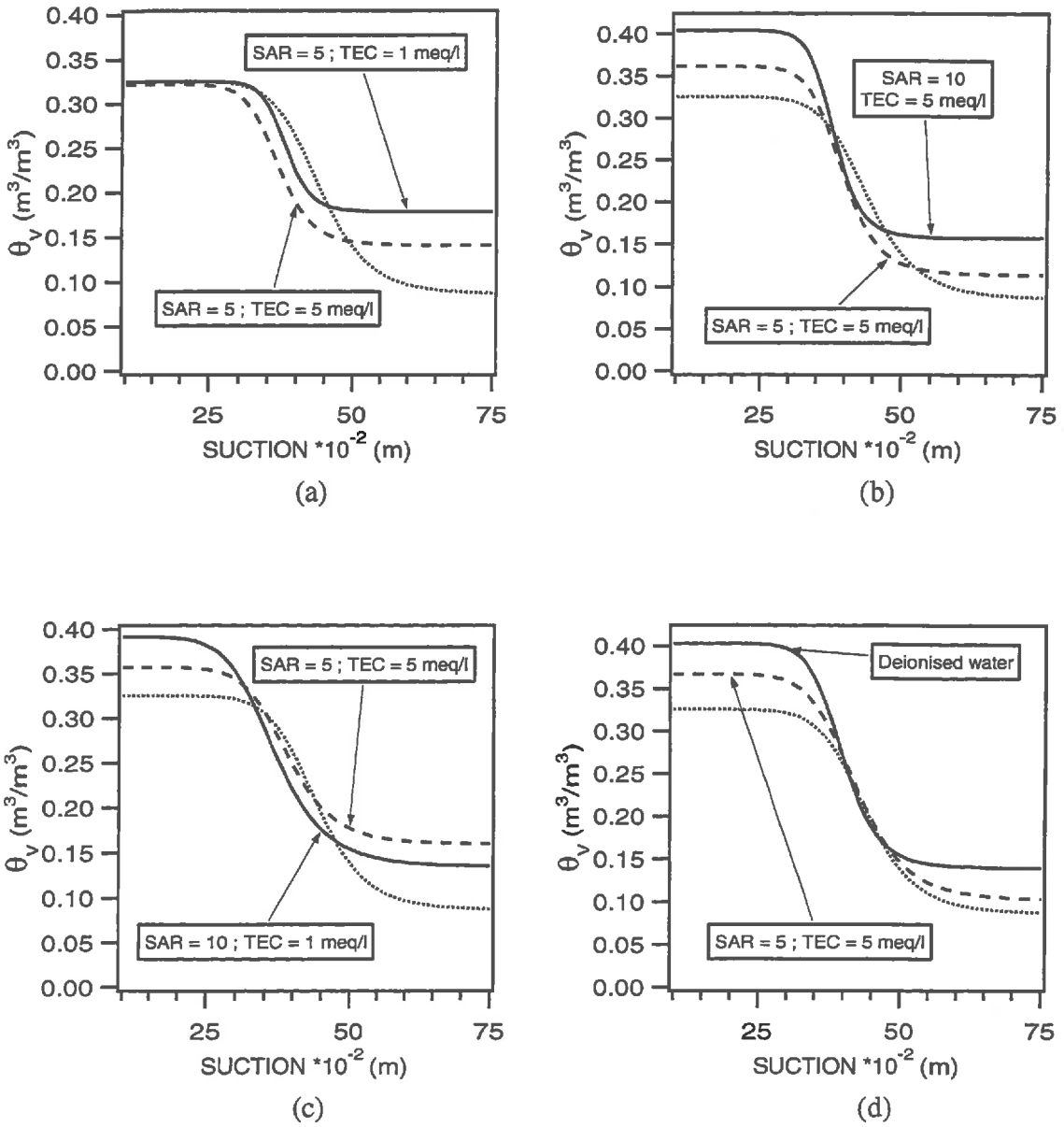

Figure 4.23. Comparison of the MRCs obtained at the end of the first (dashed line) and the second percolation period (solid line) for each column (series II) when a) the TEC is decreased, b) the SAR is increased, c) the TEC is decreased and the SAR is increased or d) deionized water replaces the leaching solution. The dotted line represents the main drying branche of the initial clay free Fontainebleau sand.

4.9. The HCC as affected by clay migration

The hydraulic conductivity curves (HCCs) were described using the same van Genuchten parameters but additional data was required to estimate the saturated hydraulic conductivity. It is worth noting that direct measurements of the saturated hydraulic conductivity were not performed at the end of the leaching period. Indeed, particle movement within the sandy column was expected with the use of solutions of low TEC (1 and 5 meq/l) or deionized water causing the direct measurement of K_s to be influenced. Consequently, the saturated hydraulic conductivities were initially calculated based on eqn. (3.15). Better HCCs can be obtained when experimental matching points are added.

One should remember that the columns were equipped with three tensiometers enabling the calculation of the hydraulic gradient. Based on the knowledge of the downward flux densities (§ 4.3.4) and the hydraulic gradients within the unsaturated layer, an unsaturated hydraulic conductivity value is obtained, associated to a corresponding mean suction. Using only the data available at the end of the percolation periods, the saturated hydraulic conductivity corresponds to the value that minimizes the sum of the squared errors between the calculated and the measured HCs, the latters being the matching points.

Performing this for the columns of the first series, it was found that K_s equalled 4.4 mm/h and 2.8 mm/h for SAR = 5 ; TEC 5 meq/ and SAR = 5 ; TEC = 1 meq/l, respectively. Comparing these values to that of Fontainebleau sand (284 mm/h), it only represents 1.5 % and 1 % of the initial K_s. The saturated conductivities of the columns leached with SAR values of 20 vary between 0.11 mm/h and 0.13 mm/h. The latter is obtained with the higher TEC (10 meq/l).

The HCCs are given in terms of relative hydraulic conductivities in figure 4.24. A logarithmic scale was chosen due to the low values obtained, especially for SAR = 20. The relative hydraulic conductivity K_r is given by the ratio of the unsaturated hydraulic conductivity to the saturated hydraulic conductivity of the initially clay-free Fontainebleau sand (K_s = 284 mm/h). These curves were calculated for the sandy layers and for Fontainebleau sand based on the four-term parameter estimation (annexe 4.14).

Two sets of curves are clearly seen, corresponding to a given SAR. The higher the SAR, the lower K_r. For a given SAR, the relative hydraulic conductivity further decreases with the TEC. When the matric potential is increased, the amount of water retained will decrease and K_r becomes smaller, reducing the clay movement. It should be noted that with a SAR value equals to 20, higher relative conductivities are maintained with a TEC = 5 meq/l rather than with TEC = 10 meq/l. As it has been mentioned to interpret the MRCs, this is probably due to differences in the clay amounts. Higher clay amounts combined to a TEC of 10 meq/l induces a lower K_r than a smaller clay quantity with a TEC of 5 meq/l.

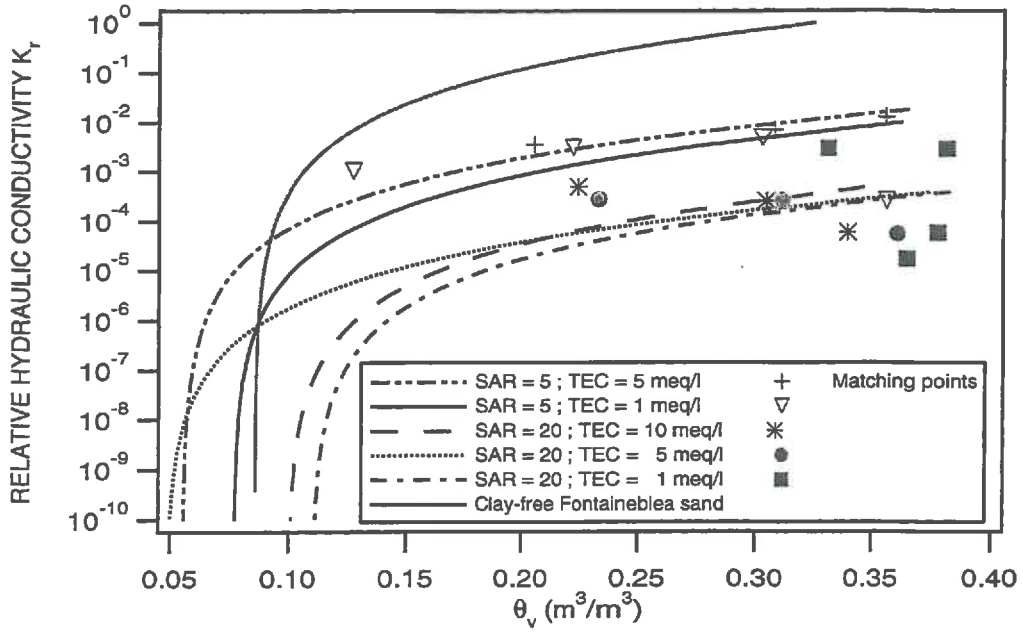

Figure 4.24. Calculated relative hydraulic conductivities of the sandy layers as affected by salinity and concentration versus the volumetric water content (series I). The markers represent the corresponding matching points to determine the saturated hydraulic conductivities.

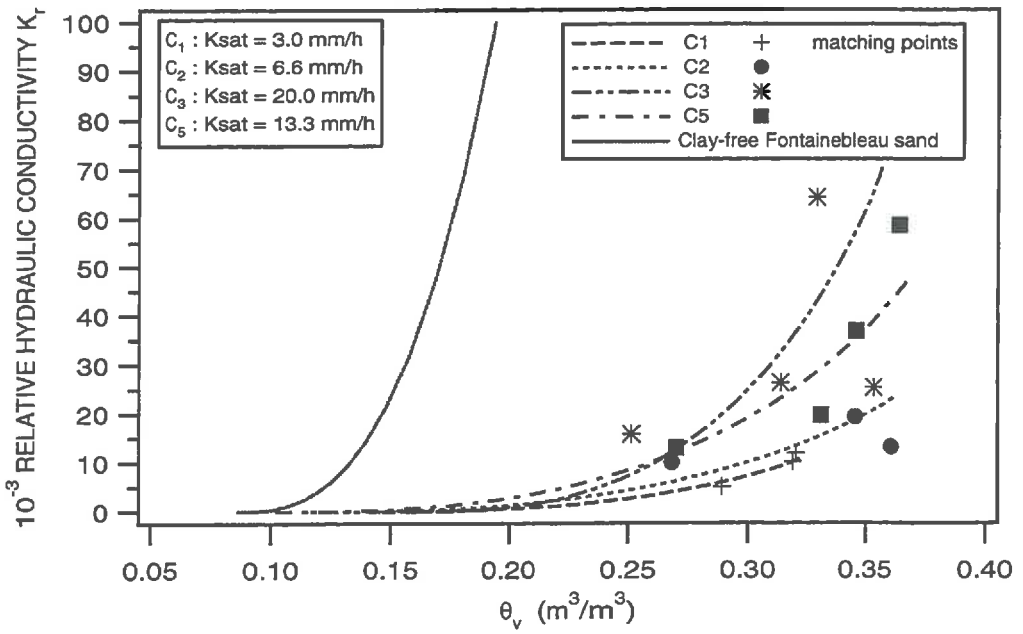

Figure 4.25. Calculated relative hydraulic conductivities of the sandy layers at the end of the first percolation period (SAR = 5 ; TEC = 5 meq/l ; series II). The markers represent the corresponding matching points to determine the saturated hydraulic conductivities.

A similar approach was applied to series II flow experiments using the four-term parameter vectors characterising the MRCs (figure 4.25). The saturated hydraulic conductivities were again obtained by minimising the sum of the squared errors between the calculated and the experimental matching points. The calculated saturated hydraulic conductivities at the end of the first leaching period (SAR = 5, TEC = 5 meq/l) ranged from 3.0 mm/h (C_1) up to 20.0 mm/h (C_3). Due to the fact that all the columns were submitted to the same experimental conditions, differences in the HCCs were interpreted by assuming a differential clay distribution within the unsaturated layer.

The effect of a change in the leaching solution on the relative hydraulic conductivities (RHCs) is presented in figure 4.26. The saturated hydraulic conductivity of the initially clay-free Fontainebleau sand is again used as reference. Increasing the SAR or diminishing the TEC caused the RHC to be reduced. Considering the TECs and the SARs used for the second percolation period, the unsaturated hydraulic conductivity reductions are the result of clay dispersion, particle translocation and limited swelling.

Maintaining a SAR equal to 5 but leaching with a more diluted solution (C_1) results in a saturated HC of 0.4 mm/h. This value only represents 13.3 % of the previous one obtained with a TEC = 5 meq/l. Increasing the SAR but maintaining a constant TEC (C_2) induced a lower reduction of K_s. Indeed, K_s diminished from 6.6 mm/h down to 1.9 mm/h, still representing 28.8 % of the former conductivity. When both SAR and TEC are modified (C_3), K_s dropped to about 5.5 % of the value obtained with SAR = 5 and TEC = 5 meq/l. Finally, leaching with deionized water (C_5) had a disastrous effect by reducing the saturated HC down to 3 % of the value obtained with the first leaching solution. RHC reductions are less pronounced with a decreasing degree of saturation.

These results seem to be in complete agreement with those of *Bresler et al. (1982)*, amongst others, who tested the effect of mixed Na-Ca salt solutions on the hydraulic conductivity of a loamy soil from Gilat, Israel. They concluded that the HC was highly dependent on the concentration and SAR in addition to their dependence on soil water content. For any given water content, HC decreased either as the solution concentration decreased or the SAR increased *(Russo and Bresler, 1977)*. The unsaturated hydraulic conductivity depends upon the size distribution of water-filled pores and upon the total water-filled porosity *(Bear and Bachmat, 1990)*. The pores created by the clay particles can be considered as isolated and simply connected voids, and are not effective from the point of view of the fluid flow. Water retained by the colloids constitutes an immobile liquid phase, whereas water in the larger pores or between the sand particles constitutes a mobile liquid phase. Consequently, for a given amount of clay and a given suction, the amount of water retained increases with an increase of the SAR or a decrease of the TEC, increasing the fraction of the immobile liquid phase. The non effective porosity is increased at the expense of the effective porosity.

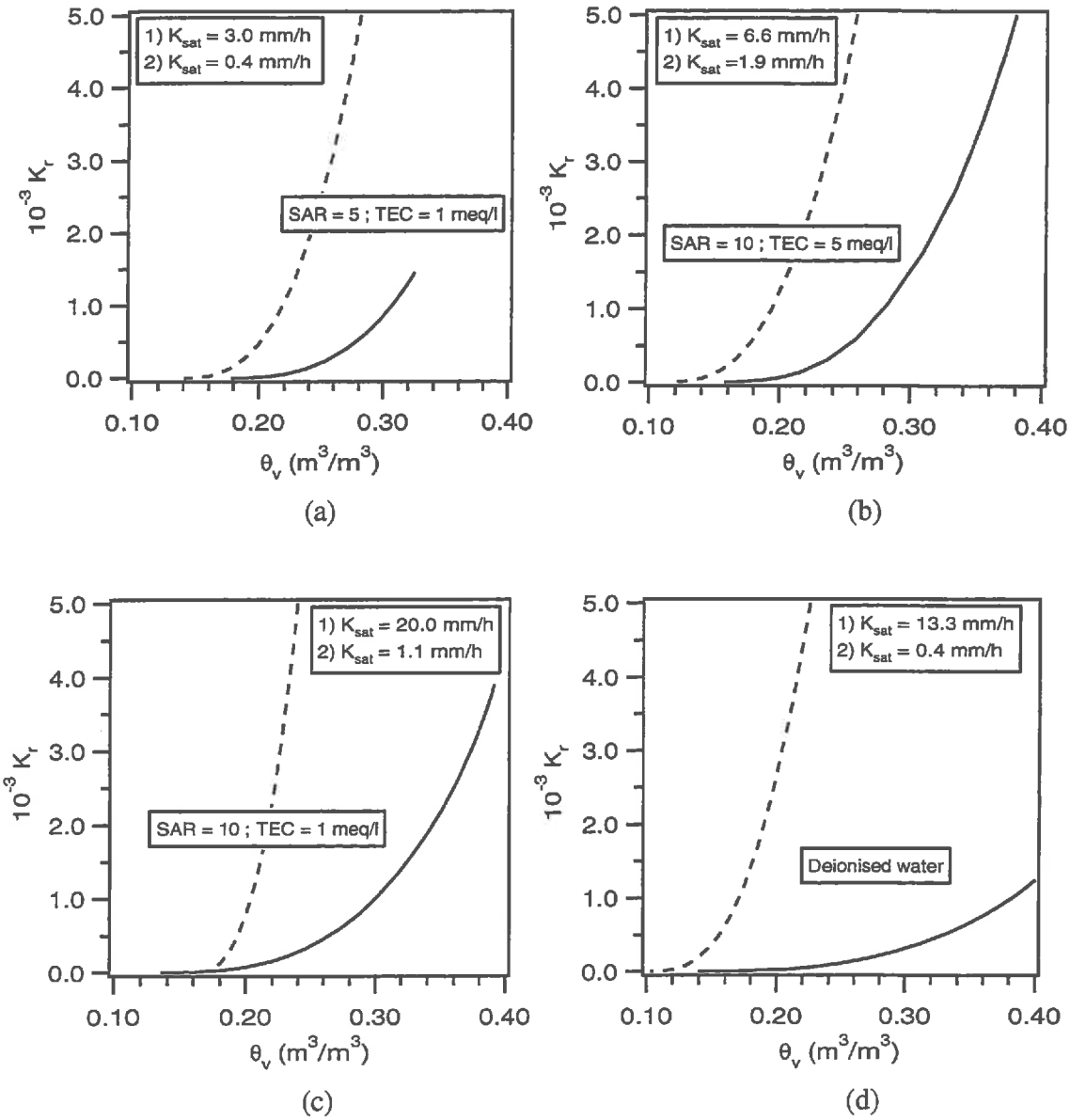

Figure 4.26. Comparison of the relative hydraulic conductivities, as a function of the volumetric water content, obtained at the end of the first (dashed line) and the second percolation period (solid line) for each column (series II) when a) SAR = 5, TEC = 1 meq/l (C_1) ; b) SAR = 10, TEC = 5 meq/l (C_2), c) SAR = 10, TEC = 1 meq/l (C_3), or d) deionized water (C_5) replaces SAR = 5, TEC = 5 meq/l.

As a result, the HC decreases. In addition, a further increase of the suction reduces the potential for movement of clay particles and the subsequent blockage of pores which contributes to soil water flow *(Bresler et al., 1982).*

4.10. Conclusions

The experimental results obtained with the flow experiments were presented and discussed in detail. By maintaining the same hydraulic conditions, i.e. constant hydraulic gradients, only the effect of different physico-chemical conditions were tested and described.

The interpretation of the measured parameters such as the suction and the water contents is not an easy task. Significant variations in the water contents can be measured without significant changes in the suctions or in the hydraulic gradients and *vice-versa*. Indeed, under a given downward flux density, one obtains specific water content and suction profiles. A reduction of the downward flux generally induces a shift of the water contents towards lower values. This is accompanied by an increase of the suctions. However, lowering the downward flux e.g. by increasing the SAR or decreasing the TEC, can also induce constant or higher water contents. The decrease of the water content due to a reduction of the flux is then balanced by an increase of the amount of water retained by dispersed clay particles. In addition, the amount of adsorbed water will increase with an augmentation of the clay amount and with the increase of the distance between clay layers. Under our experimental conditions, both dispersion, migration and limited *in situ* swelling can occur. We cannot distinguish the relative importance of each mechanism.

Considering these difficulties, it seems obvious to compare hydrodynamic properties, i.e. MRCs and HCCs rather than water content and suction profiles. Soil moisture retention curves of the sandy layers at the end of the percolation period could be described with a three or a four-term parameter vector. Imposing a constraint on the residual water content results in the estimation of three highly correlated parameters. Furthermore, the assumption that the residual water content remains unaffected by clay migration is not reasonable. It has been concluded that the MRCs had to be described using a four-term parameter vector $(\theta_r, \theta_s, \alpha, n)$.

When temporarily steady state flow conditions were assumed, it was shown that the variability of the α curve shape parameter in a given period of time expressed in terms of pore volumes could be described with an exponential relationship. In this expression, the rate of the MRC displacement influenced by the SAR and the TEC was quantified. Even though the small number of different leaching solutions, it can be seen that the higher the SAR and the lower the TEC, the more accentuated is the variation of the α curve shape parameter.

The MRCs and HCCs calculated with the parameters and estimated by the inverse approach are influenced by many factors such as the amount of clay, its spatial distribution within the column and the percolating solution. Indeed, even if identical hydraulic and chemical conditions are applied to identically packed columns, different water content profiles were measured. Because the water content appeared to be a very sensitive indicator of the presence of clay, it was concluded that these differences were only due to the amount of clay and its spatial distribution within the column. Unfortunately, this could not be verified by clay quantification because it required a complete destruction of the columns. As a consequence, different soil moisture retention curves and hydraulic conductivity curves had to be estimated for a same solution of SAR = 5 and TEC = 5 meq/l.

Increasing the SAR or decreasing the TEC generally resulted in significantly different estimated MRCs at the 0.01 level. The presence of dispersed clay particles combined to a change of the leaching solution generally resulted in an increase of the total measured volumetric water content. The latter is the summation of the immobile liquid phase retained by the clay layers and the mobile liquid phase occupying the effective porosity. It was concluded that the reduction of the RHC was due to a decrease of the relative importance of the effective porosity despite the increase of the total porosity.

REFERENCES

Aringhieri, R., and M. Capurro. (1994). Evaluating saturated hydraulic conductivity of a soil in laboratory investigations : an empirical model. *Soil Science*, **157**, 77-83.

Bear, J., and Y. Bachmat. (1990). *Introduction to Modeling of Transport Phenomena in Porous Media.* Kluwer Academic Publishers, Dordrecht, 553 p.

Bresler, E., B.L. Mc Neal, and D.L. Carter. (1982). *Saline and Sodic Soils - Principles - Dynamics - Modeling*. Springer-Verlag, Berlin, 236 p.

Chen, Y., and A. Banin. (1975). Scanning electron microscope (SEM) observations of soil structure changes induced by Na-Ca exchange in relation to hydraulic conductivity. *Soil Science*, **120**, 428-436.

Emerson, W. W., and A.C. Bakker. (1973). The comparative effect of exchangeable Ca, Mg and Na on some physical properties of red brown earth subsoils. II. The spontaneous dispersion of aggregates in water. *Australian Journal of Soil Research*, **11**, 151-157.

Frenkel, H., J.O. Goertzen, and J.D. Rhoades. (1978). Effects of clay type and content, exchangeable sodium percentage and electrolyte concentration on clay dispersion and soil hydraulic conductivity. *Soil Science Society of America Journal*, **42**, 32-39.

Frenkel, H., G.J. Levy, and M.V. Fey. (1992a). Clay dispersion and hydraulic conductivity of clay-sand mixtures as affected by the addition of various anions. *Clays and Clay Minerals*, **40**, 515-521.

Frenkel, H., M.V. Fey, and G.J. Levy. (1992b). Organic and inorganic anion effects on reference and soil clay critical flocculation concentration. *Soil Science Society of America Journal*, **56**, 1762-1766.

Goldberg, S., and H.S. Forster. (1990). Flocculation of reference clays and arid-zone soil clays. *Soil Science Society of America Journal*, **54**, 714-718.

Keren, R., and M.J. Singer. (1988). Effect of low electrolyte concentration on hydraulic conductivity of sodium/calcium-montmorillonite-sand system. *Soil Science Society of America Journal*, **52**, 368-373.

Kool, J.B., J.C. Parker, and M.Th. van Genuchten. (1987). Parameter estimation for unsaturated flow and transport models - a review. *Journal of Hydrology*, **91**, 255-293.

Kool, J.B., and J.C. Parker. (1987). Development and evaluation of closed-form expressions for hysteretic soil hydraulic properties. *Water Resources Research*, **23**, 105-114.

McNeal, B.L., W.A. Norvell, and N.T. Coleman. (1966). Effect of solution composition on the swelling of extracted soil clays. *Soil Science Society of America Proceedings*, **30**, 313-317.

Pupisky, H., and I. Shainberg. (1979). Salt effects on the hydraulic conductivity of a sandy soil. *Soil Science Society of America Journal*, **43**, 429-433.

Quirk, J.P., and R.K. Schofield. (1955). The effect of electrolyte concentration on soil permeability. *Journal of Soil Science*, **6**, 163-178.

Russo, D., and E. Bresler. (1977). Effect of mixed Na-Ca solutions on the hydraulic properties of unsaturated soils. *Soil Science Society of America Journal*, **41**, 713-717.

Shainberg, I., and A. Caiserman. (1969). Kinetics of the formation and breakdown of Ca-montmorillonite tactoids. *Soil Science Society of America Proceedings*, **33**, 547-551.

Somaratne, N.M. (1994). Characterization and modelling of surface sealing and near surface pore clogging processes. Thesis, Flinders University of South Australia.

Sumner, M.E. (1993). Sodic soils : new perspectives. *Australian Journal of Soil Research*, **31**, 683-750.

Tessier, D. (1984). Etude expérimentale de l'organisation des matériaux argileux. Hydratation, gonflement et structuration au cours de la dessication et de la réhumectation. Thèse Université Paris VII, UER des Sciences Physiques de la Terre, 361 p.

van Genuchten, M.Th., S.M. Gorelick, and W.W.G. Yeh. (1988). Application of the parameter estimation techniques to solute transport studies. In *Proceedings of the International Symposium on Water Quality Modelling of Agricultural non point Sources*, Part 2, Don G. De Coursey (ed.), Utah State University, Logan, UT, 732-753.

Verburg K., and P. Baveye. (1994). Hysteresis in the binary exchange of cations on 2:1 clay minerals : A critical review. *Clays and Clay Minerals*, **42**, 207-220.

Wan, J., and J.L. Wilson. (1994). Colloid transport in unsaturated porous media. *Water Resources Research*, **30**, 857-864.

5. Conclusions

This study was initiated to explain the abnormally large water content fluctuations recorded *in situ* in an unsaturated profile during the recharge of the bruxellian aquifer at Louvain-la-Neuve. In order to predict such fluctuations, modelling is the only tool available for a scientific approach and hopefully for management. Of course, a model remains an idealized scheme of the natural phenomena and its outputs highly depend on the input data quality. Moreover, as far as modelling of water flow is concerned, one assumes that the temporal variability of the hydrodynamic properties induced by chemical treatments is generally negligible. Once the properties are determined, either on a laboratory scale or at the field scale, they are introduced in the model to solve a direct problem. However, the assumption cannot longer been accepted especially in soils where clay dispersion can be induced and where the clay particles can further migrate in the soil profile. There is evidence through the literature that the hydraulic conductivity is highly affected by the solution electrolyte concentration and its composition in terms of Na and Ca. Most of these studies were carried out under saturated conditions and only few studies were performed in the unsaturated zone, probably because the unsaturated flow is a more complicated case requiring specific measurements such as the volumetric water content.

Within the framework of this study, smectite dispersion and mobility were investigated in two-layered experimental unsaturated columns induced by means of salty solutions and its consequences on the hydrodynamic properties of an initially clay-free sand. From these flow experiments carried out at a laboratory scale under identical hydraulic conditions but under various chemical treatments the following conclusions can be drawn :

1. Our thesis proves that Béthonvilliers smectite disperses and migrates from an upper clayey layer constituted of Béthonvilliers soil material towards an unsaturated lower layer constituted of Fontainebleau sand. This occurred under intermediate SAR values (5, 10, 20) and low total electrolyte concentrations (TECs = 1, 5, 10 meq/l).

Clay migration has been brought forth by the observation of the total hydraulic conductivities measured daily with the falling head method. Indeed, sensible increases of the hydraulic conductivities (HC) were observed after a rapid decrease at the very beginning of the flow experiments, especially for the columns leached with SAR = 5. These augmentations could neither be explained by a change of the experimental conditions nor by a change of the leaching solution. It was concluded that the departure of clay particles caused the increase of the HC and allowed to maintain it. The greater the variation is, the more clay quits the upper layer. The rise of the HC was accompanied by a simultaneous reduction of the suction measured in the first centimetres of the unsaturated sandy layer.

One should also note that clay dispersion with solutions of SAR = 5 and TEC = 5 meq/l is not familiar because this concentration is higher than some critical flocculation concentrations (CFC) mentioned in the literature. Clay dispersion can occur provided the TEC is lower than the CFC. Clay dispersion under these salty conditions was justified by the fact that soil clays are generally more dispersive than reference clays, requiring greater salt concentrations at all SARs and pH values. Furthermore, mechanical disturbance, i.e. crushing of the sample and sieving, affects clay dispersion by increasing their sensitivity to sodicity. Finally, due to the high clay amount in Béthonvilliers soil material, its sensitivity to excessive exchangeable sodium and low TECs is enhanced.

Clay dispersion is a prerequisite for particle movement. However, even if dispersive conditions are induced, one is not able yet to evaluate the amount of clay which will migrate. Exact replicates are particularly difficult to obtain even if all the experimental physico-chemical conditions are identical. Differences in the hydrodynamic properties appear probably due to differences in the amounts of clay which migrated and its spatial distribution within the unsaturated sandy layer. These two parameters are characterized by a highly stochastic behaviour.

2. Béthonvilliers smectite migrates through the unsaturated sandy layer. This was proved by quantifying dispersed smectite by means of X-ray spectrometry at the end of the percolation period. Smectite was found at all depths of the columns. There are two explanations for this. First, the smallest particles migrated probably first, those whose size is less than 0.2 µm. Second, moving interfaces created during the disconnection of the reservoir at the bottom of the column could have provoked particle translocation further down the column.

The presence of clay was also indicated through the observation of the repeated and non destructive volumetric water contents measured by gamma-radiation. Constant or even increasing water contents were measured in spite of decreasing flux densities induced by a change of the leaching solution. This also induced rapid variations in the matric potentials. The most significant variations were measured when deionized water replaced the leaching solution of SAR = 5, TEC = 5 meq/l because particularly favourable dispersive conditions were induced. Indeed, the electrolyte concentration drops and a high salt gradient is generated. In addition, applying deionized water induces an increase of the pH, which in his turn enhances the development of negative charges, thus promoting smectite dispersion and movement.

3. Extremely small amounts of smectite are required to change the hydrodynamic properties of the initially clay-free Fontainebleau sand. The ratios of the clay volume to the total volume are lower than 0.004 m^3/m^3. The soil moisture retention curves (MRCs) and the hydraulic conductivity curves (HCCs) were determined by applying an inverse approach and assuming

that these properties were well described with the functional non hysteretic van Genuchten relationships. An objective criterion was developed to allow an easy comparison of the MRCs.

4. A change in the leaching solution composition significantly affects the hydrodynamic properties. This was proved by observing the total hydraulic conductivities and by comparing the MRCs and HCCs obtained at the end of each percolation period. The total hydraulic conductivity decreases sharply when the salinity is maintained and the TEC is lowered. A more drastic effect is observed when deionized water is used. The rapidity of the HC decrease observed then suggests an immediate sealing of the pore space by the entrapped dispersed clay. On the contrary, when leaching with SAR = 10 for TECs of 1 and 5 meq/l a gradual sealing probably occurred. This suggests more a re-orientation of the dispersed clay particles than a rapid clogging of the conducting pores.

Increasing the SAR or decreasing the TEC generally resulted in significantly different estimated MRCs at the 0.01 level and in the reduction of the relative hydraulic conductivity while the total porosity was increased. Indeed, it was observed that the bulk density decreased after the leaching solution was changed inducing particle departure. If the mass of solid decreases for a constant total volume, the bulk density is reduced and the total porosity is increased. But simultaneously the distance between the clay particles increases. Consequently, more water is retained by the clay layers. If the total void volume is considered to be occupied by solution, this means that if the void ratio increases, the clay porosity also increases. However, the latter is ineffective in terms of water flow because adsorbed water constitutes a rather immobile liquid phase. Consequently, it was concluded that the reduction of the relative hydraulic conductivity was due to a decrease of the relative importance of the effective porosity despite the increase of the total porosity and the water content. This is in contradiction with the soil physics studied classically on a mechanistic point of view.

Knowing that the hydrodynamic properties change so significantly in response to the water quality as demonstrated in our thesis, a similar mechanism could be proposed to explain the field water content fluctuations related to the input of deicing salts in the ponded storm basin at Louvain-la-Neuve. Nevertheless, either in the field or in the laboratory, many problems have to be solved to improve the modelling of unsaturated flow where such physico-chemical mechanisms could occur.

6. Perspectives

This study showed interesting results but it is only a small contribution to smectite migration through unsaturated porous media and its consequences on the hydrodynamic properties. Here we will try to focus on several points requiring further research.

Dispersed clay particles constitute a mobile solid phase implicated in the transport of heavy metals, organic compounds and radionuclides amongst others. Bearing this in mind, it has important implications in the understanding and the prediction of contaminant transport. In addition to the pollutant transport, mobile particles affect the hydraulic conductivity of the media. The use of drilling muds and clay barriers for waste isolation are examples where clogging is a desirable effect. However, reduction of the hydraulic conductivity poses a major problem during recharge of aquifers. Artificial recharge has provided a means of recycling treated sewage effluents. This operation depends heavily on the ability of water to infiltrate first the unsaturated zone and then the aquifer without reducing the hydraulic conductivity of the media. However, these effluents are particularly rich in organic anions which act as dispersant enhancing clay dispersion.

Consequently, it is of uttermost importance to understand 1) the interactions between the soil particles and the liquid phase, 2) the factors affecting clay dispersion and migration within a given porous media, 3) the development of the resultant soil properties such as the soil moisture retention curve or the hydraulic conductivity curve.

One knows that the dispersive behaviour of clays depends on e.g. its mineralogy, pH, SAR, the total electrolyte concentration, the presence of other weatherable minerals and organic compounds, the use of mechanical energy which is generally required for the preparation of the samples. Data and criteria such as the Critical Flocculation Concentration (CFC) can be found through the literature. However, if they inform on the dispersive behaviour, the quantitative prediction of the amount that will be dispersed remains largely unknown. In addition, up to now no functional relationships could be drawn relating these parameters even for pure clay fractions.

In soils, the situation is more complicated because the clay fraction is rarely pure and it is further associated to other compounds such as oxides or hydroxides which also affect clay dispersion. Depending on the importance of the clay fraction, clay migration will be facilitated. This is the case in sandy porous media whereas in clay soils, particle movement is more restricted.

In order to assess the modification of the hydrodynamic properties induced chemically, one could consider a conceptual approach similar to that proposed in this work for sand-smectite mixtures. It should include relationships established experimentally bearing in mind that the preparation of the soil materials heavily affects clay swelling and dispersion. Of course, relationships established for dilute suspensions are not applicable for saturated pastes e.g. the number of layers per quasi-crystal as a function of the exchangeable sodium percentage. The experiments should also be realized e.g. on different pure smectites of varying layer charge per unit cell. Soil clays containing smectite do not necessarily behave as pure ones resulting in different relationships. Finally, once validated with independent data sets, such theoretical soil moisture retention curves could then be included in water flow modelling.

The hydrodynamic properties can also be determined by an inverse approach. Parameter estimation in this study was performed by assuming steady-state flow conditions. One should focus research on more powerful parameter estimation techniques under non steady-state conditions. Information concerning the temporal variability of the hydrodynamic properties determined by an inverse approach could then be taken into account by introducing them as new input parameter in direct flow modelling.

Finally, it seems important to discuss about the design of the laboratory experiments, the procedures and the techniques used to study the effect of water quality on the hydrodynamic properties of an unsaturated porous media affected by clay dispersion and migration.

The experimental device was appropriate but could eventually be improved regarding the system used to apply a constant suction at the bottom of the reservoir. Scanning measurements required to disconnect it generating moving interfaces which could induce particle movement further down the column. To get around the problem, the length of the experimental columns could be increased. Nevertheless, one should not forget the reservoir at the bottom which is the reference level for the hydraulic conductivity measurements with the falling head method.

Amongst the various parameters which were measured during the experiments, the flux density, the total hydraulic conductivity, the suctions at different depths and the water contents are necessary. The flux densities combined to the measurements of the suctions constitute the matching points to determine the saturated hydraulic conductivities. Direct measurements of this parameter is particularly difficult when solutions of low TECs are used because clay dispersion could take place, especially when the TEC is lower than the CFC.

The volumetric water content seems to be an interesting indicator to study the effect of water quality. Of course, repeated and non destructive measurements should be preferred e.g. using gamma-radiation or a coupled neutron-gamma probe. This equipment further allows to assess the bulk density fluctuations and, hence, the changes in the total porosity.

Reconsidering the leaching procedure explained in § 2.6.3, some modifications are suggested. The procedure explained below holds to study the effect of mixed solutions NaCl-

$CaCl_2$ but it can be modified e.g. for solutions containing different organic anions or solutions of various pH.

- Once the elements of the columns are fitted together (PVC cylinders), the small holes are filled up with silicone, and molten paraffin is poured at the junction of two consecutive cylinders.
- The dry fine textured Fontainebleau sand is then uniformly packed in the column. This is performed by placing the empty column on a vibration table (6000 oscillations/minute) and by progressively filling it within a given time, ranging from 2'30" to 3'05". The homogeneity of compaction within each column is verified using the gamma-radiation (^{137}Cs- 406 mCi or 15 GBq - ^{241}Am - 200 mCi or 7.4 GBq).

  The use of another sandy material is possible. However, one should consider that the length of the column was conditioned by the narrow suction range. Furthermore, the length has to be increased if no suction is applied at the bottom of the column. This solution should be chosen in order to avoid the mobile interfaces generated by the disconnection of the reservoir.

- The sandy layer is then progressively wetted from the bottom by capillary rise with a solution of known SAR and TEC, in order to minimize air entrapment.

  All the columns could be first leached with a solution of a given SAR but a TEC = 100 meq/l.

- The silicone is removed from the holes of the PVC cylinders. The gas phase is at atmospheric pressure.
- The drainage is started. At equilibrium i.e when the flux density equals zero, the first water content and density profiles are measured before the tensiometers are connected to the mercury manometers. The first profile corresponds to the main drying branche of the soil moisture retention curve of Fontainebleau sand in the low suction range.
- The top layer is gently placed after the drainage occurred.

  For a clayey soil material such as Béthonvilliers, the use of 20 g of air-dried raw soil material resulting in a layer thickness of approximately 0.7 cm seems perfect. If possible, one should avoid the procedure of mixing together Na and Ca-saturated soil material to obtain a desired ESP. Indeed, it requires the crushing, the sieving and the centrifugation of the material. This mechanical energy input affects the clay behaviour.

One should prefer a leaching procedure with a solution of a given SAR and a high TEC e.g. 100 meq/l. The results obtained with that specific solution could further be considered as reference. The saturation procedure could be performed separately from the flow experiment in order e.g. to establish the evolution of the saturated hydraulic conductivity of the soil material as a function of the SAR and the TEC. Turbidimetry techniques could be associated to quantify dispersed clay in the effluents.

- The top layer is covered with a glass microfibre filter to reduce surface disturbance during the leaching experiments and progressively wetted in order to minimize particle disaggregation. The wetting of the soil material is performed with the same solution of known SAR and TEC, before a constant head is applied by means of a Mariotte bottle.

  Each column could be leached with a solution of a given SAR and TEC = 100 meq/l until 10 up to 20 pore volumes are collected. This corresponds in the literature to the hydrodynamic equilibrium. Each column could then be submitted to a different solution in order to study the effect of an increase of the SAR, a decrease of the TEC, or both simultaneously. Water quality can either be gently modified by step-wise increases or decreases, or drastically modified. The effect of leaching with deionized water, which simulates rainfall, should be added.
  The experiment should at least be duplicated.

- During leaching the suction and the total hydraulic conductivity are measured daily, whereas the volumetric water content and bulk density profiles are determined weekly. All the effluent volumes are collected and the EC, pH and the respective concentrations of calcium and sodium determined. The upper layer thickness is regularly measured.
- At the end of the percolation period, the water content profile is verified by the gravimetric method. The small cylinders of the PVC column are then separated from each other. The water content on a mass basis are determined by weighting the wet sample and after drying at 105°C during 48 h.
- The amount of smectite within the sandy subsamples is quantified by the means of X-ray fluorescence spectrometry.

  X-ray fluorescence spectrometry is an interesting method but rather expensive. It further requires specific sample preparation.

Having in mind the above considerations, one can conclude that prediction of clay movement in unsaturated zone induced by salty conditions and its consequences on the hydrodynamic properties of this unsaturated zone do not seem so far to be achieved.

SYMBOLS AND ABBREVIATIONS

7. Symbols and abbreviations

Abbreviations

AAS	Atomic Absorption Spectrometry
CEC	Cation Exchange Capacity
CFC	Critical Flocculation Concentration
DCP	Direct Current Plasma
DLVO	Theory of interaction between charged particles developed independently in the 1940s by *Derjaguin and Landau (1941)* and *Verwey and Overbeek (1948)*
EC	Electrical Conductivity
ESP	Exchangeable Sodium Percentage
HCC	Hydraulic Conductivity Curve
MRC	Moisture Retention Curve
MSE	Mean Square Error
RELS	Relative Sensitivity
SAR	Sodium Adsorption Ratio
SD	Standard Deviation
SS	Sum of the Squared residuals
TEC	Total Electrolyte Concentration
OLS	Ordinary Least Squares
VG	van Genuchten

Symbols

a	limit of an interval
A	constant value
A_i	cross-sectional area [m^2]
A_v	volumetric accuracy [m^3]
b	rate of the MRC displacement ; limit of an interval
b_o	average spacing between the layers in the quasi-crystals as determined by X-ray measurements (= 9e-10 m)
B	constant value
c	Compton scatter [1/s]
C	constant value
C_b	estimated variance-covariance matrix to assess parameter uncertainty
C_i	molal concentration in the bulk solution [mole/kg H_2O]
d	as superscript to refer to drying
D	constant value

e	void ratio [m^3/m^3]
e_o	initial void ratio determined for the dry clay [m^3/m^3]
E_i	relative error
f	function
g	acceleration due to gravity [m/s^2]
G	function
h	matric head or pressure head or suction [m]
h_g	capillary pressure at the inflection point of the soil moisture retention curve [m]
h_o	matric potential at the bottom of the column [m]
H	hydraulic head [m]
$H(\hat{b})$	hessian matrix
i	indice
I	gamma count rate after dead time or/and Compton corrections [1/s]
ID	index of dispersion [kg/kg]
I_o	corrected gamma count rate through air [1/s]
I_r	recorded count rate without any correction ($I_r = N_r/t$) [1/s]
I_s	ionic strength [mole/kg H_2O]
j	indice
k	indice
K	hydraulic conductivity [m/s]
K_s	saturated hydraulic conductivity [m/s]
K_T	total hydraulic conductivity measured by the falling head method [m/s]
l	number of depths intervals ; indice
L	length of the soil column [m]
m	van Genuchten parameter $m = 1-1/n$
m_a	mass of air [kg]
m_c	mass of clay [kg]
m_s	mass of solid [kg]
m_t	total mass [kg]
m_w	mass of water [kg]
n	van Genuchten curve shape parameter
n_{obs}	number of observations
N	total corrected gamma count through the absorbing material
N_a	avogadro's number (= 6e23 $mole^{-1}$)
N_{ds}	total corrected gamma count for a dry soil column
N_o	total corrected gamma count through an empty column
N_p	number of layers per quasi-crystal (with subscript Na or Ca for Na or Ca-saturated clay)
N_s	total corrected gamma count through a column filled with sand

N_w	total corrected gamma count through a column filled with water
N_{ws}	total corrected gamma count for a wet soil column
N_{X-ray}	total corrected count obtained by X-ray fluorescence spectrometry
O	objective function
p	number of terms ; dimension of the parameter vector
p	solution pressure [Pa]
P_e	macroporosity [%]
P_m	pressure potential per unit mass [J/kg]
$P_{\max}$	maximal pressure applied to a system [Pa]
P_v	pressure potential per unit volume [Pa]
P_w	pressure potential per unit weight (= h) [m]
q	flux density [m/s]
q_e	charge of the elecron (= 1.6e-19 C)
R	gas constant (= 8.314 J mole^{-1} K^{-1})
S	surface between two soil moisture retention curves
S_e	effective saturation
S_o	total specific surface area
t	time
t_i	roots of the Legendre polynomial
T	absolute temperature
V	variance-covariance matrix
V_a	volume of air [m^3]
V_c	volume of clay [m^3]
V_s	volume of solid [m^3]
V_t	total volume [m^3]
V_w	volume of liquid [m^3]
w	as superscript to refer to wetting
w_i	weighting factors
x	uniform thickness of the absorbing material [m]
X_i	random variable
x_s	thickness of the soil material [m]
z	vertical coordinate (positive in the upward direction) or elevation head [m]
Z_i	ion valency
Z_m	gravitational potential per unit mass [J/kg]
Z_v	gravitational potential per unit volume [Pa]
Z_w	gravitational potential per unit weight [m]
$\%_c$	mass percentage of clay

Greek letters

α	van Genuchten curve shape parameter [m^{-1}]
ε	porosity [m^3/m^3]
ε_o	vacuum permittivity (= 8.85e12 F/m)
ε_r	dielectric constant of the medium (= 80 for water)
ϕ	hydraulic potential [m]
γ	contact angle (assuming here $\gamma = 0$ °)
κ	inverse of the Debye screening length [1/m]
λ_i	distance between the adjacent quasi-crystals [m]
μ_l	linear attenuation coefficient of the absorbing material, product of the mass attenuation coefficient and the density [1/m]
μ_s	mass attenuation coefficient of the soil [m^2/kg]
μ_w	mass attenuation coefficient of water [m^2/kg]
π	osmotic pressure [Pa]
θ_v	volumetric water content [m^3/m^3]
θ_m	water content on a mass basis [kg/kg]
θ_s	saturated water content [m^3/m^3] or [kg/kg]
θ_r	residual water content [m^3/m^3] or [kg/kg]
$\theta(z_i)$	water content profile (subscript 'meas' for measured and 'calc' for calculated)
ϑ	liquid ratio [m^3/m^3]
ρ_b	dry bulk density [kg/m^3]
ρ_s	density of the solid [kg/m^3]
ρ_{sc}	clay particle density of Béthonvilliers [kg/m^3]
ρ_w	density of water [kg/m^3]
σ	surface tension (7.28e-2 J/m^2 at 20° C)
σ_i	standard deviation of a random variable X_i
σ_Y	standard deviation of a function Y of independent random variable X_i
τ	dead time [µs]
ψ_v	matric potential per unit volume [J/m^3]
ψ_m	matric potential per unit mass [J/kg]
ψ_w	matric potential per unit weight [m]
π	osmotic pressure [Pa]
Φ_t	total potential
Γ_s	effective charge density of the clay (= CEC/ S_o)
Π	osmotic potential

ANNEXES

Annexe 2.1. Particle size analysis of Bethonvilliers soil samples obtained with Na-resins as dispersant (US Department of Agriculture classification).

Particle size	Mass percentage
	kg/kg *100
< 0.2 µm	50.26
0.2-0.5 µm	8.01
0.5-1 µm	3.49
1-2 µm	3.49
2-20 µm	16.15
20-50 µm	11.69
50-100 µm	3.91
100-250 µm	2.10
250-500 µm	0.32
500-1000 µm	0.46
1000-2000 µm	0.12

Annexe 2.2. Scheme of a porous cup used as tensiometer connected to a mercury manometer.

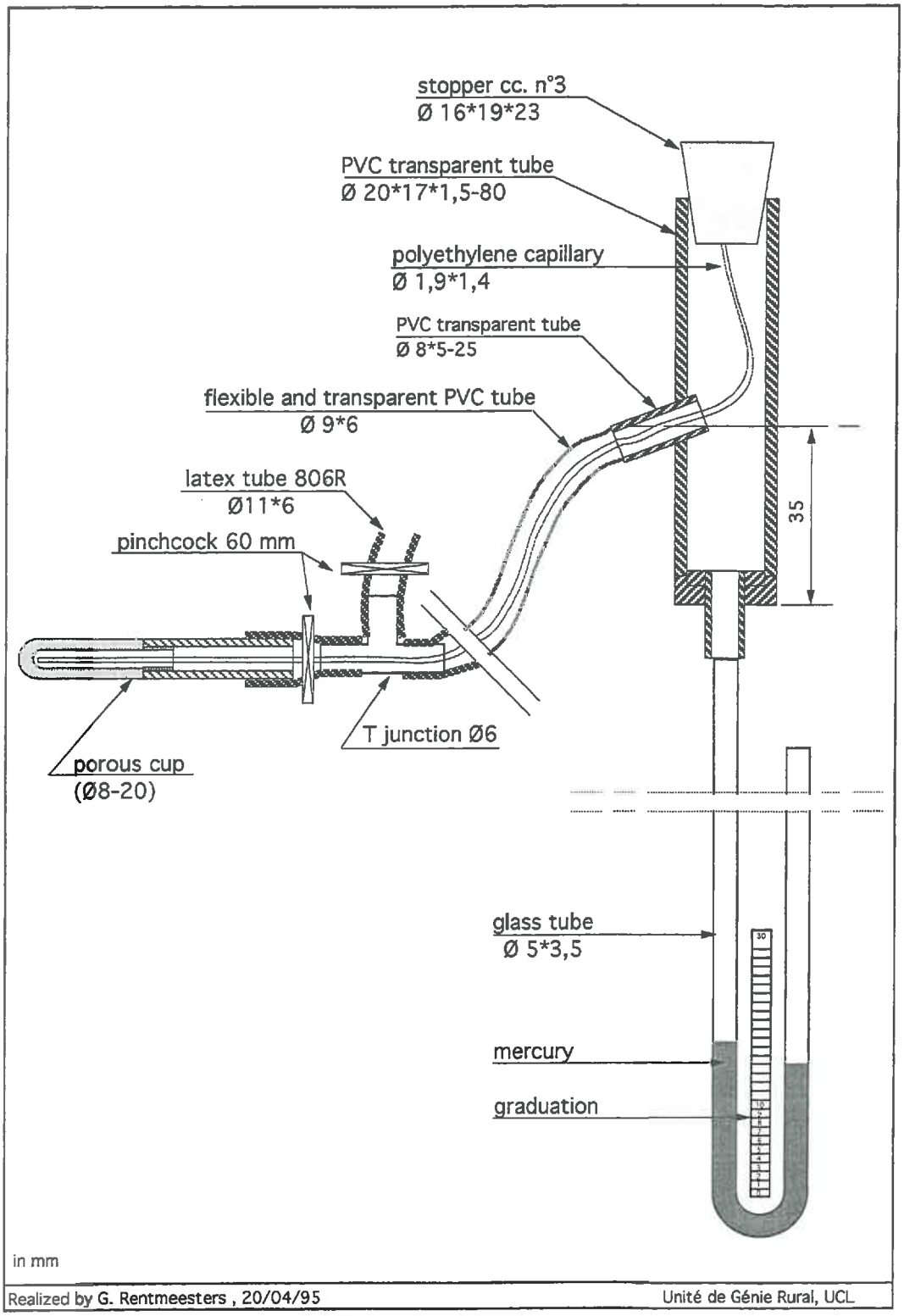

Annexe 2.3. Scheme of the upper part of the experimental column.

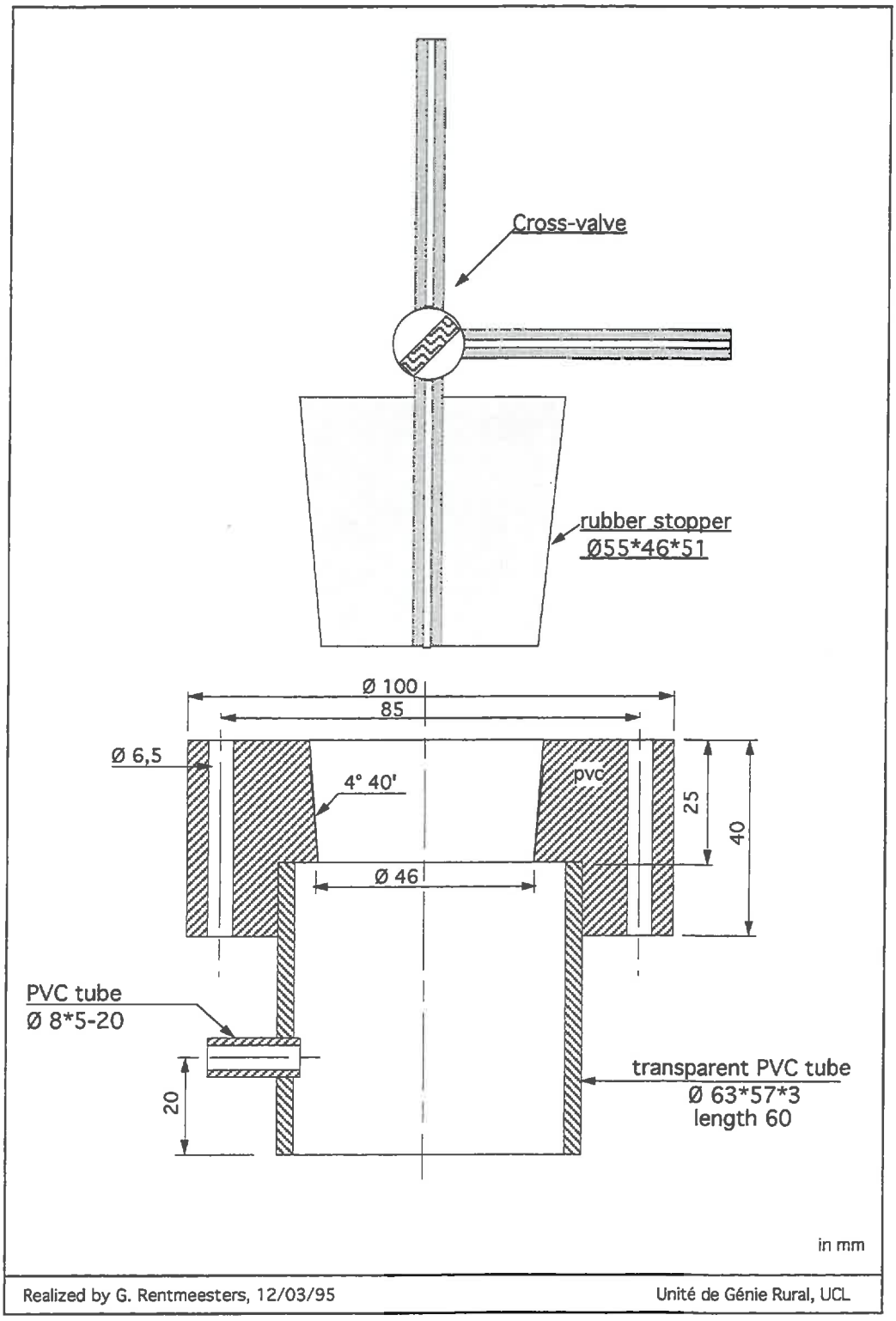

Annexe 2.4. Scheme of the lower part of the experimental column.

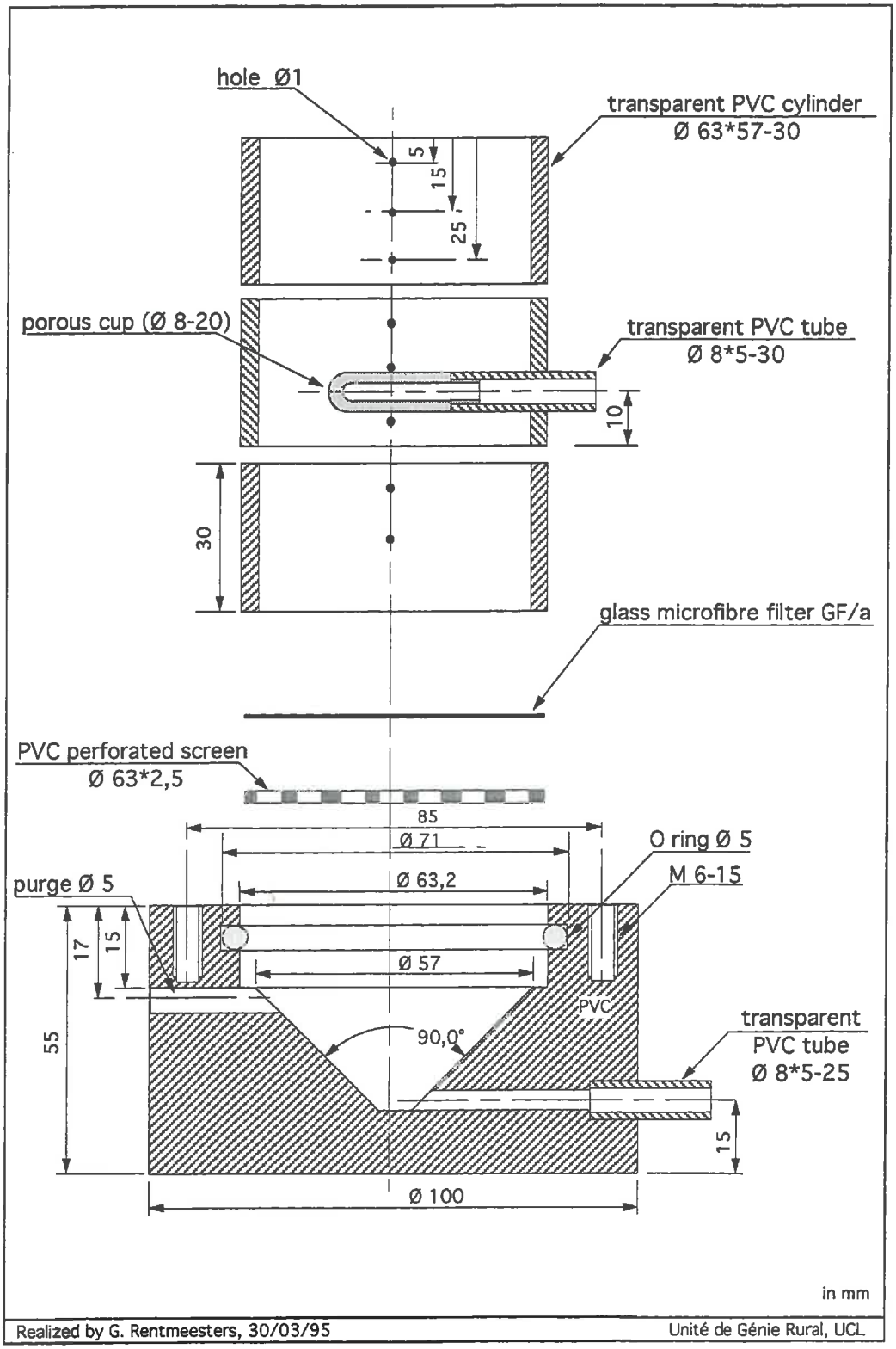

Annexe 2.5. Methodology to determine the coefficients which are necessary to take into account the ^{137}Cs interference in the low-energy band.

The two radioactive sources (^{137}Cs- 406 mCi or 15 GBq - ^{241}Am - 200 mCi or 7.4 GBq) and detectors are placed at fix cross positions on a moveable platform. The ^{241}Am source is placed in a smaller lead cylinder of 10.35 cm length and 10 cm in diameter. The beam is collimated to 3 mm. At the detector side, a lead shield-collimator cap is placed in front of the ^{241}Am detector (5.95 cm inside diameter, 22 cm length, 3.5 cm thickness, collimation = 4 mm) and ^{137}Cs detector (5.3 cm inside diameter, 7.75 cm length, 3.7 cm thickness, collimation = 2 mm).

The ^{241}Am amplifier-analyser operates with a coarse gain of 128, a voltage of 480 V, a channel width of 0.5 V with a lower level of 0.4 V. The ^{137}Cs amplifier-analyser operates with a coarse gain of 16, a voltage of 740 V, a channel width of 0.2 V with a lower level of 0.6 V. To prevent long-term drift, only the fine gain is adjusted. All the other parameters are maintained constant during the experiment.

To determine the constants of Eqn. (2.7), the ^{241}Am source is removed and only the ^{137}Cs source is used. Pulses are detected by both cross positioned detectors. Flat plates of lead of about 0.1 cm thickness are inserted into the gamma-ray beam. The thickness of the lead is progressively increased from 0.1 cm to 1.6 cm. The countings are recorded by the indivual counters, for measurements corresponding to a given thickness of lead and a recording time of 60 seconds. For count rates ranging from 1460 up to 4100 cps, Eqn. (2.7) was used with the following constants :

A = 5.26e+1 ± 11 cps ;
B = -2.10e-2 ± 1.31e-2 cps ;
C = 1.51e-5 ± 4.96e-6 cps ;
D = -2.16e-9± 5.97e-10 cps ;

and

A = -1.12e+3 ± 3.08e+2 cps ;
B = 5.60e-1 ± 1.38e-1 cps ;
C = -6.58e-5 ± 1.55e-5;

for count rates ranging from 4100 cps to 4900 cps.

Annexe 2.6. pH, electrical conductivity (EC), total electrolyte concentration (TEC) and salinity (SAR) of the leaching solutions used in the two flow experiments.

Series I	pH	CE µS/cm	$[Na^+]$ mmole/l	$[Ca^{++}]$ mmole/l	SAR $(mmole/l)^{0.5}$	TEC meq/l
SAR = 5 ; TEC = 10	-	-	5.34	1.78	4.0	8.91
SAR = 5 ; TEC = 5	5.66	629	3.22	0.62	4.1	4.44
SAR = 5 ; TEC = 1	6.23	136	0.78	0.04	4.0	0.86
SAR = 20 ; TEC = 10	6.65	1179	7.98	0.25	16.0	8.48
SAR = 20 ; TEC = 5	6.06	588	4.02	0.06	16.4	4.14
SAR = 20 ; TEC = 1	5.80	128	0.81	-	-	-
Series II						
SAR = 5 ; TEC = 5	5.76 5.84 5.65 5.78 5.65	594 587 582 583 584	3.73 3.70 3.77 3.69 3.70	0.65 0.60 0.59 0.61 0.59	4.64 4.78 4.93 4.74 4.81	5.03 4.90 4.93 4.90 4.88
SAR = 5 ; TEC = 1	5.76	120	1.38	0.05	6.29	1.47
SAR = 10 ; TEC = 5	5.63	579	4.46	0.22	9.67	4.88
SAR = 10 ; TEC = 1	5.71	121	1.01	0.02	7.66	1.05

Annexe 3.1. The relative error on the calculation of the water ratio to clay in the low pressure range (P = 55.7 kPa), for different ESP values, when each coefficient is varied independently in the range ± 3 standard deviations around the optimal value.

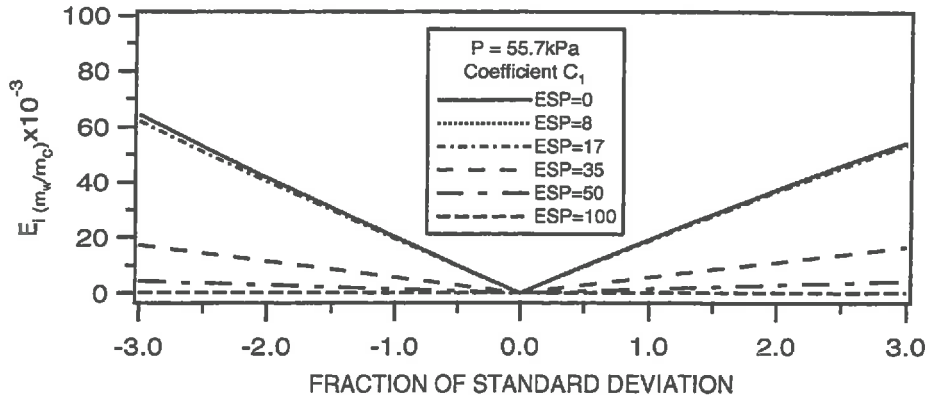

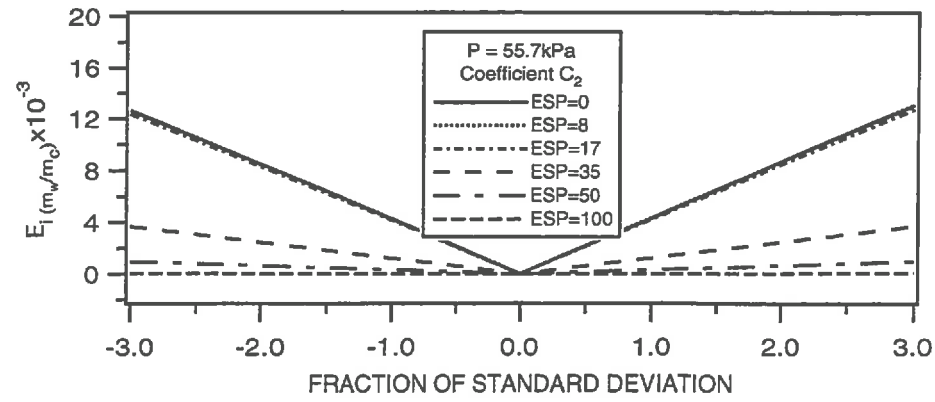

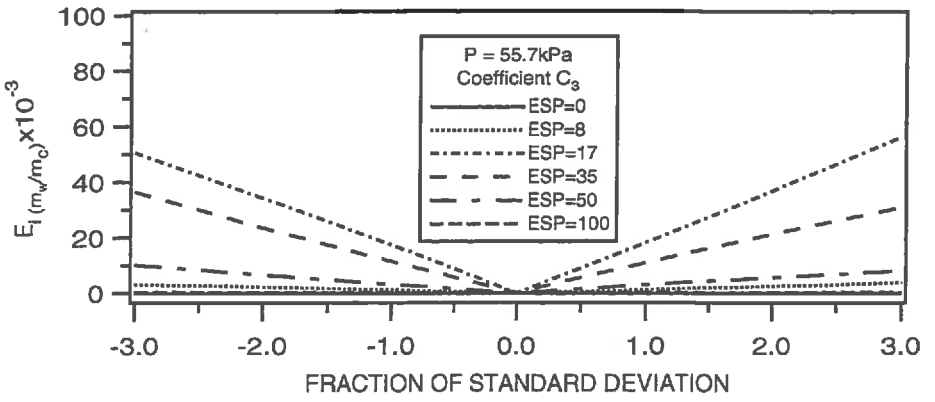

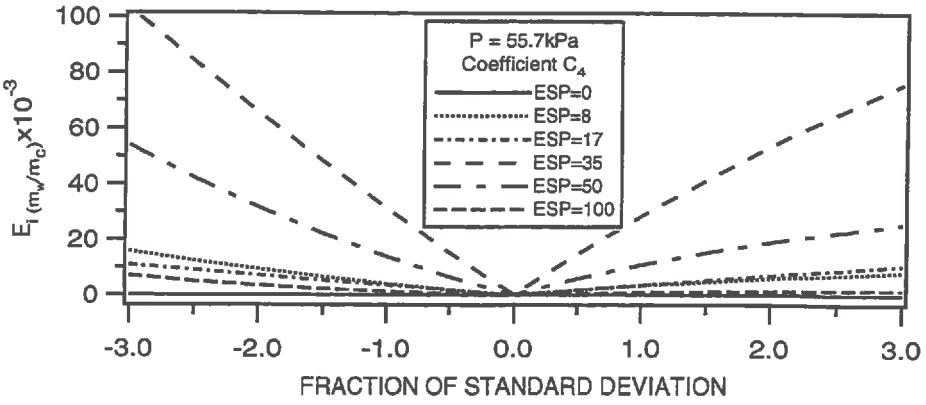
P = 55.7kPa
Coefficient C_4
ESP=0
ESP=8
ESP=17
ESP=35
ESP=50
ESP=100
$E_i\ (m_w/m_c) \times 10^{-3}$
100
80
60
40
20
0
-3.0
-2.0
-1.0
0.0
1.0
2.0
3.0
FRACTION OF STANDARD DEVIATION

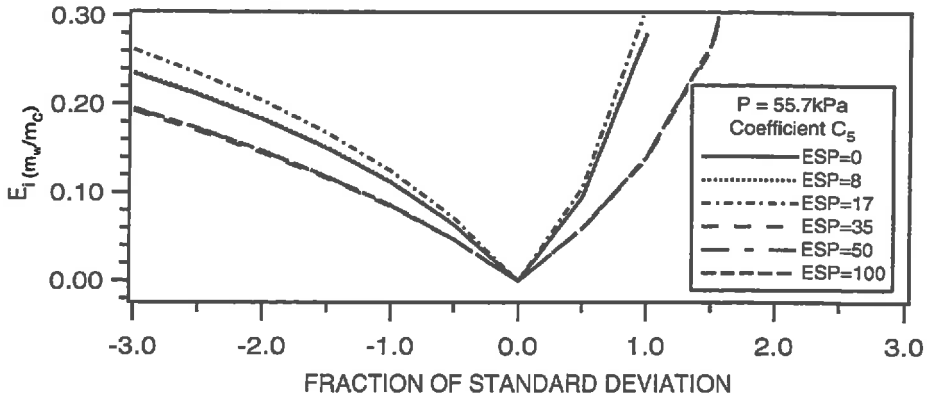
P = 55.7kPa
Coefficient C_5
ESP=0
ESP=8
ESP=17
ESP=35
ESP=50
ESP=100
$E_i\ (m_w/m_c)$
0.30
0.20
0.10
0.00
-3.0
-2.0
-1.0
0.0
1.0
2.0
3.0
FRACTION OF STANDARD DEVIATION

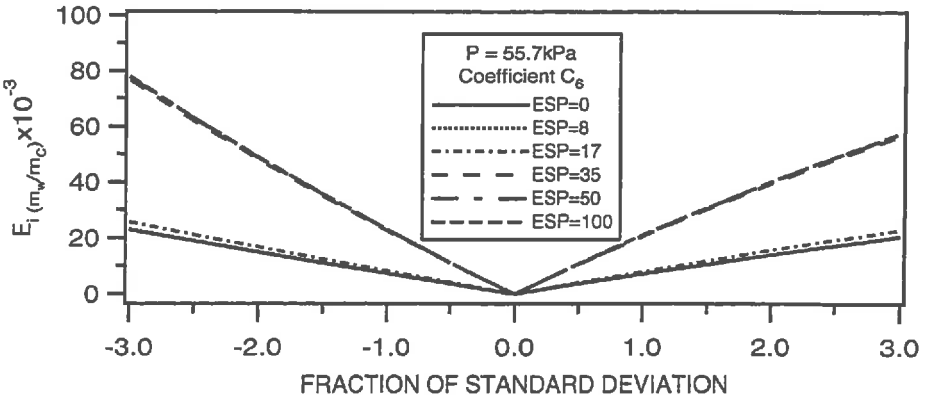
P = 55.7kPa
Coefficient C_6
ESP=0
ESP=8
ESP=17
ESP=35
ESP=50
ESP=100
$E_i\ (m_w/m_c) \times 10^{-3}$
100
80
60
40
20
0
-3.0
-2.0
-1.0
0.0
1.0
2.0
3.0
FRACTION OF STANDARD DEVIATION

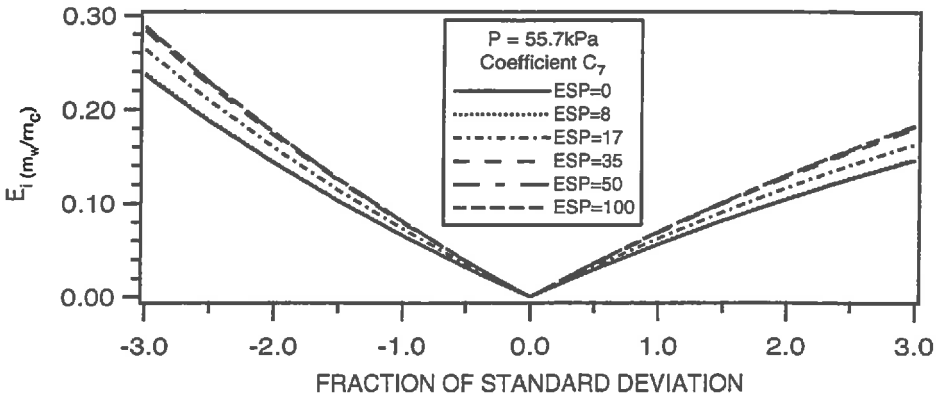
P = 55.7kPa
Coefficient C_7
ESP=0
ESP=8
ESP=17
ESP=35
ESP=50
ESP=100
$E_i\ (m_w/m_c)$
0.30
0.20
0.10
0.00
-3.0
-2.0
-1.0
0.0
1.0
2.0
3.0
FRACTION OF STANDARD DEVIATION

Annexe 3.2. The relative error on the calculation of the water ratio to clay for a pressure of 506.6 kPa and different ESP values when each coefficient is varied independently in the range ± 3 standard deviations around the optimal value.

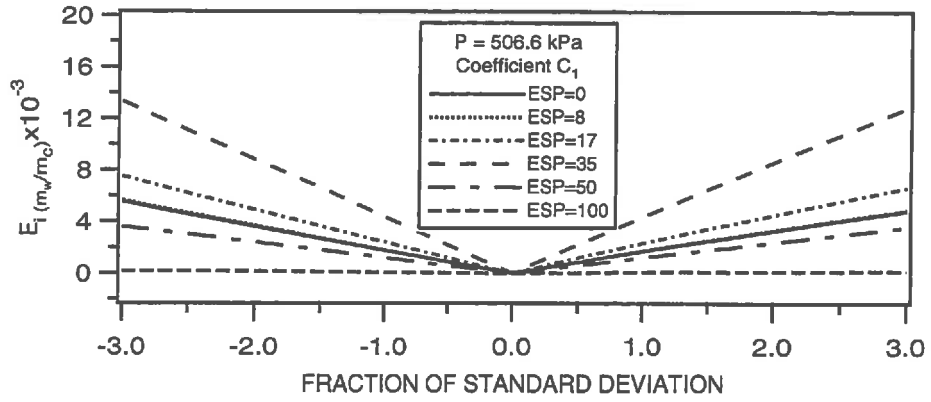

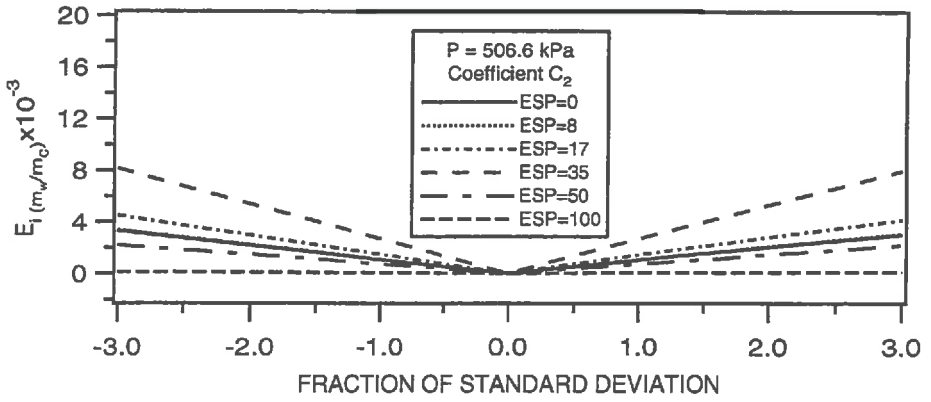

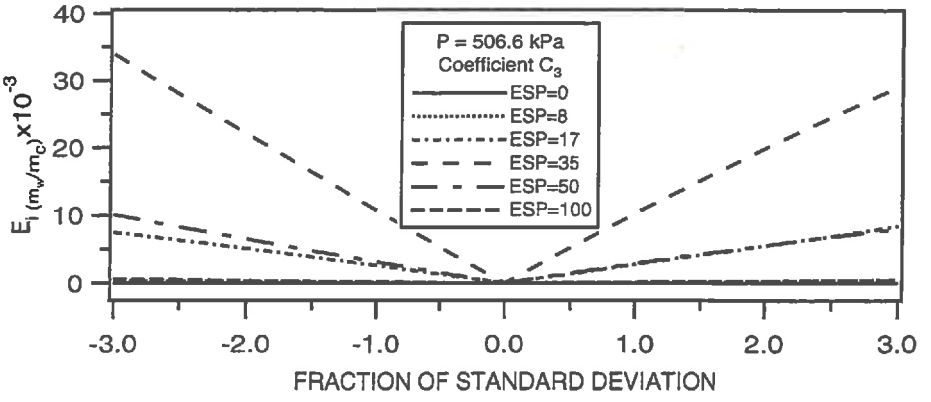

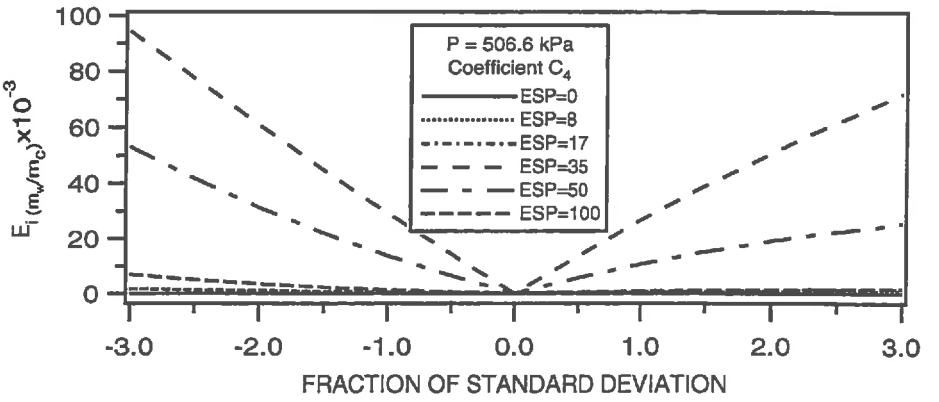
P = 506.6 kPa
Coefficient C_4
ESP=0
ESP=8
ESP=17
ESP=35
ESP=50
ESP=100
$E_i (m_w/m_c) x10^{-3}$
100
80
60
40
20
0
-3.0
-2.0
-1.0
0.0
1.0
2.0
3.0
FRACTION OF STANDARD DEVIATION

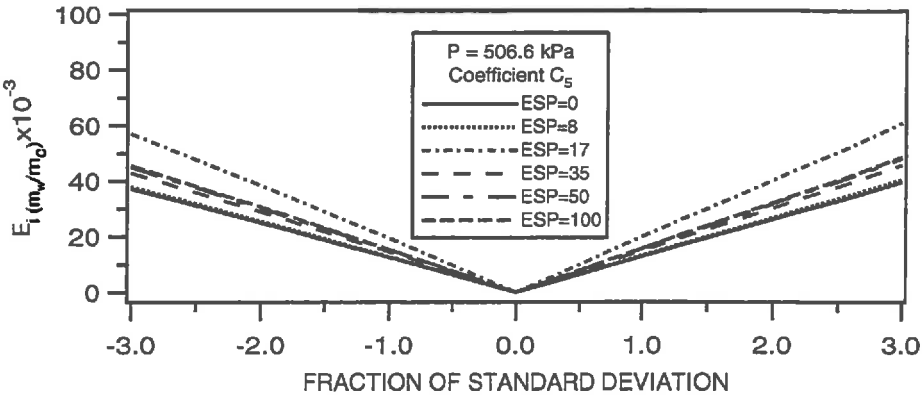
P = 506.6 kPa
Coefficient C_5
ESP=0
ESP=8
ESP=17
ESP=35
ESP=50
ESP=100
$E_i (m_w/m_c) x10^{-3}$
100
80
60
40
20
0
-3.0
-2.0
-1.0
0.0
1.0
2.0
3.0
FRACTION OF STANDARD DEVIATION

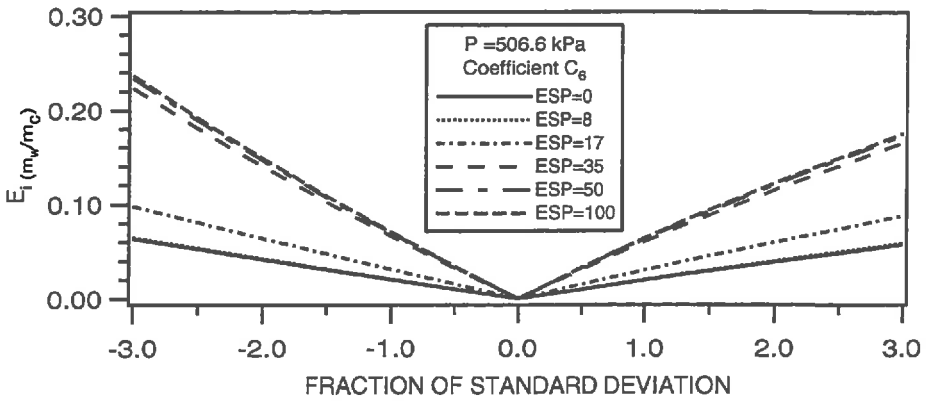
P =506.6 kPa
Coefficient C_6
ESP=0
ESP=8
ESP=17
ESP=35
ESP=50
ESP=100
$E_i (m_w/m_c)$
0.30
0.20
0.10
0.00
-3.0
-2.0
-1.0
0.0
1.0
2.0
3.0
FRACTION OF STANDARD DEVIATION

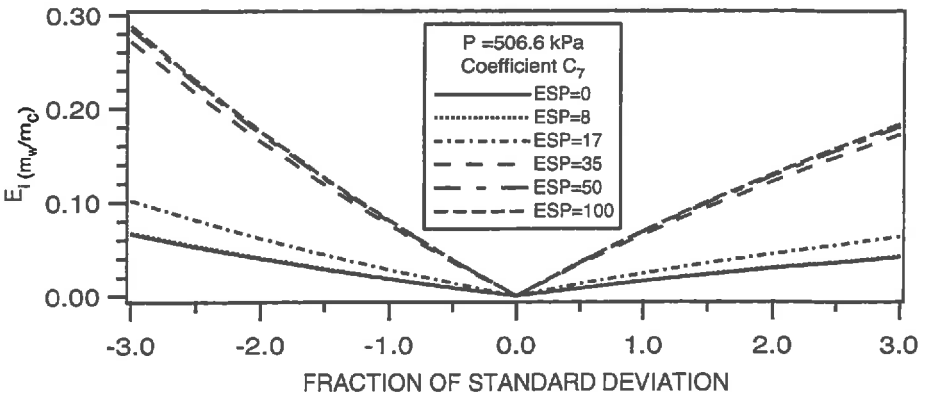
P =506.6 kPa
Coefficient C_7
ESP=0
ESP=8
ESP=17
ESP=35
ESP=50
ESP=100
$E_i (m_w/m_c)$
0.30
0.20
0.10
0.00
-3.0
-2.0
-1.0
0.0
1.0
2.0
3.0
FRACTION OF STANDARD DEVIATION

Annexe 4.1. Dry bulk density profiles, obtained by gamma-radiation, for the columns of series II. The increase of the bulk density is due to the presence of the tensiometers.

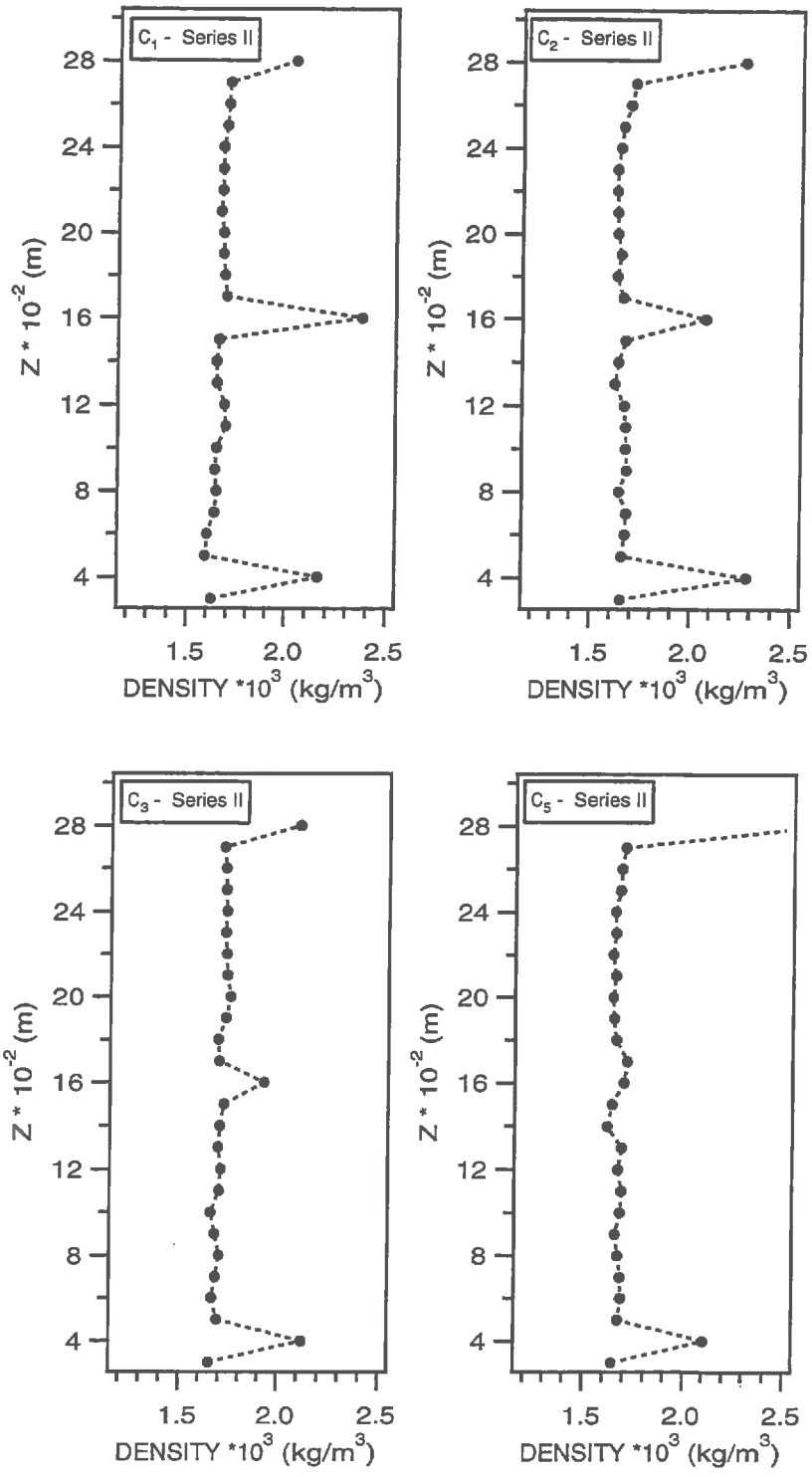

Annexe 4.2. Mean total hydraulic conductivities $\overline{K}_T$ (series I) calculated for the last 30 days associated to their standard deviation *SD*.

	Solution	$\overline{K}_T$ (m/s)	*SD* (m/s)
C_2	SAR = 5 ; TEC = 5 meq/l	1.39e-7	1.26e-8
C_3	SAR = 5 ; TEC = 1 meq/l	7.94e-9	1.31e-9
C_4	SAR = 20 ; TEC = 10 meq/l	1.55e-9	1.68e-10
C_5	SAR = 20 ; TEC = 5 meq/l	1.26e-9	2.57e-10
C_6	SAR = 20 ; TEC = 1 meq/l	1.34e-9	2.03e-10

Annexe 4.3. Mean total hydraulic conductivitites $\overline{K}_T$ (series II), calculated for the last 30 days for the first and second percolation periods associated to their standard deviation *SD*. All the columns were first leached with a solution of SAR = 5 and TEC = 5 meq/l.

	$\overline{K}_T$ (m/s)	*SD* (m/s)	2nd solution	$\overline{K}_T$ (m/s)	*SD* (m/s)
C_1	2.87e-7	1.98e-8	SAR = 5 ; TEC = 1 meq/l	5.49e-8	2.52e-9
C_2	3.09e-7	2.59e-8	SAR = 10 ; TEC = 5 meq/l	9.61e-8	8.07e-9
C_3	3.51e-7	4.83e-8	SAR = 10 ; TEC = 1 meq/l	4.94e-8	3.67e-9
C_5	2.64e-7	1.15e-8	deionized water	1.63e-8	5.45e-9

Annexe 4.4. Mean total hydraulic conductivitites $\overline{K_T}$ for the columns of series I, obtained from the slope of the linear part of the relationship between the effluent volume and time using a mean total hydraulic gradient $\overline{\nabla H}$.

	Solution	$\overline{\nabla H}$	$\overline{K_T}$ (m/s)
C_2	SAR = 5 ; TEC = 5 meq/l	2.51	1.38e-7
C_3	SAR = 5 ; TEC = 1 meq/l	2.47	8.24e-9
C_4	SAR = 20 ; TEC = 10 meq/l	2.41	1.61e-9
C_5	SAR = 20 ; TEC = 5 meq/l	2.44	1.30e-9
C_6	SAR = 20 ; TEC = 1 meq/l	2.40	1.22e-9

Annexe 4.5. Mean total hydraulic conductivitites $\overline{K_T}$ for the columns of series II obtained from the slope of the linear relationship between the effluent volume and time using a mean total hydraulic gradient $\overline{\nabla H}$.

	$\overline{\nabla H}$	$\overline{K_T}$ (m/s)	2nd solution	$\overline{\nabla H}$	$\overline{K_T}$ (m/s)
C_1	2.62	2.96e-7	SAR = 5 ; TEC = 1 meq/l	2.62	6.61e-8
C_2	2.66	3.19e-7	SAR = 10 ; TEC = 5 meq/l	2.66	1.24e-7
C_3	2.68	3.78e-7	SAR = 10 ; TEC = 1 meq/l	2.68	7.58e-8
C_5	2.66	2.80e-7	deionized water	2.66	2.22e-8

Annexe 4.6. General scheme to establish the equations required to determine the matric potential and hydraulic head for each column of the two flow experiments.

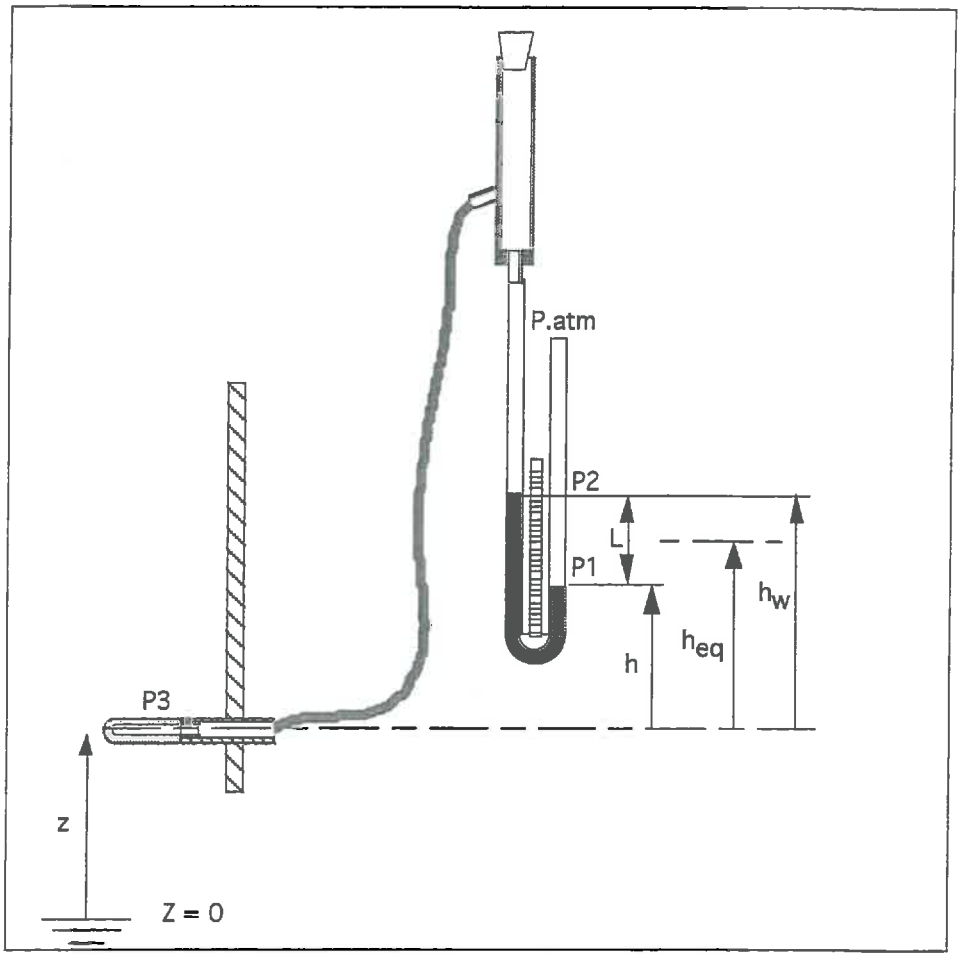

$$P_1 = P_{atm}$$

$$P_2 = P_1 - \rho_{Hg} g L \qquad avec\ L>0$$

$$P_3 = P_2 + \rho_w g h_w$$

$$\Delta P = P_3 - P_1 = \rho_w g h$$

$$P_3 - P_1 = P_{atm} - \rho_{Hg} g L + \rho_w g\left(h_{eq} + L/2\right) - P_{atm}$$

$$h = h_{eq} + L/2 - \left(\rho_{Hg}/\rho_w\right)L$$

Annexe 4.6.bis The required data relative to each column of the two flow experiments to establish the equations.

Series I

	C_1	C_2	C_3	C_4	C_5	C_6
z_1 (cm)	3.925	3.925	3.925	3.925	3.825	3.925
z_2 (cm)	16.625	16.625	16.625	16.575	16.575	16.525
z_3 (cm)	28.025	28.025	27.925	27.875	28.075	27.725
h_{1eq} (cm)	0.345	- 0.15	- 0.225	- 0.475	- 0.375	- 0.175
h_{2eq} (cm)	- 12.775	- 13.275	- 12.825	- 12.950	- 12.825	- 12.975
h_{3eq} (cm)	- 24.325	- 24.425	- 24.525	- 24.300	- 24.325	- 24.175

Series II

	C_1	C_2	C_3	C_4	C_5	C_6
z_1 (cm)	4.025	3.900	3.875	4.025	3.725	3.925
z_2 (cm)	16.350	16.650	16.650	16.550	16.450	16.425
z_3 (cm)	27.850	28.050	27.750	27.650	28.900	27.650
h_{1eq} (cm)	- 0.300	- 0.525	- 0.375	- 0.125	- 0.025	- 0.200
h_{2eq} (cm)	- 12.825	- 12.900	- 12.950	- 12.700	- 13.125	- 12.450
h_{3eq} (cm)	- 24.275	- 23.825	- 24.125	- 24.3125	- 24.375	- 24.125

Annexe 4.7. Evolution of the matric potentials measured at three different depths for the columns of series I. Those corresponding to the column leached with SAR = 20 and TEC = 1 are given in figure 4.9.

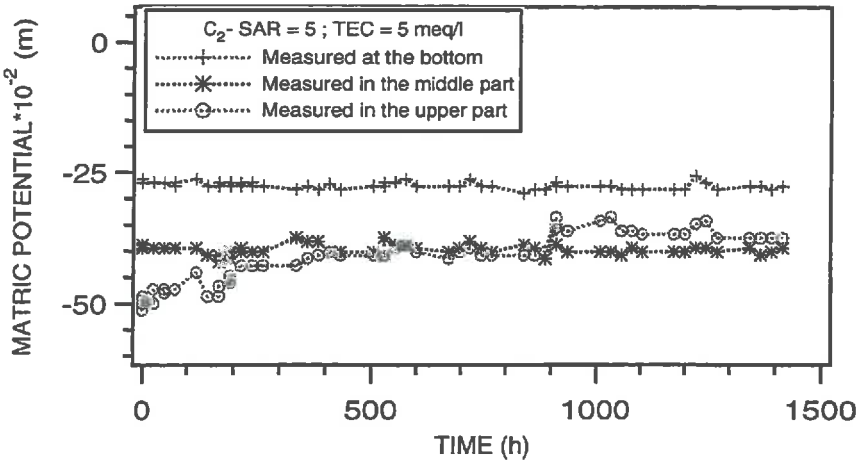

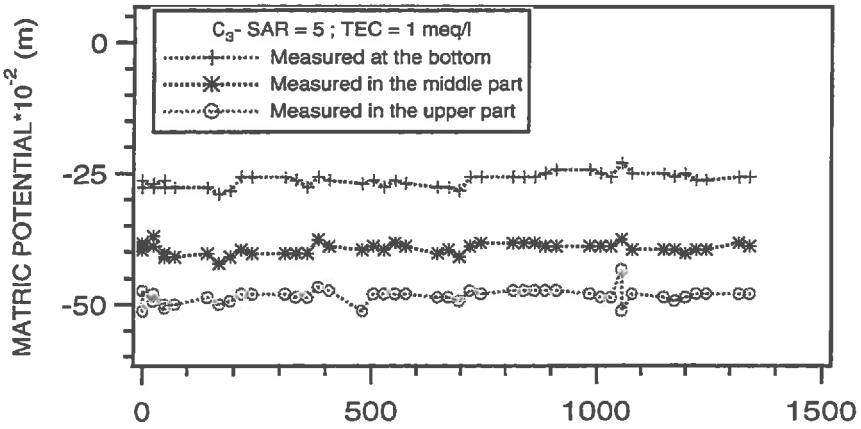

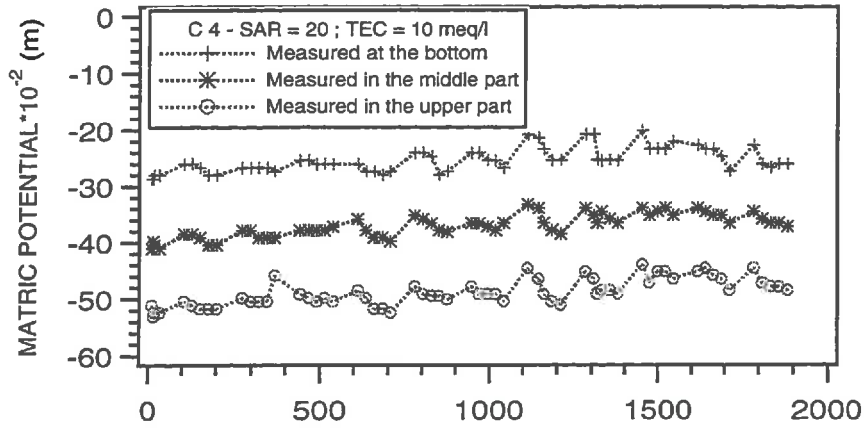

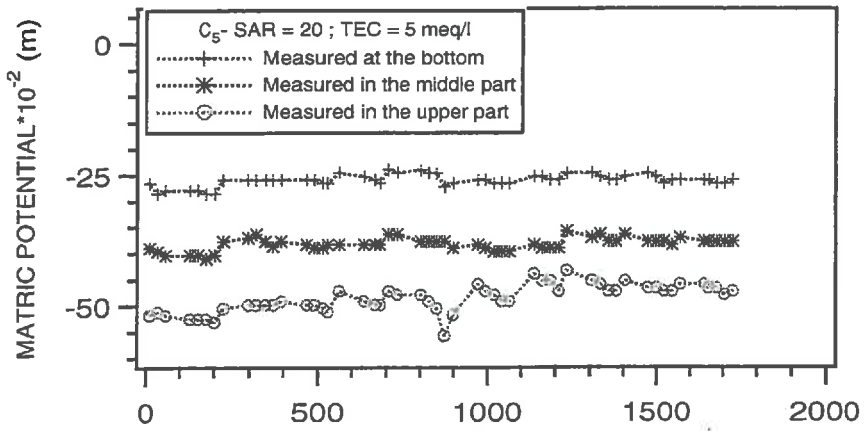

Annexe 4.8a. Evolution of the measured volumetric water contents as a function of the depth and time for the column leached with SAR = 5 and TEC = 5 meq/l (series I). The reference level Z = 0 is located at the bottom of the column.

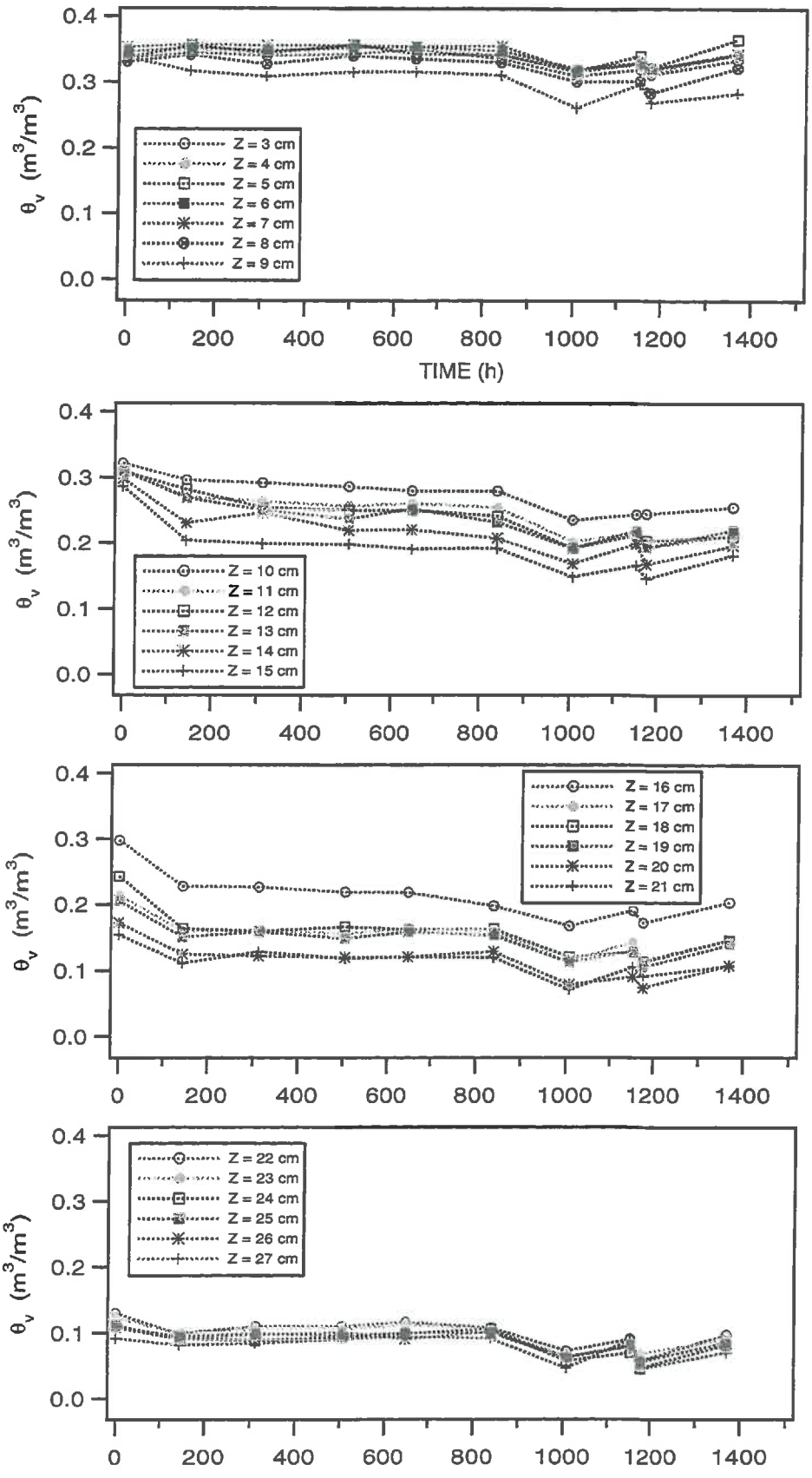

Annexe 4.8b. Evolution of the measured volumetric water contents as a function of the depth and time for the column leached with SAR = 5 and TEC = 1 meq/l (series I). The reference level Z = 0 is located at the bottom of the column.

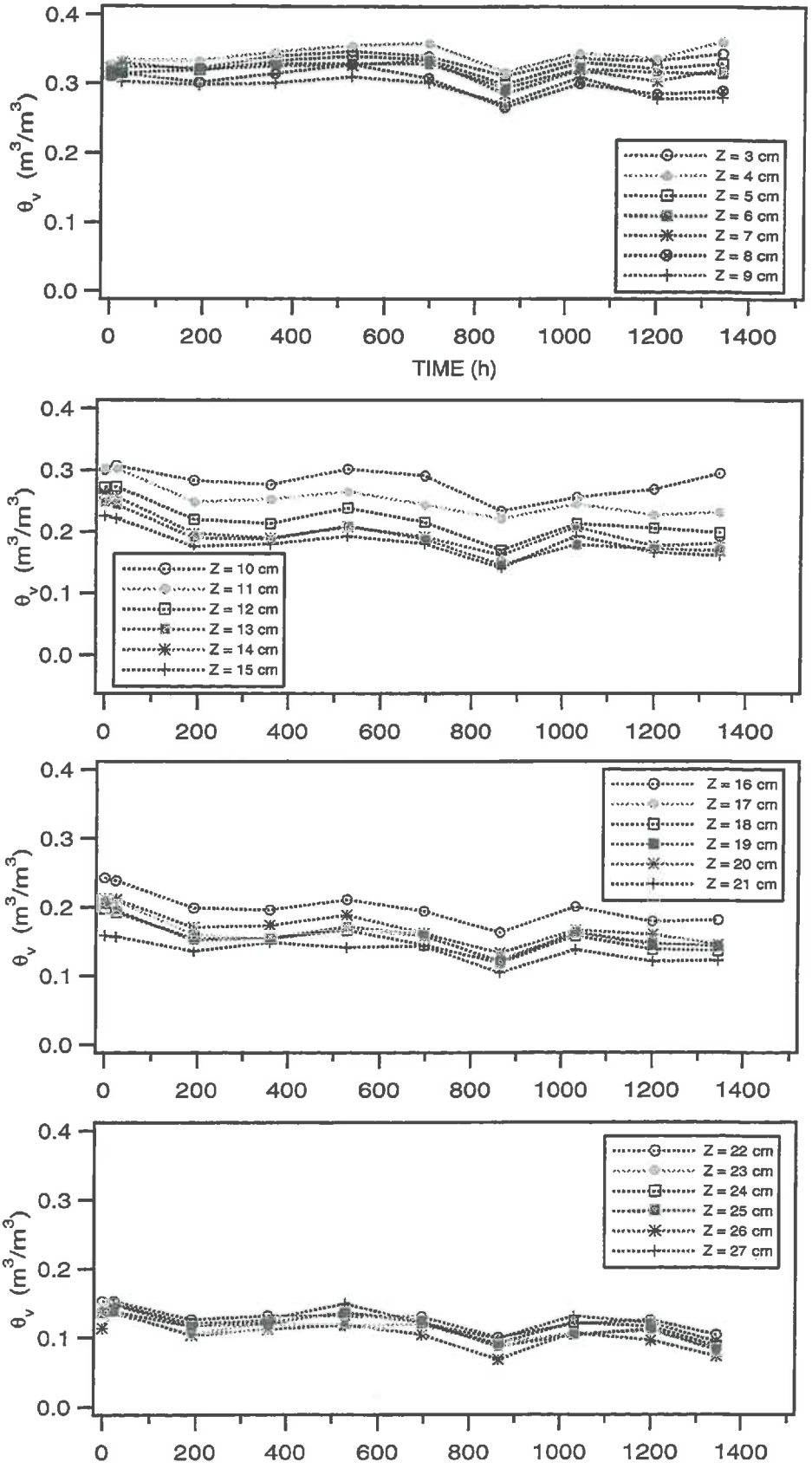

Annexe 4.8c. Evolution of the measured volumetric water contents as a function of the depth and time for the column leached with SAR = 20 and TEC = 10 meq/l (series I). The reference level Z = 0 is located at the bottom of the column.

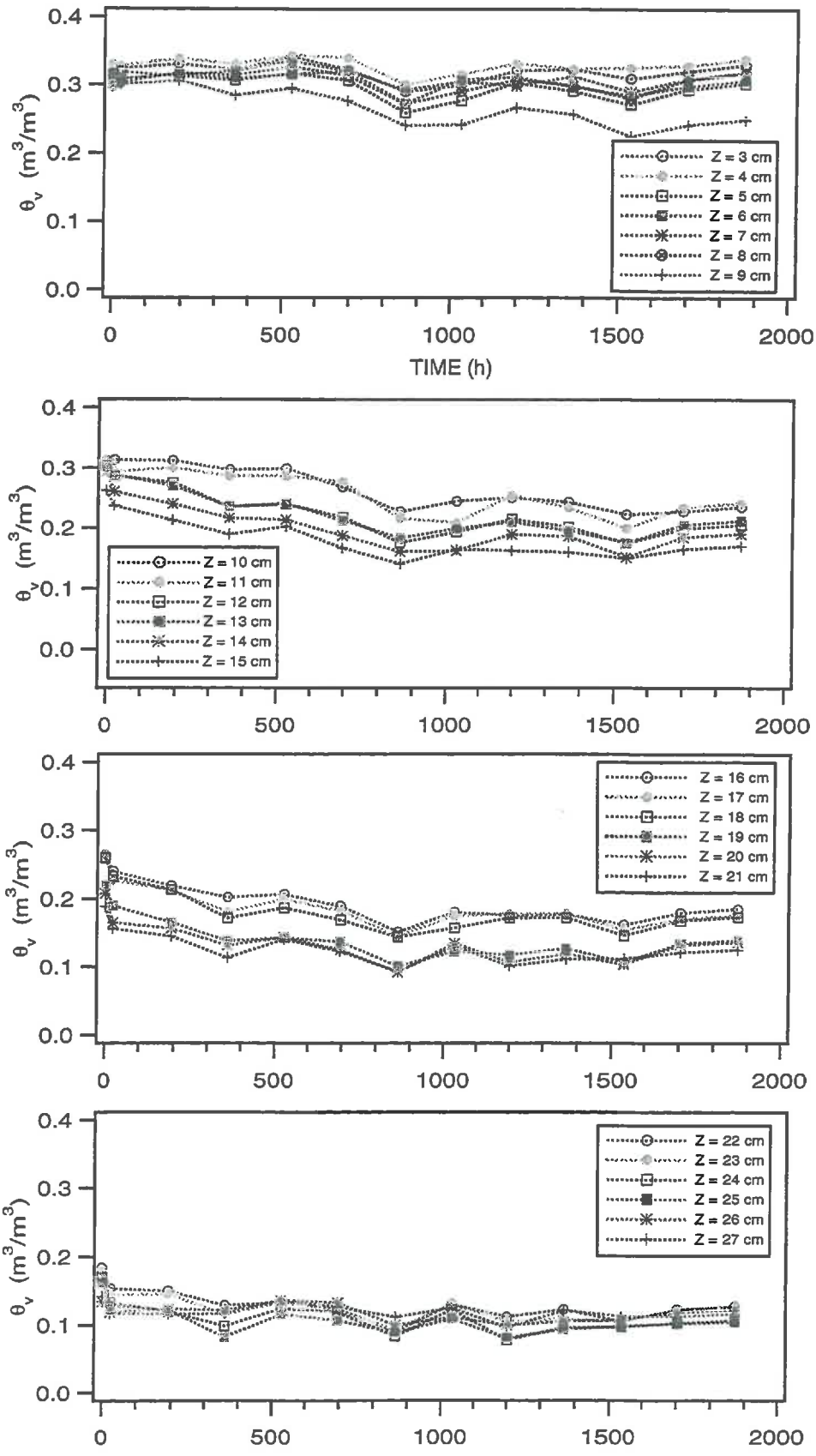

Annexe 4.8d. Evolution of the measured volumetric water contents as a function of the depth and time for the column leached with SAR = 20 and TEC = 5 meq/l (series I). The reference level Z = 0 is located at the bottom of the column.

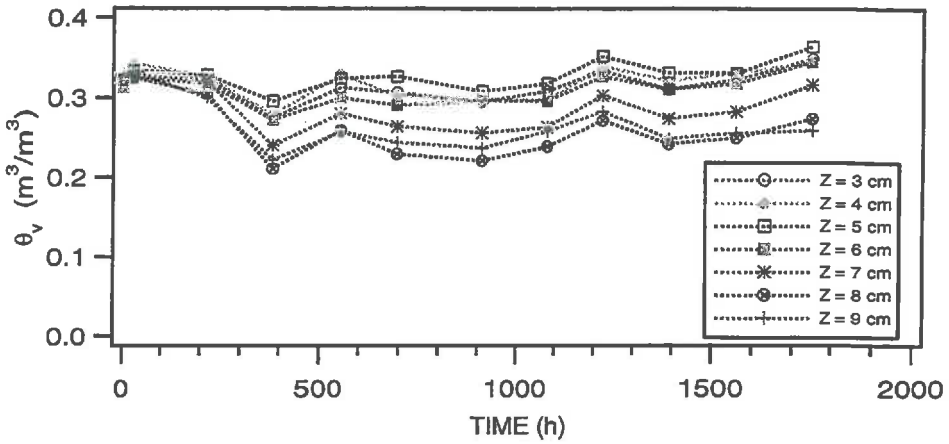

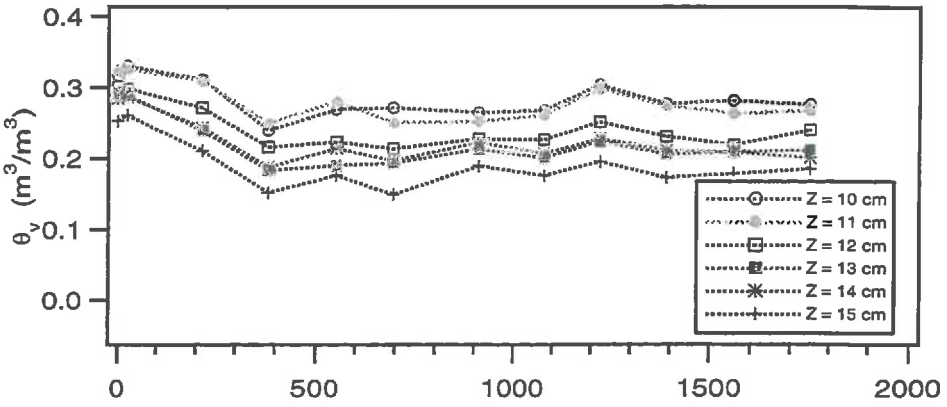

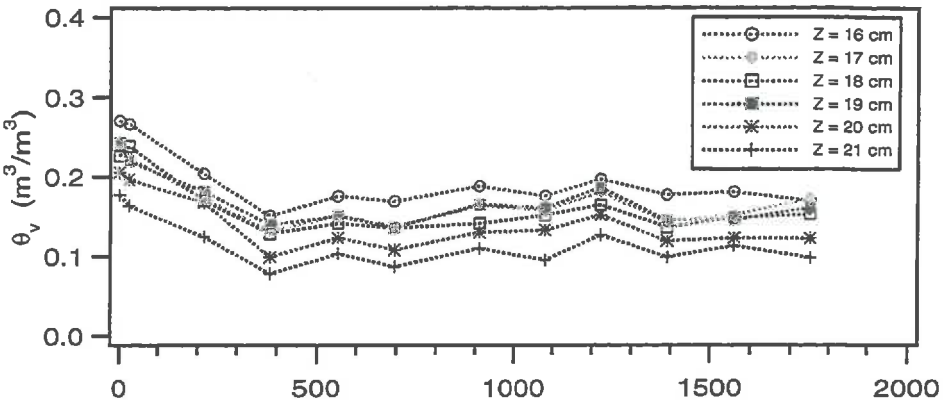

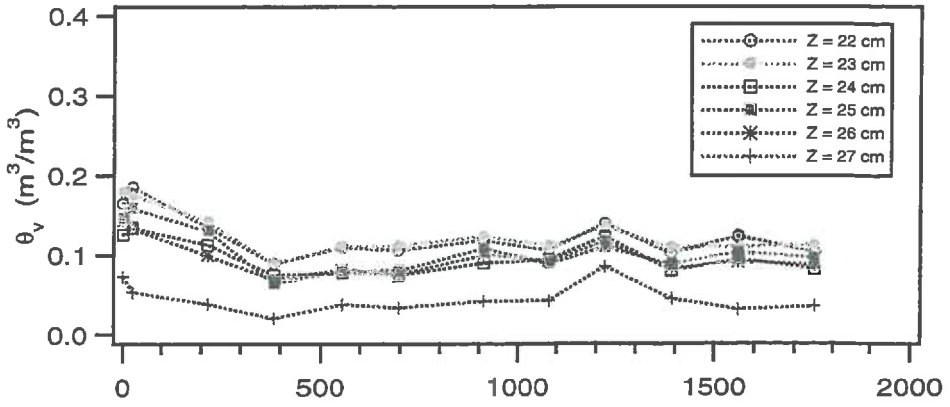

Annexe 4.8e. Evolution of the measured volumetric water contents as a function of the depth and time for the column leached with SAR = 20 and TEC = 1 meq/l (series I). The reference level Z = 0 is located at the bottom of the column.

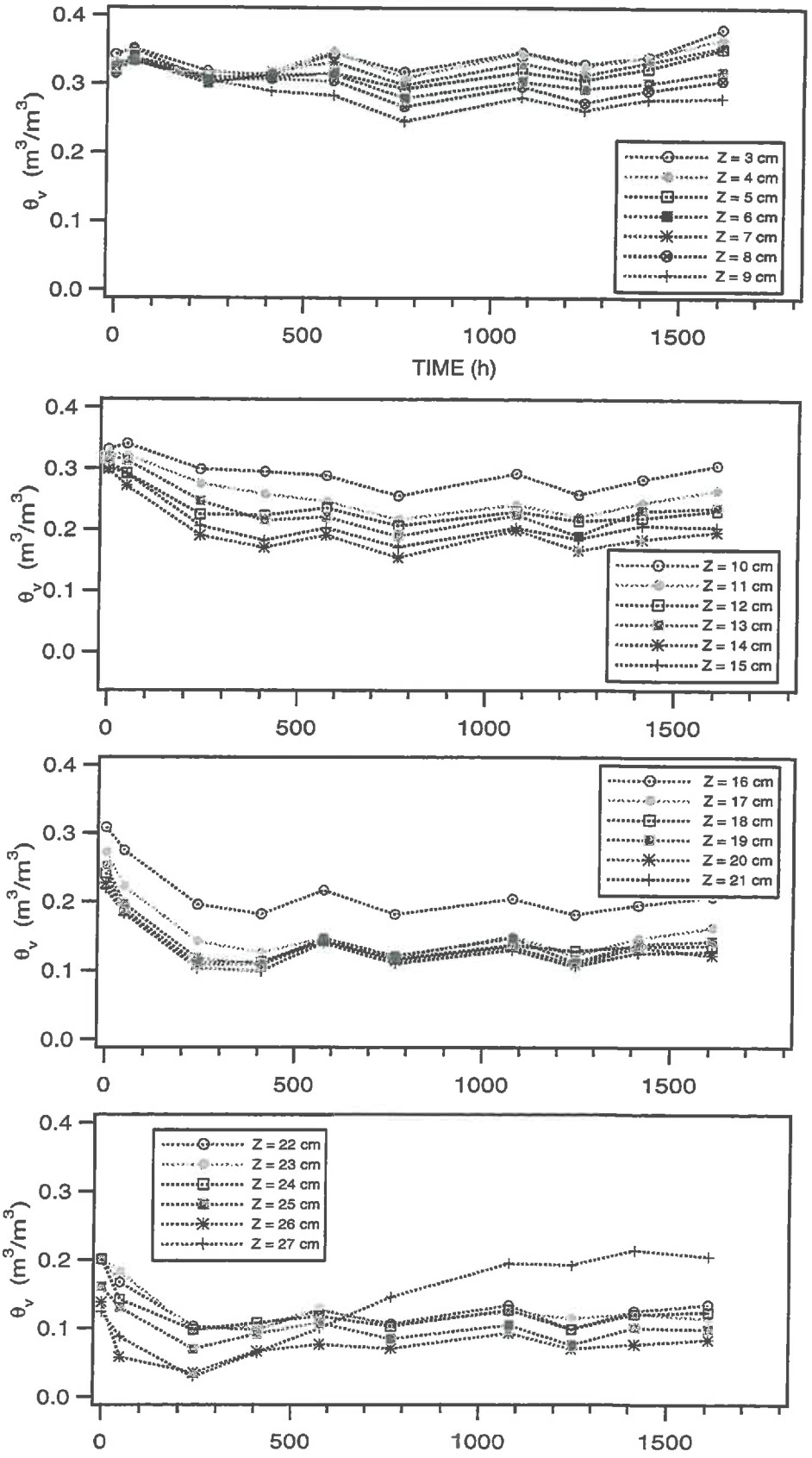

Annexe 4.9a. Evolution of the measured volumetric water contents as a function of the depth and time for the column leached first with SAR = 5, TEC = 5 meq/l and then with SAR = 5, TEC = 1 meq/l (series II). The reference level Z = 0 is located at the bottom of the column.

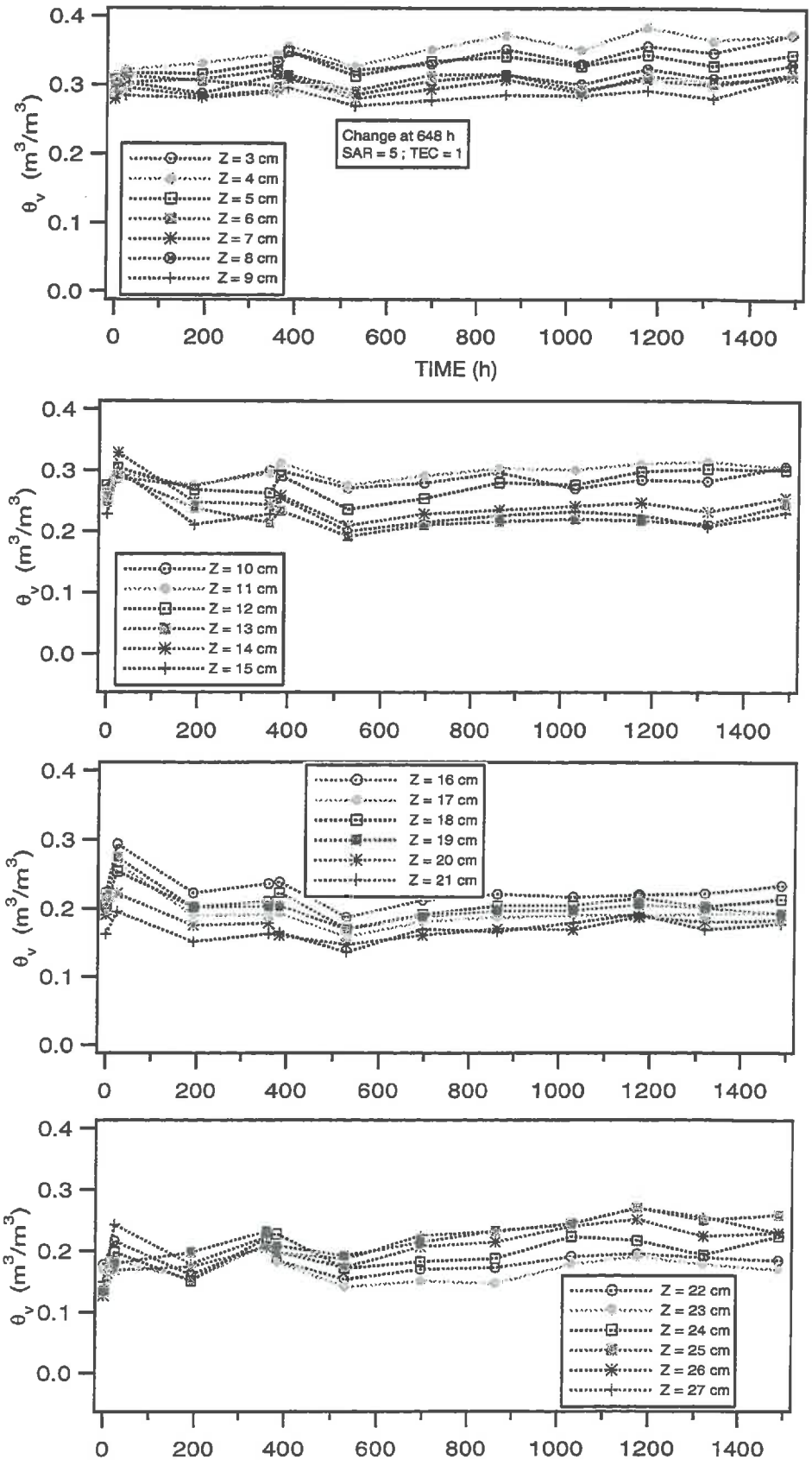

Annexe 4.9b. Evolution of the measured volumetric water contents as a function of the depth and time for the column leached first with SAR = 5, TEC = 5 meq/l and then with SAR = 10, TEC = 5 meq/l (series II). The reference level Z = 0 is located at the bottom of the column.

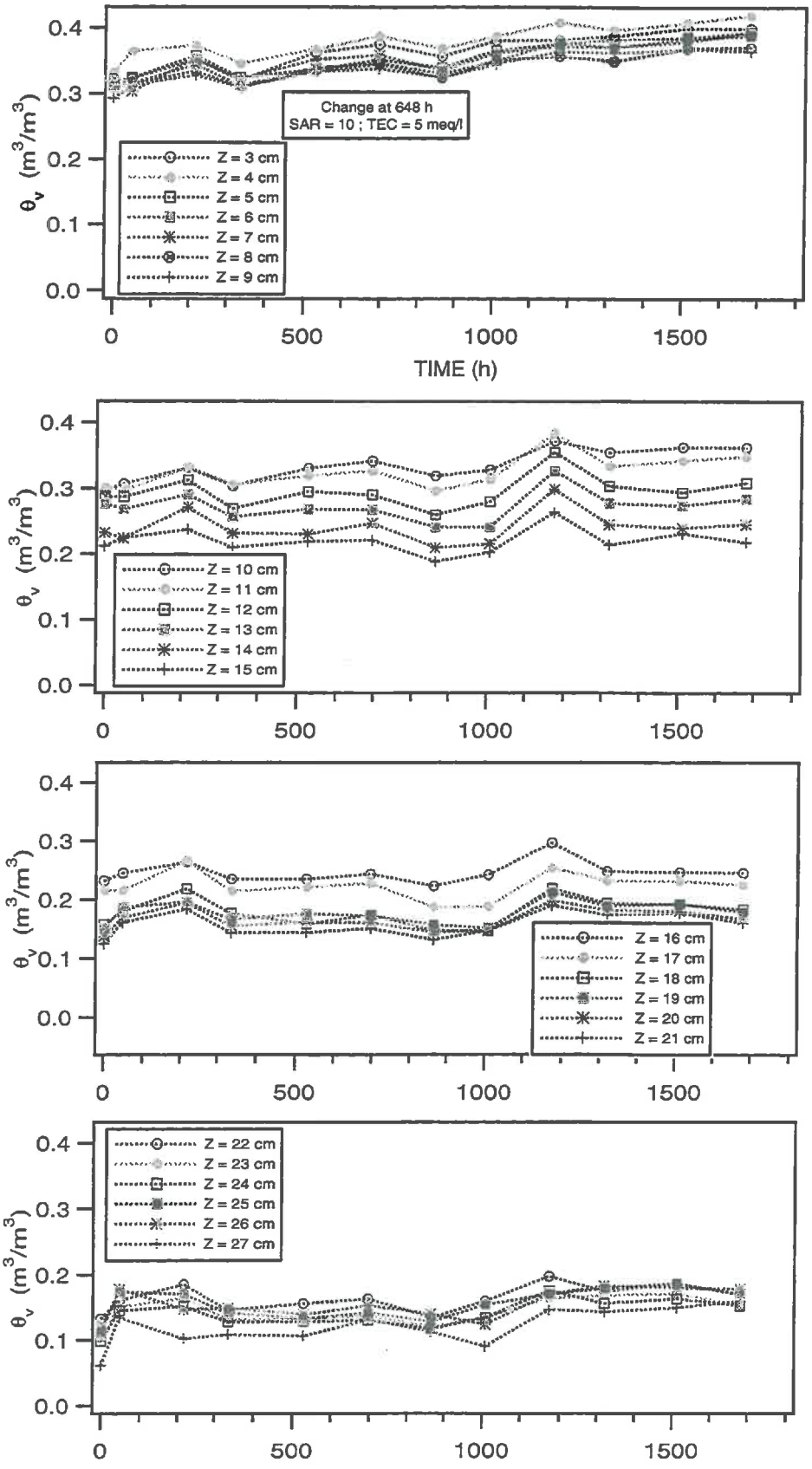

Annexe 4.9c. Evolution of the measured volumetric water contents as a function of the depth and time for the column leached first with SAR = 5, TEC = 5 meq/l and then with SAR = 10, TEC = 1 meq/l (series II). The reference level Z = 0 is located at the bottom of the column.

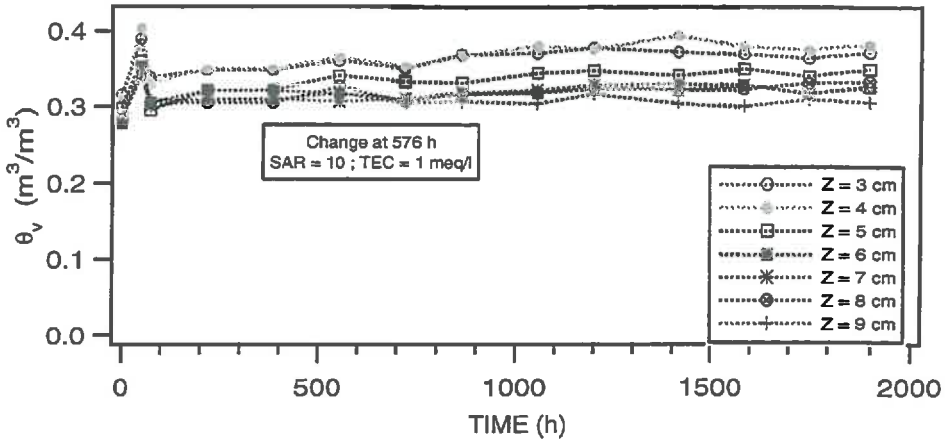

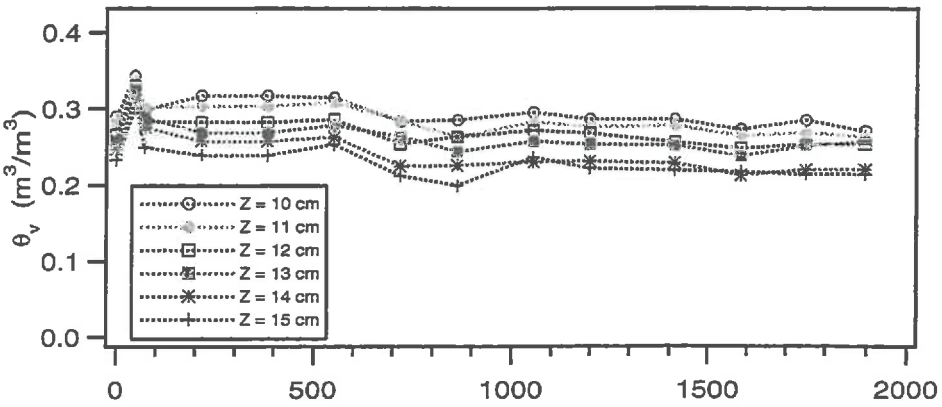

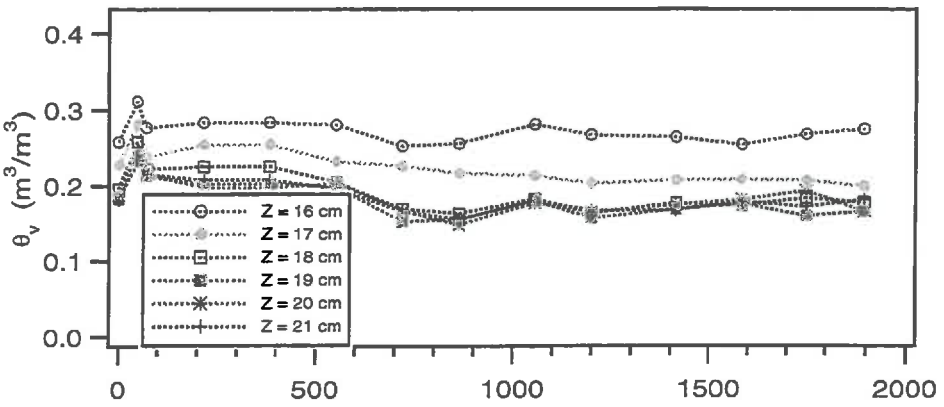

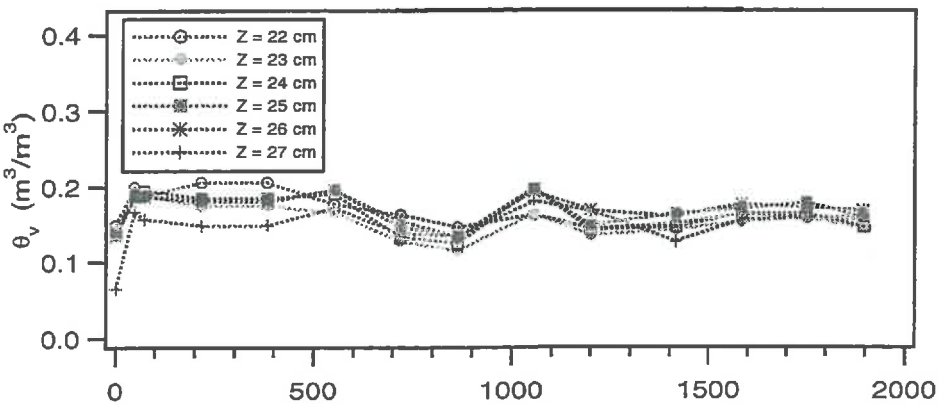

Annexe 4.9d. Evolution of the measured volumetric water contents as a function of the depth and time for the column leached first with SAR = 5, TEC = 5 meq/l and then with deionised water (series II). The reference level Z = 0 is located at the bottom of the column.

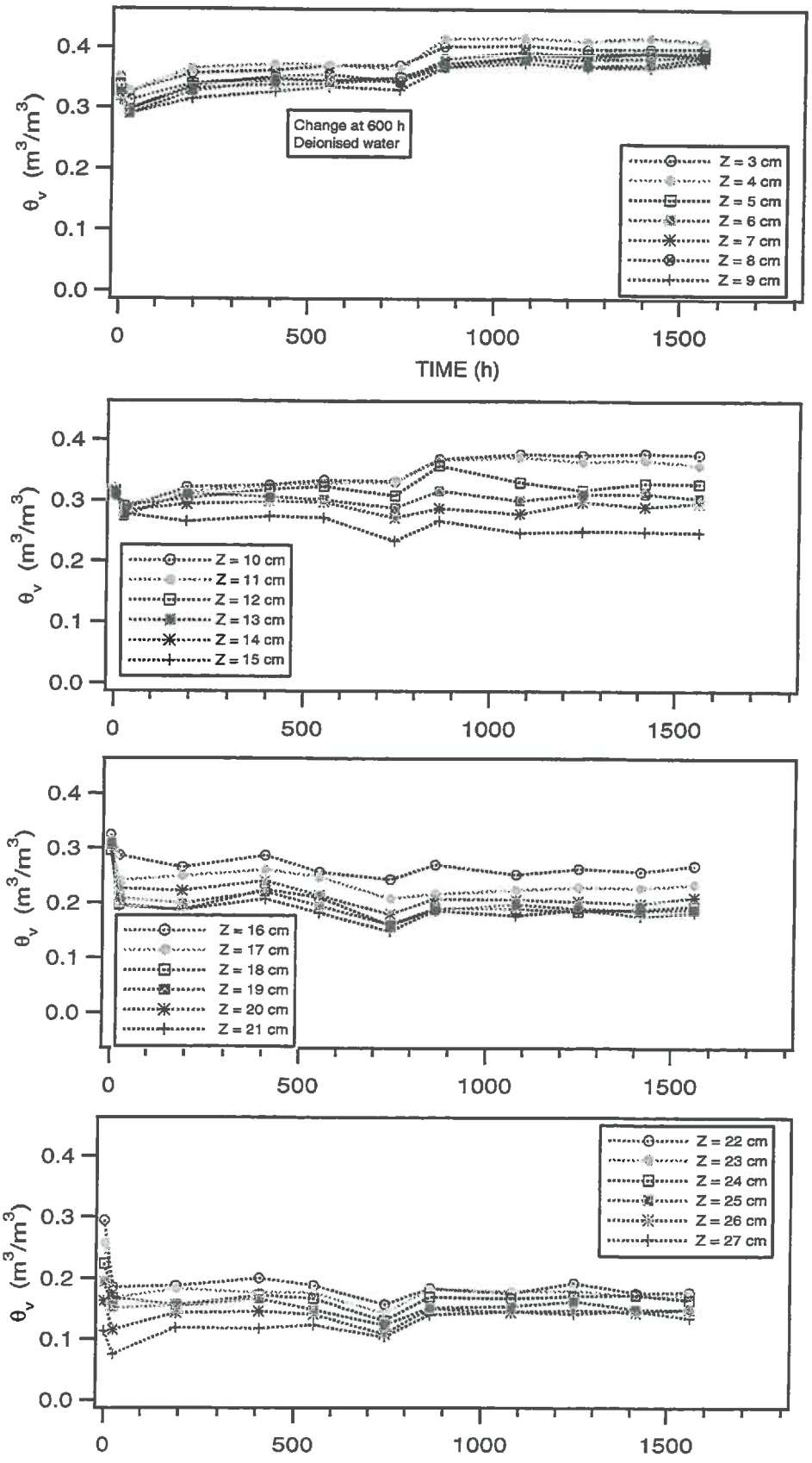

Annexe 4.10a. Evolution of the mean bulk densities obtained by gamma-radiation (^{241}Am countings during 60 s) and the 99 % confidence limit for the columns of series I.

	Solution	Dry $[\overline{\rho_b} \pm 2SD]$ (kg/m^3)	Datum	$\overline{\rho_b}$ (kg/m^3)	$[\overline{\rho_b} \pm 2SD]$ (kg/m^3)
C_2	SAR = 5 ; TEC = 5 meq/l	[1619 ; 1659]	15/02/95	1613	[1593 ; 1633]
			21/02/95	1641	[1621 ; 1661]
			28/02/95	1642	[1622 ; 1662]
			08/03/95	1636	[1616 ; 1656]
			14/03/95	1638	[1618 ; 1658]
			22/03/95	1645	[1625 ; 1665]
			29/03/95	1669	[1649 ; 1689]
			04/04/95	1654	[1634 ; 1674]
			05/04/95	1672	[1652 ; 1692]
			13/04/95	1651	[1631 ; 1671]
C_3	SAR = 5 ; TEC = 1 meq/l	[1628 ; 1668]	21/02/95	1620	[1600 ; 1640]
			22/02/95	1625	[1605 ; 1645]
			01/03/95	1647	[1627 ; 1667]
			08/03/95	1644	[1624 ; 1664]
			15/03/95	1636	[1616 ; 1656]
			22/03/95	1640	[1620 ; 1660]
			29/03/95	1670	[1650 ; 1690]
			05/04/95	1654	[1634 ; 1674]
			12/04/95	1664	[1644 ; 1684]
			18/04/95	1660	[1640 ; 1680]

C_4	SAR = 20 ; TEC = 10 meq/l	[1647 ; 1687]	23/02/95	1635	[1615 ; 1655]
			24/02/95	1654	[1634 ; 1674]
			03/03/95	1659	[1639 ; 1679]
			10/03/95	1685	[1665 ; 1705]
			17/03/95	1645	[1625 ; 1665]
			24/03/95	1651	[1631 ; 1671]
			31/03/95	1679	[1659 ; 1699]
			07/04/95	1650	[1630 ; 1670]
			14/04/95	1660	[1640 ; 1680]
			21/04/95	1648	[1628 ; 1668]
			28/04/95	1670	[1650 ; 1690]
			05/05/95	1654	[1634 ; 1674]
			12/05/95	1676	[1656 ; 1696]
C_5	SAR = 20 ; TEC = 5 meq/l	[1651 ; 1691]	14/03/95	1659	[1615 ; 1655]
			15/03/95	1649	[1629 ; 1669]
			23/03/95	1663	[1643 ; 1683]
			30/03/95	1695	[1675 ; 1715]
			06/04/95	1676	[1656 ; 1696]
			12/04/95	1683	[1663 ; 1703]
			21/04/95	1669	[1649 ; 1689]
			28/04/95	1667	[1647 ; 1697]
			04/05/95	1642	[1622 ; 1662]
			11/05/95	1663	[1643 ; 1683]
			18/05/95	1676	[1656 ; 1696]
			26/05/95		
C_6	SAR = 20 ; TEC = 1 meq/l	[1645 ; 1685]	20/03/95	1648	[1628 ; 1668]
			22/03/95	1644	[1624 ; 1664]
			30/03/95	1683	[1663 ; 1703]
			06/04/95	1686	[1666 ; 1706]
			13/04/95	1671	[1651 ; 1691]
			21/04/95	1678	[1658 ; 1698]
			27/04/95		
			04/05/95	1660	[1640 ; 1680]
			11/05/95	1672	[1652 ; 1692]
			18/05/95	1698	[1678 ; 1718]
			26/05/95	1658	[1638 ; 1678]

Annexe 4.10b. Evolution of the mean bulk densities obtained by gamma-radiation (^{241}Am countings during 60 s) and the 99 % confidence limit for the columns of series II.

	Solution	Dry $[\overline{\rho_b} \pm 2SD]$ (kg/m^3)	Datum	$\overline{\rho_b}$ (kg/m^3)	$[\overline{\rho_b} \pm 2SD]$ (kg/m^3)
C_1	SAR = 5 ; TEC = 5 meq/l	[1645 ; 1685]	08/08/95	1636	[1616 ; 1656]
			09/08/95	1610	[1590 ; 1630]
			16/08/95	1631	[1611 ; 1651]
			23/08/95	1604	[1584 ; 1624]
			24/08/95	1591	[1571 ; 1611]
			30/08/95	1620	[1600 ; 1640]
	SAR = 5 ; TEC = 1 meq/l		06/09/95	1642	[1622 ; 1662]
			13/09/95	1630	[1610 ; 1650]
			20/09/95	1605	[1585 ; 1625]
			26/09/95	1596	[1576 ; 1616]
			02/10/95	1596	[1576 ; 1616]
			09/10/95	1607	[1587 ; 1627]
C_2	SAR = 5 ; TEC = 5 meq/l	[1639 ; 1679]	16/08/95	1638	[1618 ; 1658]
			18/08/95	1611	[1591 ; 1631]
			25/08/95	1585	[1565 ; 1605]
			30/08/95	1619	[1599 ; 1639]
			07/09/95	1598	[1578 ; 1618]
	SAR = 10 ; TEC = 5 meq/l		14/09/95	1611	[1591 ; 1631]
			21/09/95	1635	[1615 ; 1655]
			27/09/95	1599	[1579 ; 1619]
			04/10/95	1583	[1563 ; 1603]
			10/10/95	1566	[1546 ; 1586]
			18/10/95	1560	[1540 ; 1580]
			25/10/95	1594	[1574 ; 1614]

C_3	SAR = 5 ; TEC = 5 meq/l	[1671 ; 1711]	21/08/95	1679	[1659 ; 1699]
			23/08/95	1659	[1639 ; 1679]
			24/08/95	1627	[1607 ; 1647]
			30/08/95	1669	[1649 ; 1689]
			06/09/95	1669	[1649 ; 1689]
			13/09/95	1667	[1647 ; 1687]
	SAR = 10 ; TEC = 1 meq/l		20/09/95	1644	[1624 ; 1664]
			26/09/95	1641	[1621 ; 1661]
			04/10/95	1646	[1626 ; 1666]
			10/10/95	1624	[1604 ; 1644]
			19/10/95	1614	[1594 ; 1634]
			26/10/95	1614	[1594 ; 1634]
			02/11/95	1611	[1591 ; 1631]
			08/11/95	1615	[1595 ; 1635]
C_5	SAR = 5 ; TEC = 5 meq/l	[1650 ; 1690]	04/09/95	1666	[1646 ; 1686]
			05/09/95	1633	[1613 ; 1653]
			12/09/95	1666	[1646 ; 1686]
			21/09/95	1633	[1613 ; 1653]
			27/09/95	1632	[1612 ; 1652]
	Deionised water		05/10/95	1600	[1580 ; 1620]
			10/10/95	1607	[1587 ; 1627]
			19/10/95	1594	[1574 ; 1614]
			26/10/95	1593	[1573 ; 1613]
			02/11/95	1608	[1588 ; 1628]
			08/11/95	1583	[1563 ; 1603]

Annexe 4.11. Evolution of the concentrations of Na and Ca in the effluents as a function of the pore volume (series II). The concentrations corresponding to the initial leaching solutions are given in annexe 2.6.

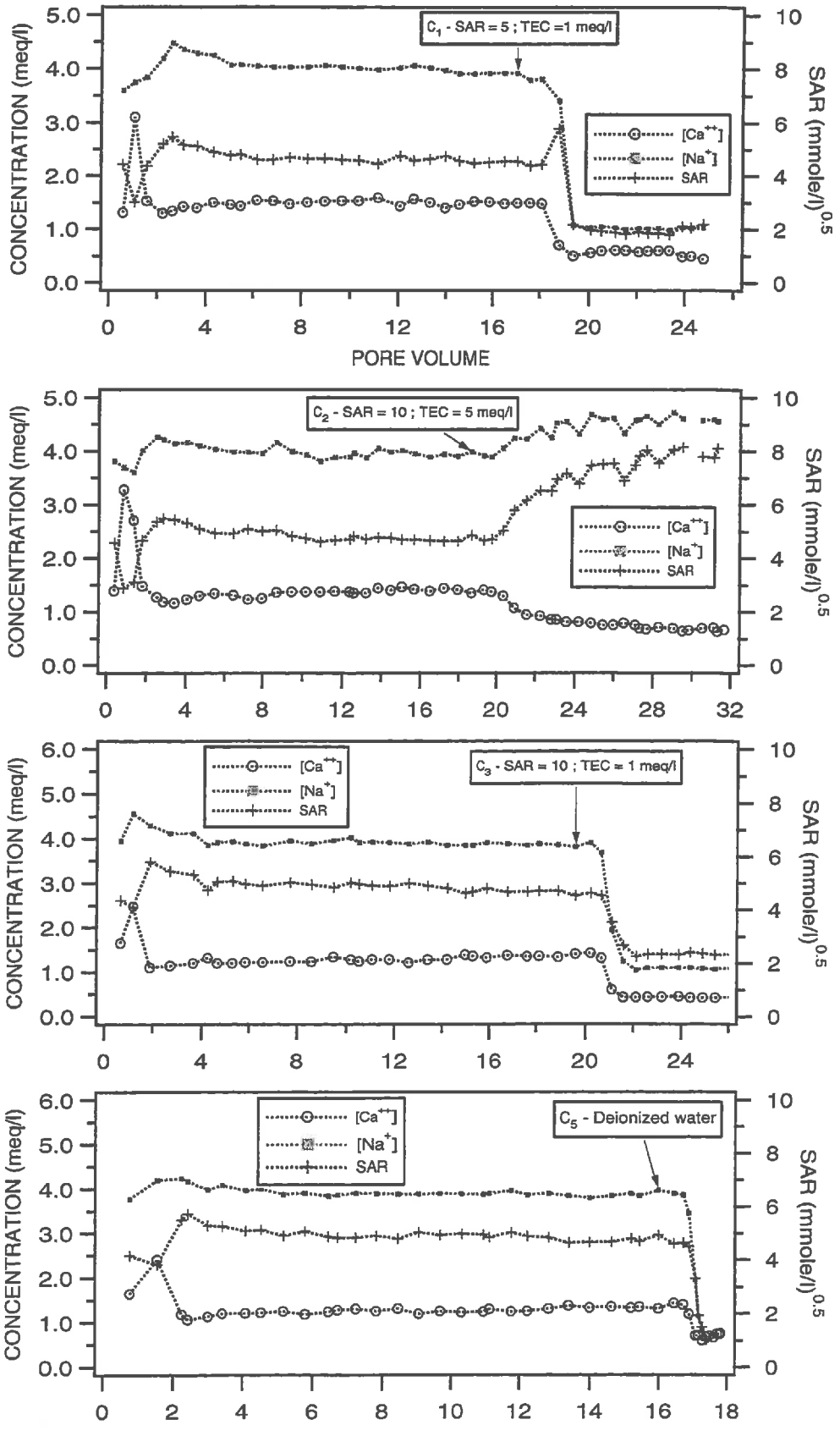

Annexe 4.12a. Measured and calculated volumetric water content profiles for the sandy layers at the end of the percolation period (series I). The residual water content is assumed to remain constant and equal to that of the initially clay-free sand. The measured profiles (filled circles) were obtained by gamma-radiation.

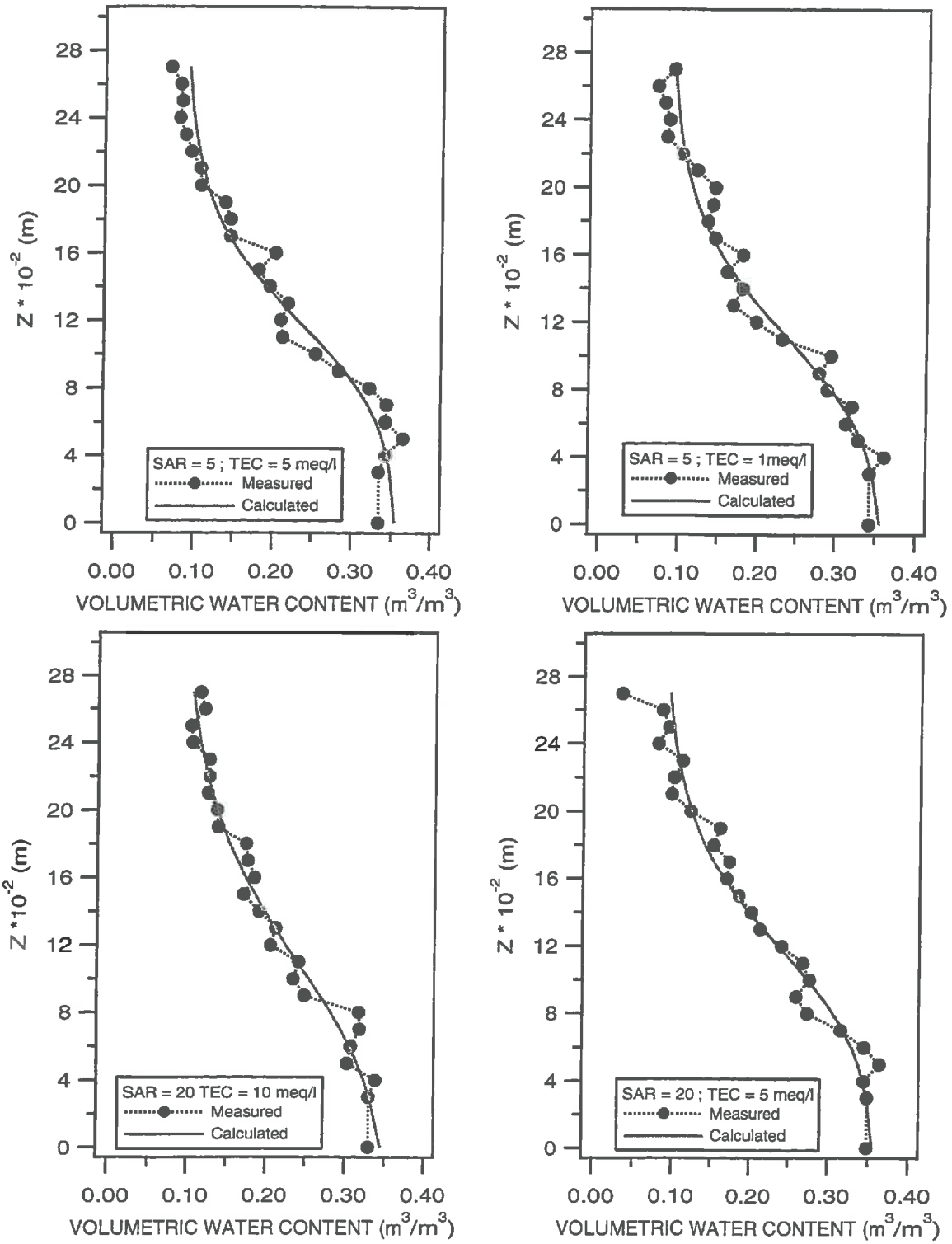

Annexe 4.12b. Measured and calculated volumetric water content profiles for the sandy layers at the end of the percolation period (series I). The residual water content is assumed to remain constant and equal to that of the initially clay-free sand. The measured profiles (filled circles) were obtained by gamma-radiation.

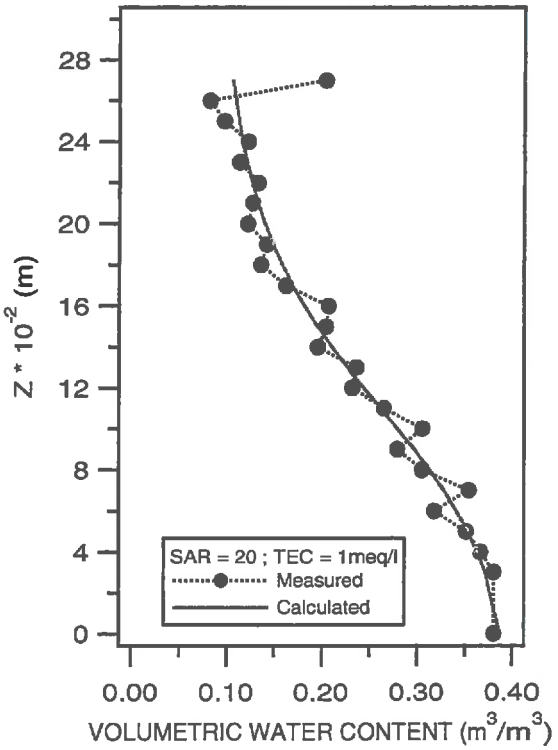

Annexe 4.13. The three-term van Genuchten parameter vectors with their estimated variances σ^2 and correlation matrixes calculated at the end of the percolation period (series I).

Solution	Parameter	Estimated Value	Estimated σ^2	Parameter	θ_S	α	n	Estimated σ^2_{res}
SAR = 5 ; TEC = 5 meq/l	θ_S	0.357	7.895e-5	θ_S	1			3.89e-4
	$\alpha^{(*)}$	0.027	9.854e-8	α	0.82	1		
	n	11.928	7.910e-1	n	-0.64	-0.66	1	
SAR = 5 ; TEC = 1 meq/l	θ_S	0.360	8.528e-5	θ_S	1			3.07e-4
	$\alpha^{(*)}$	0.0275	1.128e-7	α	0.87	1		
	n	10.912	6.550e-1	n	-0.70	-0.73	1	
SAR = 20 ; TEC = 10 meq/l	θ_S	0.355	1.185e-4	θ_S	1			2.21e-4
	$\alpha^{(*)}$	0.0274	2.456e-7	α	0.94	1		
	n	8.268	3.665e-1	n	-0.81	-0.85	1	
SAR = 20 ; TEC = 5 meq/l	θ_S	0.358	1.083e-4	θ_S	1			4.14e-4
	$\alpha^{(*)}$	0.0268	1.561e-7	α	0.87	1		
	n	10.894	8.149e-1	n	-0.73	-0.76	1	
SAR = 20 ; TEC = 1 meq/l	θ_S	0.398	4.260e-4	θ_S	1			6.64e-4
	$\alpha^{(*)}$	0.0275	6.303e-7	α	0.95	1		
	n	8.587	1.136	n	-0.84	-0.88	1	

(*) expressed in [1/cm]

Annexe 4.14. The four-term van Genuchten parameter vectors with their estimated variances σ^2 and correlation matrixes calculated at the end of the percolation period (series I).

Solution	Parameter	Estimated Value	Estimated σ^2	Parameter	θ_r	θ_s	α	n	Estimated σ^2_{res}
SAR = 5 TEC = 5 meq/l	θ_r	0.056	2.700e-4	θ_r	1				3.47e-4
	θ_s	0.366	1.330e-4	θ_s	-0.47	1			
	$\alpha^{(*)}$	0.0266	1.670e-7	α	0.47	0.47	1		
	n	9.434	1.676	n	0.87	-0.73	0.72	1	
SAR = 5 TEC = 1 meq/l	θ_r	0.077	1.441e-4	θ_r	1				3.11e-4
	θ_s	0.363	1.467e-4	θ_s	-0.57	1			
	$\alpha^{(*)}$	0.0274	1.371e-7	α	0.13	0.65	1		
	n	10.0571	2.102	n	0.86	-0.79	-0.26	1	
SAR = 20 TEC=10 meq/l	θ_r	0.100	1.145e-4	θ_r	1				2.23e-4
	θ_s	0.347	1.220e-4	θ_s	-0.56	1			
	$\alpha^{(*)}$	0.0275	1.659e-7	α	0.11	0.68	1		
	n	9.518	1.848	n	0.86	-0.80	-0.30	1	
SAR = 20 TEC = 5 meq/l	θ_r	0.048	5.727e-4	θ_r	1				2.27e-4
	θ_s	0.374	2.112e-4	θ_s	-0.67	1			
	$\alpha^{(*)}$	0.0265	2.064e-7	α	0.41	0.36	1		
	n	8.055	1.773	n	0.92	-0.86	0.07	1	
SAR = 20 TEC = 1 meq/l	θ_r	0.1104	1.4501e-4	θ_r	1				6.55e-4
	θ_s	0.383	3.180e-4	θ_s	-0.49	1			
	$\alpha^{(*)}$	0.0275	3.408e-7	α	-0.04	0.80	1		
	n	10.9678	4.468	n	0.76	-0.82	-0.55	1	

(*) expressed in [1/cm]

Annexe 4.15. Values of the surfaces between two estimated soil-moisture retention curves of series I. The simple underlined (double) values means that the MRC are significantly different at the 0.05 (0.01) level.

Solution	SAR = 5 TEC = 5 meq/l	SAR = 5 TEC = 1 meq/l	SAR = 20 TEC = 10 meq/l	SAR = 20 TEC = 5 meq/l	SAR = 20 TEC = 1 meq/l
SAR = 5 TEC = 5 meq/l	-				
SAR = 5 TEC = 1 meq/l	0.668	-			
SAR = 20 TEC = 10 meq/l	1.764	1.180	-		
SAR = 20 TEC = 5 meq/l	0.348	0.878	1.840	-	
SAR = 20 TEC = 1 meq/l	1.998	1.659	1.244	1.786	-

95 % confidence limit = [0.258 ; 1.452]
99 % confidence limit = [0.143 ; 1.856]

Annexe 4.16. Comparison between the MRCs obtained by the inverse approach (solid line) and those obtained by using the equations of the conceptual model (dashed line - main drying branche). The dotted line corresponds to the initially clay-free Fontainebleau sand (main drying branche). Experimental data from series I flow experiments were used.

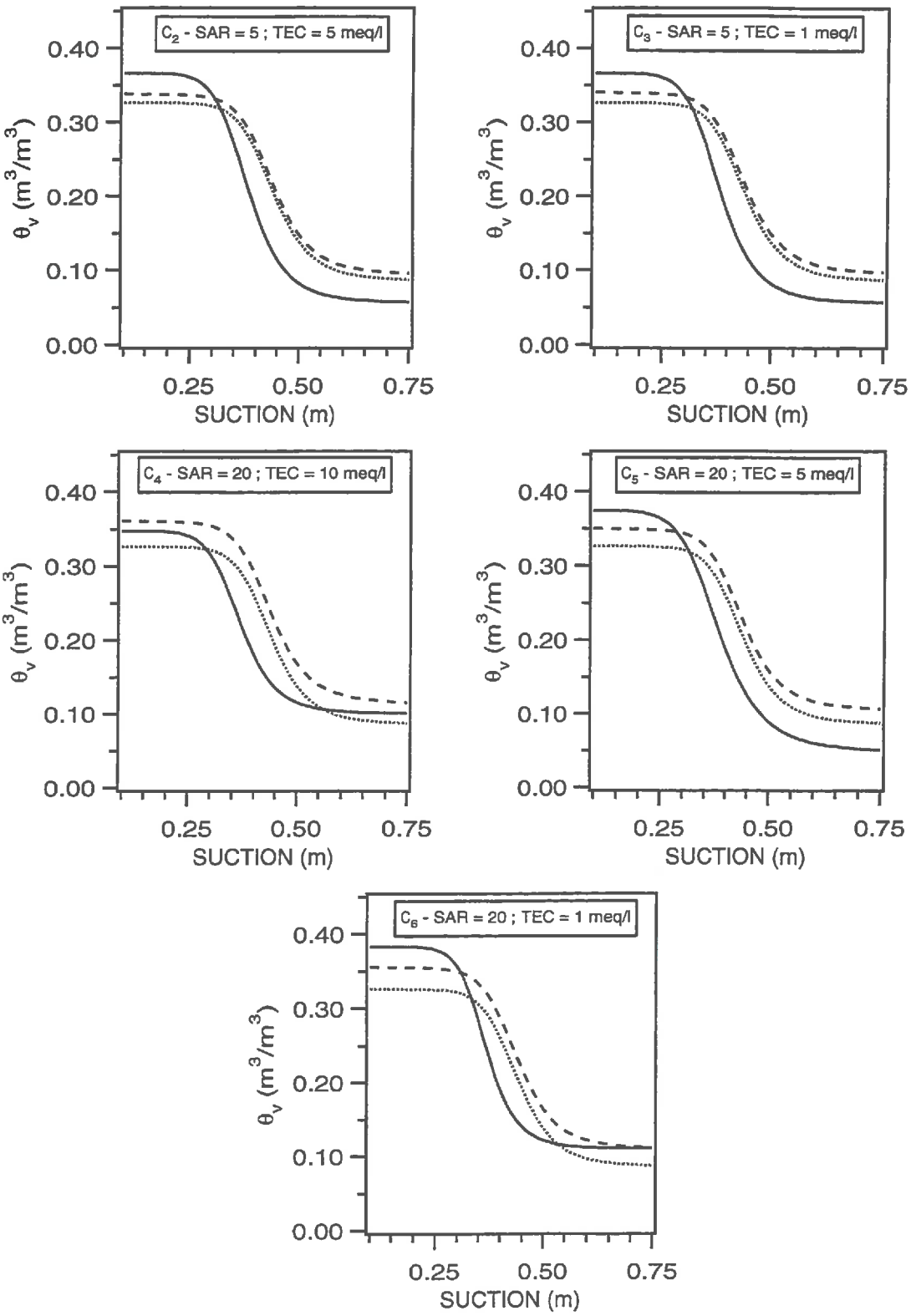

Annexe 4.17. The van Genuchten parameters with their estimated variances σ^2 and correlation matrix calculated at the end of the first percolation period (series II - SAR = 5 - TEC = 5 meq/l).

Solution	Parameter	Estimated Value	Estimated σ^2	Parameter	θ_r	θ_s	α	n	Estimated σ^2_{res}
C_1	θ_r	0.141	6.486e-5	θ_r	1				2e-4
SAR = 5	θ_s	0.322	5.148e-5	θ_s	-0.44	1			
TEC = 5 meq/l	$\alpha^{(*)}$	0.0274	1.204e-7	α	0.30	0.57	1		
	n	12.921	4.082	n	0.81	-0.71	-0.14	1	
C_2	θ_r	0.114	6.988e-5	θ_r	1				1.86e-4
SAR = 5	θ_s	0.362	2.965e-5	θ_s	-0.47	1			
TEC = 5 meq/l	$\alpha^{(*)}$	0.0255	4.130e-8	α	0.50	0.34	1		
	n	12.936	1.960	n	0.82	-0.70	0.11	1	
C_3	θ_r	0.160	2.235e-4	θ_r	1				2.30e-4
SAR = 5	θ_s	0.357	3.236e-4	θ_s	-0.54	1			
TEC = 5 meq/l	$\alpha^{(*)}$	0.0260	7.770e-7	α	-0.02	0.83	1		
	n	10.019	8.986	n	0.76	-0.92	-0.63	1	
C_5	θ_r	0.102	4.382e-4	θ_r	1				1.13e-4
SAR = 5	θ_s	0.367	3.121e-5	θ_s	-0.69	1			
TEC = 5 meq/l	$\alpha^{(*)}$	0.0240	1.304e-7	α	0.90	-0.36	1		
	n	10.042	2.008	n	0.94	-0.83	0.73	1	

(*) expressed in [1/cm]

Annexe 4.18. Values of the surfaces between two estimated MRCs at the end of the first percolation period (series II). All the columns were leached with a solution of SAR = 5 and TEC = 5 meq/l. Differences in the MRC are probably due to differences in the clay amount and their distribution within the column. The simple underlined values means that the MRC are significantly different at the 0.01 level.

Solution	C_1	C_2	C_3	C_5
C_1	-			
C_2	2.119	-		
C_3	2.198	1.804	-	
C_5	2.749	0.842	1.851	-

95 % confidence limit = [0.234 ; 1.310]
99 % confidence limit = [0.119 ; 1.657]

Annexe 4.19. The van Genuchten parameters with their estimated variances σ^2 and correlation matrix calculated at the end of the second percolation period (series II).

Solution	Parameter	Estimated Value	Estimated σ^2	Parameter	θ_r	θ_s	α	n	Estimated σ^2_{res}
C_1	θ_r	0.178	6.424e-5	θ_r	1				5.20e-4
SAR = 5	θ_s	0.325	6.643e-5	θ_s	-0.25	1			
TEC = 1 meq/l	$\alpha^{(*)}$	0.0264	1.851e-7	α	0.31	0.58	1		
	n	17.688	1.719e1	n	0.52	-0.65	-0.32	1	
C_2	θ_r	0.157	1.964e-5	θ_r	1				
SAR = 10	θ_s	0.404	2.126e-5	θ_s	-0.31	1			1.61e-4
TEC = 5 meq/l	$\alpha^{(*)}$	0.0264	2.254e-8	α	0.30	0.56	1		
	n	16.316	1.878	n	0.66	-0.63	-0.21	1	
C_3	θ_r	0.134	2.359e-4	θ_r	1				
SAR = 10	θ_s	0.391	4.176e-4	θ_s	-0.63	1			3.56e-4
TEC = 1 meq/l	$\alpha^{(*)}$	0.0278	5.698e-7	α	-0.17	0.84	1		
	n	8.604	3.296	n	0.86	-0.87	-0.59	1	
C_5	θ_r	0.140	5.487e-5	θ_r	1				
Deionised	θ_s	0.403	2.011e-5	θ_s	-0.45	1			1.35e-4
water	$\alpha^{(*)}$	0.0252	2.683e-8	α	0.53	0.33	1		
	n	13.171	1.344	n	0.83	-0.68	0.15	1	

(*) expressed in [1/cm]

Annexe 4.20. Surfaces values between the MRCs obtained at the end of the first and second percolation period (series II). The 95 % and 99 % confidence limits of the estimated probability density function of the surfaces between the generated MRC_{ig} are added.

Column	95 % confidence limit	99 % confidence limit	Surface between MRCs
C_1	[0.197 ; 0.957]	[0.113 ; 1.215]	1.676 (1)
C_2	[0.133 ; 0.707]	[0.007 ; 0.942]	2.367 (1)
C_3	[0.274 ; 1.689]	[0.165 ; 2.637]	1.595 (2)
C_5	[30.161 ; 1.133]	[0.083 ; 1.528]	1.777 (1)

(1) significantly different at the 0.01 level
(2) significantly different at the 0.0713 level